Equalization

Chapter 3

Equalization

Chapter 1's main focus was a single channel use with signal set and detector that communicate one of M messages or symbols. Chapter 1's analysis is therefore of "one-shot" use. Chapter 2 expanded this one-shot analysis to sequences or "codewords" of symbols that each pass through the channel without overlap or interference from one another. That is, the channel was **memoryless**. In practice, successive transmissions do often interfere with one another, especially as they are sent more closely together in shorter symbol periods to increase the data transmission rate. The interference between successive transmissions has the name **intersymbol interference (ISI)**. ISI can severely complicate an optimum ML detector's implementation.

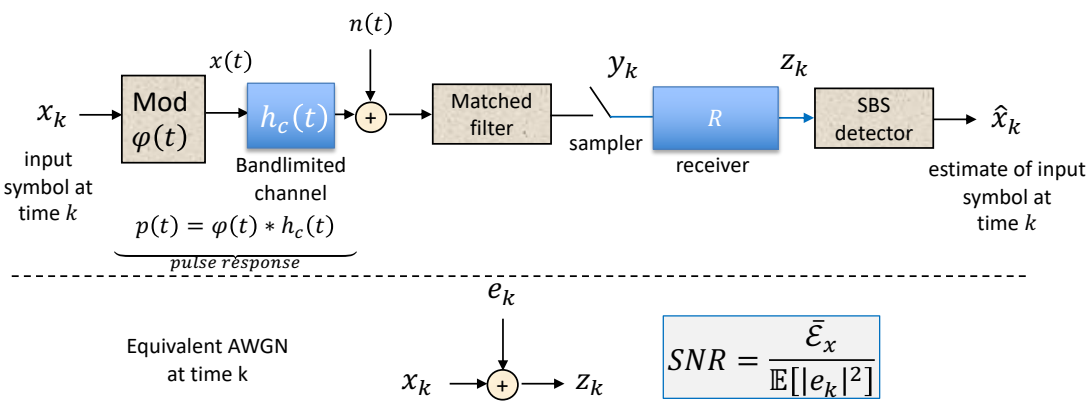

Figure 3.1: The band-limited channel with receiver and SBS detector.

Figure 3.1 illustrates a receiver for detection of successively transmitted messages. The matched filter outputs are processed by the receiver, which outputs samples, $\boldsymbol{z}_k$, that estimate the symbol transmitted at time k, $\hat{\boldsymbol{x}}_k$. Each receiver output sample is the input to the same detector that would be used on an AWGN channel without ISI. This **symbol-by-symbol (SBS)** detector, while optimum for the AWGN channel, will not be a maximum-likelihood estimator for the message sequence. Nonetheless, if the receiver is well-designed, the receiver-detector combination may work nearly as well as an optimum detector with far less complexity. The objective of this chapter's receiver will be to improve the simple SBS detector's performance. For most of this chapter, the SBS detector will be a simple scalar detector, but developments will eventually encompass the MIMO channel with first the receiver allowing $L_y > 1$ spatial dimensions in what is called "diversity" and then further expanding to $L_x > 1$ for full MIMO.

Communication designers use **equalization** to mitigate ISI effects. An equalizer is essentially the content of Figure 3.1's receiver box. This chapter studies both ISI and several equalization methods,

which amount to different structures for the receiver box. This chapter's methods are not optimal for detection, but rather find significant use as sub-optimal cost-effective methods that reduce ISI degradation. These equalization methods convert a band-limited channel with ISI into one that appears memoryless, hopefully synthesizing a new AWGN-like channel at the receiver output. The designer can then analyze the resulting memoryless, equalized channel using the methods of Chapters 1 and 2 with an appropriate equalized-system SNR, as if the channel were an AWGN with that SNR. For Chapter 2's coded systems, the decoder may no longer be SBS but it is the same decoder as would be used on the AWGN for that same SNR and does not include channel effects, grace of the equalizer. With an appropriate transmit signal choice, one of this chapter's methods - the Decision Feedback Equalizer can be generalized into a **canonical receiver**.indexreceiver!canonical A canonical receiver reliably achieves the highest possible transmission rate, or Chapter 2's capacity $\mathcal{C}$, even though not exactly an optimum ML detector.

Section 3.1 models linear intersymbol interference between successive transmissions, thereby both illustrating and measuring the ISI. In practice, as shown by a simple example, distortion from overlapping symbols can be unacceptable, suggesting that some corrective action must be taken. Section 3.1 also refines the concept of signal-to-noise ratio, which is the method used in this text to quantify receiver performance. The SNR concept will be used consistently throughout the remainder of this text as a quick and accurate means of quantifying transmission performance, as opposed to probability of error, which can be more difficult to compute, especially for suboptimum designs. As Figure 3.1 shows, the receiver's objective will be to convert the channel into an equivalent AWGN at each time k, independent of all other times k. An AWGN detector may then be applied to the derived channel, and performance computed readily using the gap approximation or other known formulas of Chapters 1 and 2 with the SNR of the derived AWGN channel. There may be loss of optimality in creating such an equivalent AWGN, which will be measured by the equivalent AWGN's SNR with respect to the best SNR that might be expected otherwise for an optimum detector. Section 3.3 discusses some desired types of channel responses that exhibit no intersymbol interference, specifically introducing the Nyquist Criterion for a linear channel (equalized or otherwise) to be free of intersymbol interference. Section 3.4 illustrates the basic concept of equalization through the zero-forcing equalizer (ZFE), which is simple to understand but often of limited effectiveness. The more widely used and higher performance, minimum mean square error linear (MMSE-LE) and decision-feedback equalizers (MMSE-DFE) are discussed in Sections 3.5 and 3.6. Section 3.7 discusses the design of finite-length equalizers, as is needed in practice. Section 3.8 discusses precoding, a method for eliminating error propagation in decision-feedback equalizers and the related concept of partial-response channels. Section 3.9 generalizes the equalization concepts to systems with one input, but several outputs (so $L_y > 1$), such as wireless transmission systems with multiple receive antennas called "diversity" receivers.

Section 3.10 generalizes the developments to MIMO channel equalization with both $L_x > 1$ and/or $L_y > 1$. Section 3.11 introduces an information-theoretic infinite-length approach to interpreting and revisiting the SISO MMSE-DFE that is then useful for optimizing the transmit filters in Section 3.12. Appendix D provides significant results on minimum mean-square estimation, including the orthogonality principle, scalar and MIMO forms of the Paley Weiner Criterion, results on linear prediction, Cholesky Factorization, and both scalar and MIMO canonical factorization results. Section 3.13 generalizes equalization to partial-response channels.

3.1 ISI and Receivers for Successive Message Transmission

Intersymbol interference (ISI) is a common practical impairment found in many transmission and storage systems, including wireless and wireline data transmission, storage disks, and even fiber-optic cables. This section introduces an ISI model. This section then continues and revisits the equivalent AWGN of Figure 3.1 for various receiver ISI-mitigating actions.

3.1.1 Successive Message Transmission

Most communication systems re-use the channel to transmit several successive messages. From Section 1.1, a new message transmits every T time units. T is the **symbol period**, and $1/T$ is the **symbol rate**.[1] Chapter 1's **data rate** for a communication system that sends one of M possible messages every T time units is

$$R \triangleq \frac{\log_2(M)}{T} = \frac{b}{T} \quad . \tag{3.1}$$

A design increases the data rate by either increasing b (which requires more signal energy to maintain P_e) or by decreasing T. Decreasing T narrows the time between message transmissions and thus increases ISI on any band-limited channel.

The transmitted signal $x(t)$ that corresponds to K successive transmissions is

$$x(t) = \sum_{k=0}^{K-1} x_k(t - kT) \quad . \tag{3.2}$$

Equation (3.2) slightly abuses previous notation in that the subscript k on $x_k(t-kT)$ refers to the index of the kth successive transmission. The K successive transmissions could be considered an aggregate or "block" symbol, $x(t)$, conveying one of M^K possible messages. The receiver could attempt to implement MAP or ML detection for this new transmission system with M^K messages. The designer then performs a Gram-Schmidt decomposition on the set of M^K signals and designs an optimum detector accordingly. Such an approach has complexity that grows exponentially (in proportion to M^K) with the block message length K. That is, the optimal detector might need M^K matched filters, one for each possible transmitted block symbol. As $K \to \infty$, the complexity can become too large for practical implementation. Chapter 8 addresses such "sequence detectors" in detail, and it may be possible to compute the à posteriori probability function with less than exponentially growing complexity.

Symbol-by-symbol detection: An alternative (suboptimal) receiver can detect each of the successive K messages independently. Such detection is called **symbol-by-symbol (SBS)** detection. Figure 3.2 contrasts the SBS detector with Chapter 1's block detector. The bank of K matched filters, $\{\phi_k^*(-t)\}_{k=1,\ldots,K}$, presumably found by Gram-Schmitt decomposition of the set of (noiseless) channel output waveforms[2], precedes a block detector that determines the K-dimensional vector symbol transmitted. The complexity would become large or infinite as K becomes large or infinite for the block detector. The lower system in Figure 3.2 has a single matched filter to the channel, with output sampled K times, followed by a receiver and an SBS detector.

[1] The symbol rate is sometimes also called the "baud rate," although abuse of the term baud (by equating it with data rate even when $M \neq 2$) has rendered the term archaic among communication engineers, and the term "baud" gradually disappears.

[2] For which it can be shown K dimensions are sufficient only if $\overline{N} = 1$, complex or real.

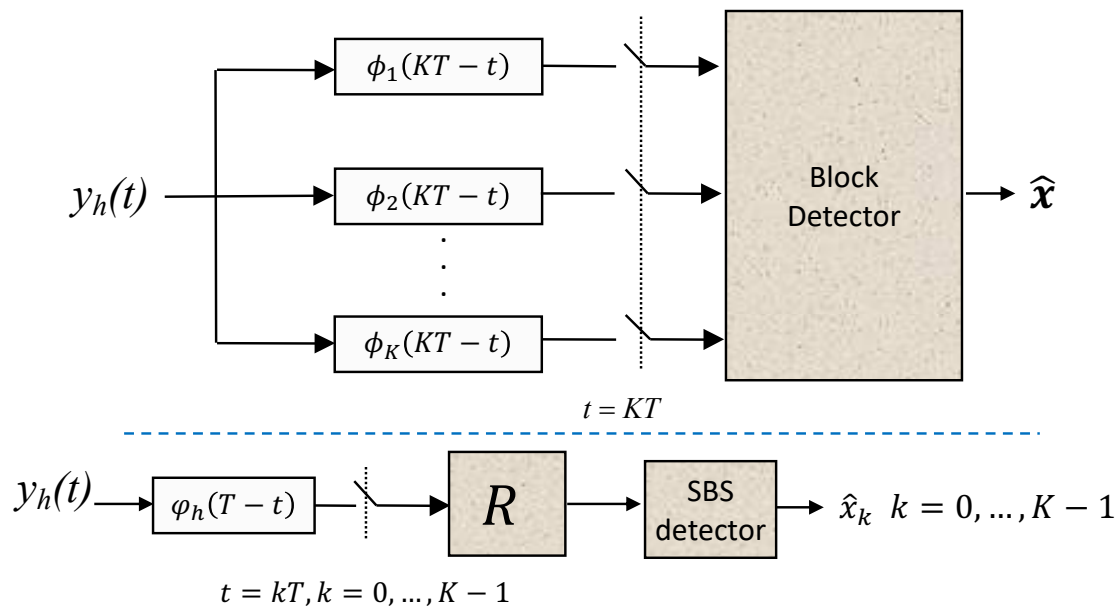

Figure 3.2: Comparison of Block and SBS detectors for successive transmission of K messages.

The SBS system has fixed (and lower) complexity per symbol/sample, but may not be optimum. ISI degrades SBS detection. This performance degradation increases as T decreases (or the symbol rate increases) in most communication channels. The designer mathematically analyzes ISI by rewriting (3.2) as

$$x(t) = \sum_{k=0}^{K-1} \sum_{n=1}^{\overline{N}} x_{kn} \cdot \varphi_n(t - kT) \ , \tag{3.3}$$

where the transmissions $x_k(t)$ have representation using a common orthonormal basis set $\{\varphi_n(t)\}$. In (3.3), $\varphi_n(t - kT)$ and $\varphi_m(t - lT)$ may be non-orthogonal when $k \neq l$. In some cases, translates of the basis functions are orthogonal. For instance, in QAM, the two band-limited basis functions

$$\varphi_1(t) = \sqrt{\frac{2}{T}} \cdot \cos\left(\frac{m\pi t}{T}\right) \cdot \text{sinc}\left(\frac{t}{T}\right) \tag{3.4}$$

$$\varphi_2(t) = -\sqrt{\frac{2}{T}} \cdot \sin\left(\frac{m\pi t}{T}\right) \cdot \text{sinc}\left(\frac{t}{T}\right) \quad , \tag{3.5}$$

or from Chapter 2, the baseband equivalent

$$\varphi(t) = \frac{1}{\sqrt{T}} \cdot \text{sinc}\left(\frac{t}{T}\right) \quad . \tag{3.6}$$

(with m a positive integer) are orthogonal for all integer-multiple-of-T time translations. In this case, the successive transmissions, when sampled at time instants kT, are free of ISI, and transmission is equivalent to a succession of "one-shot" channel uses. In this case SBS detection is optimal, and the MAP/ML detector for the entire block of messages is the same as a MAP detector used separately for each of the K independent transmissions. Signal sets for data transmission usually are orthogonal for any integer translation of symbol periods. Most linear AWGN channels, however, more accurately follow the filtered-AWGN channel of Section 1.7 and Chapter 2. The channel filtering alters the basis functions so that at the channel output the filtered basis functions are no longer orthogonal.

3.1.2 Band-limited Channels

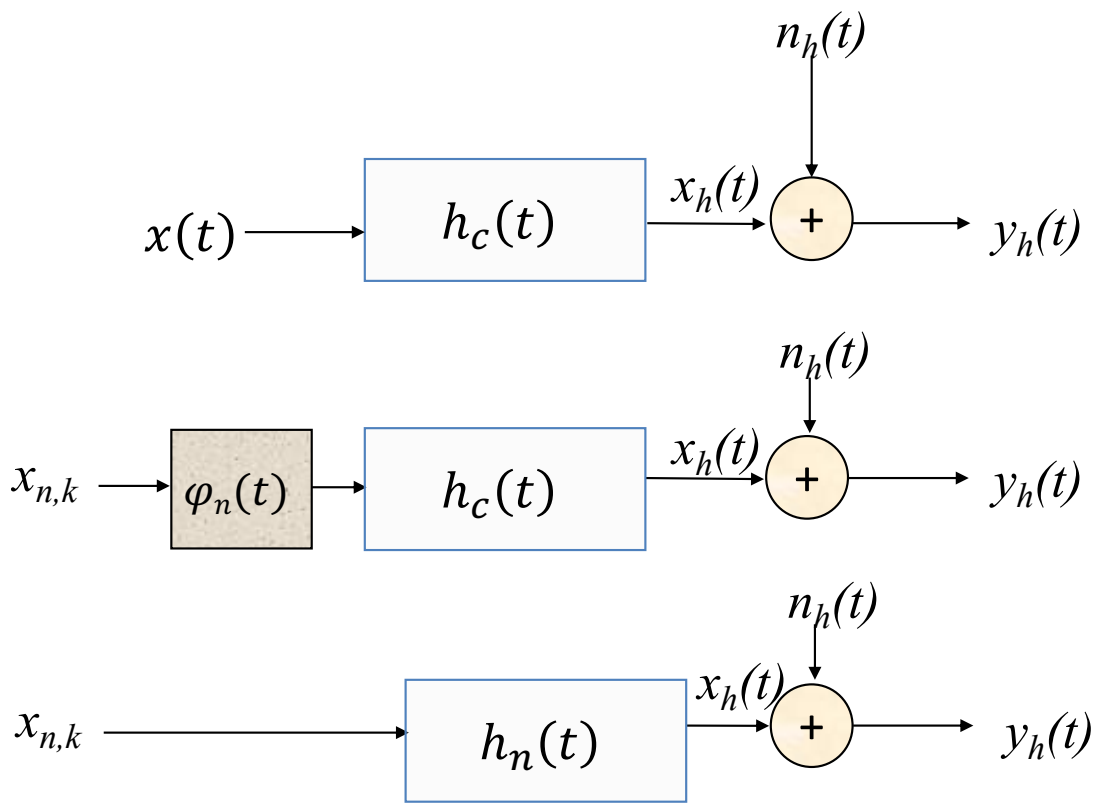

Figure 3.3: The bandlimited channel, and equivalent forms with pulse response.

Figure 3.3's bandlimited linear ISI channel is the same as the filtered AWGN channel discussed in Section 1.3.7. This subsection expands its use to successive symbol transmission, where $x_{n,k}$ denotes the symbol's component on the nth basis function at symbol time k. The (noise-free) channel output[3], $x_h(t)$, in Figure 3.3 is

$$x_h(t) = \sum_{k=0}^{K-1} \sum_{n=1}^{\overline{N}} x_{n,k} \cdot \varphi_n(t - kT) * h_c(t) \tag{3.7}$$

$$= \sum_{k=0}^{K-1} \sum_{n=1}^{\overline{N}} x_{n,k} \cdot h_n(t - kT) \tag{3.8}$$

where $h_n(t) \triangleq \varphi_n(t) * h_c(t)$. When $h(t) \neq \delta(t)$, the functions $h_n(t - kT)$ do not necessarily form an orthonormal basis, nor are they even necessarily orthogonal. Again, an optimum (MAP) detector would need to search a signal set of size M^K, which is often too complex for implementation as K gets large. When $\overline{N} = 1$ (or $\overline{N} = 2$ with complex signals and $\widetilde{N} = 1$ in both cases so that $N = 1$ or 2 respectively), there is only one pulse response $h(t)$.

[3]the subscript of h on the continuous-time signal $x_h(t)$ should not be confused with the subscripts on the discrete-time symbols x_k.

Equalization: An **equalizer** filters the channel output *to try* to convert $\{\{h_n(t-kT)\}\}_{(n,k)\in\mathbb{Z}^2}$ to an orthogonal set. Usually $n=1$ has just one value so the n index will disappear shortly. The receiver processes the equalizer output with SBS detection. Further equalizer filters discussion appears in Section 3.4. Sections 3.1 - 3.10 presume the channel-input symbol sequence x_k is independent and identically distributed at each point in time so that $\mathbb{E}\left[x_k \cdot x_j^*\right] = \delta_{kj}$. This presumption later relaxes when $x(t)$ may be the result of optimized transmit filtering, but even in those cases any equalizer typically targets the input of those filters that also have independent successive message-symbol values.

A more general ISI and equalization theory applies for any $\overline{N}$ as in Section 3.10 and also Chapters 4 and 5, but the present development sets $\overline{N}=1$. The developed equalizers here will apply equally well to any one-dimensional (e.g. PAM) or two-dimensional (e.g. QAM or hexagonal) constellation, with the later allowing filters with complex coefficients. This was the main motivation for the introduction of bandpass analysis in Chapter 1.

The **pulse response** for the transmitter/channel fundamentally quantifies ISI:

Definition 3.1.1 [Pulse Response] *A band-limited channel's* **pulse response** *is*

$$h(t) = \varphi(t) * h_c(t) \quad . \tag{3.9}$$

For the complex QAM case, $h(t)$, $\varphi(t)$, and $h_c(t)$ can be complex-baseband time functions.

The noiseless channel output $x_h(t)$ is

$$\begin{aligned} x_h(t) &= \sum_{k=0}^{K-1} x_k \cdot \varphi(t-kT) * h_c(t) & (3.10)\\ &= \sum_{k=0}^{K-1} x_k \cdot h(t-kT) \quad . & (3.11) \end{aligned}$$

The signal in (3.11) is real for a real baseband system and complex for a baseband-equivalent quadrature-modulated system. The pulse response energy $\|h\|^2$ is not necessarily equal to 1, and this text introduces the **normalized pulse response**:

$$\varphi_h(t) \triangleq \frac{h(t)}{\|h\|} \quad , \tag{3.12}$$

where

$$\|h\|^2 = \int_{-\infty}^{\infty} h(t) \cdot h^*(t) dt = \langle h(t), h(t) \rangle \quad . \tag{3.13}$$

The subscript h on $\varphi_h(t)$ indicates that $\varphi_h(t)$ is a normalized version of $h(t)$. The notation of the subscript of h here does not replace n because $n=1$ and does not appear - technically, it should be $x_{h,n=1,k}$ but notation simplifies without redundantly carrying the constant $n=1$ value. Using (3.12), Equation (3.11) becomes

$$x_h(t) = \sum_{k=0}^{K-1} x_{h,k} \cdot \varphi_h(t-kT) \quad , \tag{3.14}$$

where

$$x_{h,k} \triangleq x_k \cdot \|h\| \quad . \tag{3.15}$$

The notation $x_{h,k}$ absorbs the channel gain/attenuation $\|h\|$ into the input symbol value and thus has energy $\mathcal{E}_h = E\left[|x_{h,k}|^2\right] = \mathcal{E}_{\boldsymbol{x}} \cdot \|h\|^2$. While the functions $\varphi_h(t-kT)$ are normalized, they are not necessarily orthogonal, so SBS detection is not necessarily optimal for (3.14)'s signal.

EXAMPLE 3.1.1 [ISI and the pulse response] As an example of ISI, consider the pulse response $h(t) = \frac{1}{1+t^4}$ and two successive transmissions of opposite polarity (-1 followed by $+1$) through the corresponding channel.

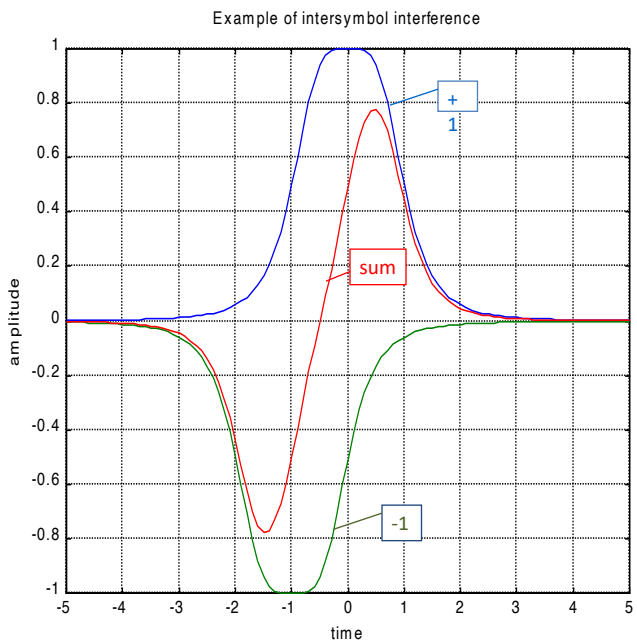

Figure 3.4: Illustration of intersymbol interference for $h(t) = \frac{1}{1+t^4}$ with $T = 1$.

Figure 3.4 illustrates the two isolated pulses with correct polarity and also the waveform corresponding to the two transmissions separated by 1 unit in time. Clearly the peaks of the pulses displace in time and also significantly reduce in amplitude. Higher transmission rates force successive transmissions closer together. Figure 3.5 illustrates the resultant sum of the two waveforms for spacings of 1 unit in time, .5 units in time, and .1 units in time. ISI severely reduces pulse strength and thereby reduces noise immunity.

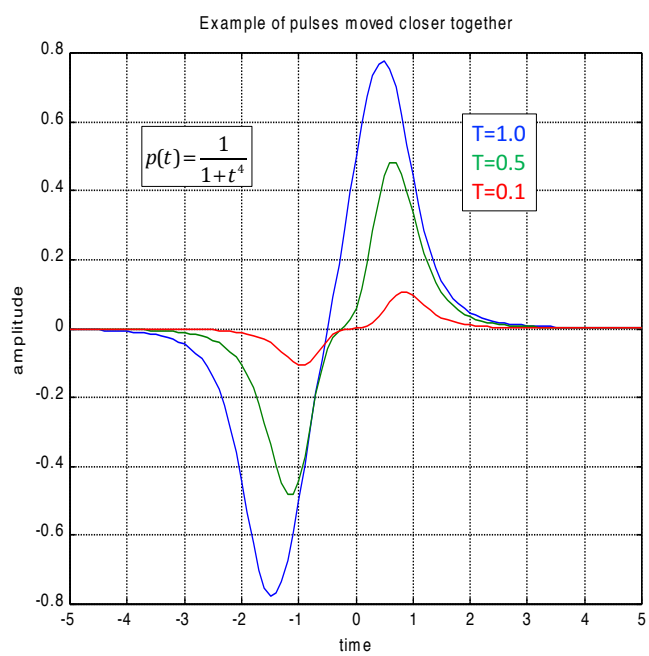

Figure 3.5: **ISI with increasing symbol rate.**

EXAMPLE 3.1.2 [Pulse Response Orthogonality - Modified Duobinary] A PAM modulated signal using rectangular pulses is

$$\varphi(t) = \frac{1}{\sqrt{T}} \cdot (u(t) - u(t-T)) \quad . \tag{3.16}$$

The channel introduces ISI, for example, according to

$$h_c(t) = \delta(t) + \delta(t-T). \tag{3.17}$$

The resulting pulse response is

$$h(t) = \frac{1}{\sqrt{T}}(u(t) - u(t-2T)) \tag{3.18}$$

and the normalized pulse response is

$$\varphi_h(t) = \frac{1}{\sqrt{2T}}(u(t) - u(t-2T)). \tag{3.19}$$

The pulse-response translates $\varphi_h(t)$ and $\varphi_h(t-T)$ are not orthogonal, even though $\varphi(t)$ and $\varphi(t-T)$ were originally orthonormal.

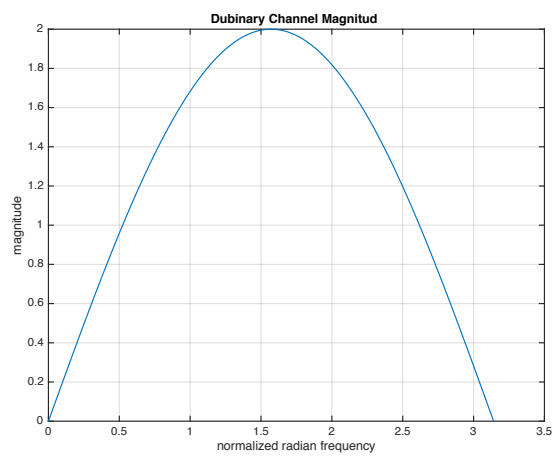

Figure 3.6: Modified Duobinary Frequency Response.

3.1.2.1 Noise Equivalent Pulse Response

Figure 3.7 models a channel with additive Gaussian noise that is not white, which often occurs in practice. The noise's power spectral density is $\frac{\mathcal{N}_0}{2} \cdot S_n(f)$. When $S_n(f) \neq 0$ (noise is never exactly zero at any frequency in practice), the noise psd has an invertible square root as in Section 1.7. The invertible square-root can be realized as a first (pre-equalizer) receiver filter. Since this filter is invertible, by Chapter 1's reversibility theorem, no information is lost in "whitening" the noise. The designer can then construe this filter as being part of, the channel as Figure 3.7's lower portion shows. The noise-equivalent pulse response then has Fourier Transform $H(f)/S_n^{1/2}(f)$ for an equivalent filtered-AWGN channel.

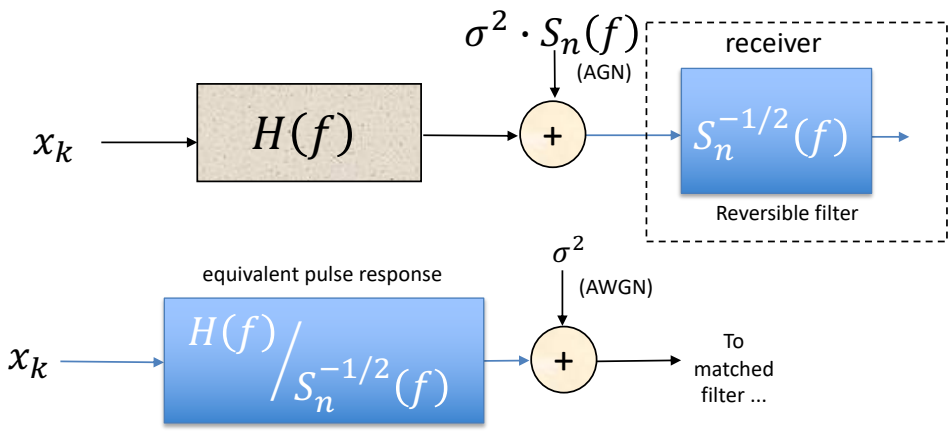

Figure 3.7: **White Noise Equivalent Channel.**

The noise-equivalent pulse response concept validates an AWGN analysis using the noise-equivalent pulse response instead of the original pulse response. Then also "colored noise" has an equivalent ISI effect, and furthermore this chapters later compensating equalizers are applicable to channels that originally have no ISI, but that do have "colored noise." An AWGN channel with a notch in $H(f)$ at some frequency is thus equivalent to a "flat channel" with $H(f) = 1$, but with narrow-band Gaussian noise at the same frequency as the notch, as Figure 3.8 illustrates.

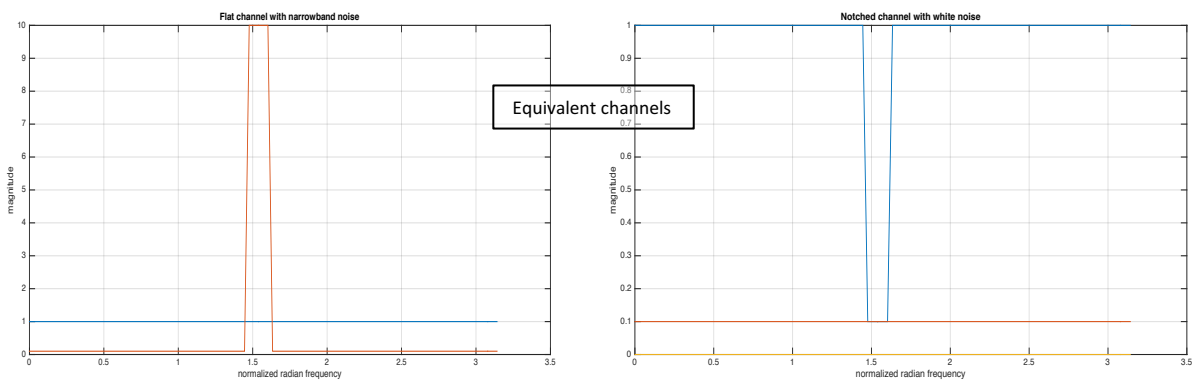

Figure 3.8: **Two "noise-equivalent" channels.**

3.1.3 The ISI-Channel Model

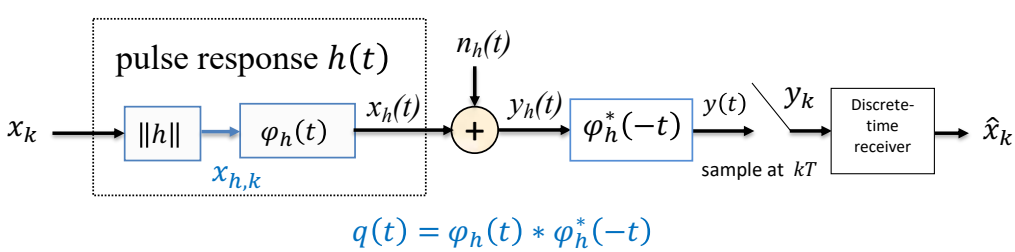

Figure 3.9: **The ISI-Channel model.**

Figure 3.9 shows a model for linear ISI channels. This model scales x_k by $\|h\|$ to form $x_{h,k}$ so that $\mathcal{E}_{\boldsymbol{x}_h} = \mathcal{E}_{\boldsymbol{x}} \cdot \|h\|^2$. The additive noise is white Gaussian. The model accommodates correlated Gaussian noise through use of the previous subsection's noise-equivalent pulse response, as in Figure 3.7. The channel output $y_h(t)$ passes through a normalized matched filter $\varphi_h^*(-t)$ to generate $y(t)$. The receiver then samples $y(t)$ at the symbol rate and subsequently processes discrete time. The following theorem illustrates that symbol-rate sampling of the matched-filter output incurs no performance loss.

Theorem 3.1.1 [ISI-Channel Model Sufficiency] *Figure 3.9's discrete-time signal samples $y_k = y(kT)$ are sufficient to represent the continuous-time ISI-model channel output $y(t)$, if $0 < \|h\| < \infty$. (i.e., a receiver with the minimum P_e exists that uses only the samples y_k).*

Proof:
Define

$$\varphi_{h,k}(t) \triangleq \varphi_h(t - kT) \quad , \tag{3.20}$$

where $\{\varphi_{h,k}(t)\}_{k\in(-\infty,\infty)}$ is a linearly independent set of functions. The set $\{\varphi_{h,k}(t)\}_{k\in(-\infty,\infty)}$ is related to a set of orthogonal basis functions $\{\phi_{h,k}(t)\}_{k\in(-\infty,\infty)}$ by an invertible transformation Γ (use Gram-Schmidt an infinite number of times). The transformation and its inverse are written

$$\{\phi_{h,k}(t)\}_{k\in(-\infty,\infty)} = \Gamma(\{\varphi_{h,k}(t)\}_{k\in(-\infty,\infty)}) \tag{3.21}$$

$$\{\varphi_{p,k}(t)\}_{k\in(-\infty,\infty)} = \Gamma^{-1}(\{\phi_{h,k}(t)\}_{k\in(-\infty,\infty)}) \quad , \tag{3.22}$$

where Γ is the invertible transformation. In Figure 3.10, the transformation outputs are the filter samples $y(kT)$. The infinite set of filters $\{\phi_{h,k}^*(-t)\}_{k\in(-\infty,\infty)}$ followed by Γ^{-1} is equivalent to an infinite set of matched filters to $\left\{\varphi_{h,k}^*(-t)\right\}_{k\in(-\infty,\infty)}$. By (3.20) this last set is equivalent to a single matched filter $\varphi_h^*(-t)$, whose output is sampled at $t = kT$ to produce $y(kT)$. Since the set $\{\phi_{h,k}(t)\}_{k\in(-\infty,\infty)}$ is orthonormal, the set of sampled filter outputs in Figure 3.10 are sufficient to represent $y_h(t)$. Since Γ^{-1} is invertible (inverse is Γ), then by Chapter 1's reversibility theorem, the sampled matched filter output $y(kT)$ is a sufficient representation of the ISI-channel output $y_h(t)$. **QED.**

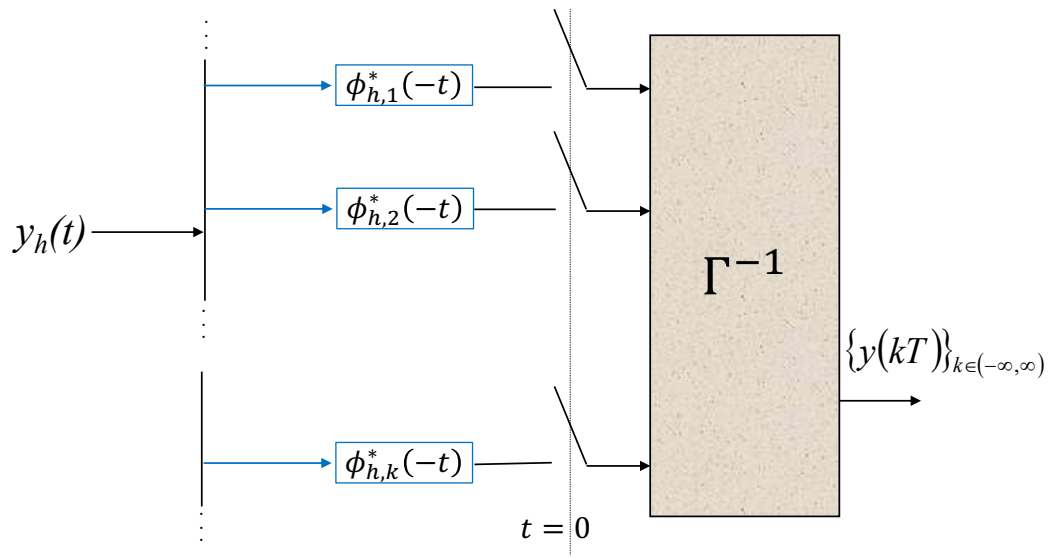

Figure 3.10: Equivalent diagram of ISI-channel model matched-filter/sampler

Referring again to Figure 3.9,

$$y(t) = \sum_k \|h\| \cdot x_k \cdot q(t - kT) + n_h(t) * \varphi_h^*(-t) \quad , \tag{3.23}$$

where

$$q(t) \triangleq \varphi_h(t) * \varphi_h^*(-t) = \frac{h(t) * h^*(-t)}{\|h\|^2} \quad . \tag{3.24}$$

The deterministic autocorrelation function $q(t)$ is Hermitian ($q^*(-t) = q(t)$). Also, $q(0) = 1$, so the symbol x_k passes at time kT to the output with amplitude scaling $\|h\|$. The function $q(t)$ can also exhibit ISI, as Figure 3.11 shows. The plotted $q(t)$ corresponds to $q_k = [-.1159\ .2029\ 1\ .2029\ -.1159]$ or, equivalently, to the pulse responsel $h(t) = \sqrt{\frac{1}{T}} \cdot (\text{sinc}(t/T) + .25 \cdot \text{sinc}((t-T)/T) - .125 \cdot \text{sinc}((t-2T)/T))$, or $H(D) = \frac{1}{\sqrt{T}} \cdot (1 + .5D)(1 - .25D)$ (Appendix D defines the notation $H(D)$). (The values for q_k can be confirmed by convolving $h(t)$ with its time reverse, normalizing, and sampling.) For notational brevity, let $y_k \triangleq y(kT)$, $q_k \triangleq q(kT)$, $n_k \triangleq n(kT)$ where $n(t) \triangleq n_h(t) * \varphi_h^*(-t)$. Thus

$$y_k = \underbrace{\|h\| \cdot x_k}_{\text{scaled input (desired)}} + \underbrace{n_k}_{\text{noise}} + \underbrace{\|h\| \cdot \sum_{m \neq k} x_m \cdot q_{k-m}}_{\text{ISI}} \quad . \tag{3.25}$$

The output y_k consists of the scaled input, noise, and ISI. The scaled input is the desired information-bearing signal. The ISI and noise are signals that distort the transmitted information. The ISI represents a new distortion component for the suboptimum SBS detector. This SBS detector is the same detector as in Chapters 1 and 2, except used under the (false) assumption that the ISI is just additional AWGN. Such a receiver can be decidedly suboptimum when the ISI is nonzero.

Using D-transform notation, (3.25) becomes

$$Y(D) = X(D) \cdot \|h\| \cdot Q(D) + N(D) \tag{3.26}$$

where $Y(D) \triangleq \sum_{k=-\infty}^{\infty} y_k \cdot D^k$. If the receiver uses symbol-by-symbol detection on the sampled output y_k, then the noise sample n_k of (one-dimensional) variance $\frac{\mathcal{N}_0}{2}$ at the matched-filter output combines with ISI from the sample times mT ($m \neq k$) in corrupting $\|h\| \cdot x_k$.

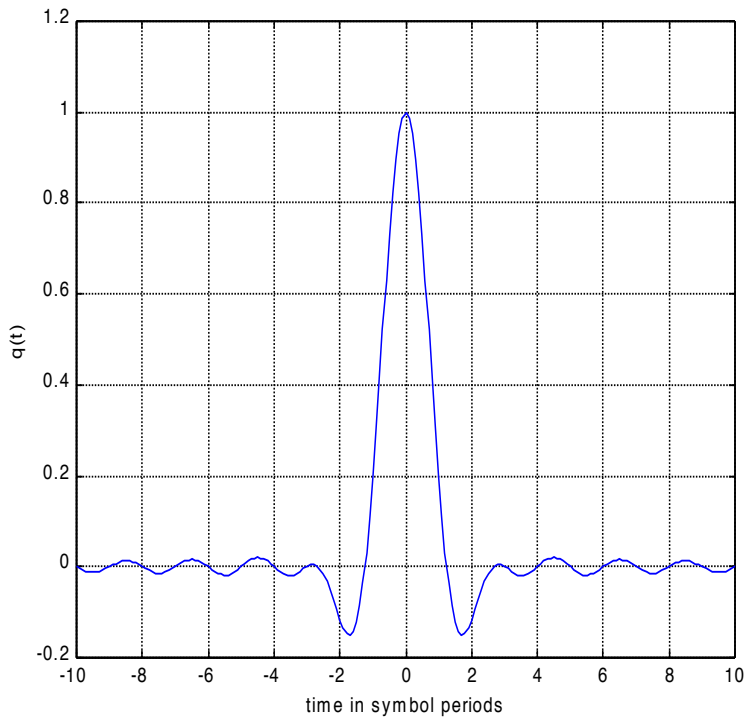

Figure 3.11: ISI in $q(t)$

ISI Distortion Measures: There are two common ISI distortion measures: The first is **Peak Distortion**, which only has meaning for real-valued $q(t)$: [4]

Definition 3.1.2 [Peak Distortion Criterion] *If $|x_{max}|$ is the maximum value for $|x_k|$, then the peak distortion is:*

$$\mathcal{D}_p \triangleq |x|_{max} \cdot \|h\| \cdot \sum_{m \neq 0} |q_m| \quad . \tag{3.27}$$

For $q(t)$ in Figure 3.11 with $x_{max} = 3$, $\mathcal{D}_p = 3 \cdot \|h\| \cdot (.1159 + .2029 + .2029 + .1159) \approx 3 \cdot \sqrt{1.078} \cdot .6376 \approx 2.0$.

The peak distortion represents a worst-case loss in minimum distance between constellation symbol values x_k, or equivalently

$$P_e \leq N_e \cdot Q \left[\frac{\|h\| \cdot \frac{d_{\min}}{2} - \mathcal{D}_p}{\sigma} \right] \quad , \tag{3.28}$$

for SBS detection. An example considers two matched-filter outputs y_k and y'_k that the receiver attempts to distinguish by suboptimally using SBS detection. These outputs arise from two different input-symbol sequences $\{x_k\}$ and $\{x'_k\}$. Without loss of generality, assume $y_k > y'_k$, and consider the difference

$$y_k - y'_k = \|h\| \cdot \left[(x_k - x'_k) + \sum_{m \neq k} (x_m - x'_m) \cdot q_{k-m} \right] + \tilde{n} \tag{3.29}$$

[4] In the real case, the magnitudes correspond to actual values. However, for complex-valued terms, the ISI is characterized by both its magnitude and phase. So, addition of the magnitudes of the symbols ignores the phase components, which may significantly change the ISI term.

The summation term inside the brackets in (3.29) represents the change in distance between y_k and y'_k caused by ISI. Without ISI, this distance is

$$y_k - y'_k \geq \|h\| \cdot d_{min} \quad , \tag{3.30}$$

while with ISI the distance can decrease to

$$y_k - y'_k \geq \|h\| \cdot \left[d_{min} - 2 \cdot |x|_{max} \cdot \sum_{m \neq 0} |q_m| \right] \quad . \tag{3.31}$$

Implicitly, the distance interpretation in (3.31) assumes $2 \cdot \mathcal{D}_p \leq \|h\| \cdot d_{\min}$.[5]

While peak distortion represents the worst-case ISI, this worst case might not occur very often in practice. For instance, with an input alphabet size $M = 4$ and a $q(t)$ that spans 15 symbol periods, worst-case value's probability of occurrence (worst level occurring in all 14 ISI contributors) is $4^{-14} = 3.7 \times 10^{-9}$, well below typical P_e's in data transmission. Nevertheless, there may be other ISI patterns of nearly just as bad interference that can also occur. Rather than separately compute each possible combination's reduction of minimum distance, its probability of occurrence, and the resulting error probability, data transmission engineers more often use the ISI measure **Mean-Square Distortion** (valid for 1 or 2 dimensions):

Definition 3.1.3 [Mean-Square Distortion] *The* **Mean-Square Distortion** *is:*

$$\mathcal{D}_{ms} \triangleq \mathbb{E}\left\{ |\sum_{m \neq k} x_{p,m} \cdot q_{k-m}|^2 \right\} \tag{3.32}$$

$$= \mathcal{E}_{\boldsymbol{x}} \cdot \|h\|^2 \cdot \sum_{m \neq 0} |q_m|^2 \quad , \tag{3.33}$$

where (3.33) is valid when the successive data symbols are independent and identically distributed with zero mean.

In Figure 3.11's example, the mean-square distortion (with $\mathcal{E}_{\boldsymbol{x}} = 5$) is $\mathcal{D}_{ms} = 5 \cdot \|h\|^2 \cdot (.1159^2 + .2029^2 + .2029^2 + .1159^2) \approx 5(1.078).109 \approx .588$. The fact $\sqrt{.588} = .767 < 1.99$ illustrates that $\mathcal{D}_{ms} \leq \mathcal{D}_p^2$. (The reader can easily prove this fact.)

The mean-square distortion criterion assumes (erroneously[6]) that $\mathcal{D}_{ms}$ is the variance of an uncorrelated Gaussian noise that adds to n_k. With this assumption, P_e is approximated by

$$P_e \approx N_e \cdot Q\left[\frac{\|h\| \cdot d_{\min}}{2\sqrt{\sigma^2 + \bar{\mathcal{D}}_{ms}}} \right] \quad . \tag{3.34}$$

Figures 3.12 and 3.13 visualize ISI through the "eye diagrams". The eye diagram is similar to what would be observed on an oscilloscope, when the trigger is synchronized to the symbol rate. The eye diagram overlays several successive symbol intervals of the modulated and filtered continuous-time waveform (except Figures 3.12 and 3.13 do not include noise). Both plots use the Lorentzian pulse response $h(t) = 1/(1 + (3t/T)^2)$. For binary transmission on this channel, there is a significant eye opening in the plot's center of Figure 3.12. With 4-level PAM transmission, the eye openings are much smaller, leading to less noise immunity. The ISI causes the spread among the path traces; more ISI results in a narrower eye opening. Clearly increasing M reduces the eye opening.

[5] On channels for which $2 \cdot \mathcal{D}_p \geq \|h\| \cdot d_{\min}$, the worst-case ISI occurs when $|2 \cdot \mathcal{D}_p - \|h\| \cdot d_{\min}|$ is maximum.

[6] This assumption is only true when x_k is Gaussian. In Chapter 2's very well-designed data transmission systems with zero gap, x_k is approximately i.i.d. and Gaussian, so that this approximation of Gaussian ISI becomes accurate.

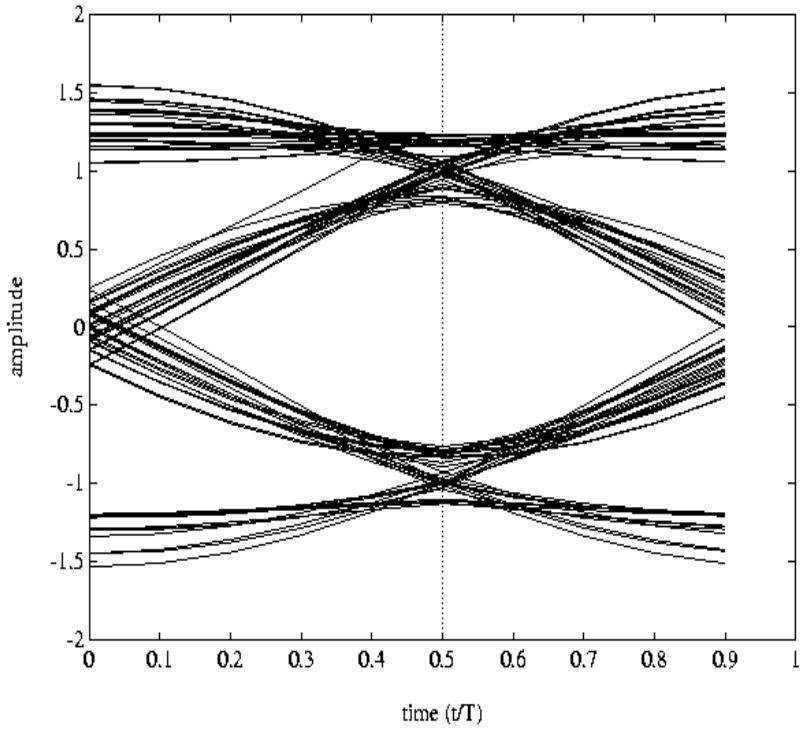

Figure 3.12: Binary eye diagram for a Lorentzian pulse response.

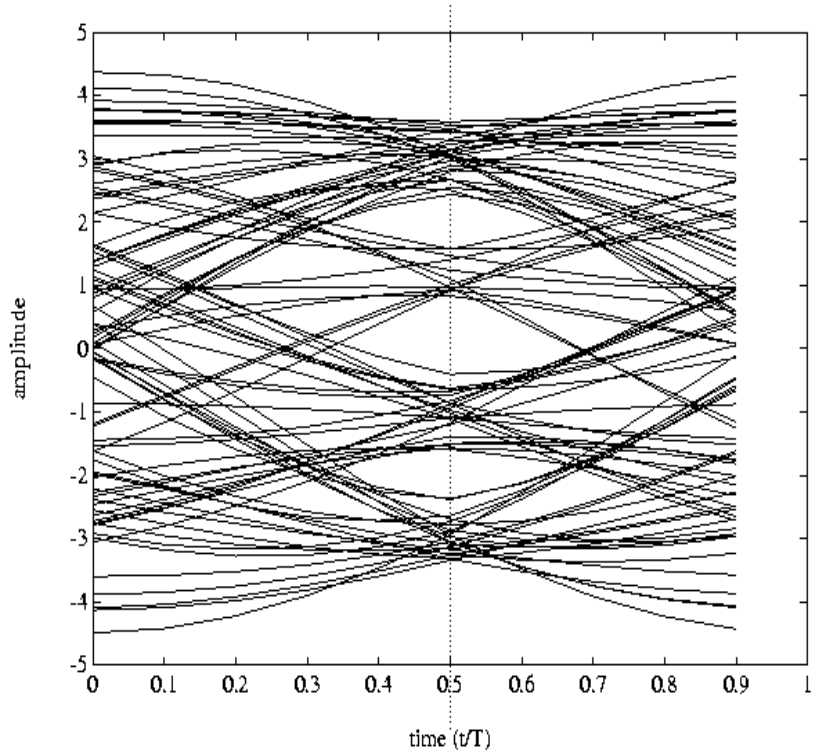

Figure 3.13: 4-Level eye diagram for a Lorentzian pulse response.

3.2 Basics of the Receiver-generated Equivalent AWGN

Figure 3.14 focuses upon the receiver and specifically the device shown generally as R. When channels have ISI, R processes the sampler output. This receiver R converts the channel into an equivalent AWGN channel approximation that also appears below the dashed line. This SBS detection approach views any deviation between the receiver output z_k and the channel input symbol x_k as additive white Gaussian noise. SBS analysis uses the Subsection 3.2.1's SNR_R to evaluate the performance of the detector that follows the receiver R. Usually, smaller deviation from the transmitted symbol means better performance, although not exactly so as Subsection 3.2.2 discusses.

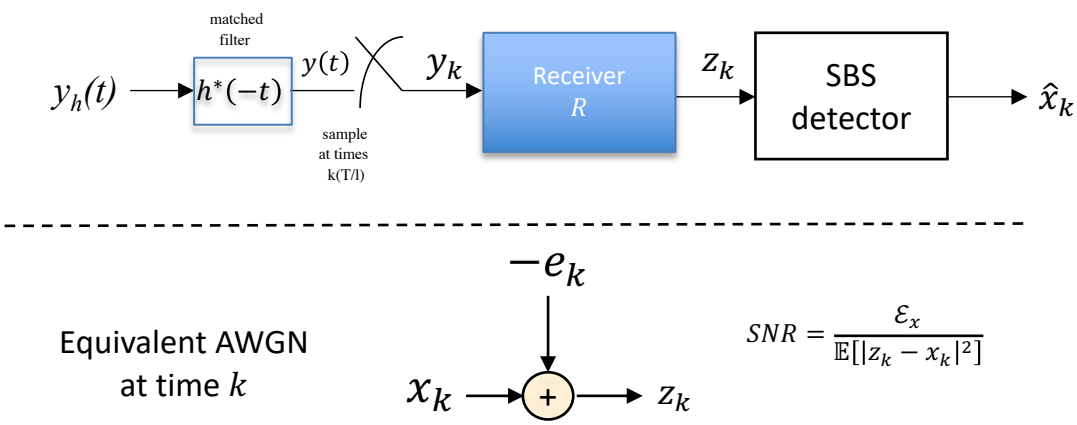

Figure 3.14: Use of possibly suboptimal receiver to approximate/create an equivalent AWGN.

Subsection 3.2.3 finishes this section with a discussion of the highest possible SNR that a designer could expect for any filtered AWGN channel, the so-called "matched-filter-bound" SNR, SNR_{MFB}. This section shall not be specific as to the content of the box shown as R, but later sections will allow both linear and slightly nonlinear structures that may often be good choices because their performance can be close to SNR_{MFB}.

3.2.1 Receiver Signal-to-Noise Ratio

Definition 3.2.1 [Receiver SNR] *The* **receiver SNR**, SNR_R *for any receiver* R *with (pre-decision) output* z_k*, and decision regions based on* x_k *(see Figure 3.14) is*

$$SNR_R \triangleq \frac{\mathcal{E}_{\boldsymbol{x}}}{E|e_k|^2} \quad , \tag{3.35}$$

where $e_k \triangleq x_k - z_k$ *is the* **receiver error**. *The denominator of (3.35) is the* **mean-square error**[7], *MSE=*$\mathbb{E}\left[|e_k|^2\right]$ *that is the same as the mean-square distortion. When* $\mathbb{E}\left[z_k|x_k\right] = x_k$*, the receiver is* **unbiased** *(otherwise* **biased***) with respect to the decision regions for* x_k*.*

Receiver SNR use will facilitate data-transmission performance evaluation of various ISI-compensation methods (i.e. equalizers). The performance measure SNR_R uses MSE or mean-square distortion, that is SNR_R jointly considers both noise and ISI in a single measure. The two right-most terms in (3.25) have normalized mean-square value $\sigma^2 + \bar{\mathcal{D}}_{ms}$, which equal the MSE. The SNR for Figure 3.14's matched

filter output y_k is the ratio of channel output sample energy $\bar{\mathcal{E}}_{\boldsymbol{x}} \cdot \|h\|^2$ to the MSE. This SNR_R often relateds directly to error probability and is a function of both the receiver and SBS-detector decision regions. This text uses SNR consistently, replacing error probability P_e as a measure of comparative performance. SNR is easier to compute than P_e, independent of M at constant $\bar{\mathcal{E}}_{\boldsymbol{x}}$, and a generally good performance measure: higher SNR means lower error probability. P_e is difficult to compute exactly because the distribution of the ISI-plus-noise is not known or is difficult to compute. This text assumes that the insertion of the appropriately scaled SNR (see Chapter 1 - Sections 1.4 - 1.6)) into the Q-function argument approximates the SBS detector's P_e. Even when this insertion into the Q-function is not sufficiently accurate, SNR_R comparison for different receivers R usually indicates which receiver is better.

3.2.2 Receiver Biases

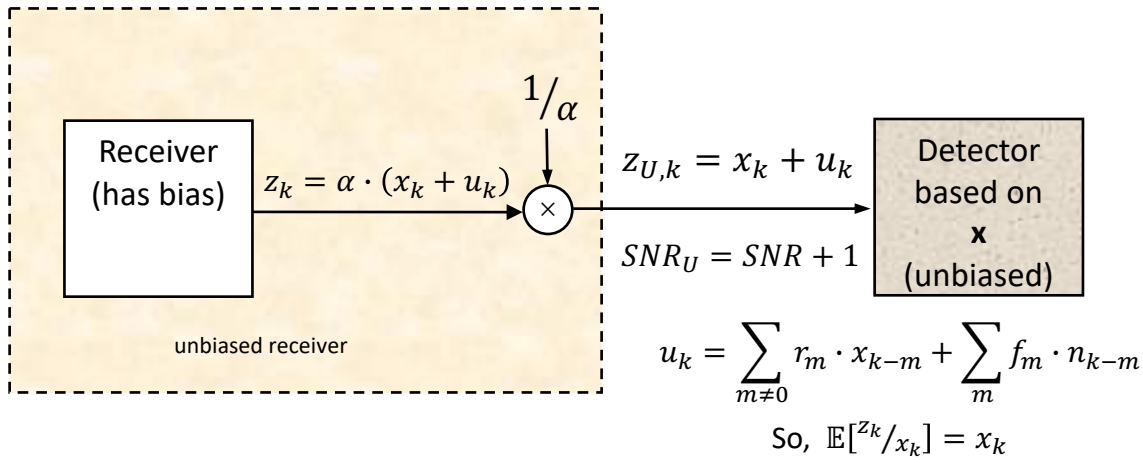

Figure 3.15: Receiver SNR concept.

Figure 3.15 illustrates a receiver that scales the error, that is the sum of ISI and noise. Any time-invariant linear receiver's output samples, z_k, satisfy

$$z_k = \alpha \cdot (x_k + u_k) \tag{3.36}$$

where α is some positive scale factor that the receiver introduces and u_k is distortion uncorrelated with x_k, $\mathbb{E}[x_k \cdot u_k^*] = 0$, so

$$u_k = \sum_{m \neq 0} r_m \cdot x_{k-m} + \sum_m f_m \cdot n_{k-m} \quad . \tag{3.37}$$

The residual ISI coefficients r_m and the filtered-noise coefficients f_k depend on the receiver and generally determine the MSE. The uncorrelated distortion has no remnant of x_k at the SBS detector input, so that $\mathbb{E}[u_k/x_k] = 0$. However, the receiver strategy may find that scaling (reducing) the x_k component in z_k by α improves SNR (small signal loss in exchange for larger uncorrelated distortion reduction). When $\mathbb{E}[z_k/x_k] = \alpha \cdot x_k \neq x_k$, the decision regions in the SBS detector are "biased." The receiver may easily remove any biasindexbias through multiplication by $1/\alpha$,as also in Figure 3.15. If the error is Gaussian noise, as is the assumption with the SBS detector, then bias removal by $1/\alpha$ scaling improves the SBS detector's error probability as in Chapter 1. (Even when the noise is not Gaussian as is the non-ideal-code case with the ISI component, scaling the signal correctly improves the average error probability if the input constellation has zero mean.)

The following theorem relates the SNR's of the unbiased and biased decision rules for any receiver R:

Theorem 3.2.1 **[Unconstrained and Unbiased Receivers]** *Given an unbiased receiver R for a decision rule based on a signal constellation corresponding to x_k, the maximum unconstrained SNR corresponding to that same receiver with any biased decision rule is*

$$SNR_R = SNR_{R,U} + 1 \quad , \tag{3.38}$$

where $SNR_{R,U}$ is the SNR using the unbiased decision rule.

Proof: From Figure 3.15, the SNR after scaling is easily

$$SNR_{R,U} = \frac{\bar{\mathcal{E}}_{\boldsymbol{x}}}{\bar{\sigma}_u^2} \quad . \tag{3.39}$$

The maximum SNR for the biased signal z_k prior to the scaling occurs when α is chosen to maximize the unconstrained SNR

$$SNR_R = \frac{\mathcal{E}_{\boldsymbol{x}}}{|\alpha|^2 \cdot \sigma_u^2 + |1-\alpha|^2 \cdot \mathcal{E}_{\boldsymbol{x}}} \quad . \tag{3.40}$$

Allowing for complex α with phase θ and magnitude $|\alpha|$, the SNR maximization over alpha is equivalent to minimizing

$$1 - 2|\alpha| \cdot cos(\theta) + |\alpha|^2 \cdot (1 + \frac{1}{SNR_{R,U}}) \quad . \tag{3.41}$$

Clearly $\theta = 0$ for a minimum and differentiating with respect to $|\alpha|$ yields $-2 + 2|\alpha| \cdot (1 + \frac{1}{SNR_{R,U}}) = 0$ or $\alpha_{opt} = 1/(1 + (SNR_{R,U})^{-1})$. Substitution of this value into the expression for SNR_R finds

$$SNR_R = SNR_{R,U} + 1 \quad . \tag{3.42}$$

Thus, a receiver R and a corresponding SBS detector that has zero bias will not correspond to a maximum SNR – the SNR can be improved by scaling (reducing) the receiver output by α_{opt}. Conversely, a receiver designed for maximum SNR can be altered slightly through simple output scaling by $1/\alpha_{opt}$ to a related receiver that has no bias and has SNR thereby reduced to $SNR_{R,U} = SNR_R - 1$. **QED**.

To illustrate the relationship of unbiased and biased receiver SNRs, suppose an ISI-free AWGN channel has an SNR=10 with $\mathcal{E}_{\boldsymbol{x}} = 1$ and $\sigma_u^2 = \frac{\mathcal{N}_0}{2} = .1$. Then, a receiver could scale the channel output by $\alpha = 10/11$. The resultant new error signal is $e_k = x_k \cdot (1 - \frac{10}{11}) - \frac{10}{11} n_k$, which has MSE=$\mathbb{E}[|e_k|^2] = \frac{1}{121} + \frac{100}{121}(.1) = \frac{1}{11}$, and SNR=11. Clearly, the biased SNR is equal to the unbiased SNR plus 1. The scaling has done nothing to improve the system, and the appearance of an improved SNR is an artifact of the SNR definition, which allows noise to reduced without accounting for the simultaneous signal-energy reduction. Removing the bias corresponds to using the actual signal energy, and the corresponding performance-characterizing SNR can always be found by subtracting 1 from the biased SNR. A natural question is then "Why compute the biased SNR?" The answer is that the biased receiver corresponds directly to minimizing the mean-square distortion, and the SNR for the "MMSE" case is often easier to compute. Figure 3.15 illustrates the usual situation that removes bias and consequently reduces SNR, but does change P_e because the SBS detector that minimizes P_e would otherwise simply scale its decision regions to match the effectively scaled input message $\alpha \cdot x_k$. The design should remove the receiver bias when minimizing mean-square error by simple scaling. The result is a more accurate SNR that subtracts 1 from the more easily computed MMSE receiver. This concept facilitates equalizer performance calculation in later sections of this chapter, and is formalized in Theorem 3.2.2 below:

Theorem 3.2.2 **[Unbiased MMSE Receiver Theorem]** *Let $\mathcal{R}$ be any allowed class of receivers R producing outputs z_k, and let R_{opt} be the receiver that achieves the maximum signal-to-noise ratio $SNR(R_{opt})$ over all $R \in \mathcal{R}$ with an unconstrained decision rule. Then the receiver that achieves the maximum SNR with an unbiased decision rule is also R_{opt}, and*

$$\max_{R \in \mathcal{R}} SNR_{R,U} = SNR(R_{opt}) - 1. \tag{3.43}$$

Proof. From Theorem 3.2.1, for any $R \in \mathcal{R}$, the relation between the signal-to-noise ratios of unbiased and unconstrained decision rules is $SNR_{R,U} = SNR_R - 1$, so

$$\max_{R\in\mathcal{R}}[SNR_{R,U}] = \max_{R\in\mathcal{R}}[SNR_R] - 1 = SNR_{R_{opt}} - 1 \quad . \tag{3.44}$$

QED.

This theorem implies that the optimum unbiased receiver and the optimum biased receiver settings are identical except for any scaling to remove bias; only the SNR measures are different. For any SBS detector, $SNR_{R,U}$ is the SNR that corresponds to best P_e. The quantity $SNR_{R,U} + 1$ is artificially high because of the bias inherent in the general SNR definition.

3.2.3 The Matched-Filter Bound

The **Matched-Filter Bound (MFB)**, also called the "one-shot" bound, specifies an upper SNR limit on the performance of data transmission systems with ISI.

Lemma 3.2.1 [Matched-Filter Bound SNR] *The SNR_{MFB} is the SNR that characterizes the best achievable performance for a given pulse response $h(t)$ and energy (on an AWGN channel) if only one message is sent. This SNR is*

$$SNR_{MFB} = \frac{\bar{\mathcal{E}}_{\boldsymbol{x}} \cdot \|h\|^2}{\frac{\mathcal{N}_0}{2}} \tag{3.45}$$

MFB *denotes the square of the Q-function argument that arises in the equivalent "one-shot" channel analysis, which typically is a scalar times SNR_{MFB}.*

Proof: Given a channel with pulse response $h(t)$ and isolated input x_0, the maximum output sample of the matched filter is $\|h\| \cdot x_0$. The normalized average energy of this sample is $\bar{\mathcal{E}}_{\boldsymbol{x}} \cdot \|h\|^2$, while the corresponding noise sample energy is $\frac{\mathcal{N}_0}{2}$, $SNR_{MFB} = \frac{\bar{\mathcal{E}}_{\boldsymbol{x}}\|h\|^2}{\frac{\mathcal{N}_0}{2}}$. **QED**.

The SBS detector's error probability satisfies $P_e \geq N_e \cdot Q(\sqrt{\text{MFB}})$. When $\bar{\mathcal{E}}_{\boldsymbol{x}}$ equals $(d_{min}^2/4)/\kappa$, then MFB $= SNR_{MFB} \cdot \kappa$. In effect the MFB corresponds to no ISI by disallowing preceding or successive transmitted symbols. An optimum detector applies directly for this "one-shot" case. The performance is tacitly a function of the transmitter basis functions, implying performance is also a function of the symbol rate $1/T$. No other (for the same input constellation) receiver for continuous band-limited transmission could have better performance when x_k is an i.i.d. sequence, since the sequence must incur some ISI. Sections 3.11 - 3.12, as well as Chapters 4 and 5 consider the possibility of correlating the input sequence $\{x_k\}$ to improve SNR.

The following example illustrates MFB computation for several constellations:

EXAMPLE 3.2.1 [Binary PAM] For binary PAM,

$$x_h(t) = \sum_k x_k \cdot h(t - kT) \quad , \tag{3.46}$$

where $x_k = \pm\sqrt{\mathcal{E}_{\boldsymbol{x}}}$. The minimum distance at the matched-filter output is $\|h\| \cdot d_{\text{min}} = \|h\| \cdot d = 2 \cdot \|h\| \cdot \sqrt{\mathcal{E}_{\boldsymbol{x}}}$, so $\mathcal{E}_{\boldsymbol{x}} = \frac{d^2_{\text{min}}}{4}$ and $\kappa = 1$. Then,

$$\text{MFB} = SNR_{MFB} \quad . \tag{3.47}$$

Thus for a binary PAM channel, the MFB (in dB) is just the "channel-output" SNR, SNR_{MFB}. If the transmitter symbols x_k are equal to ± 1 ($\mathcal{E}_{\boldsymbol{x}} = 1$), then

$$\text{MFB} = \frac{\|h\|^2}{\sigma^2} \quad , \tag{3.48}$$

where, again, $\sigma^2 = \frac{\mathcal{N}_0}{2}$. The binary-PAM P_e is then bounded by

$$P_e \geq Q(\sqrt{SNR_{_{MFB}}}) \quad . \tag{3.49}$$

EXAMPLE 3.2.2 *[M-ary PAM]* For M-ary PAM, $x_k = \pm\frac{d}{2}, \pm\frac{3d}{2}, \ldots, \pm\frac{(M-1)d}{2}$ and

$$\frac{d}{2} = \sqrt{\frac{3 \cdot \mathcal{E}_{\boldsymbol{x}}}{M^2 - 1}} \quad , \tag{3.50}$$

so $\kappa = 3/(M^2 - 1)$. Thus,

$$\text{MFB} = \frac{3}{M^2 - 1} \cdot SNR_{_{MFB}} \quad , \tag{3.51}$$

for $M \geq 2$. If the transmitter symbols x_k are equal to $\pm 1, \pm 3, \ , \ldots, \pm(M-1)$, then

$$\text{MFB} = \frac{\|h\|^2}{\sigma^2} \quad . \tag{3.52}$$

Equation (3.52) is the same result as (3.48), which should be expected since the minimum distance is the same at the transmitter, and thus also at the channel output, for both (3.48) and (3.52). The M'ary-PAM P_e is then bounded by

$$P_e \geq 2 \cdot (1 - 1/M) \cdot Q(\sqrt{\frac{3 \cdot SNR_{_{MFB}}}{M^2 - 1}}) \quad . \tag{3.53}$$

EXAMPLE 3.2.3 **[QPSK]** For QPSK, $x_k = \pm\frac{d}{2} \pm \jmath\frac{d}{2}$, and $d = 2 \cdot \sqrt{\bar{\mathcal{E}}_{\boldsymbol{x}}}$, so $\kappa = 1$. Thus

$$\text{MFB} = SNR_{_{MFB}} \quad . \tag{3.54}$$

Thus, for a QPSK (or 4SQ QAM) channel, MFB (in dB) equals the channel output SNR. If the transmitter symbols x_k are $\pm 1 \pm \jmath$, then

$$\text{MFB} = \frac{\|h\|^2}{\sigma^2} \quad . \tag{3.55}$$

The best QPSK P_e is then approximated by

$$\bar{P}_e \approx Q(\sqrt{SNR_{_{MFB}}}) \quad . \tag{3.56}$$

EXAMPLE 3.2.4 **[M-ary QAM Square]** For M-ary QAM, $\Re\{x_k\} = \pm\frac{d}{2}, \pm\frac{3d}{2}, \ldots, \pm\frac{(\sqrt{M}-1)d}{2}$, $\Im\{x_k\} = \pm\frac{d}{2}, \pm\frac{3d}{2}, \ldots, \pm\frac{(\sqrt{M}-1)d}{2}$, (recall that $\Re$ and $\Im$ denote real and imaginary parts, respectively) and

$$\frac{d}{2} = \sqrt{\frac{3 \cdot \bar{\mathcal{E}}_{\boldsymbol{x}}}{M - 1}} \quad , \tag{3.57}$$

so $\kappa = 3/(M - 1)$. Thus

$$\text{MFB} = \frac{3}{M - 1} SNR_{_{MFB}} \quad , \tag{3.58}$$

for $M \geq 4$. If the real and imaginary components of the transmitter symbols x_k equal $\pm 1, \pm 3, \ , \ldots, \pm(\sqrt{M} - 1)$, then

$$\text{MFB} = \frac{\|h\|^2}{\sigma^2} \quad . \tag{3.59}$$

The best M'ary QAM P_e is then approximated by

$$\bar{P}_e \approx 2 \cdot (1 - 1/\sqrt{M}) \cdot Q(\sqrt{\frac{3 \cdot SNR_{_{MFB}}}{M - 1}}) \quad . \tag{3.60}$$

In general for square QAM constellations,

$$\text{MFB} = \frac{3}{4^{\bar{b}} - 1} \cdot SNR_{_{MFB}} \quad . \tag{3.61}$$

For the QAM Cross constellations,

$$\text{MFB} = \frac{\frac{2 \cdot \bar{\mathcal{E}}_{\boldsymbol{x}} \cdot \|h\|^2}{\frac{31}{48} \cdot M - \frac{2}{3}}}{\sigma^2} = \frac{96}{31 \cdot 4^{\bar{b}} - 32} \cdot SNR_{_{MFB}} \quad . \tag{3.62}$$

For later sections' suboptimum receivers, $SNR_U \leq SNR_{_{MFB}}$. As $SNR_U \rightarrow SNR_{_{MFB}}$, then the receiver performs increasingly well. It is not always possible to design a receiver that attains, nor even approaches, $SNR_{_{MFB}}$, even with infinite complexity, unless one allows co-design of the input symbols x_k in a channel-dependent way (see Sections 3.11 - 3.12 and Chapters 4 and 5). The loss with respect to matched filter bound for any receiver is $SNR_u / SNR_{_{MFB}} \leq 1$, in effect determining a signal-energy loss because successive transmissions interfere with one another – it may well be that the loss in signal power is an acceptable exchange for a higher data rate.

Use of Gap with ISI: The gap originally applied to noise increases or energy decreases. Clearly an energy increase relative to noise also increases the ISI, causing two offsetting effects: higher margin for more signal energy but lower margin for greater MSE (ISI). Fundamentally, the signal energy increase is a larger multiple than the MSE increase (for non-zero noise), so the application of a gap to the MSE is conservative, but almost universally accepted in practice. Thus, it's ok to apply the gap to SNR even with ISI present.

3.3 Nyquist Criterion

The Nyquist Criterion specifies the conditions on $q(t) = \varphi_h(t) * \varphi_h^*(-t)$ for an ISI-free channel, on which a symbol-by-symbol detector is optimal. This section first reviews some fundamental frequency-domain relationships between $q(t)$ and its samples $q_k = q(kT)$.

$$\begin{aligned} q(kT) &= \frac{1}{2\pi}\int_{-\infty}^{\infty} Q(\omega)\cdot e^{\jmath\omega kT}\cdot d\omega && (3.63)\\ &= \frac{1}{2\pi}\sum_{n=-\infty}^{\infty}\int_{\frac{(2n-1)\pi}{T}}^{\frac{(2n+1)\pi}{T}} Q(\omega)\cdot e^{\jmath\omega kT}\cdot d\omega && (3.64)\\ &= \frac{1}{2\pi}\sum_{n=-\infty}^{\infty}\int_{-\frac{\pi}{T}}^{\frac{\pi}{T}} Q(\omega+\frac{2\pi n}{T})\cdot e^{\jmath(\omega+\frac{2\pi n}{T})kT}\cdot d\omega && (3.65)\\ &= \frac{1}{2\pi}\int_{-\frac{\pi}{T}}^{\frac{\pi}{T}} Q_{eq}(\omega)\cdot e^{\jmath\omega kT}\cdot d\omega \quad , && (3.66)\end{aligned}$$

where $Q_{eq}(\omega)$, the **equivalent frequency response**, becomes

$$Q_{eq}(\omega) \triangleq \sum_{n=-\infty}^{\infty} Q(\omega+\frac{2\pi n}{T}) \quad . \tag{3.67}$$

The function $Q_{eq}(\omega)$ is periodic in ω with period $\frac{2\pi}{T}$. This function is also known as the **folded** or **aliased** spectrum of $Q(\omega)$ because the sampling process causes the frequency response outside of the fundamental interval $(-\frac{\pi}{T}, \frac{\pi}{T})$ to be added (i.e. "folded in"). Writing the Fourier Transform of the sequence q_k as $Q(e^{-\jmath\omega T}) = \sum_{k=-\infty}^{\infty} q_k e^{-\jmath\omega kT}$ leads to

$$\frac{1}{T}\cdot Q_{eq}(\omega) = Q(e^{-\jmath\omega T}) \triangleq \sum_{k=-\infty}^{\infty} q_k e^{-\jmath\omega kT} \quad , \tag{3.68}$$

a well-known digital-signal-processing relation between any waveform's sampled discrete-time and continuous-time representations:

Theorem 3.3.1 **[Nyquist's Criterion]** *A channel specified by pulse response $p(t)$ (and resulting in $q(t) = \frac{p(t)*p^*(-t)}{\|p\|^2}$) is ISI-free if and only if*

$$Q(e^{-\jmath\omega T}) = \frac{1}{T}\sum_{n=-\infty}^{\infty} Q(\omega+\frac{2\pi n}{T}) = 1 \quad . \tag{3.69}$$

Proof:
By definition the channel is ISI-free if and only if $q_k = 0$ for all $k \neq 0$ (recall $q_0 = 1$ by definition). The proof follows directly by substitution of $q_k = \delta_k$ into (3.68). **QED.**

Functions that satisfy (3.69) are called "Nyquist pulses." One function that satisfies Nyquist's Criterion is

$$q(t) = \text{sinc}\left(\frac{t}{T}\right) \quad , \tag{3.70}$$

which corresponds to normalized pulse response

$$\varphi_h(t) = \frac{1}{\sqrt{T}}\cdot\text{sinc}\left(\frac{t}{T}\right) \quad . \tag{3.71}$$

The function $q(kT) = \text{sinc}(k) = \delta_k$ satisfies Nyquist's ISI-free condition. One feature of $\text{sinc}(t/T)$ is that it has minimum bandwidth for no ISI.

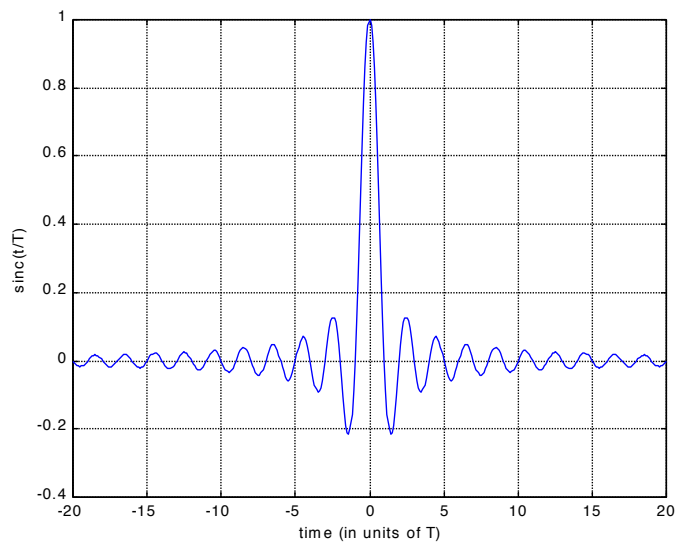

Figure 3.16: **The sinc(t/T) function.**

No other function has this same minimum bandwidth and also satisfies the Nyquist Criterion. (Proof is left as an exercise to the reader.) Figure 3.16 plots the $\text{sinc}(t/T)$ function for $-20T \leq t \leq 20T$.

The frequency $\frac{1}{2T}$ (1/2 the symbol rate) is often construed as the maximum frequency of a sampled signal that can be represented by samples at the sampling rate. In terms of positive-frequencies, $1/2T$ represents a minimum bandwidth necessary to satisfy the Nyquist Criterion, and thus has a special name in data transmission:

> **Definition 3.3.1 [Nyquist Frequency]** *The frequency* $\omega = \frac{\pi}{T}$ *or* $f = \frac{1}{2T}$ *is called the* **Nyquist frequency**.[8]

3.3.1 Vestigial Symmetry

In addition to the $\text{sinc}(t/T)$ Nyquist pulse, data-transmission engineers use transmit-filter responses with up to twice the minimum bandwidth. For the corresponding pulse responses, $Q(\omega) = 0$ for $|\omega| > \frac{2\pi}{T}$. These wider-bandwidth responses are less sensitive to sampling-time errors as follows: The $\text{sinc}(t/T)$ function decays in amplitude only linearly with time. Thus, any sampling-phase error in the sampling process of Figure 3.9 introduces residual ISI with amplitude that only decays linearly with time. In fact for $q(t) = \text{sinc}(t/T)$, the ISI term $\sum_{k \neq 0} q(\tau + kT)$ with a sampling timing error of $\tau \neq 0$ is not absolutely summable, resulting in infinite peak distortion. The time-domain-response envelope decays more rapidly if the frequency response is smooth (i.e. continuously differentiable). To meet this smoothness condition and also satisfy Nyquist's Criterion, the response must occupy a larger than minimum bandwidth that is between $1/2T$ and $1/T$. A $q(t)$ with higher bandwidth can exhibit significantly faster decay as $|t|$ increases, thus reducing sensitivity to timing phase errors. Designers also desire any bandwidth increase to be as small as possible, while still meeting other system requirements including acceptable sampling-time-error sensitivity. The **percent excess bandwidth**[9], or **percent roll-off**, is a measure of the extra bandwidth.

[8] This text distinguishes the Nyquist Frequency from the Nyquist Rate in sampling theory, where the latter is twice the highest frequency of a signal to be sampled and is not the same as the Nyquist Frequency here.

[9] The quantity α used here is not a bias factor, and similarly $Q(\cdot)$ is a measure of ISI and not the integral of a unit-variance Gaussian function – uses should be clear to reasonable readers who'll understand that sometimes symbols are re-used in obviously different contexts.

Definition 3.3.2 **[Percent Excess Bandwidth]** *The* **percent excess bandwidth** α *follows from a strictly band-limited* $Q(\omega)$ *and is the highest frequency in* $Q(\omega)$ *for which there is nonzero energy transfer. That is*

$$Q(\omega) = \begin{cases} nonzero & |\omega| \leq (1+\alpha)\cdot\frac{\pi}{T} \\ 0 & |\omega| > (1+\alpha)\cdot\frac{\pi}{T} \end{cases} \quad . \tag{3.72}$$

Thus, if $\alpha = .15$ (a typical value), the pulse $q(t)$ is said to have "15% excess bandwidth." Usually, data transmission systems have $0 \leq \alpha \leq 1$. In this case in equation (3.69), only the terms $n = -1, 0, +1$ contribute to the folded spectrum and the Nyquist Criterion becomes

$$\begin{aligned} 1 &= Q(e^{-\jmath\omega T}) && (3.73) \\ &= \frac{1}{T}\left\{Q\left(\omega + \frac{2\pi}{T}\right) + Q(\omega) + Q\left(\omega - \frac{2\pi}{T}\right)\right\} \quad -\frac{\pi}{T} \leq \omega \leq \frac{\pi}{T} \quad . && (3.74) \end{aligned}$$

Further, recalling that $q(t) = \varphi_h(t) * \varphi_h^*(-t)$ is Hermitian and has the properties of an autocorrelation function, then $Q(\omega)$ is real and $Q(\omega) \geq 0$. For the region $0 \leq \omega \leq \frac{\pi}{T}$ (for real signals), (3.74) reduces to

$$\begin{aligned} 1 &= Q(e^{-\jmath\omega T}) && (3.75) \\ &= \frac{1}{T}\left\{Q(\omega) + Q\left(\omega - \frac{2\pi}{T}\right)\right\} \quad . && (3.76) \end{aligned}$$

For complex signals, the negative frequency region $(-\frac{\pi}{T} \leq \omega \leq 0)$ should also have

$$\begin{aligned} 1 &= Q(e^{-\jmath\omega T}) && (3.77) \\ &= \frac{1}{T}\left\{Q(\omega) + Q\left(\omega + \frac{2\pi}{T}\right)\right\} \quad . && (3.78) \end{aligned}$$

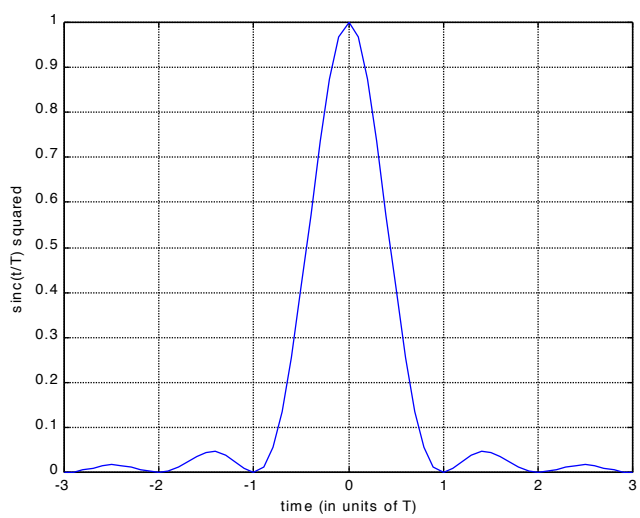

Figure 3.17: The $sinc^2(t/T)$ Function – time-domain

Any $Q(\omega)$ satisfying (3.76) (and (3.78) in the complex case) is vestigially symmetric with respect to the Nyquist Frequency. An example of a vestigially symmetric response with 100% excess bandwidth is $q(t) = \text{sinc}^2(t/T)$, which apperas in Figures 3.17 and 3.18.

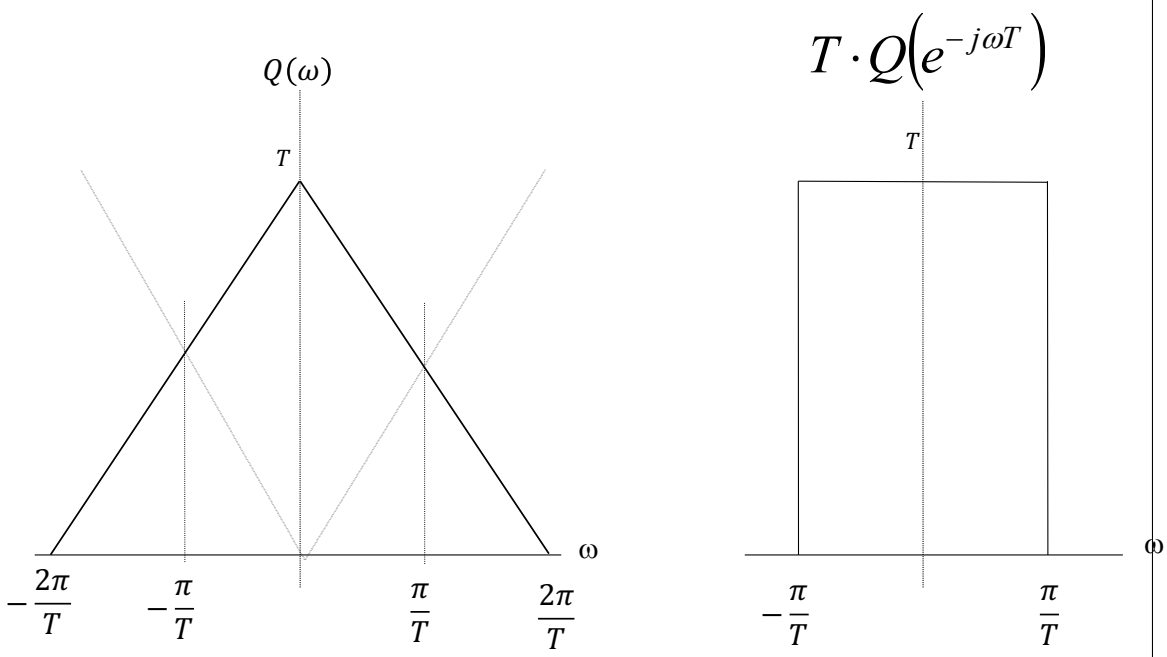

Figure 3.18: The $sinc^2(t/T)$ function – frequency-domain

3.3.2 Raised Cosine Pulses

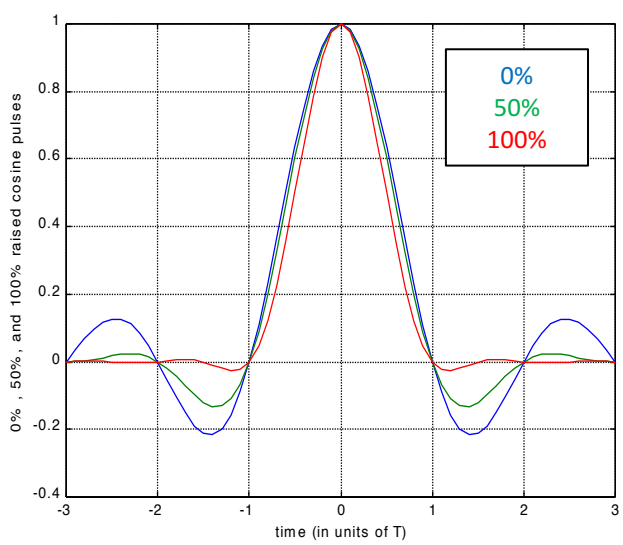

Figure 3.19: Raised cosine pulse shapes – time-domain

The most widely used set of functions that satisfy the Nyquist Criterion are the **raised-cosine** pulse shapes:

Definition 3.3.3 **[Raised-Cosine Pulse Shapes]** *The raised cosine family of pulse shapes (indexed by $0 \leq \alpha \leq 1$) is given by*

$$q(t) = sinc\left(\frac{t}{T}\right) \cdot \left[\frac{\cos\left(\frac{\alpha\pi t}{T}\right)}{1-\left(\frac{2\alpha t}{T}\right)^2}\right] \quad , \tag{3.79}$$

and have Fourier Transforms

$$Q(\omega) = \begin{cases} T & |\omega| \leq \frac{\pi}{T}\cdot(1-\alpha) \\ \frac{T}{2}\cdot\left[1-\sin\left(\frac{T}{2\alpha}\cdot\left\{|\omega|-\frac{\pi}{T}\right\}\right)\right] & \frac{\pi}{T}\cdot(1-\alpha) \leq |\omega| \leq \frac{\pi}{T}\cdot(1+\alpha) \\ 0 & \frac{\pi}{T}\cdot(1+\alpha) \leq |\omega| \end{cases} \quad . \tag{3.80}$$

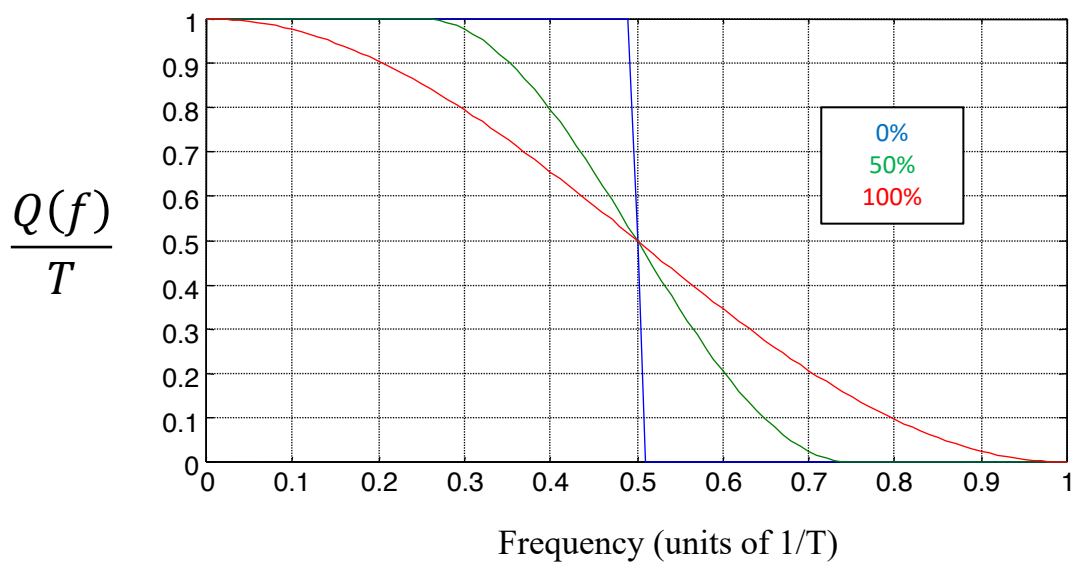

Figure 3.20: Raised Cosine Pulse Shapes – frequency-domain

The raised cosine pulse shapes are shown in Figure 3.19 (time-domain) and Figure 3.20 (frequency-domain) for $\alpha = 0, .5$, and 1. When $\alpha = 0$, the raised cosine reduces to a sinc function, which decays asymptotically as $\frac{1}{t}$ for $t \to \infty$, while for $\alpha \neq 0$, the function decays as $\frac{1}{t^3}$ for $t \to \infty$.

Raised Cosine Derivation: The raised-cosine's time-domain inverse transform

$$q_{RCR}(t) \triangleq \frac{1}{2\pi}\int_{-\infty}^{\infty} Q_{RCR}(\omega)\cdot e^{j\omega t}d\omega \quad .$$

Before inserting the expression for $Q_{RCR}(\omega)$, the inverse transform of this even function simplifies to

$$q_{RCR}(t) = \frac{1}{\pi}\int_{0}^{\infty} Q_{RCR}(\omega)\cdot\cos(\omega t)\,d\omega \quad ,$$

which separates into 2 integrals over successive positive frequency ranges with insertion of (3.80)

$$q_{RCR}(t) = \frac{1}{\pi}\int_{0}^{(1-\alpha)\pi/T} T\cdot\cos(\omega t)\,d\omega + \frac{1}{2\pi}\int_{(1-\alpha)\pi/T}^{(1+\alpha)\pi/T}\frac{T}{2}\cdot\left[1-\sin\left(\frac{T}{2\alpha}(\omega-\pi/T)\right)\right]\cdot\cos(\omega t)\cdot d\omega \quad . \tag{3.81}$$

Equation (3.81)'s first integral reduces to

$$q_{RCR,1}(t) = (1-\alpha)\cdot \mathrm{sinc}\left[\frac{(1-\alpha)t}{T}\right] \ , \tag{3.82}$$

Equation (3.82) also can be rewritten using $\sin(A-B) = \sin(A)\cdot\cos(B) - \cos(A)\sin(B)$ as

$$\begin{aligned} q_{RCR,1}(t) &= \frac{\sin\left[\frac{(1-\alpha)\pi t}{T}\right]}{\frac{pit}{T}} \\ &= \frac{1}{\frac{\pi t}{T}}\cdot\left[\sin\left(\frac{\pi t}{T}\right)\cdot\cos\left(\frac{\alpha\pi t}{T}\right) - \cos\left(\frac{\pi t}{T}\right)\cdot\sin\left(\frac{\alpha\pi t}{T}\right)\right] \\ &= \mathrm{sinc}\left(\frac{\pi t}{T}\right)\cdot\cos\left(\frac{\alpha\pi t}{T}\right) - \frac{\cos\left(\frac{\pi t}{T}\right)}{\frac{\pi t}{T}}\cdot\sin\left(\frac{\alpha\pi t}{T}\right) \ , \end{aligned}$$

which will be a convenient form later in this derviation.

The second integral in Equation (3.81) follows as the sum of two more integrals for the constant term (2a) and the sinusoidal term (2b) as

$$q_{RCR,2a}(t) = -\frac{T}{2\pi t}\left[\sin\left(\frac{(1+\alpha)\pi t}{T}\right) - \sin\left(\frac{(1-\alpha)\pi t}{T}\right)\right] \text{ and}$$

Using the formula $\cos(A)\sin(B) = \frac{1}{2}\left[\sin(A+B) - \sin(A-B)\right]$, then $q_{RCR,2a}(t)$ becomes:

$$q_{RCR,2a}(t) = \frac{\cos\left(\frac{\pi}{T}\right)}{\pi t/T}\cdot\sin\left(\frac{\alpha\pi t}{T}\right) \ .$$

It follows then that

$$q_{RCR,1}(t) + q_{RCR,2a}(t) = \mathrm{sinc}\left(\frac{\pi t}{T}\right)\cdot\cos\left(\frac{\alpha\pi t}{T}\right) \ .$$

$$q_{RCR,2b}(t) = -\frac{T}{2\pi t}\int_{(1-\alpha)\pi/T}^{(1+\alpha)\pi/T} \sin\left[\frac{T}{2\alpha}\left(\omega - \frac{\pi}{T}\right)\right]\cdot\cos(\omega t)\cdot d\omega \ .$$

Using the formula $\sin(A)\cos(B) = \frac{1}{2}\left[\sin(A+B) + \sin(A-B)\right]$, then $q_{RCR,2b}(t)$ becomes:

$$
\begin{aligned}
q_{RCR,2b}(t) &= -\frac{T}{4\pi}\int_{(1-\alpha)\pi/T}^{(1+\alpha)\pi/T}\left\{\sin\left[\frac{T}{2\alpha}(\omega-\pi/T)+\omega t\right]+\sin\left[\frac{T}{2\alpha}(\omega-\pi/T)-\omega t\right]\right\}\cdot d\omega \\
&= -\frac{T}{4\pi}\int_{(1-\alpha)\pi/T}^{(1+\alpha)\pi/T}\left\{\sin\left[\omega\left(\frac{T}{2\alpha}+t\right)-\frac{\pi}{2\alpha}\right]+\sin\left[\omega\left(\frac{T}{2\alpha}-t\right)-\frac{\pi}{2\alpha}\right]\right\}\cdot d\omega \\
&= \frac{T}{4\pi}\left\{\frac{1}{\frac{T}{2\alpha}+t}\cos\left[\frac{(1+\alpha)\pi}{T}\left(\frac{T}{2\alpha}+t\right)-\frac{\pi}{2\alpha}\right]-\frac{1}{\frac{T}{2\alpha}+t}\cos\left[\frac{(1-\alpha)\pi}{T}\left(\frac{T}{2\alpha}+t\right)-\frac{\pi}{2\alpha}\right]\right. \\
&\quad \left.+\frac{1}{\frac{T}{2\alpha}-t}\cos\left[\frac{(1+\alpha)\pi}{T}\left(\frac{T}{2\alpha}-t\right)-\frac{\pi}{2\alpha}\right]-\frac{1}{\frac{T}{2\alpha}-t}\cos\left[\frac{(1-\alpha)\pi}{T}\left(\frac{T}{2\alpha}-t\right)-\frac{\pi}{2\alpha}\right]\right\} \\
&= \frac{T}{4\pi}\left\{-\frac{1}{\frac{T}{2\alpha}+t}\sin\left[\frac{(1+\alpha)\pi t}{T}\right]-\frac{1}{\frac{T}{2\alpha}+t}\sin\left[\frac{(1-\alpha)\pi t}{T}\right]\right. \\
&\quad \left.+\frac{1}{\frac{T}{2\alpha}-t}\sin\left[\frac{(1+\alpha)\pi t}{T}\right]+\frac{1}{\frac{T}{2\alpha}-t}\sin\left[\frac{(1-\alpha)\pi t}{T}\right]\right\} \\
&= \frac{T}{2\pi}\left\{-\frac{1}{\frac{T}{2\alpha}+t}\sin\left(\frac{\pi t}{T}\right)\cdot\cos\left(\frac{\alpha\pi t}{T}\right)+\frac{1}{\frac{T}{2\alpha}-t}\sin\left(\frac{\pi t}{T}\right)\cdot\cos\left(\frac{\alpha\pi t}{T}\right)\right\} \\
&= -\frac{T}{2\pi}\left\{-\frac{\frac{T}{2\alpha}-t-\frac{T}{2\alpha}-t}{\left(\frac{T}{2\alpha}\right)^2-t^2}\cdot\sin\left(\frac{\pi t}{T}\right)\cdot\cos\left(\frac{\alpha\pi t}{T}\right)\right\} \\
&= \frac{T}{2\pi}\left[\frac{8\alpha^2 t}{T^2-4\alpha^2t^2}\right]\cdot\sin\left(\frac{\pi t}{T}\right)\cdot\cos\left(\frac{\alpha\pi t}{T}\right) \\
&= \frac{T}{\pi t}\left[\frac{4\alpha^2t^2}{1-4\alpha^2(t/T)^2}\right]\cdot\sin\left(\frac{\pi t}{T}\right)\cdot\cos\left(\frac{\alpha\pi t}{T}\right) \\
&= \left[\frac{4\alpha^2t^2}{1-4\alpha^2(t/T)^2}\right]\cdot\operatorname{sinc}\left(\frac{t}{T}\right)\cdot\cos\left(\frac{\alpha\pi t}{T}\right) \quad .
\end{aligned}
$$

Then, the sum is the RCR so

$$
\begin{aligned}
q_{RCR}(t) &= q_{RCR,1}(t)+q_{RCR,2a}(t)+q_{RCR,2b}(t) \\
&= \left[1+\frac{4\alpha^2t^2}{1-4\alpha^2(t/T)^2}\right]\cdot\operatorname{sinc}\left(\frac{t}{T}\right)\cdot\cos\left(\frac{\alpha\pi t}{T}\right) \\
&= \left[\frac{\operatorname{sinc}\left(\frac{t}{T}\right)\cdot\cos\left(\frac{\alpha\pi t}{T}\right)}{1-4\alpha^2(t/T)^2}\right] \\
&= \left[\frac{\operatorname{sinc}\left(\frac{t}{T}\right)\cdot\cos\left(\frac{\alpha\pi t}{T}\right)}{1-(\frac{2\alpha t}{T})^2}\right] \quad ,
\end{aligned}
$$

which is the desired result.

3.3.3 Square-Root Splitting of the Nyquist Pulse

This section describes an ISI-free transmission system that has transmit-and-channel filtering $\varphi_h(t)$ and receiver matched filter $\varphi_h^*(-t)$ such that $q(t)=\varphi_h(t)*\varphi_h^*(-t)$ or equivalently

$$\Phi_h(\omega)=Q^{1/2}(\omega) \tag{3.83}$$

so that the matched filter and transmit/channel filters are "square-roots" of the Nyquist pulse. When $h(t)=\delta(t)$ or equivalently $\varphi_h(t)=\varphi(t)$, the transmit filter (and the receiver matched filters) are

square-roots of a Nyquist pulse shape. Such square-root transmit filtering finds significant use even when $\varphi_h(t) \neq \varphi(t)$ and the pulse response is the convolution of $h(t)$ with the square-root filter.

The square-root form of raised-cosine pulse shapes then is

$$\sqrt{Q(\omega)} = \begin{cases} \sqrt{T} & |\omega| \leq \frac{\pi}{T} \cdot (1-\alpha) \\ \sqrt{\frac{T}{2}} \cdot \left[1 - \sin\left(\frac{T}{2\alpha} \cdot (|\omega| - \frac{\pi}{T})\right)\right]^{1/2} & \frac{\pi}{T} \cdot (1-\alpha) \leq |\omega| \leq \frac{\pi}{T} \cdot (1+\alpha) \\ 0 & \frac{\pi}{T} \cdot (1+\alpha) \leq |\omega| \end{cases} \quad . \tag{3.84}$$

This expression can be inverted to the time-domain via use of the identity $sin^2(\theta) = .5(1 - \cos(2\theta))$, as in the section below, to obtain

$$\varphi_h(t) = \frac{4\alpha}{\pi\sqrt{T}} \cdot \frac{\cos\left([1+\alpha]\frac{\pi t}{T}\right) + \frac{T \cdot \sin\left([1-\alpha]\frac{\pi t}{T}\right)}{4\alpha t}}{1 - \left(\frac{4\alpha t}{T}\right)^2} \quad . \tag{3.85}$$

Another simpler form for seeing the value at time 0 (which is $[1/\sqrt{T}] \cdot (1 - \alpha + 4\alpha/\pi)$) is

$$\varphi_h(t) = \frac{(1-\alpha)}{\sqrt{T}} \cdot \frac{\text{sinc}\left[\frac{(1-\alpha)t}{T}\right]}{\left[(1 - \frac{4\alpha t}{T})^2\right]} + \frac{4\alpha t \cdot \cos\left(\frac{(1+\alpha)\pi t}{T}\right)}{\sqrt{T}\pi t\left[(\frac{4\alpha t}{T})^2 - 1\right]} \quad . \tag{3.86}$$

However, Equation (3.85) seems best to see the limiting value at $t = \pm\frac{T}{4\alpha}$, where the denominator is readily seen as zero. However, the numerator is also zero if one recalls that $cos(x) = sin(\pi/2 - x)$. The value at these two times (through use of L'Hopital's rule) is

$$\varphi_{SR}(\pm\frac{T}{4\alpha}) = \frac{\alpha}{\sqrt{2T}}\left[\left(1 + \frac{2}{\pi}\right) \cdot \sin\left(\frac{\pi}{4\alpha}\right) + \left(1 - \frac{2}{\pi}\right) \cdot \cos\left(\frac{\pi}{4\alpha}\right)\right] \quad . \tag{3.87}$$

The reader is reminded that the square-root of a Nyquist-satisfying pulse shape does not need to be Nyquist by itself, only in combination with its matched square-root filter. Thus, this square-root raised-cosine pulse is not zero at integer sampling instants.

Square-Root Raised Cosine Derviation: The square-root of a raised-cosine function has inverse transform

$$\varphi_{SR}(t) \triangleq \frac{1}{2\pi}\int_{-\infty}^{\infty} \sqrt{Q_{RCR}(\omega)} \cdot e^{\jmath\omega t} \cdot d\omega \quad .$$

Before inserting the expression for $Q_{RCR}(\omega)$, the inverse transform of this even function simplifies to

$$\varphi_{SR}(t) \triangleq \frac{1}{\pi}\int_{0}^{\infty} \sqrt{Q_{RCR}(\omega)} \cdot \cos(\omega t) \cdot d\omega \quad ,$$

which (3.84)'s insertion separates into 2 integrals over successive positive frequency ranges:

$$\varphi_{SR}(t) = \frac{1}{\pi}\int_{0}^{(1-\alpha)\pi/T} \sqrt{T} \cdot \cos(\omega t) \cdot d\omega + \frac{1}{\pi}\int_{(1-\alpha)\pi/T}^{(1+\alpha)\pi/T} \sqrt{\frac{T}{2} \cdot \left[1 - \sin\left(\frac{T}{2\alpha}(\omega - \pi/T)\right)\right]} \cdot \cos(\omega t) \cdot d\omega \quad . \tag{3.88}$$

The first integral in Equation (3.88) easily is performed to obtain

$$\varphi_{SR,1}(t) = \frac{(1-\alpha)}{\sqrt{T}} \cdot \text{sinc}\left[\frac{(1-\alpha)t}{T}\right] \quad . \tag{3.89}$$

Using the half-angle formula $1 - \sin(x) = 1 - cos(x - \pi/2) = 2\sin^2\left(\frac{x}{2} - \frac{\pi}{4}\right)$, the 2nd integral in Equation (3.88) expands into integrable terms as

$$\begin{aligned} \varphi_{SR,2}(t) &= \frac{\sqrt{T}}{\pi}\int_{(1-\alpha)\pi/T}^{(1+\alpha)\pi/T} \sin\left(\frac{T}{4\alpha}\left[\omega - \frac{\pi}{T}\right] - \frac{\pi}{4}\right) \cdot \cos(\omega t) \cdot d\omega \\ &= \frac{\sqrt{T}}{\pi}\int_{(1-\alpha)\pi/T}^{(1+\alpha)\pi/T} \sin\left(\frac{T}{4\alpha}\left[\omega - \frac{\pi}{T} - \frac{\pi\alpha}{T}\right]\right) \cdot \cos(\omega t) \cdot d\omega \\ &= \frac{\sqrt{T}}{\pi}\int_{(1-\alpha)\pi/T}^{(1+\alpha)\pi/T} \sin\left(\frac{T}{4\alpha}\left[\omega - \frac{(1+\alpha)\pi}{T}\right]\right) \cdot \cos(\omega t) \cdot d\omega \quad . \end{aligned}$$

A basic trig formula is $\sin(A)\cdot\cos(B) = \frac{1}{2}\left[\sin(A+B)+\sin(A-B)\right]$, so

$$\begin{aligned}
\varphi_{SR,2}(t) &= \frac{\sqrt{T}}{2\pi}\int_{(1-\alpha)\pi/T}^{(1+\alpha)\pi/T}\left\{\sin\left(\frac{T}{4\alpha}\left[\omega-\frac{(1+\alpha)\pi}{T}\right]+\omega t\right)+\sin\left(\frac{T}{4\alpha}\left[\omega-\frac{(1+\alpha)\pi}{T}\right]-\omega t\right)\right\}\cdot d\omega \\
&= \frac{\sqrt{T}}{2\pi}\int_{(1-\alpha)\pi/T}^{(1+\alpha)\pi/T}\left\{\sin\left[\omega\left(t+\frac{T}{4\alpha}\right)-\frac{\pi(1+\alpha)}{4\alpha}\right]+\sin\left[\omega\left(\frac{T}{4\alpha}-t\right)-\frac{\pi(1+\alpha)}{4\alpha}\right]\right\}\cdot d\omega \\
&= \frac{\sqrt{T}}{2\pi}\left\{\frac{-4\alpha}{4\alpha t+T}\cos\left[\omega\left(t+\frac{T}{4\alpha}\right)-\frac{\pi(1+\alpha)}{4\alpha}\right]\Bigg|_{(1-\alpha)\pi/T}^{(1+\alpha)\pi/T}\right. \\
&\quad \left.+\frac{-4\alpha}{T-4\alpha t}\cos\left[\omega\left(\frac{T}{4\alpha}-t\right)-\frac{\pi(1+\alpha)}{4\alpha}\right]\Bigg|_{(1-\alpha)\pi/T}^{(1+\alpha)\pi/T}\right\} \\
&= \frac{-4\alpha\sqrt{T}}{2\pi(4\alpha t+T)}\left\{\cos\left[\frac{(1+\alpha)\pi}{T}(t+\frac{T}{4\alpha})-\frac{\pi}{4\alpha}(1+\alpha)\right]-\cos\left[\frac{(1-\alpha)\pi}{T}(t+\frac{T}{4\alpha})-\frac{\pi}{4\alpha}(1+\alpha)\right]\right\} \\
&\quad +\frac{-4\alpha\sqrt{T}}{2\pi(T-4\alpha t)}\left\{\cos\left[\frac{(1+\alpha)\pi}{T}(\frac{T}{4\alpha}-t)-\frac{\pi}{4\alpha}(1+\alpha)\right]-\cos\left[\frac{(1-\alpha)\pi}{T}(\frac{T}{4\alpha}-t)-\frac{\pi}{4\alpha}(1+\alpha)\right]\right\}
\end{aligned}$$

Continuing with algebra at this point:

$$\begin{aligned}
\varphi_{SR,2}(t) &= \frac{-2\alpha\sqrt{T}}{\pi(4\alpha t+T)}\left\{\cos\left(\frac{(1+\alpha)\pi t}{T}\right)+\sin\left(\frac{(1-\alpha)\pi t}{T}\right)\right\} \\
&\quad +\frac{2\alpha\sqrt{T}}{\pi(T-4\alpha t)}\left\{\cos\left(\frac{(1+\alpha)\pi t}{T}\right)-\sin\left(\frac{(1-\alpha)\pi t}{T}\right)\right\} \\
&= \frac{2\alpha\sqrt{T}}{\pi}\left[\frac{-1}{4\alpha t+T}+\frac{1}{T-4\alpha t}\right]\cos\left(\frac{(1+\alpha)\pi t}{T}\right) \\
&\quad +\frac{2\alpha\sqrt{T}}{\pi}\left[\frac{1}{4\alpha t+T}+\frac{1}{T-4\alpha t}\right]\sin\left(\frac{(1-\alpha)\pi t}{T}\right) \\
&= \frac{2\alpha\sqrt{T}}{\pi}\left[\frac{2T}{(4\alpha t)^2-T^2}\right]\cos\left(\frac{(1+\alpha)\pi t}{T}\right) \\
&\quad +\frac{2\alpha\sqrt{T}}{\pi}\left[\frac{8\alpha t}{(4\alpha t)^2-T^2}\right]\sin\left(\frac{(1-\alpha)\pi t}{T}\right) \\
&= \frac{4\alpha t\cdot\cos\left(\frac{(1+\alpha)\pi t}{T}\right)}{\sqrt{T}\pi t\left[(\frac{4\alpha t}{T})^2-1\right]}+\frac{16\alpha^2t^2\sqrt{T}\cdot\sin\left(\frac{(1-\alpha)\pi t}{T}\right)}{T^2\pi t\left[(\frac{4\alpha t}{T})^2-1\right]} \\
&= \frac{4\alpha t\cdot\cos\left(\frac{(1+\alpha)\pi t}{T}\right)}{\sqrt{T}\pi t\left[(\frac{4\alpha t}{T})^2-1\right]}+\frac{16\alpha^2t^2/T^2\cdot\mathrm{sinc}\left(\frac{(1-\alpha)t}{T}\right)}{\left[(\frac{4\alpha t}{T})^2-1\right]} \quad .
\end{aligned}$$

Addition of the first term from Equation (3.88) produces

$$\varphi_{SR}(t)=\frac{(1-\alpha)}{\sqrt{T}}\cdot\mathrm{sinc}\left[\frac{(1-\alpha)t}{T}\right]+\frac{4\alpha t\cdot\cos\left(\frac{(1+\alpha)\pi t}{T}\right)}{\sqrt{T}\pi t\left[(\frac{4\alpha t}{T})^2-1\right]}+\frac{16\alpha^2t^2/T^2\cdot\mathrm{sinc}\left(\frac{(1-\alpha)t}{T}\right)}{\left[(\frac{4\alpha t}{T})^2-1\right]} \quad .$$

Combining the sinc terms provides one convenient form of the square-root raised cosine of

$$\varphi_{SR}(t)=\frac{(1-\alpha)}{\sqrt{T}}\cdot\frac{\mathrm{sinc}\left[\frac{(1-\alpha)t}{T}\right]}{\left[(1-\frac{4\alpha t}{T})^2\right]}+\frac{4\alpha t\cdot\cos\left(\frac{(1+\alpha)\pi t}{T}\right)}{\sqrt{T}\pi t\left[(\frac{4\alpha t}{T})^2-1\right]} \quad ,$$

from which limiting results like $\varphi_{SR}(0)=1/\sqrt{T}$ follow easily. The preferred form for most engineering

texts follows by combining the two fractional terms and simplifying.

$$\varphi_{SR}(t) = \varphi_h(t) = \frac{4\alpha}{\pi\sqrt{T}} \cdot \frac{\cos\left([1+\alpha]\frac{\pi t}{T}\right) + \frac{T\cdot\sin\left([1-\alpha]\frac{\pi t}{T}\right)}{4\alpha t}}{1-\left(\frac{4\alpha t}{T}\right)^2} \quad .$$

3.4 Linear Zero-Forcing Equalization

This section examines the **Zero-Forcing Equalizer** (ZFE), which is the easiest equalizer to analyze and understand, but has inferior performance to some other equalizers to be introduced in later sections. Figure 3.9's ISI model helps describe the ZFE.

The ZFE sets R equal to a linear time-invariant filter with discrete impulse response w_k that acts on y_k to produce z_k, which is an estimate of x_k. Ideally, for SBS detection to be optimal, $q_k = \delta_k$ by Nyquist's Criterion. The ZFE tries to restore the Nyquist pulse shape to q_k. In so doing, the ZFE ignores the noise and shapes the signal y_k so that it is ISI free. From Section 3.1's ISI-channel model and Figure 3.9,

$$y_k = \|h\| \cdot x_k * q_k + n_k \quad . \tag{3.90}$$

In the ZFE case, n_k is initially viewed as being zero. The D-transform of y_k is (See Appendix D.2)

$$Y(D) = \|h\| \cdot X(D) \cdot Q(D) \quad . \tag{3.91}$$

The ZFE output, z_k, has D Transform

$$Z(D) = W(D) \cdot Y(D) = W(D) \cdot Q(D) \cdot \|h\| \cdot X(D) \quad , \tag{3.92}$$

and will be free of ISI if $Z(D) = X(D)$, leaving the ZFE filter characteristic:

Definition 3.4.1 **[Zero-Forcing Equalizer]** *The ZFE transfer characteristic is*

$$W(D) = \frac{1}{Q(D) \cdot \|h\|} \quad . \tag{3.93}$$

The ZFE processes the sampled matched-filter output sequence. The ZFE's name reinforces that ISI is "forced to zero" at all sampling instants kT except $k = 0$. The receiver finishes with SBS detection for the input x_k constellation's decision regions,

3.4.1 ZFE Performance Analysis

The ZFE output noise variance, which is nonzero in practice, is however also important in determining performance. Because this noise arises through linear filter acting of the discrete Gaussian noise process n_k, it is also Gaussian. The designer can compute the discrete autocorrelation function (the bar denotes normalized to one dimension, so $N = 2$ for the complex QAM case) for the noise n_k as

$$\begin{aligned}
\bar{r}_{nn,k} &= E\left[n_l n_{l-k}^*\right]/N && (3.94)\\
&= \int_{-\infty}^{\infty}\int_{-\infty}^{\infty} \overline{E\left[n_h(t) \cdot n_h^*(s)\right]} \cdot \varphi_h^*(t - lT) \cdot \varphi_h(s - (l-k)T) \cdot dt \cdot ds && (3.95)\\
&= \int_{-\infty}^{\infty}\int_{-\infty}^{\infty} \frac{\mathcal{N}_0}{2}\delta(t-s) \cdot \varphi_h^*(t - lT)\varphi_h(s - (l-k)T) \cdot dt \cdot ds && (3.96)\\
&= \frac{\mathcal{N}_0}{2}\int_{-\infty}^{\infty} \varphi_h^*(t - lT) \cdot \varphi_h(t - (l-k)T) \cdot dt && (3.97)\\
&= \frac{\mathcal{N}_0}{2}\int_{-\infty}^{\infty} \varphi_h^*(u) \cdot \varphi_h(u + kT)du \quad (\text{letting } u = t - lT) && (3.98)\\
&= \frac{\mathcal{N}_0}{2} \cdot q_{-k}^* = \frac{\mathcal{N}_0}{2} \cdot q_k \quad , && (3.99)
\end{aligned}$$

or more simply

$$\bar{R}_{nn}(D) = \frac{\mathcal{N}_0}{2} \cdot Q(D) \quad , \tag{3.100}$$

where the analysis uses the substitution $u = t - lT$ in going from (3.97) to (3.98), and assumes baseband equivalent signals for the complex case. The complex baseband-equivalent noise has (one-dimensional) sample variance $\frac{\mathcal{N}_0}{2}$ at the normalized matched-filter output. The ZFE-output noise, $n_{ZFE,k}$, has autocorrelation function

$$\bar{r}_{ZFE,k} \triangleq \mathbb{E}\left[n_{ZFE,l} \cdot n^*_{ZFE,l-k}\right] = \bar{r}_{nn,k} * w_k * w^*_{-k} \quad . \tag{3.101}$$

The D-Transform of $\bar{r}_{ZFE,k}$ is then

$$\bar{R}_{ZFE}(D) = \frac{\mathcal{N}_0}{2} \frac{Q(D)}{\|h\|^2 \cdot Q^2(D)} = \frac{\frac{\mathcal{N}_0}{2}}{\|h\|^2 \cdot Q(D)} \quad . \tag{3.102}$$

The ZFE noise's power spectral density is then $\bar{R}_{ZFE}(e^{-\jmath\omega T})$. The ZFE-output noise's (per-dimensional) variance is the (per-dimensional) mean-square error between the desired x_k and the ZFE output z_k. Since

$$z_k = x_k + n_{ZFE,k} \quad , \tag{3.103}$$

then σ^2_{ZFE} is

$$\begin{aligned}
\sigma^2_{ZFE} &= \frac{T}{2\pi} \int_{-\frac{\pi}{T}}^{\frac{\pi}{T}} \bar{R}_{ZFE}(e^{-\jmath\omega T}) \cdot d\omega & (3.104)\\
&= \frac{T}{2\pi} \int_{-\frac{\pi}{T}}^{\frac{\pi}{T}} \frac{\frac{\mathcal{N}_0}{2}}{\|h\|^2 \cdot Q(e^{-\jmath\omega T})} \cdot d\omega & (3.105)\\
&= \frac{\frac{\mathcal{N}_0}{2}}{\|h\|^2} \gamma^{-1}_{ZFE} = \frac{\frac{\mathcal{N}_0}{2}}{\|h\|} \cdot w_0 \quad , & (3.106)
\end{aligned}$$

where

$$\gamma^{-1}_{ZFE} = \frac{T}{2\pi} \int_{-\frac{\pi}{T}}^{\frac{\pi}{T}} \frac{d\omega}{Q(e^{-\jmath\omega T})} = w_0 \cdot \|h\| \quad . \tag{3.107}$$

The ZFE's **center tap** is $w_{ZFE,0}$. This ZFE tap always has the largest magnitude and thus spotted readily when plotting the ZFE's impulse response. From (3.103) and the fact that $\mathbb{E}[n_{ZFE,k}] = 0$, $\mathbb{E}[z_k/x_k] = x_k$, so that the ZFE is unbiased for a detection rule based on x_k. The ZFE-output SNR is

$$SNR_{ZFE} = \frac{\bar{\mathcal{E}}_{\boldsymbol{x}}}{\sigma^2_{ZFE}} = SNR_{MFB} \cdot \gamma_{ZFE} \quad . \tag{3.108}$$

Computation of $d_{\min}$ over x_k's constellation leads to a relation between $\bar{\mathcal{E}}_{\boldsymbol{x}}$, $d_{\min}$, and M, and the NNUB on error probability for an SBS detector at the ZFE output is (please, do not confuse the Q function with the channel autocorrelation $Q(D)$)

$$P_{ZFE,e} \approx N_e \cdot Q\left(\frac{d_{\min}}{2\sigma_{ZFE}}\right) \quad . \tag{3.109}$$

Since SBS detection can never have performance that exceeds the MFB,

$$\begin{aligned}
\sigma^2 \le \sigma^2_{ZFE} \cdot \|h\|^2 &= \sigma^2 \cdot \frac{T}{2\pi} \int_{-\frac{\pi}{T}}^{\frac{\pi}{T}} \frac{d\omega}{Q(e^{-\jmath\omega T})} & (3.110)\\
&= \frac{\sigma^2}{\gamma_{ZFE}} & (3.111)\\
SNR_{MFB} &\ge SNR_{ZFE} & (3.112)\\
\gamma_{ZFE} &\le 1 \quad , & (3.113)
\end{aligned}$$

with equality if and only if $Q(D) = 1$.

Finally, the ZFE equalization loss, γ_{ZFE}, defines the SNR reduction with respect to the SNR_{MFB}:

Definition 3.4.2 [ZFE Equalization Loss] *The* **ZFE Equalization Loss**, γ_{ZFE} *in decibels is*

$$\gamma_{ZFE} \triangleq 10 \cdot \log_{10}\left(\frac{SNR_{ZFE}}{SNR_{MFB}}\right) = 10\log_{10}\frac{\sigma^2}{\|h\|^2 \cdot \sigma^2_{ZFE}} = -10\log_{10}\|h\| \cdot w_{ZFE,0} \quad , \tag{3.114}$$

and is a measure of ZFE loss (in dB) with respect to the MFB. The sign of the loss is often ignored since only its magnitude is of concern.

Equation (3.114) always thus provides a number greater than or equal to zero in dB.

3.4.2 Noise Enhancement

The ZFE design ignored noise effects. This oversight can lead to **noise enhancement**, a σ^2_{ZFE} that is unacceptably large, and consequent poor performance.

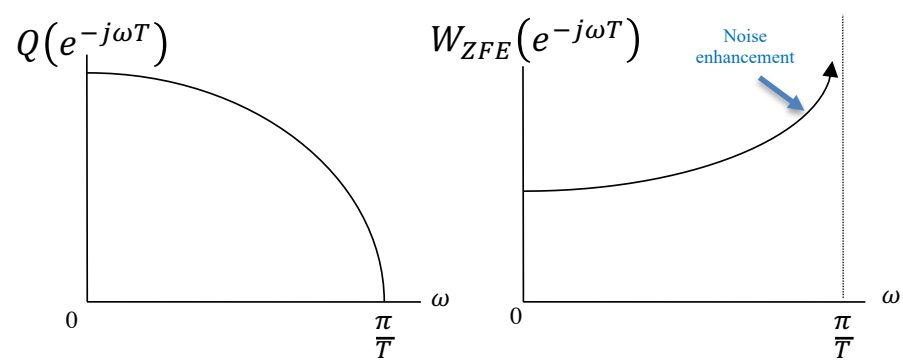

Figure 3.21: Noise Enhancement

Figure 3.21 illustrates a lowpass-channel example with zero Nyquist Frequency transfer, that is, $Q(e^{-j\omega T}) = 0$ at $\omega = \frac{\pi}{T}$. Since $W(e^{-j\omega T}) = 1/(\|h\| \cdot Q(e^{-j\omega T}))$, then the ZFE amplifies any noise energy near the Nyquist Frequency, in this case so much that $\sigma^2_{ZFE} \to \infty$. Even when there is no channel notch at any frequency, σ^2_{ZFE} can be finite, but large, leading to unacceptable performance degradation.

3.4.3 Signal Processing Relationship Review

In actual example computation, this text's readers often find Table 3.1 useful in recalling basic digital signal processing equivalences related to scale factors between continuous time convolution and discrete-time convolution.

time	frequency	
$p(t) \leftrightarrow P(\omega)$		continuous-time
$p_k = p(kT) \leftrightarrow P\left(e^{-j\omega T}\right) = \frac{1}{T}\sum_{n=-\infty}^{\infty} P\left(\omega + \frac{2\pi n}{T}\right)$		discrete-time
$y(t) = x(t) * p(t) \leftrightarrow Y(\omega) = X(\omega)\cdot P(\omega)$		continuous-time
$y(kT) = T\cdot x_k * p_k \leftrightarrow Y\left(e^{-j\omega T}\right) = T\cdot X\left(e^{-j\omega T}\right)\cdot P\left(e^{-j\omega T}\right)$		discrete-time
	$Y\left(e^{-j\omega T}\right) = \frac{1}{T}\cdot X(\omega)\cdot P(\omega)$	sampling theorem satisfied
$\|p\|^2 = \int_{-\infty}^{\infty} \|p(t)\|^2 dt$	$= \frac{1}{2\pi}\int_{-\infty}^{\infty} \|P(\omega)\|^2 d\omega$	continuous-time
$\|p\|^2 = T\sum_{k=-\infty}^{\infty} \|p_k\|^2$	$= \frac{T^2}{2\pi}\int_{-\frac{\pi}{T}}^{\frac{\pi}{T}} \left\|P\left(e^{-j\omega T}\right)\right\|^2 d\omega$	discrete-time (sampling thm satisfied)

Table 3.1: Conversion factors of T.

The following example clearly illustrates the noise-enhancement effect:

EXAMPLE 3.4.1 *[$1 + .9 \cdot D^{-1}$ - ZFE]* A bandlimited channel's pulse response is

$$H(\omega) = \begin{cases} \sqrt{T}\cdot\left(1 + .9\cdot e^{\jmath\omega T}\right) & |\omega| \le \frac{\pi}{T} \\ 0 & |\omega| > \frac{\pi}{T} \end{cases} . \tag{3.115}$$

The modulation is binary PAM. Then $\|h\|^2$ is

$$\begin{aligned} \|h\|^2 &= \frac{1}{2\pi}\int_{-\frac{\pi}{T}}^{\frac{\pi}{T}} |H(\omega)|^2 \cdot d\omega & (3.116) \\ &= \frac{1}{2\pi}\int_{-\frac{\pi}{T}}^{\frac{\pi}{T}} T\cdot[1.81 + 1.8\cos(\omega T)]\cdot d\omega & (3.117) \\ &= \frac{T}{2\pi}\cdot 1.81\cdot\frac{2\pi}{T} = 1.81 = 1^2 + .9^2 \quad . & (3.118) \end{aligned}$$

Figure 3.22 plots this pulse response's Fourier Transform magnitude. Thus, with $\Phi_h(\omega)$ as the Fourier transform of $\{\varphi_h(t)\}$,

$$\Phi_h(\omega) = \begin{cases} \sqrt{\frac{T}{1.81}}\cdot\left(1 + .9\cdot e^{\jmath\omega T}\right) & |\omega| \le \frac{\pi}{T} \\ 0 & |\omega| > \frac{\pi}{T} \end{cases} . \tag{3.119}$$

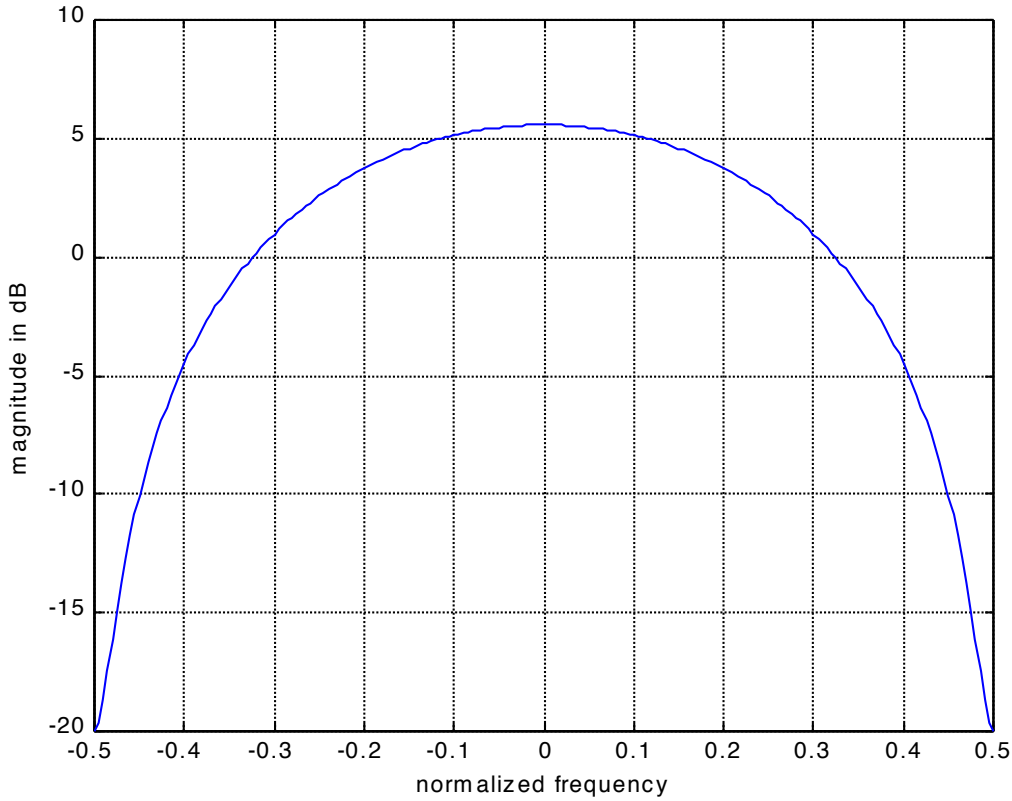

Figure 3.22: Magnitude of Fourier transform of (sampled) pulse response.

Then, (using the bandlimited property of $H(\omega)$ in this example)

$$
\begin{aligned}
Q(e^{-\jmath\omega T}) &= \frac{1}{T}\cdot|\Phi_h(\omega)|^2 && (3.120)\\
&= \frac{1}{1.81}|1+.9\cdot e^{\jmath\omega T}|^2 && (3.121)\\
&= \frac{1.81+1.8\cdot\cos(\omega T)}{1.81} && (3.122)\\
Q(D) &= \frac{.9\cdot D^{-1}+1.81+.9\cdot D}{1.81} \quad . && (3.123)
\end{aligned}
$$

Then

$$
W(D) = \frac{\sqrt{1.81}\cdot D}{.9+1.81\cdot D+.9\cdot D^2} \quad . \qquad (3.124)
$$

The ZFE's Fourier Transform magnitude appears in Figure 3.23.

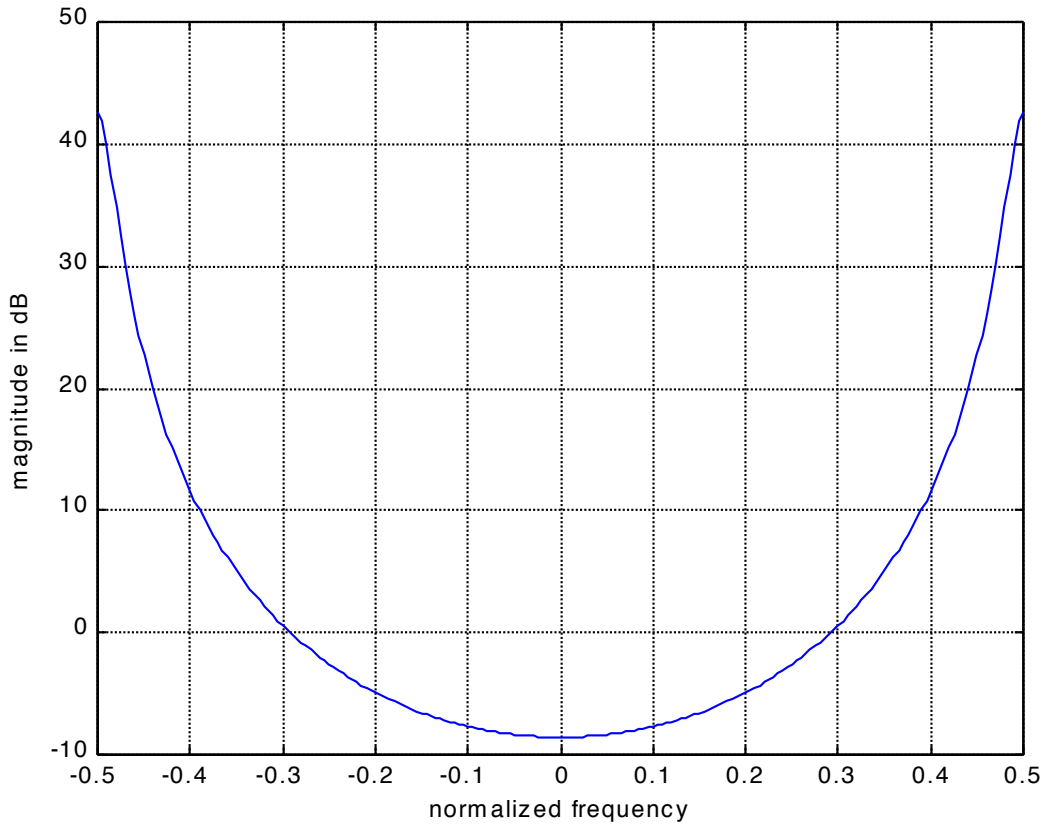

Figure 3.23: ZFE magnitude for example.

The time-domain sample response of the equalizer is shown in Figure 3.24.

Computation of σ^2_{ZFE} allows performance evaluation, [10]

$$\sigma^2_{ZFE} = \frac{T}{2\pi}\int_{-\frac{\pi}{T}}^{\frac{\pi}{T}} \frac{\frac{\mathcal{N}_0}{2}}{Q(e^{-\jmath\omega T})\cdot\|h\|^2}d\omega \tag{3.125}$$

$$= \frac{T}{2\pi}\int_{-\frac{\pi}{T}}^{\frac{\pi}{T}} \frac{(1.81/1.81)\cdot\frac{\mathcal{N}_0}{2}}{1.81+1.8\cdot\cos(\omega T)}d\omega \tag{3.126}$$

$$= \frac{\mathcal{N}_0}{2}\frac{1}{2\pi}\int_{-\pi}^{\pi}\frac{1}{1.81+1.8\cdot\cos u}du \tag{3.127}$$

$$= (\frac{\mathcal{N}_0}{2})\frac{2}{2\pi}\left[\frac{2}{\sqrt{1.81^2-1.8^2}}\mathrm{Tan}^{-1}\left\{\frac{\sqrt{1.81^2-1.8^2}\cdot\tan\frac{u}{2}}{1.81+1.8}\right\}\right|_0^{\pi} \tag{3.128}$$

$$= (\frac{\mathcal{N}_0}{2})\frac{4}{2\pi\sqrt{1.81^2-1.8^2}}\cdot\frac{\pi}{2} \tag{3.129}$$

$$= (\frac{\mathcal{N}_0}{2})\frac{1}{\sqrt{1.81^2-1.8^2}} \tag{3.130}$$

$$= \frac{\mathcal{N}_0}{2}(5.26) \quad . \tag{3.131}$$

[10] From a table of integrals
$\int\frac{1}{a+b\cos u}du = \frac{2}{\sqrt{a^2-b^2}}\mathrm{Tan}^{-1}\left(\frac{\sqrt{a^2-b^2}\tan(\frac{u}{2})}{a+b}\right)$.

The ZFE-output SNR is

$$SNR_{ZFE} = \frac{\bar{\mathcal{E}}_{\boldsymbol{x}}}{5.26 \cdot \frac{\mathcal{N}_0}{2}} \quad . \tag{3.132}$$

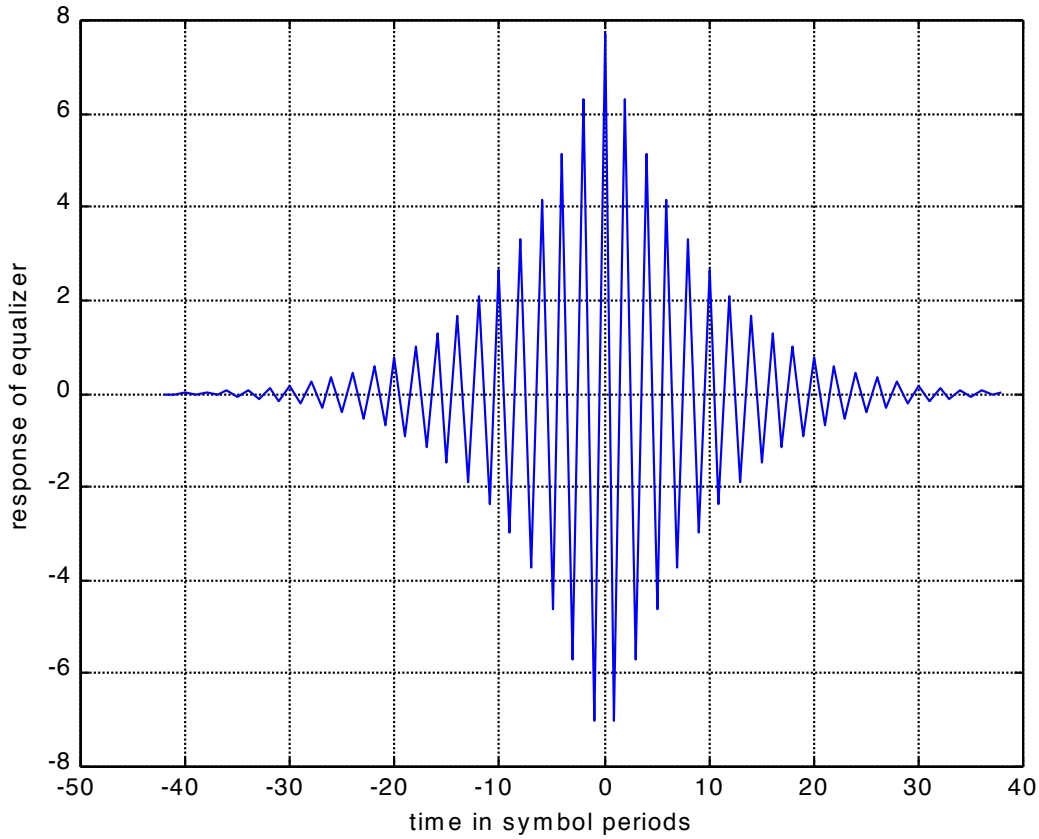

Figure 3.24: ZFE time-domain response.

This SNR_{ZFE} is also the Q-function argument for a binary SBS detector at the ZFE output. Assuming the two transmitted levels are $x_k = \pm 1$, then

$$\text{MFB} = \frac{\|h\|^2}{\sigma^2} = \frac{1.81}{\sigma^2} \quad , \tag{3.133}$$

leaving

$$\gamma_{ZFE} = 10 \log_{10}(1.81 \cdot 5.26) \approx 9.8\text{dB} \tag{3.134}$$

for any value of the noise variance. This is very poor performance on this channel. No matter what b is used, the loss is almost 10 dB from best performance. Thus, noise enhancement can be a serious problem. Chapter 8 demonstrates a non-SBS maximum-likelihood detector by which to ensure that there is no loss with respect to the matched filter bound for this channel. Chapter 4 will use codes with $b \leq 1.55$ that ensure $P_e < 10^{-5}$ on this channel, which is far below the error rate achievable even when the MFB is attained. Thus, there are good solutions, but the ZFE is not a good solution.

It may help when dealing with pole-zero channels $Q(D)$ and thus $W_{ZFE}(D) = [\|h\| \cdot Q(D)]^{-1}$ to note that Equation (3.124) expands using matlab's residue command[11] after multiplying

[11] There is also a direct partial fraction expansion matlab command, but it only exists in special add-on packages.

numerator and denominator by D:

```
>> [r,p,k1]=residue([sqrt(1.81) 0],[.9 1.81 .9])
r =
    7.8676
   -6.3728
p =
   -1.1111
   -0.9000
k1 =  []
```

where r is the "residue" or numerator of a term $r/(D-p)$ for each of the residues and poles (equal in number). (k is a constant that is nonzero only when the numerator is of equal or greater than the denominator. It is zero in this example, can be a constant, or can even have powers of D associated if a vector) The expansion D-transform (assuming k is constant, when not it expands in obvious way for $k(1)+k(2)\cdot D+...$). Further, $W(D)$'s positive real nature ensures that each pole $p(m)$ has a corresponding paired pole $1/p^*(m)$. Choose the $|p(m)| \leq 1$, and the following holds, summing over the poles with magnitude less/equal to one)

$$W(D) = k1 + \underbrace{\sum_m \frac{r(m)/p(m)}{1-p(m)\cdot D}}_{\text{causal in } w_0} + \underbrace{\frac{r(m)\cdot D^{-1}}{1-p^*(m)\cdot D^{-1}}}_{\text{strictly noncausal, no } w_0} \quad . \tag{3.135}$$

with corresponding time-domain sequence (k is time index and m is pole index over poles with magnitude less than or equal to one - only take 1/2 of those with a pole that is exactly one)

$$k1\cdot\delta_k - \sum_m \left\{ r(m)\cdot[p(m)]^{k-1}\cdot u_k - r(m)\cdot[p^*(m)]^{-k-1}\cdot u_{1-mk} \right\} \quad , \tag{3.136}$$

from which w_0 follows as

$$w_0 = k - \sum_m r(m)/p(m) \ . \tag{3.137}$$

Another example generalizes Example 3.4.1 to a complex baseband pulse response (corresponding to a QAM channel):

EXAMPLE 3.4.2 *[QAM: $-.5D^{-1}+(1+.25\jmath)-.5\jmath D$ Channel]* Given a baseband equivalent channel

$$h(t) = \frac{1}{\sqrt{T}}\left\{ -\frac{1}{2}\cdot\text{sinc}\left(\frac{t+T}{T}\right) + \left(1+\frac{\jmath}{4}\right)\cdot\text{sinc}\left(\frac{t}{T}\right) - \frac{\jmath}{2}\cdot\text{sinc}\left(\frac{t-T}{T}\right)\right\} \quad , \tag{3.138}$$

the discrete-time channel samples are

$$h_k = \frac{1}{\sqrt{T}}\cdot\left[-\frac{1}{2}\ ,\ \left(1+\frac{\jmath}{4}\right)\ ,\ -\frac{\jmath}{2}\right] \quad . \tag{3.139}$$

This channel has the transfer function of Figure 3.25.

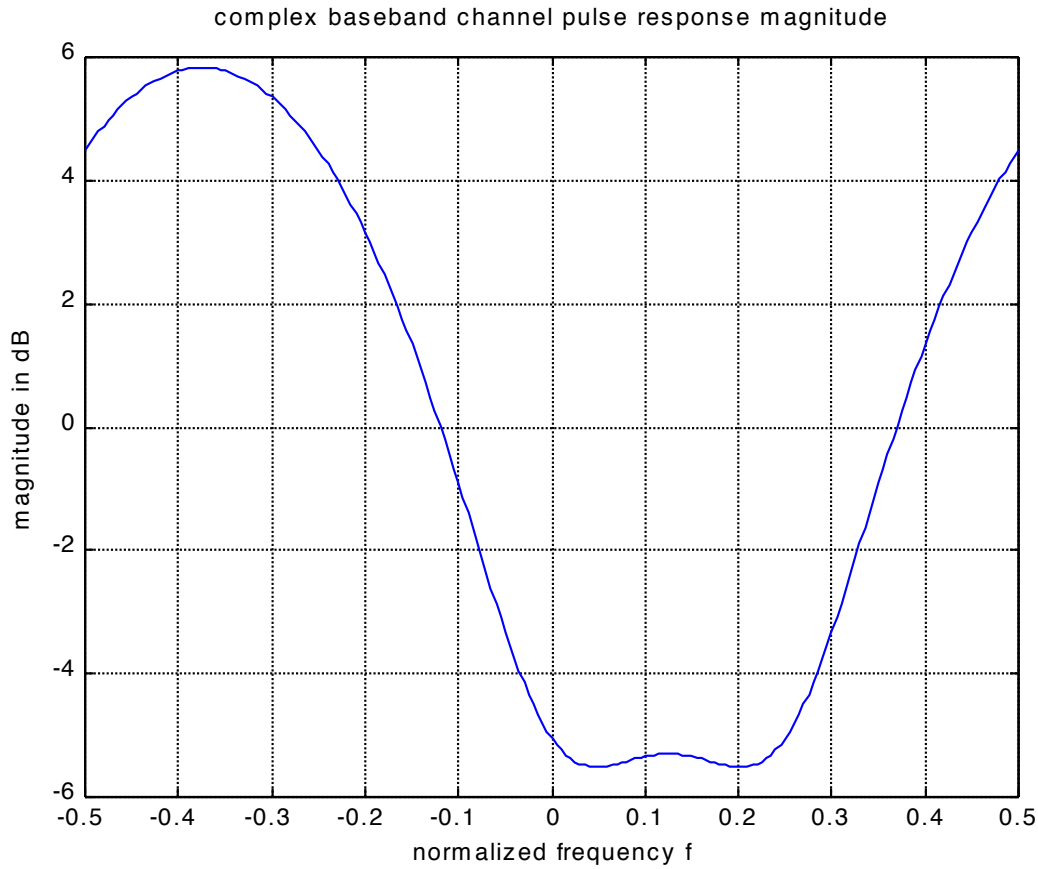

Figure 3.25: Fourier transform magnitude for for Example 3.4.2.

The pulse response norm (squared) is

$$\|h\|^2 = \frac{T}{T}\left(.25 + 1 + .0625 + .25\right) = 1.5625 \quad . \tag{3.140}$$

Then q_k is given by

$$q_k = q(kT) = T\left(\varphi_{h,k} * \varphi^*_{h,-k}\right) = \frac{1}{1.5625}\left[\, -\frac{\jmath}{4}\ ,\ \frac{5}{8}(-1+\jmath)\ ,\ 1.5625\ ,\ -\frac{5}{8}(1+\jmath)\ ,\ \frac{\jmath}{4}\,\right] \tag{3.141}$$

or

$$Q(D) = \frac{1}{1.5625}\left[\, -\frac{\jmath}{4}\cdot D^{-2} + \frac{5}{8}(-1+\jmath)\cdot D^{-1} + 1.5625 - \frac{5}{8}(1+\jmath)\cdot D + \frac{\jmath}{4}\cdot D^2\,\right] \tag{3.142}$$

Then, $Q(D)$ factors into

$$Q(D) = \frac{1}{1.5625}\left\{(1 - .5\jmath\cdot D)\left(1 - .5\cdot D^{-1}\right)\left(1 + .5\jmath\cdot D^{-1}\right)(1 - .5\cdot D)\right\} \quad , \tag{3.143}$$

and

$$W_{ZFE}(D) = \frac{1}{Q(D)\cdot\|h\|} \tag{3.144}$$

or

$$W_{ZFE}(D) = \frac{\sqrt{1.5625}}{\left(-.25\jmath\cdot D^{-2} + .625(-1+\jmath)\cdot D^{-1} + 1.5625 - .625(1+\jmath)\cdot D + .25\jmath\cdot D^2\right)} \quad . \tag{3.145}$$

The ZFE's Fourier Transform appears in Figure 3.26.

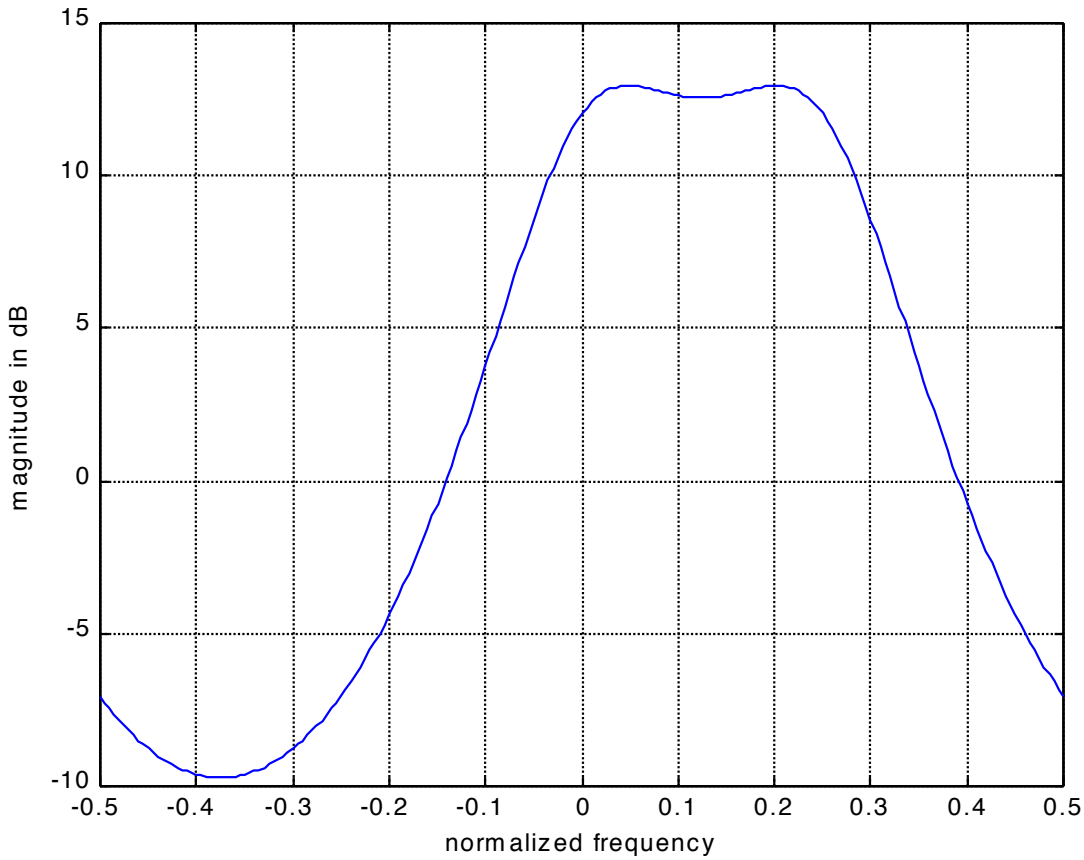

Figure 3.26: ZFE Fourier transform magnitude for Example 3.4.2.

Figure 3.27 plots the real and imaginary parts of the equalizer response in the time domain

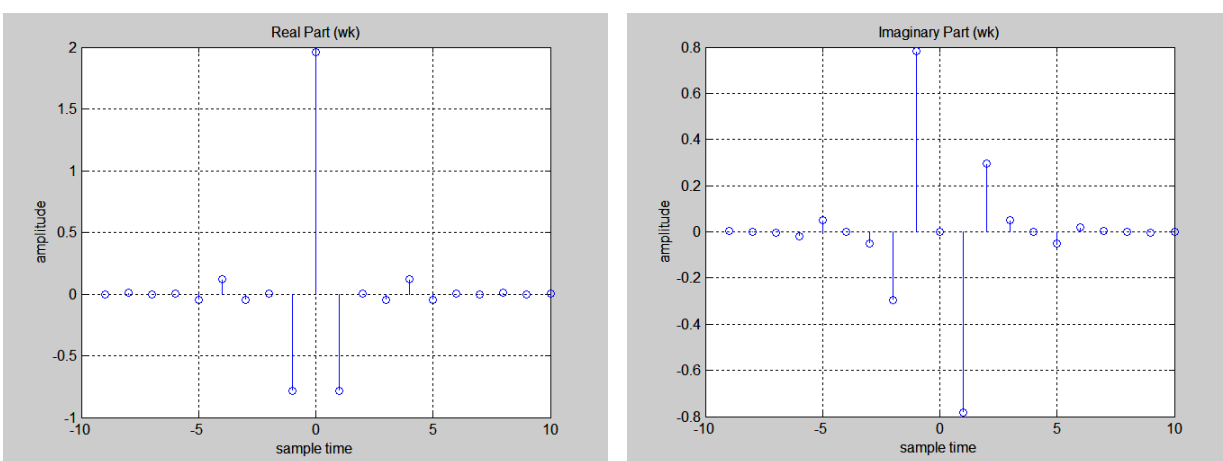

Figure 3.27: Time-domain equalizer coefficients for complex channel.

Then

$$\sigma^2_{ZFE} = \frac{T}{2\pi}\int_{-\frac{\pi}{T}}^{\frac{\pi}{T}} \frac{\frac{\mathcal{N}_0}{2}}{\|h\|^2 \cdot Q(e^{-\jmath\omega T})} \cdot d\omega \quad , \tag{3.146}$$

or

$$\sigma^2_{ZFE} = \frac{\mathcal{N}_0}{2} \cdot \frac{w_0}{\|h\|} \quad , \tag{3.147}$$

where w_0 is the zero (center) coefficient of the ZFE. This coefficient can be extracted from

$$\begin{aligned} W_{ZFE}(D) &= \sqrt{1.5625} \cdot \left[\frac{D^2 \cdot (-4\jmath)}{\{(D+2\jmath)\,(D-2)\,(D-.5)\,(D+.5\jmath)\}}\right] \\ &= \sqrt{1.5625} \cdot \left[\frac{A}{D-2} + \frac{B}{D+2\jmath} + \text{terms not contributing to } w_0\right] \quad , \end{aligned}$$

where A and B are coefficients in the partial-fraction expansion (Matlab's residuez and residue commands ican be very useful here):

$$A = \frac{4(-4\jmath)}{(2+2\jmath)(2+.5\jmath)(1.5)} = -1.5686 - \jmath.9412 = 1.8293\angle -2.601 \tag{3.148}$$

$$B = \frac{-4(-4\jmath)}{(-2\jmath-.5)(-2\jmath-2)(-1.5\jmath)} = .9412 + \jmath 1.5685 = 1.8293\angle 1.030 \quad . \tag{3.149}$$

Finally

$$W_{ZFE}(D) = \sqrt{1.5625}\left[\frac{A(-.5)}{1-.5\cdot D} + \frac{B(-.5\jmath)}{(1-.5\jmath\cdot D)} + \text{terms}\right] \quad , \tag{3.150}$$

and

$$w_0 = \sqrt{1.5625}\,[(-.5)(-1.5686-\jmath.9412) - .5\jmath(.9412+\jmath 1.5686)] \tag{3.151}$$

$$= \sqrt{1.5625}(1.57) = 1.96 \tag{3.152}$$

The ZFE loss can be shown to be

$$\gamma_{ZFE} = 10\cdot\log_{10}(w_0\cdot\|h\|) = 3.9 \text{ dB} \quad , \tag{3.153}$$

which is better than the last channel because the frequency spectrum is not as near zero in this complex example as it was earlier on the PAM example. Nevertheless, considerably better performance is also possible on this complex channel, but not with the ZFE.

To compute P_e for 4QAM, the designer calculates

$$\bar{P}_e \approx Q\left(\sqrt{SNR_{MFB} - 3.9 \text{ dB}}\right) \quad . \tag{3.154}$$

If $SNR_{MFB} = 10$dB, then $\bar{P}_e \approx 2.2\times 10^{-2}$. If $SNR_{MFB} = 17.4$dB, then $\bar{P}_e \approx 1.0\times 10^{-6}$. If $SNR_{MFB} = 23.4$dB for 16QAM, then $\bar{P}_e \approx 2.0\times 10^{-5}$. similar to the real example, the matlab commands are

```
>> [r,p,k]=residue([sqrt(1.5625) 0 0],[-i/4  (5/8)*(-1+i) 1.5625 -5/8*(1+j) i/4]);
>> transpose(r)  =  -1.9608 + 1.1765i   1.1765 - 1.9608i   0.2941 + 0.4902i   0.4902 + 0.2941i
>> transpose(p) =   2.0000 - 0.0000i  -0.0000 + 2.0000i  -0.0000 + 0.5000i   0.5000 + 0.0000i
>> k =     []
>> r(3)/p(3) =   0.9804 - 0.5882i
>> r(4)/p(4) =   0.9804 + 0.5882i
>> w0= r(3)/p(3) + r(4)/p(4) = 1.9608
```

3.5 Minimum Mean-Square Error Linear Equalization

The **Minimum Mean-Square Error Linear Equalizer** (MMSE-LE) balances ISI reduction and noise enhancement. The MMSE-LE always performs as well as, or better than, the ZFE and uses also a linear discrete-time filter, w_k for R The MMSE-LE is slightly more complex to describe and analyze than the ZFE.

The MMSE-LE iacts on y_k to form an output sequence z_k that is the best MMSE estimate of x_k. That is, the filter w_k minimizes the Mean Square Error (MSE):

Definition 3.5.1 *[Mean Square Error (for the LE)] The* **LE error** *signal is*

$$e_k = x_k - w_k * y_k = x_k - z_k \quad . \tag{3.155}$$

The LE's **Minimum Mean Square Error** *(MMSE) is then*

$$\sigma^2_{MMSE-LE} \triangleq \min_{w_k} \mathbb{E}\left[|x_k - z_k|^2\right] \quad . \tag{3.156}$$

The MSE criteria for w_k does not ignore noise enhancement because this filter's optimization balances ISI elimination with noise-power increase. The MMSE-LE output is as close as possible, in the Minimum MSE sense, to the data symbol x_k.

3.5.1 Linear Equalizer Optimization

Using D-transforms,

$$E(D) = X(D) - W(D) \cdot Y(D) \tag{3.157}$$

By Appendix' D orthogonality principle, and at any discrete sample time k, the error sample e_k must be uncorrelated with any equalizer input signal y_m. Succinctly,

$$\mathbb{E}\left[E(D) \cdot Y^*(D^{-*})\right] = 0 \quad . \tag{3.158}$$

Evaluating (3.158), using (3.157), yields

$$0 = \bar{R}_{xy}(D) - W(D) \cdot \bar{R}_{yy}(D) \quad , \tag{3.159}$$

where ($N = 1$ for PAM, $N = 2$ for Quadrature Modulation)[12]

$$\bar{R}_{xy}(D) = E\left[X(D) \cdot Y^*(D^{-*})\right]/N = \bar{\mathcal{E}}_{\boldsymbol{x}} \cdot \|h\| \cdot Q(D) \tag{3.160}$$

$$\begin{aligned} \bar{R}_{yy}(D) &= E\left[Y(D) \cdot Y^*(D^{-*})\right]/N = \bar{\mathcal{E}}_{\boldsymbol{x}} \cdot \|h\|^2 \cdot Q^2(D) + \frac{\mathcal{N}_0}{2} \cdot Q(D) \\ &= \bar{\mathcal{E}}_{\boldsymbol{x}} \cdot Q(D) \cdot \left(\|h\|^2 \cdot Q(D) + \frac{\mathcal{N}_0}{2}\right) \quad . \end{aligned} \tag{3.161}$$

Then the MMSE-LE becomes

$$W(D) = \frac{\bar{R}_{xy}(D)}{\bar{R}_{yy}(D)} = \frac{1}{\|h\| \cdot (Q(D) + 1/SNR_{MFB})} \quad . \tag{3.162}$$

The MMSE-LE differs from the ZFE only in the additive positive constant $1/SNR_{MFB}$ in (3.162)'s denominator. The equalizer transfer function $W(e^{-\jmath\omega T})$ is also real and positive for all finite signal-to-noise ratios. This finite positive term prevents the denominator from ever becoming zero, and thus well conditions the MMSE-LE even when the channel (or pulse response) is zero for some frequencies or frequency bands. Also $W(D) = W^*(D^{-*})$.

[12] The expression $R_{xx}(D) \triangleq E\left[X(D) \cdot X^*(D^{-*})\right]$ is used in a symbolic sense, since the terms of $X(D) \cdot X^*(D^{-*})$ have form $\sum_k x_k \cdot x^*_{k-j}$, implying the additional operation $\lim_{K\to\infty}[1/(2K+1)] \cdot \sum_{-K\le k\le K}$ on the sum in such terms. This is permissible for stationary (and ergodic) discrete-time sequences.

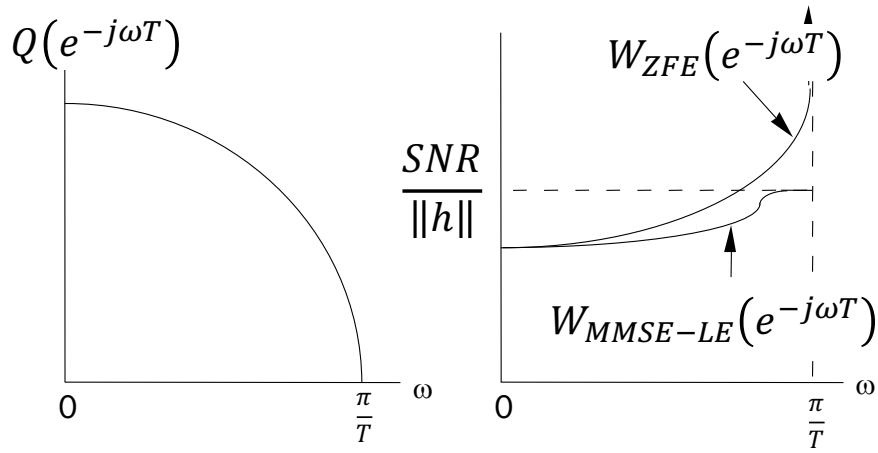

Figure 3.28: **Example of MMSE-LE versus ZFE.**

Figure 3.28 repeats Figure 3.21 with addition of the MMSE-LE transfer characteristic. The MMSE-LE transfer function has magnitude $\bar{\mathcal{E}}_{\boldsymbol{x}}/\sigma^2$ at $\omega = \frac{\pi}{T}$, while the ZFE becomes infinite at this same frequency. This MMSE-LE leads to better performance, as the next subsection computes.

3.5.2 Performance of the MMSE-LE

The MMSE is error-autocorrelation-sequence's time-0 coefficient

$$\begin{aligned}
\bar{R}_{ee}(D) &= \mathbb{E}\left[E(D)\cdot E^*(D^{-*})\right]/N \qquad (3.163)\\
&= \bar{\mathcal{E}}_{\boldsymbol{x}} - W^*(D^{-*})\cdot \bar{R}_{xy}(D) - W(D)\cdot \overline{R}^*_{xy}(D^{-*}) + W(D)\cdot \bar{R}_{yy}(D)\cdot W^*(D^{-*})\\
&= \bar{\mathcal{E}}_{\boldsymbol{x}} - W(D)\cdot \bar{R}_{yy}(D)\cdot W^*(D^{-*})\\
&= \bar{\mathcal{E}}_{\boldsymbol{x}} - \frac{Q(D)\cdot\left(\bar{\mathcal{E}}_{\boldsymbol{x}}\cdot\|h\|^2\cdot Q(D) + \frac{\mathcal{N}_0}{2}\right)}{\|h\|^2\cdot\left(Q(D)+1/SNR_{MFB}\right)^2}\\
&= \bar{\mathcal{E}}_{\boldsymbol{x}} - \frac{\bar{\mathcal{E}}_{\boldsymbol{x}}Q(D)}{\left(Q(D)+1/SNR_{MFB}\right)}\\
&= \frac{\frac{\mathcal{N}_0}{2}}{\|h\|^2\cdot\left(Q(D)+1/SNR_{MFB}\right)} \qquad (3.164)
\end{aligned}$$

The third equality follows from

$$\begin{aligned}
W(D)\cdot\bar{R}_{yy}(D)W^*(D^{-*}) &= W(D\cdot\bar{R}_{yy}(D)\cdot\bar{R}_{yy}(D)^{-1}\cdot\bar{R}^*_{xy}(D^{-*})\\
&= W(D)\cdot\bar{R}^*_{xy}(D^{-*}) \quad ,
\end{aligned}$$

and that

$$\left(W(D)\cdot\bar{R}_{yy}(D)\cdot W^*(D^{-*})\right)^* = W(D)\cdot\bar{R}_{yy}(D)\cdot W^*(D^{-*}) \quad .$$

The MMSE then becomes

$$\sigma^2_{MMSE-LE} = \frac{T}{2\pi}\int_{-\frac{\pi}{T}}^{\frac{\pi}{T}} \bar{R}_{ee}(e^{-\jmath\omega T})\cdot d\omega = \frac{T}{2\pi}\int_{-\frac{\pi}{T}}^{\frac{\pi}{T}} \frac{\frac{\mathcal{N}_0}{2}\cdot d\omega}{\|h\|^2\cdot\left(Q(e^{-\jmath\omega T})+1/SNR_{MFB}\right)} \quad . \qquad (3.165)$$

The constant $\frac{\mathcal{N}_0}{2}/\|h\|$ scales $W(e^{-\jmath\omega T})$ in (3.165), so then

$$\sigma^2_{MMSE-LE} = w_0\cdot\frac{\frac{\mathcal{N}_0}{2}}{\|h\|} \quad . \qquad (3.166)$$

From comparison of (3.165) and (3.106), that

$$\sigma^2_{MMSE-LE} \leq \sigma^2_{ZFE} \quad , \tag{3.167}$$

with equality if and only if $SNR_{MFB} \to \infty$. Infinite SNR implies zero noise, and thus the ZFE and LE become the same at zero noise. Furthermore, since the ZFE is unbiased, and $\text{SNR}_{MMSE-LE} = \text{SNR}_{MMSE-LE,U} + 1$ and $\text{SNR}_{MMSE-LE,U}$ are the maximum-SNR corresponding to unconstrained and unbiased linear equalizers, respectively,

$$SNR_{ZFE} \leq \text{SNR}_{MMSE-LE,U} = \frac{\bar{\mathcal{E}}_{\boldsymbol{x}}}{\sigma^2_{MMSE-LE}} - 1 \leq SNR_{MFB} \quad . \tag{3.168}$$

Confirmation of MMSE-LE bias follows from the equalizer output

$$\begin{aligned}
Z(D) &= W(D) \cdot Y(D) && (3.169)\\
&= \frac{1}{\|h\| \cdot [Q(D) + 1/SNR_{MFB}]} \cdot [Q(D) \cdot \|h\| \cdot X(D) + N(D)] && (3.170)\\
&= X(D) - \frac{1/SNR_{MFB}}{Q(D) + 1/SNR_{MFB}} \cdot X(D) + \frac{N(D)}{\|h\| \cdot [Q(D) + 1/SNR_{MFB}]} \quad , && (3.171)
\end{aligned}$$

for which the x_k-dependent residual ISI term contains a component

$$\begin{aligned}
\text{signal-basis term} &= -\frac{1}{SNR_{MFB}} \cdot w_0 \cdot \|h\| \cdot x_k && (3.172)\\
&= -\frac{1}{SNR_{MFB}} \cdot \frac{\sigma^2_{MMSE-LE} \cdot \|h\|^2}{\frac{N_0}{2}} \cdot x_k && (3.173)\\
&= -\frac{\sigma^2_{MMSE-LE}}{\bar{\mathcal{E}}_{\boldsymbol{x}}} \cdot x_k && (3.174)\\
&= -\frac{1}{\text{SNR}_{MMSE-LE}} \cdot x_k \quad . && (3.175)\\
& && (3.176)
\end{aligned}$$

So $z_k = \left(1 - \frac{1}{\text{SNR}_{MMSE-LE}}\right) x_k - e'_k$ where e'_k is the error for unbiased detection and R. The optimum unbiased receiver with decision regions scaled by $1 - \frac{1}{\text{SNR}_{MMSE-LE}}$ (see Section 3.2.1) has the signal energy given by

$$\left(1 - \frac{1}{\text{SNR}_{MMSE-LE}}\right)^2 \cdot \bar{\mathcal{E}}_{\boldsymbol{x}} \quad . \tag{3.177}$$

A new error for the scaled decision regions is $e'_k = (1 - 1/\text{SNR}_{MMSE-LE}) \cdot x_k - z_k = e_k - \frac{1}{\text{SNR}_{MMSE-LE}} x_k$, which is also the old error with the x_k dependent term removed. Since e'_k and x_k are then independent,

$$\sigma^2_e = \sigma^2_{MMSE-LE} = \sigma^2_{e'} + \left(\frac{1}{\text{SNR}_{MMSE-LE}}\right)^2 \bar{\mathcal{E}}_{\boldsymbol{x}} \quad , \tag{3.178}$$

leaving

$$\begin{aligned}
\sigma^2_{e'} &= \sigma^2_{MMSE-LE} - \left(\frac{1}{\text{SNR}_{MMSE-LE}}\right)^2 \bar{\mathcal{E}}_{\boldsymbol{x}}\\
&= \frac{\text{SNR}^2_{MMSE-LE}\sigma^2_{MMSE-LE} - \bar{\mathcal{E}}_{\boldsymbol{x}}}{\text{SNR}^2_{MMSE-LE}}\\
&= \frac{\bar{\mathcal{E}}_{\boldsymbol{x}} \left(\text{SNR}_{MMSE-LE} - 1\right)}{\text{SNR}^2_{MMSE-LE}} \quad . && (3.179)
\end{aligned}$$

The SNR for the unbiased MMSE-LE then becomes (taking the ratio of (3.177) to $\sigma^2_{e'}$)

$$\text{SNR}_{MMSE-LE,U} = \frac{\bar{\mathcal{E}}_{\boldsymbol{x}} \cdot \frac{(\text{SNR}_{MMSE-LE}-1)^2}{\text{SNR}^2_{MMSE-LE}}}{\bar{\mathcal{E}}_{\boldsymbol{x}} \cdot \frac{(\text{SNR}_{MMSE-LE}-1)}{\text{SNR}^2_{MMSE-LE}}} = \text{SNR}_{MMSE-LE} - 1 \quad , \tag{3.180}$$

which corroborates the earlier relation of the optimum biased and unbiased SNR's for any particular receiver structure (at least for the LE structure). The unbiased SNR is

$$\text{SNR}_{MMSE-LE,U} = \frac{\bar{\mathcal{E}}_{\boldsymbol{x}}}{\sigma^2_{MMSE-LE}} - 1 \quad , \tag{3.181}$$

which is the performance level that this text always uses because it corresponds to the best SBS detector error probability, as was discussed earlier in Section 3.1. Figure **??** shows explicitly the scaling effect on a 4QAM decision regions. Again, MMSE receivers (of which the MMSE-LE is one) reduce noise energy and introduce bias, the "scaling up" removes the bias, and ensures the detector achieves the best P_e.

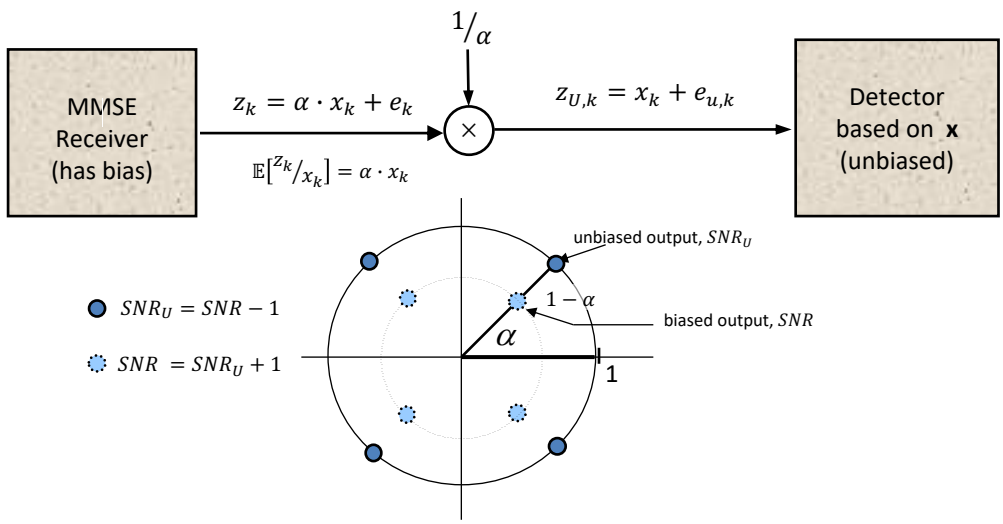

Figure 3.29: Illustration of bias and its removal.

Since the ZFE is also an unbiased receiver, (3.168) must hold. The first inequality in (3.168) tends to equality if the ratio $\frac{\bar{\mathcal{E}}_{\boldsymbol{x}}}{\sigma^2} \to \infty$ or if the channel is free of ISI ($Q(D) = 1$). The second inequality tends to equality if $\frac{\bar{\mathcal{E}}_{\boldsymbol{x}}}{\sigma^2} \to 0$ or if the channel is free of ISI ($Q(D) = 1$).

The unbiased MMSE-LE loss with respect to the MFB is

$$\gamma^{-1}_{MMSE-LE} = \frac{SNR_{MFB}}{\text{SNR}_{MMSE-LE,U}} = \left(\frac{\|h\|^2 \cdot \sigma^2_{MMSE-LE}}{\sigma^2}\right)\left(\frac{\bar{\mathcal{E}}_{\boldsymbol{x}}}{\bar{\mathcal{E}}_{\boldsymbol{x}} - \sigma^2_{MMSE-LE}}\right) \quad . \tag{3.182}$$

The $\frac{\|h\|^2 \cdot \sigma^2_{MMSE-LE}}{\sigma^2}$ in (3.182) is the increase in noise variance of the MMSE-LE, while the term $\frac{\bar{\mathcal{E}}_{\boldsymbol{x}}}{\bar{\mathcal{E}}_{\boldsymbol{x}} - \sigma^2_{MMSE-LE}}$ term represents the equalizer-output signal-energy reduction that accrues to lower noise enhancement.

The MMSE-LE also requires no additional complexity to implement and should always be used in place of the ZFE when the receiver uses symbol-by-symbol detection on the equalizer output. The error is not necessarily Gaussian in distribution. Nevertheless, engineers commonly make this assumption in

practice, with a good degree of accuracy, despite the potential non-Gaussian residual ISI component in $\sigma^2_{MMSE-LE}$. This text also follows this practice. Thus,

$$P_e \approx N_e \cdot Q\left(\sqrt{\kappa \cdot \text{SNR}_{MMSE-LE,U}}\right) \quad , \tag{3.183}$$

where κ depends on the relation of $\bar{\mathcal{E}}_{\boldsymbol{x}}$ to $d_{\min}$ for the particular constellation of interest, for instance $\kappa = 3/(M-1)$ for Square QAM. The reader may recall that the symbol Q is used in two separate ways, for the Q-function, and for the transform of the matched-filter-pulse-response cascade. The actual meaning should always be obvious in context.)

3.5.3 Examples Revisited

This section returns to the earlier ZFE examples to compute the improvement of the MMSE-LE on these same channels.

EXAMPLE 3.5.1 [PAM - MMSE-LE] The pulse response of a channel used with binary PAM is again given by

$$H(\omega) = \begin{cases} \sqrt{T}\left(1 + .9 \cdot e^{\jmath\omega T}\right) & |\omega| \leq \frac{\pi}{T} \\ 0 & |\omega| > \frac{\pi}{T} \end{cases} \quad . \tag{3.184}$$

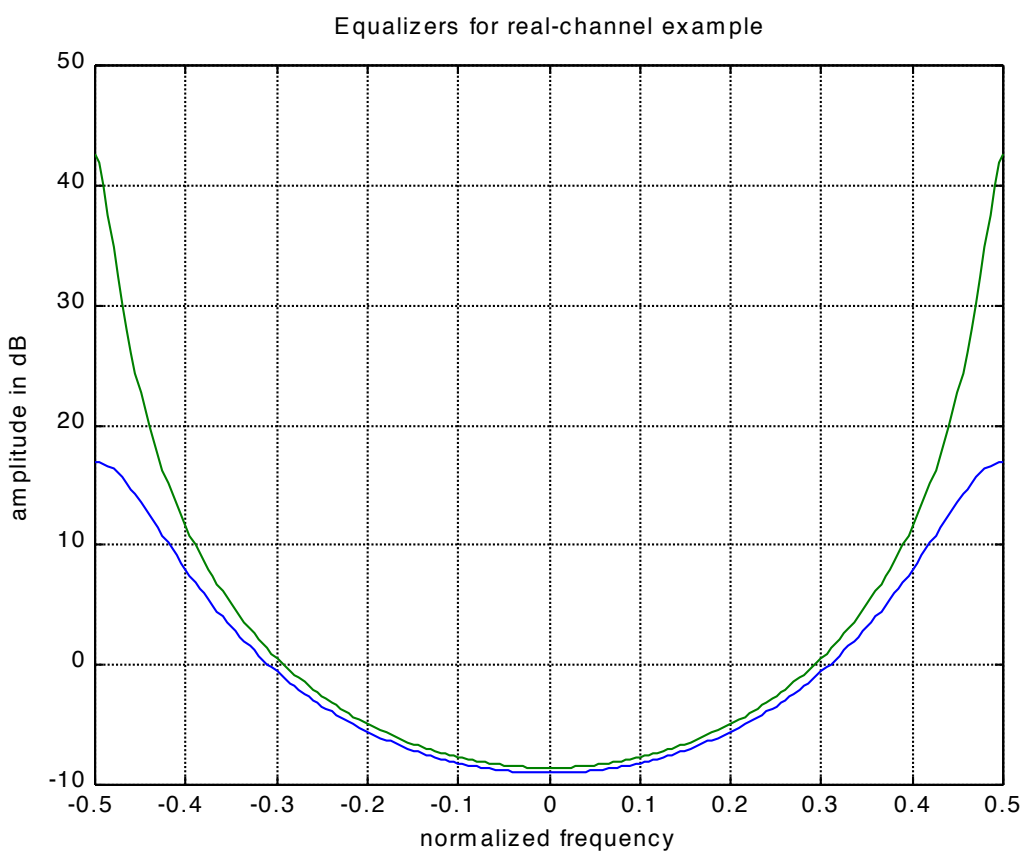

Figure 3.30: Comparison of Example 3.5.1 equalizer frequency responses for MMSE-LE and ZFE.

Let us suppose $SNR_{MFB} = 10\text{dB}$ $(= \bar{\mathcal{E}}_{\boldsymbol{x}} \cdot \|h\|^2/\frac{\mathcal{N}_0}{2})$ and that $\bar{\mathcal{E}}_{\boldsymbol{x}} = 1$. The equalizer is

$$W(D) = \frac{1}{\|h\| \cdot \left(\frac{.9}{1.81} \cdot D^{-1} + 1.1 + \frac{.9}{1.81} \cdot D\right)} \quad . \tag{3.185}$$

Figure 3.30 shows the frequency response of the equalizer for both the ZFE and MMSE-LE. Clearly the MMSE-LE has a lower magnitude.

The $\sigma^2_{MMSE-LE}$ is

$$\sigma^2_{MMSE-LE} = \frac{T}{2\pi} \int_{-\frac{\pi}{T}}^{\frac{\pi}{T}} \frac{\frac{\mathcal{N}_0}{2}}{1.81 + 1.8 \cdot \cos(\omega T) + 1.81/10} \cdot d\omega \tag{3.186}$$

$$= \frac{\mathcal{N}_0}{2} \frac{1}{\sqrt{1.991^2 - 1.8^2}} \tag{3.187}$$

$$= \frac{\mathcal{N}_0}{2}(1.175) \quad , \tag{3.188}$$

which is considerably smaller than σ^2_{ZFE}. The SNR for the MMSE-LE is

$$\text{SNR}_{MMSE-LE,U} = \frac{1 - 1.175(.181)}{1.175(.181)} = 3.7 \ (5.7\text{dB}) \quad . \tag{3.189}$$

The loss with respect to the MFB is 10dB - 5.7dB = 4.3dB. This is 5.5dB better than the ZFE (9.8dB - 4.3dB = 5.5dB), but still not good for this channel.

Figure 3.31 compares the frequency-domain responses of the equalized channel.

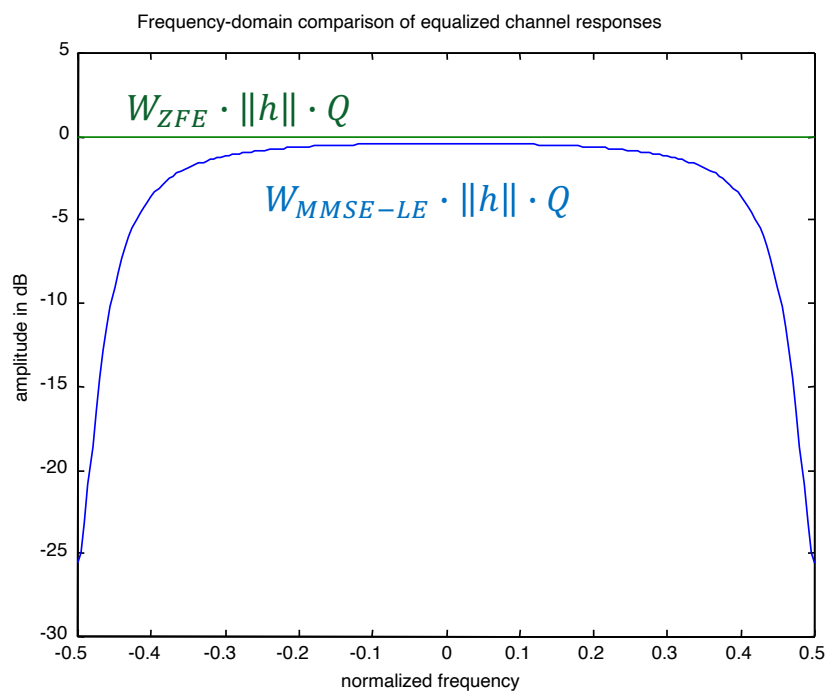

Figure 3.31: Example 3.5.1's Equalized frequency MMSE and ZF response comparison.

Figure 3.32 compares the time-domain responses of the equalized channel. The MMSE-LE clearly does not have an ISI-free response, but mean-square error/distortion is minimized and the MMSE-LE has better performance than the ZFE.

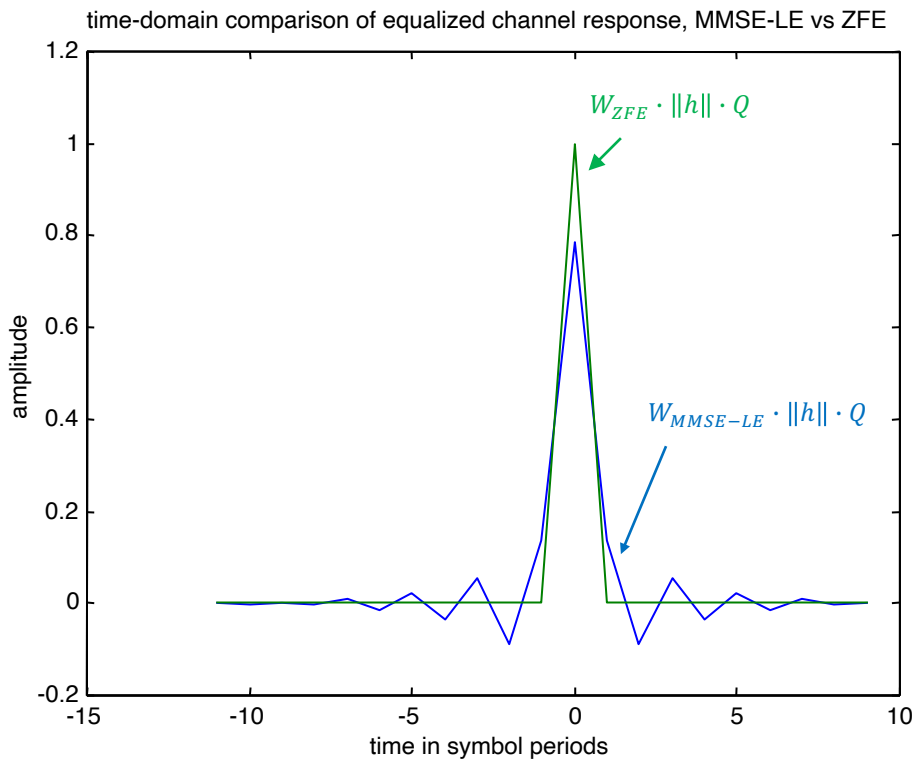

Figure 3.32: Example 3.5.1's equalized time-domain responses for MMSE-LE and ZFE.

This example's relatively small energy near the Nyquist Frequency is the reason for both the MMSE-LE's and the ZFE's poor performance. To improve performance further, decision-assisted equalization is examined in Section 3.6 (or codes combined with equalization, as discussed in Chapter 2). Chapter 4 provides a bettertway to address this channel.

The complex example also follows in a straightforward manner.

EXAMPLE 3.5.2 [QAM - MMSE-LE] Recall that the equivalent baseband pulse response samples were given by

$$h_k = \frac{1}{\sqrt{T}} \cdot \left[-\frac{1}{2} \, , \, \left(1 + \frac{\jmath}{4}\right) \, , \, -\frac{\jmath}{2} \right] \quad . \tag{3.190}$$

Again, $SNR_{MFB} = 10\text{dB}$ $(= \bar{\mathcal{E}}_{\boldsymbol{x}} \cdot \|h\|^2 / \frac{\mathcal{N}_0}{2})$, $\bar{\mathcal{E}}_{\boldsymbol{x}} = 1$, and thus

$$\sigma^2_{MMSE-LE} = w_0 \cdot \frac{\mathcal{N}_0}{2} \cdot \|h\|^{-1} \quad . \tag{3.191}$$

The equalizer is, noting that $\frac{\mathcal{N}_0}{2} = \frac{\bar{\mathcal{E}}_{\boldsymbol{x}} \cdot \|h\|^2}{SNR_{MFB}} = 1.5625/10 = .15625$,

$$W(D) = \frac{1}{(Q(D) + 1/SNR_{MFB}) \cdot \|h\|} \tag{3.192}$$

or

$$= \frac{\sqrt{1.5625}}{-.25\jmath \cdot D^{-2} + .625(-1+\jmath) \cdot D^{-1} + 1.5625(1+.1) - .625(1+\jmath) \cdot D^1 + .25\jmath \cdot D^2} \quad . \tag{3.193}$$

Figure 3.33 compares the MMSE-LE and ZFE equalizer responses for this same channel. The MMSE-LE high response values are considerably more limited than the ZFE values.

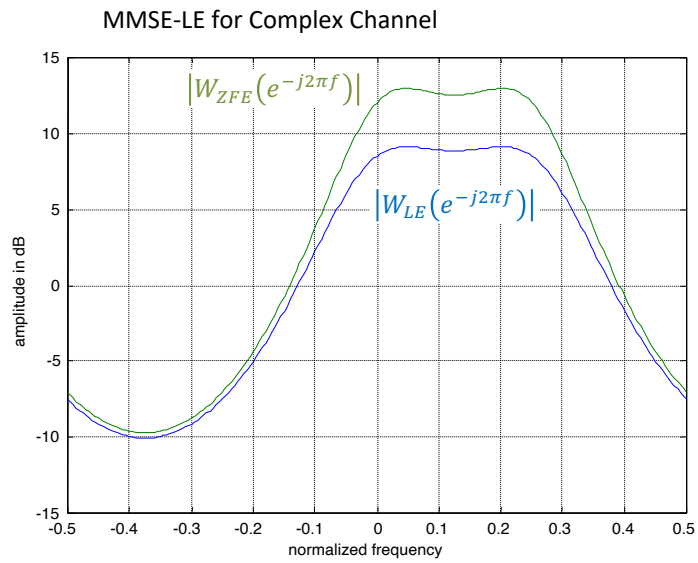

Figure 3.33: Comparison of MMSE-LE and ZFE for complex channel example.

The roots of $Q(D) + 1/SNR_{MFB}$, or of the denominator in (3.193), are

$$D = 2.217\angle^{-1.632} = -.1356 - \jmath 2.213 \tag{3.194}$$
$$D = 2.217\angle^{.0612} = 2.213 + \jmath .1356 \tag{3.195}$$
$$D = .451\angle^{-1.632} = -.0276 - \jmath .4502 \tag{3.196}$$
$$D = .451\angle^{.0612} = .4502 + \jmath .0276 \quad , \tag{3.197}$$

and (3.193) becomes

$$W(D) = \frac{\left[\sqrt{1.5625}D^2/(.25\jmath)\right]}{(D - 2.22\angle^{-1.632})(D - 2.22\angle^{.0612})(D - .451\angle^{-1.632})(D - .451\angle^{.0612})} \tag{3.198}$$

or

$$W(D) = \frac{A}{D - 2.22\angle^{-1.632}} + \frac{B}{D - 2.22\angle^{.0612}} + \ldots \quad , \tag{3.199}$$

where the second expression (3.199) ignores any partial-fraction terms that do not contribute to w_0. Then,

$$\begin{aligned} A &= \frac{\sqrt{1.5625}(-4\jmath)(2.22\angle^{-1.632})^2}{(2.22\angle^{-1.632} - 2.22\angle^{.0612})(2.22\angle^{-1.632} - .451\angle^{-1.632})(2.22\angle^{-1.632} - .451\angle^{.0612})} \\ &= \sqrt{1.5625}(-\jmath .805 + 1.20)\jmath = 1.0079 + \jmath 1.5025 \end{aligned} \tag{3.200}$$

$$\begin{aligned} B &= \frac{\sqrt{1.5625}(-4\jmath)(2.22\angle^{.0612})^2}{(2.22\angle^{.0612} - 2.22\angle^{-1.632})(2.22\angle^{.0612} - .451\angle^{-1.632})(2.22\angle^{.0612} - .451\angle^{.0612})} \\ &= \sqrt{1.5625}(\jmath 1.20 - .805)\jmath = -1.5025 - 1.0079\jmath \quad . \end{aligned} \tag{3.201}$$

Then, from (3.199),

$$w_0 = A(-.451\angle^{1.632}) + B(-.451\angle^{-.0612}) = \sqrt{1.5625}(1.125) \quad . \tag{3.202}$$

Then

$$\sigma^2_{MMSE-LE} = 1.125\frac{\mathcal{N}_0}{2} = 1.125(.15625) = .1758 \quad , \tag{3.203}$$

$$\text{SNR}_{MMSE-LE,U} = \frac{[1 - 1.125(.15625)]}{1.125(.15625)} = 4.69 \text{ (6.7 dB)} \quad , \tag{3.204}$$

which is 3.3 dB below $SNR_{MFB} = 10$ dB, or equivalently,

$$\gamma_{MMSE-LE} = 10 \cdot \log_{10}(10/4.69) = 10 \cdot \log_{10}(2.13) = 3.3 \text{ dB} \quad , \tag{3.205}$$

but .6 dB better than the ZFE. Better designs yet also exist for this channel with structures not yet introduced. Nevertheless, the MMSE-LE is one of the most commonly used equalization structures in practice.

Figure 3.33 compares the equalized channel responses for both the MMSE-LE and ZFE. While the MMSE-LE performs better, there is a significant deviation from the ideal flat response. This deviation is good and gains .6 dB improvement. Also, because of biasing, the MMSE-LE output is everywhere slightly lower than the ZFE output (which is unbiased). This bias can be removed by scaling by 5.69/4.69.

3.5.4 Fractionally Spaced Equalization

Previous developments always insert a matched filter $\varphi_h^*(-t)$ before the sampler, as in Figure 3.9. While this simplifies analysist, there are several practical problems with the matched-filter use. First, $\varphi_h^*(-t)$ is a continuous-time filter and may be much more difficult to design accurately than an equivalent digital filter. Secondly, the precise sampling frequency and especially its phase, must be known so that the signal can be sampled when it is at maximum strength. Third, the receiver may not know the channel pulse response accurately, and the receiver instead uses an adaptive equalizer (see Chapter 7). It may be difficult to design an adaptive, analog, matched filter.

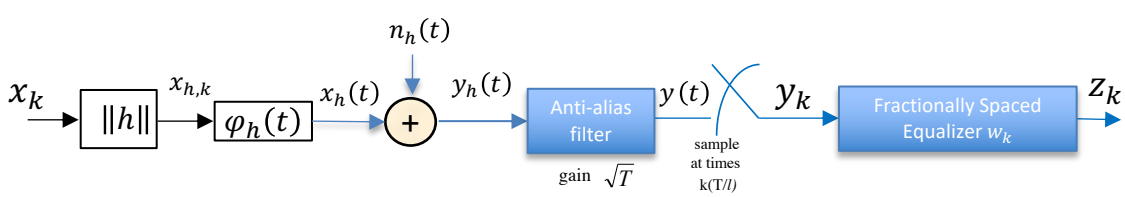

Figure 3.34: Fractionally spaced equalization.

For these reasons, sophisticated data transmission systems often replace Figure 3.9's matched-filter, symbol-rate sampler, and equalizer system with Figure 3.34's **Fractionally Spaced Equalizer (FSE)**. The FSE basically interchanges the sampler and the matched filter. Also the FSE increases the sampling rate by some rational number ℓ ($\ell > 1$). The new sampling rate is sufficiently high to be greater than twice the highest frequency of $x_h(t)$. Then, the matched-filtering operation and the equalization filtering are performed at rate ℓ/T, and the cascade of the two filters is realized as a single filter in practice. An anti-alias or noise-rejection filter always precedes the sampling device (usually an analog-to-digital converter). This text assumes this filter is an ideal lowpass filter with gain $\sqrt{T}$ transfer over the frequency range $-\ell \cdot \frac{\pi}{T} \leq \omega \leq \ell \cdot \frac{\pi}{T}$. The variance of the noise samples at the filter output will then be $\ell \cdot \frac{\mathcal{N}_0}{2}$ per dimension.

In practical systems, the four most commonly found values for ℓ are $\frac{4}{3}$, 2, 3, and 4. The FSE's major drawback is that to span the same interval in time (when implemented as an FIR filter, as is typical in practice), it requires a factor of ℓ more coefficients, leading to a possible increase in memory by a factor of as much as ℓ. The FSE outputs may also appear to be computed ℓ times more often in real time. However, only $\left(\frac{1}{\ell}\right)^{th}$ of the output samples need be computed (that is, those at the symbol rate, as that

is when we need them to make a decision), so computation is approximately ℓ times that of symbol-spaced equalization, corresponding to ℓ times as many coefficients to span the same time interval, or equivalently, to ℓ times as many input samples per symbol.

FSE Timing Phase Improvement: The FSE digitally realizes the cascade of the matched filter and the equalizer, eliminating the need for an analog matched filter. (The entire filter for the FSE can also be easily implemented adaptively, see Chapter 7.) The FSE can also exhibit a significant improvement in sensitivity to sampling-phase errors. To investigate this improvement briefly, the original symbol-spaced equalizers (ZFE or MMSE-LE) may have the sampling-phase on the sampler in error by some small offset t_0. Then, the sampler will sample the matched filter output at times $kT + t_0$, instead of times kT. Then,

$$y(kT + t_0) = \sum_m x_m \cdot \|h\| \cdot q(kT - mT + t_0) + n_k \quad , \tag{3.206}$$

which corresponds to $q(t) \to q(t + t_0)$ or $Q(\omega) \to Q(\omega)e^{-\jmath\omega t_0}$. For the system with sampling offset,

$$Q(e^{-\jmath\omega T}) \to \frac{1}{T} \cdot \sum_n Q(\omega - \frac{2\pi n}{T}) \cdot e^{-\jmath(\omega - \frac{2\pi n}{T})t_0} \quad , \tag{3.207}$$

which is no longer nonnegative real across the entire frequency band. In fact, it is now possible (for certain nonzero timing offsets t_0, and at frequencies just below the Nyquist Frequency) that the two aliased frequency characteristics $Q(\omega) \cdot e^{-\jmath\omega t_0}$ and $Q(\omega - \frac{2\pi}{T}) \cdot e^{-\jmath(\omega - \frac{2\pi}{T})t_0}$add to approximately zero, thus producing a notch within the critical frequency range (-$\frac{\pi}{T}$, $\frac{\pi}{T}$). This notch can significantly reduce the LE and ZFE performance, because of noise enhancement. The loss in performance can be several dB for reasonable timing offsets. When the receiver samples anti-alias filter output at greater than twice the highest frequency in $x_h(t)$, the samples retain full information about the entire signal. Equivalently, the FSE can synthesize, via its transfer characteristic, a phase adjustment (effectively interpolating to the correct phase) so as to correct the timing offset, t_0, in the sampling device. The symbol-spaced equalizer cannot interpolate to the correct phase, because no interpolation is correctly performed at the symbol rate. Equivalently, information has been lost about the signal by sampling at a speed that is too low in the symbol-spaced equalizer without matched filter. This possible notch is an example of information loss at some frequency. In effect, the FSE equalizes before it aliases (aliasing does occur at the output of the equalizer where it decimates by l for symbol-by-symbol detection), whereas the symbol-spaced equalizer aliases before it equalizes; the former alternative is often the one of choice in practical system implementation, if the extra memory and computation can be accommodated. Effectively, with an FSE, the sampling device need only be locked to the symbol rate, but can otherwise provide any sampling phase. The phase is tacitly corrected to the optimum phase inside the linear filter implementing the FSE.

The sensitivity to sampling phase is channel dependent: In particular, there is usually significant channel energy near the Nyquist Frequency in applications that exhibit a significant improvement of the FSE with respect to the symbol-spaced equalizer. In channels with little energy near the Nyquist Frequency, the FSE provides little performance gain, and is significantly more complex to implement (more parameters and higher sampling rate).

Infinite-Length FSE Settings: To derive FSE settings, this section assumes that ℓ, the oversampling factor, is an integer. The anti-alias filter's sampled output decomposes into ℓ sampled-at-rate-$1/T$ interleaved sequences with D-transforms $Y_0(D)$, $Y_2(D)$, ..., $Y_{\ell-1}(D)$, where $Y_\ell(D)$ corresponds to the sample sequence $y[kT - iT/\ell]$. Then,

$$Y_i(D) = H_i(D) \cdot X(D) + N_i(D) \tag{3.208}$$

where $H_i(D)$ is the transform of the symbol-rate-spaced-i^{th}-phase-of-$h(t)$ sequence $h[kT - (i-1)T/l]$, and similarly $N_i(D)$ is the transform of a symbol-rate sampled white noise sequence with autocorrelation function $R_{nn}(D) = l \cdot \frac{\mathcal{N}_0}{2}$ per dimension, and these noise sequences are also independent of one another.

A column vector transform is

$$\boldsymbol{Y}(D) = \begin{bmatrix} Y_0(D) \\ \vdots \\ Y_{\ell-1}(D) \end{bmatrix} = \boldsymbol{H}(D) \cdot X(D) + \boldsymbol{N}(D) \quad . \tag{3.209}$$

Also

$$\boldsymbol{H}(D) \triangleq \begin{bmatrix} H_0(D) \\ \vdots \\ H_{\ell-1}(D) \end{bmatrix} \text{ and } \boldsymbol{N}(D) = \begin{bmatrix} N_0(D) \\ \vdots \\ N_{\ell-1}(D) \end{bmatrix} \quad . \tag{3.210}$$

By considering the FSE output at sampling rate $1/T$, the interleaved FSE coefficients rewrite in a row vector $\boldsymbol{W}(D) = [W_1(D)\ ,...,\ W_l(D)]$. Thus the FSE output is

$$Z(D) = \boldsymbol{W}(D) \cdot \boldsymbol{Y}(D) \quad . \tag{3.211}$$

Again, the orthogonality condition says that $E(D) = X(D) - Z(D)$ should be orthogonal to $Y(D)$, which in vector form is

$$\mathbb{E}\left[E(D) \cdot \boldsymbol{Y}^*(D^{-*})\right] = \boldsymbol{R}_{x\boldsymbol{Y}}(D) - \boldsymbol{W}(D) \cdot \boldsymbol{R}_{\boldsymbol{YY}}(D) = 0 \quad , \tag{3.212}$$

where

$$\boldsymbol{R}_{x\boldsymbol{Y}}(D) \triangleq \mathbb{E}\left[X(D) \cdot \boldsymbol{Y}^*(D^{-*})\right] = \bar{\mathcal{E}}_{\boldsymbol{x}} \cdot \boldsymbol{H}^*(D^{-*}) \tag{3.213}$$

$$\boldsymbol{R}_{\boldsymbol{YY}}(D) \triangleq \mathbb{E}\left[\boldsymbol{Y}(D) \cdot \boldsymbol{Y}^*(D^{-*})\right] = \bar{\mathcal{E}}_{\boldsymbol{x}} \cdot \boldsymbol{H}(D) \cdot \boldsymbol{H}^*(D^{-*}) + \ell \cdot \frac{\mathcal{N}_0}{2} \cdot I \quad . \tag{3.214}$$

MMSE-FSE filter setting is then

$$W(D) = \boldsymbol{R}_{x\boldsymbol{Y}}(D) \cdot \boldsymbol{R}_{\boldsymbol{YY}}^{-1}(D) = \boldsymbol{H}^*(D^{-*}) \cdot \left[\boldsymbol{H}(D) \cdot \boldsymbol{H}^*(D^{-*}) + \ell/SNR\right]^{-1} \quad . \tag{3.215}$$

The corresponding error sequence has autocorrelation function

$$\bar{R}_{ee}(D) = \bar{\mathcal{E}}_{\boldsymbol{x}} - \boldsymbol{R}_{x\boldsymbol{Y}}(D) \cdot \boldsymbol{R}_{\boldsymbol{YY}}^{-1}(D)\boldsymbol{R}_{\boldsymbol{Y}x}(D) = \frac{\ell \cdot \frac{\mathcal{N}_0}{2}}{\boldsymbol{H}^*(D^{-*}) \cdot \boldsymbol{H}(D) + \ell/SNR} \quad . \tag{3.216}$$

The MMSE is then computed as

$$\text{MMSE}_{MMSE-FSE} = \frac{T}{2\pi} \int_{-\frac{\pi}{T}}^{\frac{\pi}{T}} \frac{\ell \cdot \frac{\mathcal{N}_0}{2} d\omega}{\|\boldsymbol{H}(e^{-\jmath\omega T})\|^2 + \ell/SNR} = \text{MMSE}_{MMSE-LE} \quad , \tag{3.217}$$

where $\|\boldsymbol{H}(e^{-\jmath\omega T})\|^2 = \sum_{i=1}^{\ell} |H_i(e^{-\jmath\omega T})|^2$. The SNR's, biased and unbiased, are also then exactly the same as given for the MMSE-LE, as long as the sampling rate exceeds twice the highest frequency of $H(f)$.

The reader is cautioned against letting $\frac{\mathcal{N}_0}{2} \to 0$ to get the ZF-FSE. This is because the matrix $\boldsymbol{R}_{\boldsymbol{YY}}(D)$ will often be singular when this occurs. To avoid problems with singularity, an appropriate pseudoinverse, which zeros the FSE characteristic when $H(\omega) = 0$ is recommended.

3.5.4.1 Passband Equalization

Quadrature modulation methods (for instance Chapter 1's CAP) sometimes use an alternative passband representation. Passband "direct conversion" methods also find use. When ω_c is not too high (or there is intermediate-frequency up/down conversion), filtering can directly implement in passband. Passband equalizers commute the carrier demodulation and filtering, as in Figure 3.35. This can be done with either symbol-spaced or fractionally spaced equalizers, whence combining again matched-filter and equalizer. A reason for this interchange is the recovery of the carrier-frequency recovery. Postponing the carrier demodulation to the equalizer output can significantly improve the system's tolerance carrier-frequency

estimate errors, as Chapter 6 investigates. In the present (perfect carrier phase lock) development, passband equalization and baseband equalization are exactly equivalent and the settings for the passband equalizer are identical to those of the corresponding baseband equalizer, other than a translation in frequency by ω_c radians/sec.

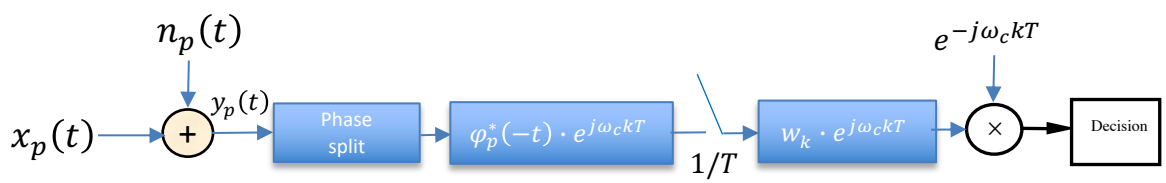

Figure 3.35: Passband equalization, direct synthesis of analytic-equivalent equalizer.

Passband equalization is best suited to CAP implementations (See Chapter 1) where the complex channel is the analytic equivalent. The complex equalizer then acts on the analytic equivalent channel and signals to eliminate ISI in a MMSE sense. When used with CAP, the final rotation shown in Figure 3.35 is not necessary – such a rotation is only necessary with a QAM transmit signal.

Nyquist Inband Implementation: Figure 3.35's phase splitter forms the analytic equivalent with the use of the Hilbert Transform, as discussed in Chapter 1. The linear filter w_k can be a ZFE, a MMSE-LE, or any other desired setting. The equalizer implementation will need ractional spacing if w_k absorbs the matched-filter function. Designers often will also absorb the phase splitters Hilbert transform into the realization also. This is then a **Nyquist Inband Equalization**. A particularly common variant samples both phase-splitter streams at rate $2/T$ and stagger one stream by $T/4$ with respect to the other. The corresponding $T/2$ complex equalizer can then be implemented adaptively with four independent adaptive equalizers (rather than the two filters, real and imaginary part, that nominally characterize complex convolution). The adaptive filters will then correct for any imperfections in the phase-splitting process, whereas the two filters with fixed conjugate symmetry could not.

3.6 Decision Feedback Equalization

Decision Feedback Equalization uses also previous SBS decisions to reduce ISI. The DFE thereby reconstructs and subtracts any "trailing" ISI caused by previously transmitted symbols. Thus, the DFE is inherently a nonlinear receiver. However, analysis is possible with linear techniques under the assumption that all previous decisions are correct. There are both MMSE and ZF DFEs, following Sections 3.4 and 3.5's linear equalization; the zero-forcing solution is a special case of the MMSE-DFE with $SNR \to \infty$. This section then derives the MMSE solution, which subsumes the zero-forcing case when $SNR \to \infty$.

Figure 3.36 illustrates he Decision Feedback Equalizer (DFE). The DFE contains a linear "feedforward equalizer," $W(D)$, (the settings for this linear equalizer are not necessarily the same as those for the ZFE or MMSE-LE), augmented by a linear, causal, **feedback filter**, $1 - B(D)$, where $b_0 = 1$. The feedback filter inputs are the previous symbols' decisions; thus, the name "decision feedback." The feedforward filter output is $Z(D)$, and the SBS decision input is $Z'(D)$. The feedforward filter shapes the channel output signal so that it is a causal minimum-phase signal. The feedback section will then subtract (without noise enhancement) any trailing ISI. Figure 3.36's SBS absorbs any bias removal.

This section assumes that previous decisions are correct. In practice, this may not be true, and can be a significant DFE weakness. Nevertheless, the analysis becomes intractable if it includes decision-error propagation in the feedback section. The most efficient way to study the effect of feedback errors has often been through measurement. Section 3.7 provides an exact error-propagation analysis for finite-length DFE's that can (unfortunately) require enormous computation. Section 3.8.1 introduces precoders to eliminate error propagation.

3.6.1 Minimum-Mean-Square-Error Decision Feedback Equalizer

The **Minimum-Mean-Square Error Decision Feedback Equalizer** (MMSE-DFE) jointly optimizes the settings of both the feedforward filter w_k and the feedback filter $\delta_k - b_k$ to minimize the MSE:

Definition 3.6.1 [Mean Square Error (for DFE)] *The* **MMSE-DFE error** *signal is*

$$e_k = x_k - z'_k \quad . \tag{3.218}$$

The MMSE *for the* MMSE-DFE *is*

$$\sigma^2_{MMSE-DFE} \triangleq \min_{w_k, b_k} \mathbb{E}\left[|x_k - z'_k|^2\right] \quad . \tag{3.219}$$

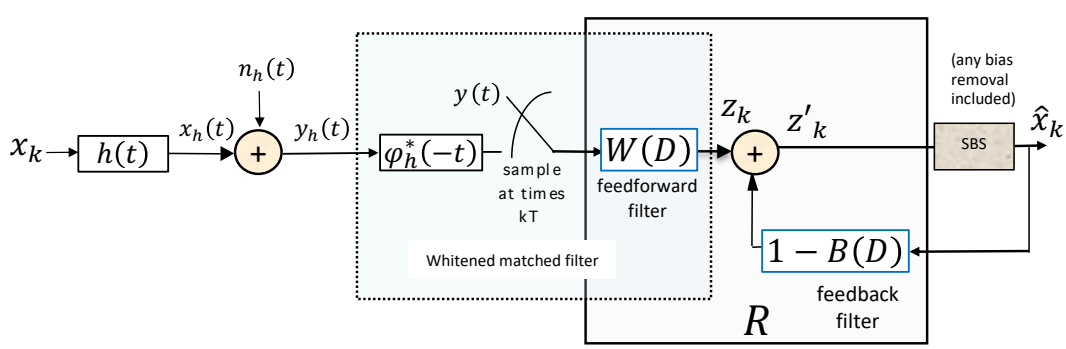

Figure 3.36: Decision feedback equalization.

The error sequence can be written as

$$E(D) = X(D) - W(D) \cdot Y(D) - [1 - B(D)] \cdot X(D) = B(D) \cdot X(D) - W(D) \cdot Y(D) \quad . \tag{3.220}$$

For any fixed $B(D)$, $\mathbb{E}\left[E(D) \cdot Y^*(D^{-*})\right] = 0$ to minimize MSE, which leads to

$$B(D) \cdot \bar{R}_{xy}(D) - W(D) \cdot \bar{R}_{yy}(D) = 0 \quad . \tag{3.221}$$

Thus,

$$W(D) = \frac{B(D)}{\|h\| \cdot \left(Q(D) + \frac{1}{SNR_{MFB}}\right)} = B(D) \cdot W_{\text{MMSE-LE}}(D) \quad , \tag{3.222}$$

for any $B(D)$ with $b_0 = 1$. (Also, $W(D) = W_{\text{MMSE-LE}}(D) \cdot B(D)$, a consequence of the linearity of the MMSE estimate, so that $E(D) = B(D) \cdot E_{\text{MMSE-LE}}(D)$)

Error-sequence autocorrelation: The error-sequence autocorrelation function with arbitrary monic $B(D)$ is

$$\begin{aligned}
\bar{R}_{ee}(D) &= B(D) \cdot \bar{\mathcal{E}}_{\boldsymbol{x}} \cdot B^*(D^{-*}) - 2\Re\left\{B(D) \cdot \bar{R}_{xy}(D) \cdot W^*(D^{-*})\right\} + W(D) \cdot \bar{R}_{yy}(D) \cdot W^*(D^{-*}) \\
&= B(D) \cdot \bar{\mathcal{E}}_{\boldsymbol{x}} \cdot B^*(D^{-*}) - W(D) \cdot \bar{R}_{yy}(D) \cdot W^*(D^{-*}) && (3.223) \\
&= B(D) \cdot \bar{\mathcal{E}}_{\boldsymbol{x}} \cdot B^*(D^{-*}) - B(D) \cdot \frac{\bar{R}_{xy}(D)}{\|h\| \cdot \left(Q(D) + \frac{1}{SNR_{MFB}}\right)} \cdot B^*(D^{-*}) && (3.224) \\
&= B(D) \cdot R_{MMSE-LE}(D) \cdot B^*(D^{-*}) && (3.225)
\end{aligned}$$

where $R_{MMSE-LE}(D) = \frac{\frac{\mathcal{N}_0}{2}}{\|h\|^2} \cdot [1/(Q(D) + 1/SNR_{MFB})]$ is the MMSE-LE error-sequence autocorrelation function. The solution for $B(D)$ is then the forward-prediction filter associated with this error sequence as in Appendix D. Problem 3.8 develops further the linear prediction approach as the "noise predictive DFE," and reorganizes the MMSE-DFE to be the concatenation of a MMSE-LE and a linear-predictor that "whitens" the error sequence.

Canonical factorization: In more detail on $B(D)$, the (scaled) inverse autocorrelation has spectral factorization:

$$Q(D) + \frac{1}{SNR_{MFB}} = \gamma_0 \cdot G(D) \cdot G^*(D^{-*}), \tag{3.226}$$

where γ_0 is a positive real number and $G(D)$ is a canonical filter response. A filter response $G(D)$ is called **canonical** if it is **causal** ($g_k = 0$ for $k < 0$), **monic** ($g_0 = 1$), and **minimum-phase** (all its poles are outside the unit circle, and all its zeroes are on or outside the unit circle). If $G(D)$ is canonical, then $G^*(D^{-*})$ is **anti-canonical**, i.e., anti-causal, monic, and "maximum-phase" (all poles inside the unit circle, and all zeros in or on the unit circle). Using this factorization,

$$\begin{aligned}
\bar{R}_{ee}(D) &= \frac{B(D) \cdot B^*(D^{-*})}{Q(D) + 1/SNR_{MFB}} \cdot \frac{\frac{\mathcal{N}_0}{2}}{\|h\|^2} && (3.227) \\
&= \frac{B(D)}{G(D)} \cdot \frac{B^*(D^{-*})}{G^*(D^{-*})} \cdot \frac{\frac{\mathcal{N}_0}{2}}{\gamma_0 \cdot \|h\|^2} && (3.228) \\
r_{ee,0} &\geq \frac{\frac{\mathcal{N}_0}{2}}{\gamma_0 \cdot \|h\|^2} \quad , && (3.229)
\end{aligned}$$

with equality if and only if $B(D) = G(D)$. Thus, the MMSE will then be $\sigma^2_{MMSE-DFE} = \frac{\frac{\mathcal{N}_0}{2}}{\gamma_0 \cdot \|h\|^2}$. The feedforward filter then becomes

$$W(D) = \frac{G(D)}{\|h\| \cdot \gamma_0 \cdot G(D) \cdot G^*(D^{-*})} = \frac{1}{\|h\| \cdot \gamma_0 \cdot G^*(D^{-*})} \quad . \tag{3.230}$$

The last step in (3.229) follows from the observations that

$$r_{ee,0} = \|\frac{B}{G}\|^2 \frac{\frac{\mathcal{N}_0}{2}}{\gamma_0 \cdot \|h\|^2} \quad , \tag{3.231}$$

the fractional polynomial inside the squared norm is necessary monic and causal, and therefore the squared norm has a minimum value of 1. $B(D)$ and $W(D)$ specify the MMSE-DFE:

Lemma 3.6.1 **[MMSE-DFE]** *The MMSE-DFE has* **feedforward section**

$$W(D) = \frac{1}{\|h\| \cdot \gamma_0 \cdot G^*(D^{-*})} \tag{3.232}$$

(realized with delay, as it is strictly noncausal) and **feedback section**

$$B(D) = G(D) \tag{3.233}$$

where $G(D)$ is the unique **canonical factor** *of:*

$$Q(D) + \frac{1}{SNR_{MFB}} = \gamma_0 \cdot G(D) \cdot G^*(D^{-*}) \quad . \tag{3.234}$$

*This text also calls the joint matched-filter/sampler/$W(D)$ combination in the forward path of the DFE the "***Mean-Square Whitened Matched Filter (MS-WMF)***". These settings for the MMSE-DFE minimize the MSE as was shown above.*

3.6.2 MMSE-DFE Performance Analysis

Again, the MMSE-DFE error-sequence autocorrelation function is

$$\bar{R}_{ee}(D) = \frac{\frac{\mathcal{N}_0}{2}}{\gamma_0 \cdot \|h\|^2} \quad . \tag{3.235}$$

Thus, the minimized MMSE-DFE error sequence is "white" (since $\bar{R}_{ee}(D)$ is a constant) and has MMSE or average energy (per real dimension) $\frac{\frac{\mathcal{N}_0}{2}}{\|h\|^2}\gamma_0^{-1}$. Also,

$$\begin{aligned} \frac{T}{2\pi}\int_{-\frac{\pi}{T}}^{\frac{\pi}{T}} \ln\left(Q(e^{-\jmath\omega T}) + \frac{1}{SNR_{MFB}}\right) \cdot d\omega &= \ln(\gamma_0) + \frac{T}{2\pi}\int_{-\frac{\pi}{T}}^{\frac{\pi}{T}} \ln\left(G(e^{-\jmath\omega T}) \cdot G^*(e^{-\jmath\omega T})\right) \cdot d\omega \\ &= \ln(\gamma_0) \quad . \end{aligned} \tag{3.236}$$

(The last line follows from $\ln\left(G(e^{-\jmath\omega T})\right)$ being a periodic function integrated over one period of its fundamental frequency, and similarly for $\ln\left(G^*(e^{-\jmath\omega T})\right)$.) This last result leads to a famous expression for $\sigma^2_{MMSE-DFE}$, which was first derived by Salz in 1977 [4],

$$\sigma^2_{MMSE-DFE} = \frac{\frac{\mathcal{N}_0}{2}}{\|h\|^2} \cdot e^{-\frac{T}{2\pi}\int_{-\frac{\pi}{T}}^{\frac{\pi}{T}} \ln\left(Q(e^{-\jmath\omega T}) + \frac{1}{SNR_{MFB}}\right) \cdot d\omega} \quad . \tag{3.237}$$

MMSE-DFE SNR: The MMSE-DFE's SNR follows easily as

$$SNR_{MMSE-DFE} = \frac{\bar{\mathcal{E}}_{\boldsymbol{x}}}{\sigma^2_{MMSE-DFE}} = \gamma_0 \cdot SNR_{MFB} \tag{3.238}$$

$$= SNR_{MFB} \cdot e^{\frac{T}{2\pi}\int_{-\frac{\pi}{T}}^{\frac{\pi}{T}} \ln\left(Q(e^{-\jmath\omega T}) + \frac{1}{SNR_{MFB}}\right) \cdot d\omega} \quad . \tag{3.239}$$

From the $k = 0$ term in (3.234), γ_0 is also

$$\gamma_0 = \frac{1 + 1/SNR_{MFB}}{\|g\|^2} = \frac{1 + 1/SNR_{MFB}}{1 + \sum_{i=1}^{\infty} |g_i|^2} \quad . \tag{3.240}$$

From this expression with $G(D) = 1$ (no ISI), then $SNR_{MMSE-DFE} = SNR_{MFB} + 1$, which again illustrates the bias in MMSE equalizer estimates.

Bias Calculation: This bias follows directly from

$$\begin{aligned}
Z'(D) &= X(D) - E(D) && (3.241)\\
&= X(D) - G(D) \cdot X(D) + \frac{1}{\|h\| \cdot \gamma_0 \cdot G^*(D^{-*})} \cdot Y(D) && (3.242)\\
&= X(D) - G(D) \cdot X(D) + \frac{Q(D)}{\gamma_0 \cdot G^*(D^{-*})} \cdot X(D) + N(D) \cdot \frac{1}{\|h\| \cdot \gamma_0 \cdot G^*(D^{-*})} && (3.243)\\
&= X(D) - \frac{1/SNR_{MFB}}{\gamma_0 \cdot G^*(D^{-*})} \cdot X(D) + N(D) \cdot \frac{1}{\|h\| \cdot \gamma_0 \cdot G^*(D^{-*})} \quad . && (3.244)
\end{aligned}$$

The current sample, x_k, corresponds to the time zero sample of $1 - \frac{1/SNR_{MFB}}{\gamma_0 \cdot G^*(D^{-*})}$, and is equal to $(1 - \frac{1}{SNR_{MMSE-DFE}}) \cdot x_k$. Thus z'_k contains a signal component of x_k that is reduced in magnitude. Thus, again using the result from Section 3.2.1, the SNR corresponding to the lowest probability of error corresponds to the same MMSE-DFE receiver with output scaled to remove the bias. This leads to the more informative SNR

$$SNR_{MMSE-DFE,U} = SNR_{MMSE-DFE} - 1 = \gamma_0 \cdot SNR_{MFB} - 1 \quad . \tag{3.245}$$

If $G(D) = 1$, then $SNR_{MMSE-DFE,U} = SNR_{MFB}$. Also,

$$\gamma_{MMSE-DFE} = \frac{SNR_{MMSE-DFE,U}}{SNR_{MFB}} = \frac{\gamma_0 \cdot SNR_{MFB} - 1}{SNR_{MFB}} = \gamma_0 - 1/SNR_{MFB} \quad . \tag{3.246}$$

Feedforward Bias-Removal Alternative: Rather than scale the decision input, the receiver scales (up) the feedforward output by $\frac{1}{1 - \frac{1}{SNR_{MMSE-DFE}}}$. This removes the bias, but also increases MSE by the square of the same factor. The SNR will then be $SNR_{MMSE-DFE,U}$. This result is verified by writing the MS-WMF output

$$Z(D) = [X(D) \cdot \|h\| \cdot Q(D) + N(D)] \cdot \frac{1}{\|h\| \cdot \gamma_0 \cdot G^*(D^{-*})} \tag{3.247}$$

where $N(D)$, again, has autocorrelation $\bar{R}_{nn}(D) = \frac{\mathcal{N}_0}{2} \cdot Q(D)$. $Z(D)$ expands to

$$\begin{aligned}
Z(D) &= [X(D) \cdot \|h\| \cdot Q(D) + N(D)] \frac{1}{\|h\| \cdot \gamma_0 \cdot G^*(D^{-*})} && (3.248)\\
&= X(D) \cdot \frac{\gamma_0 \cdot G(D) \cdot G^*(D^{-*}) - 1/SNR_{MFB}}{\gamma_0 \cdot G^*(D^{-*})} + N(D) \frac{1}{\|h\| \cdot \gamma_0 \cdot G^*(D^{-*})} && (3.249)\\
&= X(D) \cdot G(D) - \frac{X(D)}{SNR_{MFB} \cdot \gamma_0 \cdot G^*(D^{-*})} + N'(D) && (3.250)\\
&= X(D) \cdot \left[G(D) - \frac{1}{SNR_{MMSE-DFE}}\right] + \frac{1}{SNR_{MMSE-DFE}} \left[1 - \frac{1}{G^*(D^{-*})}\right] X(D) + N'(D)\\
&= X(D) \cdot \left[G(D) - \frac{1}{SNR_{MMSE-DFE}}\right] + E'(D) \quad , && (3.251)
\end{aligned}$$

where $N'(D)$ is the filtered noise at the MS-WMF output, which has autocorrelation function

$$\bar{R}_{n'n'}(D) = \frac{\frac{\mathcal{N}_0}{2} \cdot Q(D)}{\|h\|^2 \cdot \gamma_0^2 \cdot G(D) \cdot G^*(D^{-*})} = \frac{\bar{\mathcal{E}}_{\boldsymbol{x}}}{SNR_{MMSE-DFE}} \left[1 - \frac{1/SNR_{MFB}}{Q(D) + 1/SNR_{MFB}}\right] \quad , \tag{3.252}$$

and

$$e'_k = -e_k + \frac{1}{SNR_{MMSE-DFE}} \cdot x_k \quad . \tag{3.253}$$

The error e'_k is not a white sequence in general. Since x_k and e'_k are uncorrelated, $\sigma_e^2 = \sigma_{MMSE-DFE}^2 = \sigma_{e'}^2 + \frac{\bar{\mathcal{E}}_{\boldsymbol{x}}}{SNR_{MMSE-DFE}^2}$.

Unbiased Feedback Section: An "unbiased" monic, causal polynomial is

$$G_U(D) = 1 + \frac{SNR_{MMSE-DFE}}{SNR_{MMSE-DFE,U}} \cdot [G(D) - 1] \quad , \tag{3.254}$$

then the MMSE-DFE output is

$$Z(D) = \frac{SNR_{MMSE-DFE,U}}{SNR_{MMSE-DFE}} \cdot X(D) \cdot G_U(D) + E'(D) \quad . \tag{3.255}$$

$Z_U(D)$ removes the scaling

$$Z_U(D) = Z(D) \cdot \frac{SNR_{MMSE-DFE}}{SNR_{MMSE-DFE,U}} = X(D) \cdot G_U(D) + E_U(D) \quad , \tag{3.256}$$

where $E_U(D) = \frac{SNR_{MMSE-DFE}}{SNR_{MMSE-DFE,U}} \cdot E'(D)$ and has energy

$$\begin{aligned}
\sigma_{e_U}^2 &= \left(\sigma_{MMSE-DFE}^2 - \frac{\bar{\mathcal{E}}_{\boldsymbol{x}}}{SNR_{MMSE-DFE}^2}\right) \cdot \left(\frac{SNR_{MMSE-DFE}}{SNR_{MMSE-DFE,U}}\right)^2 && (3.257)\\
&= \frac{SNR_{MMSE-DFE}^2 \cdot \sigma_{MMSE-DFE}^2 - \bar{\mathcal{E}}_{\boldsymbol{x}}}{SNR_{MMSE-DFE}^2} \cdot \frac{SNR_{MMSE-DFE}^2}{SNR_{MMSE-DFE,U}^2} && (3.258)\\
&= \frac{\bar{\mathcal{E}}_{\boldsymbol{x}} \cdot [(SNR_{MMSE-DFE}/\bar{\mathcal{E}}_{\boldsymbol{x}}) \cdot SNR_{MMSE-DFE} \cdot \sigma_{MMSE-DFE}^2 - 1]}{SNR_{MMSE-DFE,U}^2} && (3.259)\\
&= \frac{\bar{\mathcal{E}}_{\boldsymbol{x}} \cdot [SNR_{MMSE-DFE} - 1]}{SNR_{MMSE-DFE,U}^2} && (3.260)\\
&= \frac{\bar{\mathcal{E}}_{\boldsymbol{x}}}{SNR_{MMSE-DFE,U}} \quad . && (3.261)
\end{aligned}$$

This new unbiased MMSE-DFE has SNR $\frac{\bar{\mathcal{E}}_{\boldsymbol{x}}}{\bar{\mathcal{E}}_{\boldsymbol{x}}/SNR_{MMSE-DFE,U}} = SNR_{MMSE-DFE,U}$. The feedback section is $1 - G_U(D)$, if the scaling occurs before the summing junction, but is $1 - G(D)$ if scaling occurs after the summing junction. Figure 3.37 shows the alternative unbiased MMSE-DFE.

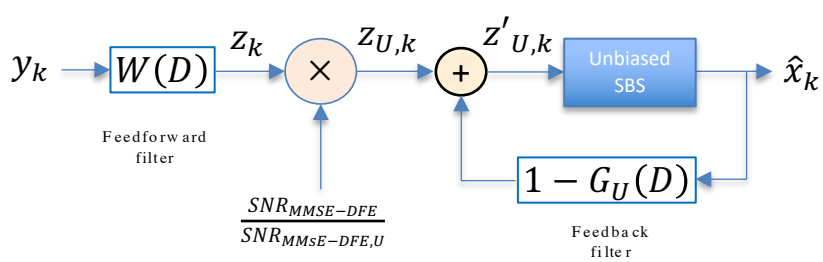

Figure 3.37: Decision feedback equalization with unbiased feedback filter.

All the results on fractional spacing for the LE still apply to the DFE's feedforward section, albeit now for the DFE's W_K. Again, any feedforward filter's realization is either with a matched filter and symbol-spaced sampling or with an anti-alias filter and fractionally spaced sampling, as in Section 3.5.4.

3.6.3 Zero-Forcing DFE

A designer finds the ZF-DFE feedforward and feedback filters by setting $SNR_{MFB} \to \infty$ in the MMSE-DFE expressions. The spectral factorization (assuming $\ln(Q(e^{\jmath\omega T})$ is integrable over $(-\frac{\pi}{T}, \frac{\pi}{T})$, see Appendix D)

$$Q(D) = \eta_0 \cdot P_c(D) \cdot P_c^*(D^{-*}) \tag{3.262}$$

then determines the ZF-DFE filters as

$$B(D) = P_c(D) \quad , \tag{3.263}$$

$$W(D) = \frac{1}{\eta_0 \cdot \|h\| \cdot P_c^*(D^{-*})} \quad . \tag{3.264}$$

P_c is sometimes called a **canonical pulse response** for the channel. Since $q_0 = 1 = \eta_0 \cdot \|P_c\|^2$, then

$$\eta_0 = \frac{1}{1 + \sum_{i=1}^{\infty} |p_{c,i}|^2} \quad . \tag{3.265}$$

Equation (3.265) shows that there is a signal energy loss of the ratio of the squared first tap magnitude in the canonical pulse response to the squared norm of all the taps. This loss ratio is minimized for a minimum-phase polynomial, and $P_c(D)$ is the minimum-phase equivalent of the channel pulse response. The noise at the output of the feedforward filter has (white) autocorrelation function $\frac{\mathcal{N}_0}{2}/(\|p\|^2 \cdot \eta_0)$, so that

$$\sigma^2_{ZFDFE} = \frac{\frac{\mathcal{N}_0}{2}}{\|h\|^2} \cdot \frac{1}{\eta_0} = \frac{\frac{\mathcal{N}_0}{2}}{\|h\|^2} e^{-\frac{T}{2\pi}\int_{-\frac{\pi}{T}}^{\frac{\pi}{T}} \ln\left(Q(e^{\jmath\omega T})\right) d\omega} \quad . \tag{3.266}$$

The corresponding SNR is then

$$SNR_{ZF-DFE} = \eta_0 \cdot SNR_{MFB} = \frac{1}{1 + \sum_{i=1}^{\infty} |p_{c,i}|^2} \cdot SNR_{MFB} \quad . \tag{3.267}$$

3.6.4 Examples Revisited

EXAMPLE 3.6.1 [PAM - DFE] The pulse response of a channel used with binary PAM is again given by

$$H(\omega) = \begin{cases} \sqrt{T} \cdot \left(1 + .9 \cdot e^{\jmath\omega T}\right) & |\omega| \le \frac{\pi}{T} \\ 0 & |\omega| > \frac{\pi}{T} \end{cases} \quad . \tag{3.268}$$

Again, the $SNR_{MFB} = 10$ dB and $\mathcal{E}_{\boldsymbol{x}} = 1$.

Then $\tilde{Q}(D) \triangleq Q(D) + 1/SNR_{MFB}$ is

$$\tilde{Q}(e^{-\jmath\omega T}) = \frac{1.81 + 1.8 \cdot \cos(\omega T) + 1.81/10}{1.81} \tag{3.269}$$

$$\tilde{Q}(D) = \frac{1}{1.81} \cdot (1 + .9 \cdot D)(1 + .9 \cdot D^{-1}) + .1 \tag{3.270}$$

$$= \frac{1}{1.81}\left(.9 \cdot D + 1.991 + .9 \cdot D^{-1}\right) \quad . \tag{3.271}$$

The roots of $\tilde{Q}(D)$ are $-.633$ and -1.58. The function $\tilde{Q}(D)$ has canonical factorization

$$\tilde{Q}(D) = .785 \cdot (1 + .633 \cdot D)(1 + .633 \cdot D^{-1}) \quad . \tag{3.272}$$

Then, $\gamma_0 = .785$. The feedforward section is

$$W(D) = \frac{1}{\sqrt{1.81}(.785)(1 + .633 \cdot D^{-1})} = \frac{.9469}{1 + .633 \cdot D^{-1}} \quad , \tag{3.273}$$

and the feedforward filter transfer function appears in Figure 3.38.

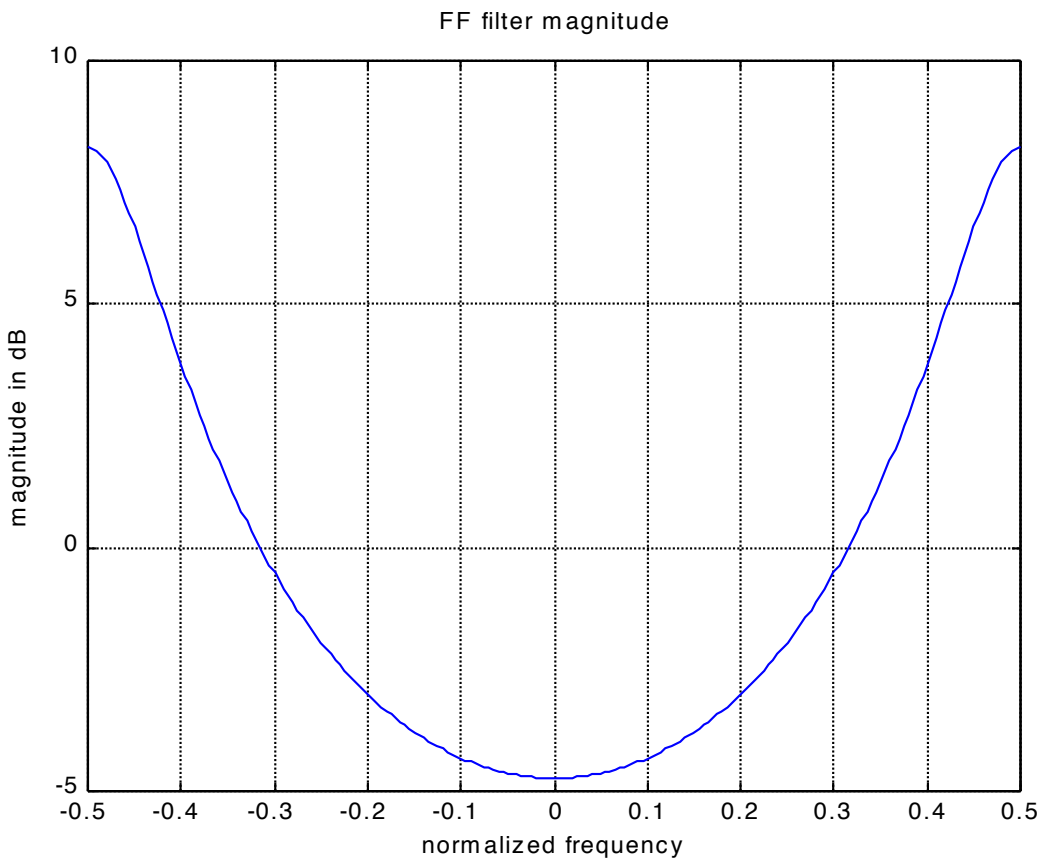

Figure 3.38: Feedforward filter transfer function for real-channel example.

The feedback section is

$$B(D) = G(D) = 1 + .633D \quad , \tag{3.274}$$

with magnitude in Figure 3.39. The MS-WMF filter transfer function appears in Figure 3.40, illustrating the near all-pass character of this filter. The MMSE is

$$\sigma^2_{MMSE-DFE} = \frac{\mathcal{N}_0}{2}\frac{1}{\|p\|^2\gamma_0} = \cdot\frac{.181}{1.81 \cdot .785} = .1274 \tag{3.275}$$

and

$$SNR_{MMSE-DFE,U} = \frac{1 - .1274}{.1274} = 6.85 \;\; (8.4\text{dB}) \quad . \tag{3.276}$$

Thus, the MMSE-DFE is only 1.6dB below the MFB on this channel. However, the ZF-DFE for this same channel would produce $\eta_0 = 1/\|p_c\|^2$=.5525. In this case $\sigma^2_{ZFDFE} = .181/(.5525)1.81 = .181$ and the loss with respect to the MFB would be $\eta_0 = 2.6$ dB, 1 dB lower than the MMSE-DFE for this channel.

It will in fact be possible to do yet better on this channel, using sequence detection, as discussed in Chapter 9, and/or by codes (Chapters 10 and 11). However, what originally appeared as a a stunning loss of 9.8 dB with the ZFE has now been reduced to a much smaller 1.6 dB.

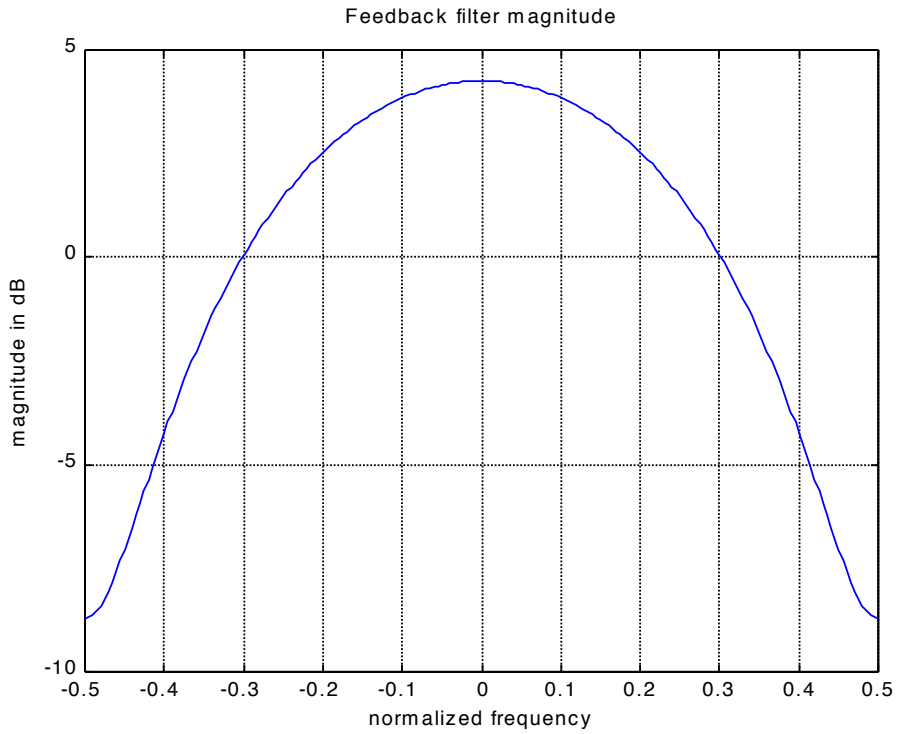

Figure 3.39: Feedback filter transfer function for real-channel example.

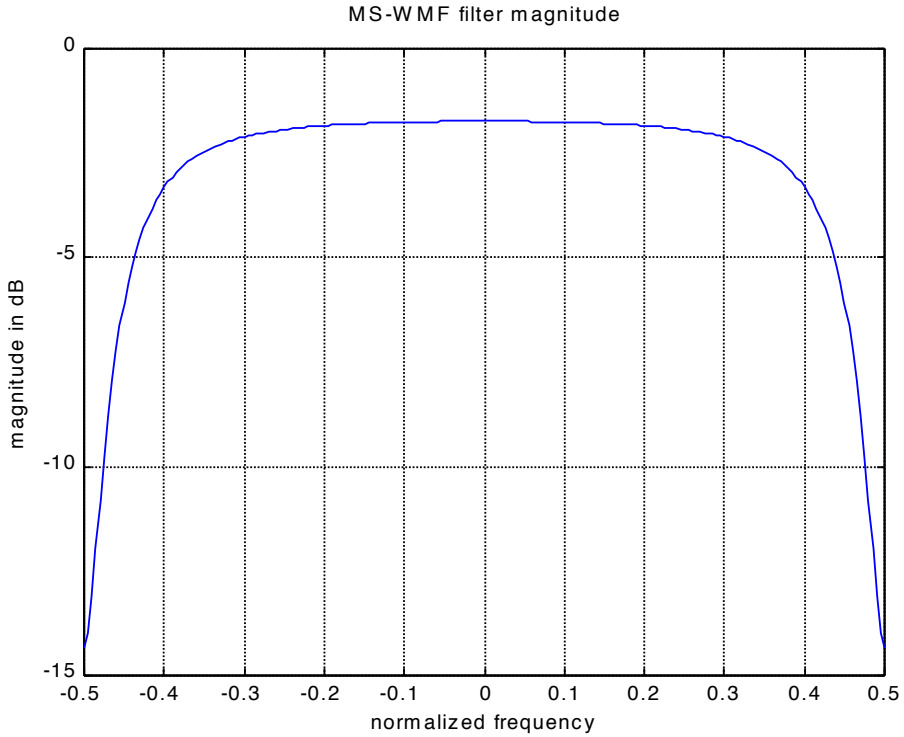

Figure 3.40: MS-WMF transfer function for real-channel example.

The QAM example is also revisited here:

EXAMPLE 3.6.2 [QAM - DFE] Recall that the equivalent baseband pulse response samples were given by

$$h_k = \frac{1}{\sqrt{T}} \cdot \left[-\frac{1}{2} \quad \left(1 + \frac{\jmath}{4}\right) \quad -\frac{\jmath}{2} \right] \quad . \tag{3.277}$$

The $SNR_{MFB} = 10$ dB. Then,

$$\tilde{Q} = \frac{-.25\jmath \cdot D^{-2} + .625(-1+\jmath) \cdot D^{-1} + 1.5625(1+.1) - .625(1+\jmath) \cdot D + .25\jmath \cdot D^2}{1.5625} \quad . \tag{3.278}$$

or

$$\begin{aligned} \tilde{Q} &= (1 - .451\angle^{1.632} D)(1 - .451\angle^{-.0612} D)(1 - .451\angle^{-1.632} D^{-1})(1 - .451\angle^{.0612} D^{-1}) \cdot \\ &\cdot \frac{-\jmath}{1.5625 \cdot 4 \cdot (.451\angle^{-1.632})(.451\angle^{.0612})} \quad . \end{aligned} \tag{3.279}$$

Thus with algebra, $\gamma_0 = .7865$ and $G(D) = 1 - .4226(1+\jmath) \cdot D + .2034\jmath \cdot D^2$. The feedforward and feedback sections follow straightforwardly as

$$B(D) = G(D) = 1 - .4226(1+\jmath) \cdot D + .2034\jmath \cdot D^2 \tag{3.280}$$

and

$$W(D) = \frac{1.017}{1 - .4226(1-\jmath) \cdot D^{-1} - .2034\jmath \cdot D^{-2}} \quad . \tag{3.281}$$

The MSE is

$$\sigma^2_{MMSE-DFE} = (.15625)\frac{1}{.7865(1.5625)} = .1271 \quad . \tag{3.282}$$

and the corresponding SNR is

$$SNR_{MMSE-DFE,U} = \frac{1}{.1271} - 1 = 8.4\text{dB} \quad . \tag{3.283}$$

The loss is (also coincidentally) 1.6 dB with respect to the MFB and is 1.7 dB better than the MMSE-LE on this channel.

For the ZF-DFE,

$$Q(D) = (1 - .5\angle^{\pi/2} D)(1 - .5 \cdot D)(1 - .5\angle^{-\pi/2} \cdot D^{-1})(1 - .5 \cdot D^{-1}) \cdot \tag{3.284}$$

$$\cdot \frac{-\jmath}{1.5625 \cdot 4 \cdot (.5\angle^{-\pi/2})(.5)} \tag{3.285}$$

and thus $\eta_0 = .6400$ and $P_c(D) = 1 - .5(1+\jmath) \cdot D + .25\jmath \cdot D^2$. The feedforward and feedback sections can be computed in a straightforward manner, as

$$B(D) = P_c(D) = 1 - .5 \cdot (1+\jmath) \cdot D + .25\jmath \cdot D^2 \tag{3.286}$$

and

$$W(D) = \frac{1.25}{1 - .5(1-\jmath) \cdot D^{-1} - .25\jmath \cdot D^{-2}} \quad . \tag{3.287}$$

The output noise variance is

$$\sigma^2_{ZFDFE} = (.15625)\frac{1}{.6400(1.5625)} = .1563 \quad . \tag{3.288}$$

and the corresponding SNR is

$$SNR_{ZFDFE} = \frac{1}{.1563} = 6.4 = 8.0\text{dB} \quad . \tag{3.289}$$

The loss is 2.0 dB with respect to the MFB and is .4 dB worse than the MMSE-DFE.

3.7 Finite Length Equalizers

The previous section's discrete-time equalizers admit infinite-length filtering. Practice often implements equalization filters, w_k, as finite-impulse-response (FIR) filters. Usually FIR structures have better numerical properties than IIR structures. Even more importantly, adaptive equalizers (see Section 3.8 and Chapter 7) often use FIR structures for w_k (and also for b_k, with the adaptive DFE). This section studies FIR equalizer's design and analyses their performance.

Both the FIR LE and DFE cases have zero-forcing and least-squares designs. This section describes MMSE design and then examines SNR$\rightarrow \infty$ to obtain the zero-forcing special case with some FIR adjustments. Because of the finite length, the FIR ZFE cannot completely eliminate ISI in general.

3.7.1 FIR MMSE-LE

Returning to Figure 3.34's FSE, the FIR receiver also implements both matched filter and equalizater digitally at sampling rate ℓ/T as a single filter. Perfect anti-alias filtering with constant gain $\sqrt{T}$ precedes the sampler, and the combined pulse-response/anti-alias filter is $h(t)$. The assumption that $\ell \in \mathbb{Z}^+$ simplifies matrix specification.

One view of the oversampled channel output is as a set of ℓ parallel T-spaced subchannels whose pulse responses are offset by T/ℓ from each other as in Figure 3.41.

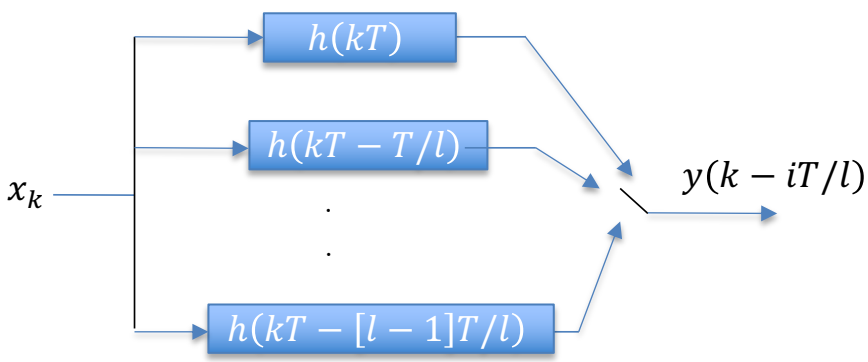

Figure 3.41: Polyphase subchannel representation of the channel pulse response.

Each subchannel produces one of the ℓ filter-output phases per symbol period at sampling rate ℓ/T. The channel output $y(t)$ is

$$y(t) = \sum_m x_m \cdot h(t - mT) + n(t) \quad , \tag{3.290}$$

which, if sampled at time instants $t = kT - \frac{iT}{\ell}$, $i = 0, ..., \ell - 1$, becomes

$$y(kT - \frac{iT}{\ell}) = \sum_{m=-\infty}^{\infty} x_m \cdot h(kT - \frac{iT}{\ell} - mT) + n(kT - \frac{iT}{\ell}) \quad . \tag{3.291}$$

The (per-dimensional) sampled-noise variance is $\frac{\mathcal{N}_0}{2} \cdot \ell$ because $h(t)$ absorbes the anti-alias filter gain, $\sqrt{T}$. Mathematically, it is convenient to represent such a system with vectors. The ℓ phases per symbol period of the oversampled $y(t)$ define the vector

$$\boldsymbol{y}_k = \begin{bmatrix} y(kT) \\ y(kT - \frac{T}{\ell}) \\ \vdots \\ y(kT - \frac{\ell-1}{\ell}T) \end{bmatrix} \quad . \tag{3.292}$$

The vector $\boldsymbol{y}_k$ can be written as

$$\boldsymbol{y}_k = \sum_{m=-\infty}^{\infty} x_m \cdot \boldsymbol{h}_{k-m} + \boldsymbol{n}_k = \sum_{m=-\infty}^{\infty} x_{k-m} \cdot \boldsymbol{h}_m + \boldsymbol{n}_k \quad , \tag{3.293}$$

where

$$\boldsymbol{h}_k = \begin{bmatrix} h(kT) \\ h(kT - \frac{T}{\ell}) \\ \vdots \\ h(kT - \frac{\ell-1}{\ell}T) \end{bmatrix} \quad \text{and} \quad \boldsymbol{n}_k = \begin{bmatrix} n(kT) \\ n(kT - \frac{T}{\ell}) \\ \vdots \\ n(kT - \frac{\ell-1}{\ell}T) \end{bmatrix} \tag{3.294}$$

The design assumes the response $h(t)$ extends only over a finite time interval. In practice, this assumption requires any nonzero component of $h(t)$ outside of this time interval to be negligible. This time interval is $0 \le t \le \nu T$. Thus, $\boldsymbol{h}_k = 0$ for $k < 0$, and for $k > \nu$. The sum in (3.291) becomes

$$\boldsymbol{y}_k = [\ \boldsymbol{h}_0 \ \ \boldsymbol{h}_1 \ , ..., \ \boldsymbol{h}_\nu \ ] \begin{bmatrix} x_k \\ x_{k-1} \\ \vdots \\ \vdots \\ x_{k-\nu} \end{bmatrix} + \boldsymbol{n}_k \quad . \tag{3.295}$$

Each row in (3.295) corresponds to a sample at the output of one of the filters in Figure 3.41. More generally, for N_f successive ℓ-tuples of samples of $y(t)$,

$$\boldsymbol{Y}_k \triangleq \begin{bmatrix} \boldsymbol{y}_k \\ \boldsymbol{y}_{k-1} \\ \vdots \\ \boldsymbol{y}_{k-N_f+1} \end{bmatrix} \tag{3.296}$$

$$= \begin{bmatrix} \boldsymbol{h}_0 & \boldsymbol{h}_1 & ... & \boldsymbol{h}_\nu & 0 & 0 & ... & 0 \\ 0 & \boldsymbol{h}_0 & \boldsymbol{h}_1 & ... & ... & \boldsymbol{h}_\nu & ... & 0 \\ \vdots & \vdots & \ddots & \ddots & \ddots & \ddots & \vdots & \\ 0 & ... & 0 & 0 & \boldsymbol{h}_0 & \boldsymbol{h}_1 & ... & \boldsymbol{h}_\nu \end{bmatrix} \begin{bmatrix} x_k \\ x_{k-1} \\ \vdots \\ \vdots \\ x_{k-N_f-\nu+1} \end{bmatrix} + \begin{bmatrix} \boldsymbol{n}_k \\ \boldsymbol{n}_{k-1} \\ \vdots \\ \boldsymbol{n}_{k-N_f+1} \end{bmatrix} \quad . \tag{3.297}$$

This text uses $\boldsymbol{H}$ to denote the large $(N_f \cdot \ell) \times (N_f + \nu)$ matrix in (3.297), while $\boldsymbol{X}_k$ denotes the data vector, and $\boldsymbol{N}_k$ denotes the noise vector. Then, the oversampled vector representation of the channel is

$$\boldsymbol{Y}_k = \boldsymbol{H} \cdot \boldsymbol{X}_k + \boldsymbol{N}_k \quad . \tag{3.298}$$

When $\ell = n/m$ (a rational fraction), then (3.298) still holds with $\boldsymbol{H}$ an $[N_f \cdot \frac{n}{m}] \times (N_f + \nu)$ matrix that does not follow the form in (3.297), with each row possibly having a set of coefficients unrelated to the other rows.[13]

An equalizer processes the sampled channel output vector $\boldsymbol{Y}_k$ by taking the inner product of an $(N_f \cdot \ell)$-dimensional row vector of equalizer coefficients, $\boldsymbol{w}$, and $\boldsymbol{Y}_k$, so $Z(D) = W(D) \cdot Y(D)$ can be written

$$z_k = \boldsymbol{w} \cdot \boldsymbol{Y}_k \quad . \tag{3.299}$$

For causal practical implementation, the designer picks a channel-equalizer system delay $\Delta \cdot T$ symbol periods,

$$\Delta \approx \frac{\nu + N_f}{2} \quad , \tag{3.300}$$

[13] In this case, (3.290) is used to compute each row at the appropriate sampling instants. $N_f \cdot \frac{n}{m}$ should also be an integer so that $\boldsymbol{H}$ is constant. Otherwise, $\boldsymbol{H}$ becomes a "time-varying" matrix $\boldsymbol{H}_k$.

with the exact value being of little consequence unless the equalizer length N_f is very short. This delay allows time for the transmit data symbol to reach the receiver in real (causal) deployment. With infinite-length filters, the need for such a delay does not enter the mathematics because the infinite-length filters are not realizable, so that infinite-length analysis simply provides best performance bounds. Δ is approximately the sum of the channel and equalizer delays in symbol periods. The equalizer output error is then

$$e_k = x_{k-\Delta} - z_k \quad , \tag{3.301}$$

and the corresponding MSE is

$$\sigma^2_{MMSE-LE} = \mathbb{E}\left\{|e_k|^2\right\} = \mathbb{E}\left\{e_k \cdot e_k^*\right\} = \mathbb{E}\left\{(x_{k-\Delta} - z_k)\cdot(x_{k-\Delta} - z_k)^*\right\} \quad . \tag{3.302}$$

Using the Orthogonality Principle of Appendix D.2, the MSE in (3.302) is minimimun when

$$\mathbb{E}\left\{e_k \cdot \boldsymbol{Y}_k^*\right\} = 0 \quad . \tag{3.303}$$

Thus, the best equalizer setting occurs when the equalizer error signal is uncorrelated with any channel output sample upon which the FIR MMSE-LE acts. Thus

$$\mathbb{E}\left\{x_{k-\Delta} \cdot \boldsymbol{Y}_k^*\right\} - \boldsymbol{w} \cdot \mathbb{E}\left\{\boldsymbol{Y}_k \cdot \boldsymbol{Y}_k^*\right\} = 0 \quad . \tag{3.304}$$

Equation (3.304)'s two quantities (both $y(t)$ and x_k remain stationary)are Appendix D's: per-dimensional **FIR MMSE** autocorrelation matrix

$$\boldsymbol{R}_{\boldsymbol{YY}} \stackrel{\Delta}{=} \mathbb{E}\left\{\boldsymbol{Y}_k \cdot \boldsymbol{Y}_k^*\right\} \quad , \tag{3.305}$$

and per-dimensional **FIR MMSE-LE** cross correlation vector

$$\boldsymbol{R}_{\boldsymbol{Y}x} \stackrel{\Delta}{=} \mathbb{E}\left\{\boldsymbol{Y}_k \cdot x_{k-\Delta}^*\right\} \quad . \quad , \tag{3.306}$$

Note $\boldsymbol{R}_{x\boldsymbol{Y}} = \boldsymbol{R}^*_{\boldsymbol{Y}x}$, and $\boldsymbol{R}_{\boldsymbol{YY}}$ is not a function of Δ.

The MMSE-LE then directly follows as

Definition 3.7.1 **[FIR MMSE-LE]** *The FIR MMSE-LE for sampling rate ℓ/T, delay Δ, and length N_f symbol periods has coefficients*

$$\boldsymbol{w} = \boldsymbol{R}^*_{\boldsymbol{Y}x} \cdot \boldsymbol{R}^{-1}_{\boldsymbol{YY}} = \boldsymbol{R}_{x\boldsymbol{Y}} \cdot \boldsymbol{R}^{-1}_{\boldsymbol{YY}} \quad , \tag{3.307}$$

or equivalently,

$$\boldsymbol{w}^* = \boldsymbol{R}^{-1}_{\boldsymbol{YY}} \cdot \boldsymbol{R}_{\boldsymbol{Y}x} \quad . \tag{3.308}$$

The dimensionality (real for one-dimension or complex with two real dimensions) should be the same consistently for $\boldsymbol{w}$'s calculation.

In general, it may be of interest to derive more specific expressions for $\boldsymbol{R}_{\boldsymbol{YY}}$ and $\boldsymbol{R}_{x\boldsymbol{Y}}$.

$$\begin{aligned}
\boldsymbol{R}_{x\boldsymbol{Y}} &= \overline{\mathbb{E}\left\{x_{k-\Delta} \cdot \boldsymbol{Y}_k^*\right\}} = \overline{\mathbb{E}\left\{x_{k-\Delta} \cdot \boldsymbol{X}_k^*\right\}} \cdot \boldsymbol{H}^* + \overline{\mathbb{E}\left\{x_{k-\Delta} \cdot \boldsymbol{N}_k^*\right\}} && (3.309)\\
&= \left[\, 0 \ldots 0 \; \bar{\mathcal{E}}_{\boldsymbol{x}} \; 0 \ldots 0 \,\right] \cdot \boldsymbol{H}^* + 0 && (3.310)\\
&= \bar{\mathcal{E}}_{\boldsymbol{x}} \cdot \left[\, 0 \ldots 0 \; \boldsymbol{h}_\nu^* \ldots \boldsymbol{h}_0^* \; 0 \ldots 0 \,\right] && (3.311)
\end{aligned}$$

$$\begin{aligned}
\boldsymbol{R}_{\boldsymbol{YY}} &= \overline{\mathbb{E}\left\{\boldsymbol{Y}_k \cdot \boldsymbol{Y}_k^*\right\}} = \boldsymbol{H} \cdot \overline{\mathbb{E}\left\{\boldsymbol{X}_k \cdot \boldsymbol{X}_k^*\right\}} \cdot \boldsymbol{H}^* + \overline{\mathbb{E}\left\{\boldsymbol{N}_k \cdot \boldsymbol{N}_k^*\right\}} && (3.312)\\
&= \bar{\mathcal{E}}_{\boldsymbol{x}} \cdot \boldsymbol{H} \cdot \boldsymbol{H}^* + R_{\boldsymbol{NN}} \quad , && (3.313)
\end{aligned}$$

where $R_{\boldsymbol{NN}}$ is the (possibly fractionally spaced) noise autocorrelation matrix and is equal to $\ell \cdot \frac{\mathcal{N}_0}{2} \cdot I$ when the noise is white. A convenient expression is

$$[0 \ldots 0 \; \boldsymbol{h}_\nu^* \ldots \boldsymbol{h}_0^* \; 0 \ldots 0] = \boldsymbol{1}_\Delta^* \cdot \boldsymbol{H}^* \stackrel{\Delta}{=} \boldsymbol{H}_\Delta^* \quad , \tag{3.314}$$

so that $\mathbf{1}_\Delta$ is an $N_f+\nu$-vector of 0's and a 1 in the $(\Delta+1)^{th}$ position. Then the FIR MMSE-LE becomes (in terms of $\boldsymbol{h}$, $\bar{\mathcal{E}}_{\boldsymbol{x}}$ and Δ)

$$\begin{aligned}
\boldsymbol{w} &= \mathbf{1}_\Delta^* \cdot \boldsymbol{H}^* \cdot \left[\boldsymbol{H}\cdot\boldsymbol{H}^* + \frac{1}{\bar{\mathcal{E}}_{\boldsymbol{x}}}\cdot \boldsymbol{R}_{\boldsymbol{nn}}\right]^{-1} && (3.315)\\
&= \mathbf{1}_\Delta^* \cdot \left[\boldsymbol{H}^*\cdot\boldsymbol{R}_{\boldsymbol{nn}}^{-1}\cdot\boldsymbol{H} + \frac{1}{\bar{\mathcal{E}}_{\boldsymbol{x}}}\cdot I\right]^{-1}\cdot \boldsymbol{H}^*\cdot\boldsymbol{R}_{\boldsymbol{nn}}^{-1} && (3.316)\\
\text{with } R_{\boldsymbol{NN}} &= \ell\cdot\frac{\mathcal{N}_0}{2}\cdot I, \text{ (3.315) becomes}\\
&= \boldsymbol{H}_\Delta^*\cdot\left[\boldsymbol{H}\cdot\boldsymbol{H}^* + \frac{\ell}{SNR}\cdot I\right]^{-1} \quad , && (3.317)
\end{aligned}$$

with the abbreviation $SNR = \bar{\mathcal{E}}_{\boldsymbol{x}}/\frac{\mathcal{N}_0}{2}$. Appendix C's matrix inversion lemma helps derive (3.316).

The position of the nonzero elements in (3.311) depend on the choice of Δ. The MMSE, $\sigma^2_{MMSE-LE}$ follows from (3.302) and (3.307):

$$\begin{aligned}
\sigma^2_{MMSE-LE} &= \overline{\mathbb{E}\left\{x_{k-\Delta}\cdot x_{k-\Delta}^* - x_{k-\Delta}\cdot\boldsymbol{Y}_k^*\cdot\boldsymbol{w}^* - \boldsymbol{w}\cdot\boldsymbol{Y}_k\cdot x_{k-\Delta}^* + \boldsymbol{w}\cdot\boldsymbol{Y}_k\cdot\boldsymbol{Y}_k^*\cdot\boldsymbol{w}^*\right\}} && (3.318)\\
&= \bar{\mathcal{E}}_{\boldsymbol{x}} - \boldsymbol{R}_{x\boldsymbol{Y}}\cdot\boldsymbol{w}^* - \boldsymbol{w}\cdot\boldsymbol{R}_{\boldsymbol{Y}x} + \boldsymbol{w}\cdot\boldsymbol{R}_{\boldsymbol{YY}}\cdot\boldsymbol{w}^* && (3.319)\\
&= \bar{\mathcal{E}}_{\boldsymbol{x}} - \boldsymbol{w}\cdot\boldsymbol{R}_{\boldsymbol{YY}}\cdot\boldsymbol{w}^* && (3.320)\\
&= \bar{\mathcal{E}}_{\boldsymbol{x}} - \boldsymbol{R}_{x\boldsymbol{Y}}\cdot\boldsymbol{R}_{\boldsymbol{YY}}^{-1}\cdot\boldsymbol{R}_{\boldsymbol{Y}x} && (3.321)\\
&= \bar{\mathcal{E}}_{\boldsymbol{x}} - \boldsymbol{w}\cdot\boldsymbol{R}_{\boldsymbol{Y}x} \quad , && (3.322)
\end{aligned}$$

With algebra, (3.322) is the same as

$$\sigma^2_{MMSE-LE} = \overline{\frac{\ell\cdot\frac{\mathcal{N}_0}{2}}{\|h\|^2}\mathbf{1}_\Delta^*\cdot\left(\frac{\boldsymbol{H}^*\cdot\boldsymbol{R}_{\boldsymbol{nn}}^{-1}\cdot\boldsymbol{H}}{\|h\|^2} + \frac{\ell}{SNR_{MFB}}I\right)^{-1}\cdot\mathbf{1}_\Delta} = \frac{\ell\cdot\frac{\mathcal{N}_0}{2}}{\|h\|^2}\mathbf{1}_\Delta^*\cdot\bar{Q}^{-1}\cdot\mathbf{1}_\Delta \quad , \tag{3.323}$$

so that the best value of Δ (the position of the 1 in the vectors above) corresponds to the smallest diagonal element of the inverted ("Q-tilde") matrix in (3.323) – this means that only one matrix need be inverted to obtain the correct Δ value as well as compute the equalizer settings. Problem 3.17 develops some interesting relationships for $\boldsymbol{w}$ in terms of $\boldsymbol{H}$ and SNR. Thus, the SNR for the FIR MMSE-LE is

$$\text{SNR}_{MMSE-LE} = \frac{\bar{\mathcal{E}}_{\boldsymbol{x}}}{\sigma^2_{MMSE-LE}} \quad , \tag{3.324}$$

and the corresponding unbiased SNR is

$$\text{SNR}_{MMSE-LE,U} = \text{SNR}_{MMSE-LE} - 1 \quad . \tag{3.325}$$

The loss with respect to the MFB is, again,

$$\gamma_{MMSE-LE} = \frac{\text{SNR}_{MMSE-LE,U}}{SNR_{MFB}} \quad . \tag{3.326}$$

3.7.2 FIR ZFE

One obtains the FIR ZFE by letting the SNR$\rightarrow\infty$ in the FIR MMSE, which alters $\boldsymbol{R}_{\boldsymbol{YY}}$ to

$$\boldsymbol{R}_{\boldsymbol{YY}} = \bar{\mathcal{E}}_{\boldsymbol{x}}\cdot\boldsymbol{H}\cdot\boldsymbol{H}^* \tag{3.327}$$

and then $\boldsymbol{w}$ remains as

$$\boldsymbol{w} = \boldsymbol{R}_{x\boldsymbol{Y}}\cdot\boldsymbol{R}_{\boldsymbol{YY}}^{-1} \quad . \tag{3.328}$$

Because the FIR equalizer may not be sufficiently long to cancel all ISI, the FIR ZFE may still have nonzero residual ISI. This ISI power is

$$\sigma^2_{MMSE-ZFE} = \bar{\mathcal{E}}_{\boldsymbol{x}} - \boldsymbol{w}\cdot\boldsymbol{R}_{\boldsymbol{Y}x} \quad . \tag{3.329}$$

However, (3.329) still ignores the enhanced noise at the FIR ZFE output. This noise's variance is

$$\text{FIR ZFE noise power} = \boldsymbol{w} \cdot \boldsymbol{R_{nn}} \cdot \boldsymbol{w}^* \quad . \tag{3.330}$$

The FIR ZFE's residual interference introduces a bias that follows from the gain of $x_{k-\Delta}$ in the equalizer output z_k:

$$1/\omega_{zfe} \stackrel{\Delta}{=} \boldsymbol{w} \cdot \boldsymbol{H} \cdot \boldsymbol{1}_\Delta \quad . \tag{3.331}$$

So multiplying the equalizer output to $\omega_{zfe} \cdot \boldsymbol{z}$ removes the bias but sales the noise and residual ISI by the same factor, making the ZFE output SNR

$$SNR_{ZFE} = \frac{\bar{\mathcal{E}}_{\boldsymbol{x}}}{\omega_{zfe} \cdot \left(\bar{\mathcal{E}}_{\boldsymbol{x}} - \boldsymbol{w} \cdot \boldsymbol{R_{Y_x}} + \boldsymbol{w} \cdot \boldsymbol{R_{nn}} \cdot \boldsymbol{w}^*\right)} \quad . \tag{3.332}$$

The loss is the ratio of the SNR to SNR_{ZFE},

$$\gamma_{\text{ZFE}} = \frac{SNR_{ZFE}}{SNR_{MFB}} \quad . \tag{3.333}$$

3.7.3 examples

EXAMPLE 3.7.1 *[Return to $1 = .9 \cdot D^{-1}$]*

For the earlier PAM example, one notes that sampling with $\ell = 1$ is sufficient to represent all signals. First, choose $N_f = 3$ and note that ν=1. Then

$$\boldsymbol{H} = \begin{bmatrix} .9 & 1 & 0 & 0 \\ 0 & .9 & 1 & 0 \\ 0 & 0 & .9 & 1 \end{bmatrix} \quad . \tag{3.334}$$

With a choice of $\Delta = 2$, then

$$\boldsymbol{R_{Y_x}} = \bar{\mathcal{E}}_{\boldsymbol{x}} \cdot \boldsymbol{H} \begin{bmatrix} 0 \\ 0 \\ 1 \\ 0 \end{bmatrix} \tag{3.335}$$

$$= \begin{bmatrix} 0 \\ 1 \\ .9 \end{bmatrix} \quad , \tag{3.336}$$

and

$$\boldsymbol{R_{YY}} = \bar{\mathcal{E}}_{\boldsymbol{x}} \cdot \left(\boldsymbol{H} \cdot \boldsymbol{H}^* + \frac{1}{SNR} \cdot I\right) \tag{3.337}$$

$$= \begin{bmatrix} 1.991 & .9 & 0 \\ .9 & 1.991 & .9 \\ 0 & .9 & 1.991 \end{bmatrix} \quad , \tag{3.338}$$

The FIR MMSE is

$$\boldsymbol{w}^* = \boldsymbol{R_{YY}^{-1}} \cdot \boldsymbol{R_{Y_x}} = \begin{bmatrix} .676 & -.384 & .174 \\ -.384 & .849 & -.384 \\ .174 & -.384 & .676 \end{bmatrix} \begin{bmatrix} 0 \\ 1 \\ .9 \end{bmatrix} = \begin{bmatrix} -.23 \\ .51 \\ .22 \end{bmatrix} \tag{3.339}$$

Then

$$\sigma^2_{MMSE-LE} = \left(1 - [-.23\ .51\ .22] \begin{bmatrix} 0 \\ 1 \\ .9 \end{bmatrix}\right) = .294 \tag{3.340}$$

The SNR is

$$\text{SNR}_{MMSE-LE,U} = \frac{1}{.294} - 1 = 2.4 \text{ (3.8 dB)} \quad . \tag{3.341}$$

which is 6.2dB below MFB performance and 1.9dB worse than the infinite length MMSE-LE for this channel.

Figure 3.42 plots The 3-tap equalizer frequency response (bias removal not included) on the left and the (with bias removed) equalized channel on the right.

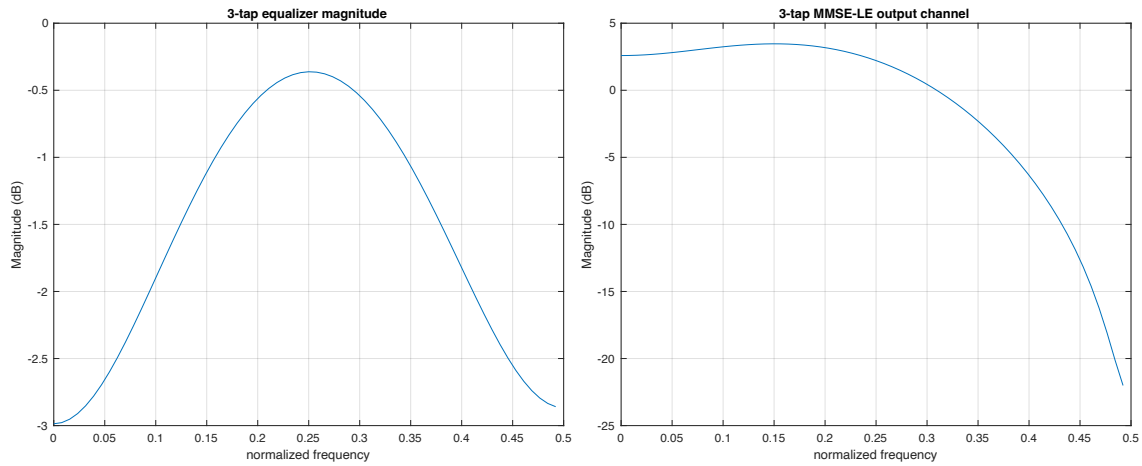

Figure 3.42: 3-tap FIR equalizer spectrum magnitude and equalized channel

Figure 3.43 repeats Figure 3.42 with 7 taps, and the improvement is noticeable.

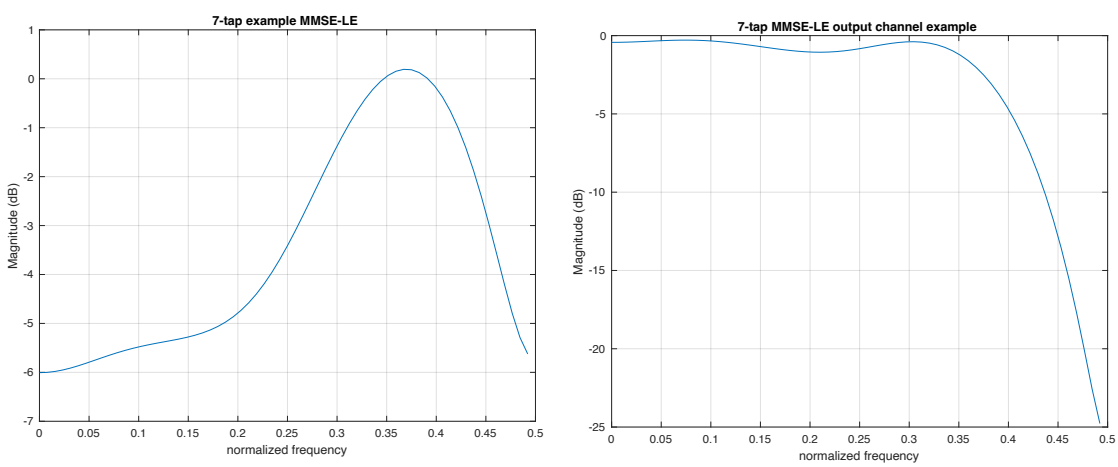

Figure 3.43: 7-tap FIR equalizer spectrum magnitude and equalized channel

With sufficiently large number of taps for this channel, the infinite length performance level can be attained. Figure 3.44 plots this performance versus the number of equalizer taps:

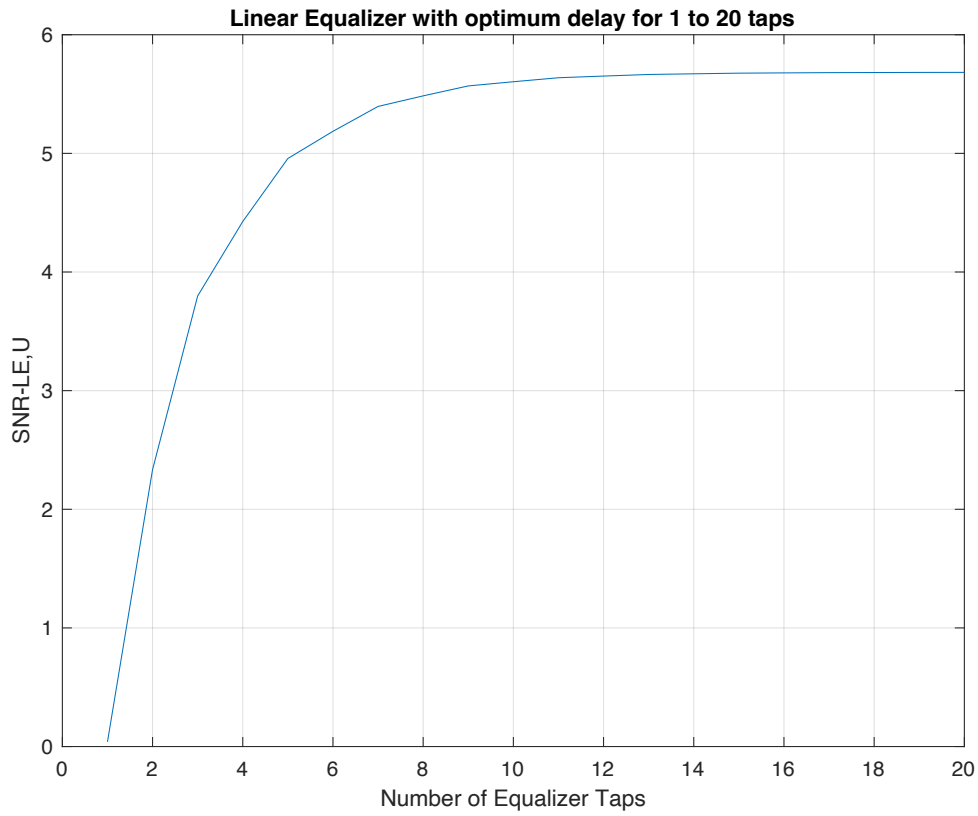

Figure 3.44: FIR equalizer performance for $1 + .9D^{-1}$ versus number of equalizer taps.

Clearly, 15 taps are sufficient for infinite-length performance.

ZFE: The zero-forcing version of this equalizer zeros noise in the MMSE equations, but then removes bias and adds the actual enhanced noise. For the ZFE on this noncausal maximum phase will desire maximum delay of $\Delta = 3$ (which can be verified by trial and error also with lower values. Matlab equations are:

```
>> H = [
    0.9000    1.0000         0         0
         0    0.9000    1.0000         0
         0         0    0.9000    1.0000 ];
>> Hdelstar=H(:,4)' =     0     0     1
>> wzfe=Hdelstar*inv(H*H') =    0.2702   -0.5434    0.8227
>> chan=wzfe*H =    0.2432   -0.2189    0.1970    0.8227
>> wnobias=1/chan(4) =    1.2155
>> MMSEzf=1-wzfe*H(:,4) =  0.1773
>> SNRzfu=1/.1773-1 =    4.6402
>> omega = 1/chan(4) =    1.2155
>> (SNRzfu+1)/SNRzfu =    1.2155 %checks
>> enoise=.181*norm(w)^2  =    0.1892
>> SNRall=10*log10(1/(wnobias*(MMSEzf+enoise)))   = 3.0813  dB (< 3.78 dB for MMSE-LE,U)
```

This verifies as always that the ZFE (with same number of taps/parameters) never performs better than the MMSE equalizer.

EXAMPLE 3.7.2 *[revisit QAM]* For the earlier complex QAM example, sampling with $\ell = 1$ is sufficient to represent all signals. First, choose $N_f = 4$ and note that $\nu = 2$. Then

$$\boldsymbol{H} = \begin{bmatrix} -.5 & 1+\jmath/4 & -\jmath/2 & 0 & 0 & 0 \\ 0 & -.5 & 1+\jmath/4 & -\jmath/2 & 0 & 0 \\ 0 & 0 & -.5 & 1+\jmath/4 & -\jmath/2 & 0 \\ 0 & 0 & 0 & -.5 & 1+\jmath/4 & -\jmath/2 \end{bmatrix} \quad . \tag{3.342}$$

The matrix $(\boldsymbol{H}^* \cdot \boldsymbol{H} + .15625 \cdot I)^{-1}$ has the same smallest element 1.3578 for both $\Delta = 2, 3$, so choosing $\Delta = 2$ will not unnecessarily increase system delay. With a choice of $\Delta = 2$, then

$$\boldsymbol{R}_{\boldsymbol{Y}_x} = \bar{\mathcal{E}}_{\boldsymbol{x}} \cdot \boldsymbol{H} \cdot \begin{bmatrix} 0 \\ 0 \\ 1 \\ 0 \\ 0 \\ 0 \end{bmatrix} \tag{3.343}$$

$$= \begin{bmatrix} -.5\jmath \\ 1+\jmath/4 \\ -.5 \\ 0 \end{bmatrix} \quad , \tag{3.344}$$

and

$$\boldsymbol{R}_{\boldsymbol{Y}\boldsymbol{Y}} = \bar{\mathcal{E}}_{\boldsymbol{x}} \cdot \left(\boldsymbol{H} \cdot \boldsymbol{H}^* + \frac{1}{SNR} I \right) \tag{3.345}$$

$$= \begin{bmatrix} 1.7188 & -0.6250 - 0.6250\jmath & \jmath/4 & 0 \\ -0.6250 + 0.6250\jmath & 1.7188 & -0.6250 - 0.6250\jmath & \jmath/4 \\ -\jmath/4 & -0.6250 + 0.6250\jmath & 1.7188 & -0.6250 - 0.6250\jmath \\ 0 & -\jmath/4 & -0.6250 + 0.6250\jmath & 1.7188 \end{bmatrix} \quad .$$

The FIR MMSE is

$$\boldsymbol{w}^* = \boldsymbol{R}_{\boldsymbol{Y}\boldsymbol{Y}}^{-1} \cdot \boldsymbol{R}_{\boldsymbol{Y}_x} = \begin{bmatrix} 0.2570 - 0.0422\jmath \\ 0.7313 - 0.0948\jmath \\ -0.1182 - 0.2982\jmath \\ -0.1376 + 0.0409\jmath \end{bmatrix} \quad . \tag{3.346}$$

Then

$$\sigma^2_{MMSE-LE} = (1 - \boldsymbol{w} \cdot \boldsymbol{R}_{\boldsymbol{Y}_x}) \tag{3.347}$$

$$= .2121 \quad . \tag{3.348}$$

The SNR is

$$SNR_{MMSE-LE,U} = \frac{1}{.2121} - 1 = 3.714 \text{ (5.7 dB)} \quad , \tag{3.349}$$

which is 4.3 dB below MFB performance and 2.1 dB worse than the infinite-length MMSE-LE for this channel. With sufficiently large number of taps for this channel, the infinite-length performance level can be attained.

3.7.4 FIR MMSE-DFE

The FIR DFE case is similar to the feed-forward equalizers just discussed, except that the receiver now augments the fractionally spaced feed-forward section with a symbol-spaced feedback section. The MSE for the DFE case, as long as $\boldsymbol{w}$ and $\boldsymbol{b}$ are sufficiently long, is

$$MSE = \mathbb{E}\left\{ |x_{k-\Delta} - \boldsymbol{w} \cdot \boldsymbol{Y}_k + \boldsymbol{b} \cdot \boldsymbol{x}_{k-\Delta-1}|^2 \right\} \quad , \tag{3.350}$$

where $\boldsymbol{b}$ is the vector of coefficients for the feedback FIR filter

$$\boldsymbol{b} \triangleq [\, b_1 \; b_2 \; ... \; b_{N_b}] \quad , \tag{3.351}$$

and $\boldsymbol{x}_{k-\Delta-1}$ is the vector of data symbols in the feedback path. It is mathematically convenient to define an augmented response vector for the DFE as

$$\tilde{\boldsymbol{w}} \triangleq \left[\boldsymbol{w} \vdots \; -\boldsymbol{b} \right] \quad , \tag{3.352}$$

and a corresponding augmented DFE input vector as

$$\tilde{\boldsymbol{Y}}_k \triangleq \left[\begin{array}{c} \boldsymbol{Y}_k \\ \boldsymbol{x}_{k-\Delta-1} \end{array} \right] \quad . \tag{3.353}$$

Then, (3.350) becomes

$$MSE = \mathbb{E}\left\{ |x_{k-\Delta} - \tilde{\boldsymbol{w}} \cdot \tilde{\boldsymbol{Y}}_k|^2 \right\} \quad . \tag{3.354}$$

The solution, paralleling (3.306) - (3.308), uses the **FIR MMSE-DFE autocorrelation matrix**:

$$\begin{aligned} \boldsymbol{R}_{\tilde{\boldsymbol{Y}}\tilde{\boldsymbol{Y}}} &\triangleq \mathbb{E}\left\{ \tilde{\boldsymbol{Y}}_k \cdot \tilde{\boldsymbol{Y}}_k^* \right\} & (3.355) \\ &= \left[\begin{array}{cc} \boldsymbol{R}_{\boldsymbol{Y}\boldsymbol{Y}} & \mathbb{E}[\boldsymbol{Y}_k \cdot \boldsymbol{x}_{k-\Delta-1}^*] \\ \mathbb{E}[\boldsymbol{x}_{k-\Delta-1} \cdot \boldsymbol{Y}_k^*] & \bar{\mathcal{E}}_{\boldsymbol{x}} \cdot I_{N_b} \end{array} \right] & (3.356) \\ &= \left[\begin{array}{cc} \bar{\mathcal{E}}_{\boldsymbol{x}} \cdot \left(\boldsymbol{H}\boldsymbol{H}^* + \frac{{}^R\boldsymbol{N}\boldsymbol{N}}{\bar{\mathcal{E}}_{\boldsymbol{x}}} \right) & \bar{\mathcal{E}}_{\boldsymbol{x}} \cdot \boldsymbol{H} \cdot J_\Delta] \\ \bar{\mathcal{E}}_{\boldsymbol{x}} \cdot J_\Delta^* \cdot \boldsymbol{H}^* & \bar{\mathcal{E}}_{\boldsymbol{x}} \cdot I_{N_b} \end{array} \right] \quad , & (3.357) \end{aligned}$$

where J_Δ is an $(N_f + \nu) \times N_b$ matrix of 0's and 1's, which has the upper $\Delta + 1$ rows zeroed and an identity matrix of dimension $\min(N_b, N_f + \nu - \Delta - 1)$ with zeros to the right (when $N_f + \nu - \Delta - 1 < N_b$), zeros below (when $N_f + \nu - \Delta - 1 > N_b$), or no zeros to the right or below exactly fitting in the bottom of J_Δ (when $N_f + \nu - \Delta - 1 = N_b$).

The corresponding **FIR MMSE-DFE cross-correlation vector** is

$$\begin{aligned} \boldsymbol{R}_{\tilde{\boldsymbol{Y}}x} &\triangleq E\left\{ \tilde{\boldsymbol{Y}}_k \cdot x_{k-\Delta}^* \right\} & (3.358) \\ &= \left[\begin{array}{c} \boldsymbol{R}_{\boldsymbol{Y}x} \\ 0 \end{array} \right] & (3.359) \\ &= \left[\begin{array}{c} \bar{\mathcal{E}}_{\boldsymbol{x}} \cdot \boldsymbol{H} \cdot \boldsymbol{1}_\Delta \\ 0 \end{array} \right] \quad , & (3.360) \end{aligned}$$

where, again, $\overline{N} = 1$ for real signals and $\overline{N} = 2$ for complex signals.

The FIR MMSE-DFE for sampling rate ℓ/T, delay Δ, and of length N_f and N_b has coefficients

$$\tilde{\boldsymbol{w}} = \boldsymbol{R}_{x\tilde{\boldsymbol{Y}}} \cdot \boldsymbol{R}_{\tilde{\boldsymbol{Y}}\tilde{\boldsymbol{Y}}}^{-1} \quad . \tag{3.361}$$

Equation (3.361) can be rewritten in detail as

$$\left[\boldsymbol{w} \vdots -\boldsymbol{b} \right] \cdot \bar{\mathcal{E}}_{\boldsymbol{x}} \cdot \left[\begin{array}{cc} \boldsymbol{H} \cdot \boldsymbol{H}^* + \frac{1}{\bar{\mathcal{E}}_{\boldsymbol{x}}} \cdot {}^R\boldsymbol{N}\boldsymbol{N} & \boldsymbol{H} \cdot J_\Delta \\ J_\Delta^* \boldsymbol{H}^* & I_{N_b} \end{array} \right] = \left[\bar{\mathcal{E}}_{\boldsymbol{x}} \cdot \boldsymbol{1}_\Delta^* \cdot \boldsymbol{H}^* \vdots 0 \right] \quad , \tag{3.362}$$

which reduces to

$$\begin{aligned} \boldsymbol{w} \cdot \left(\boldsymbol{H} \cdot \boldsymbol{H}^* + \frac{1}{\bar{\mathcal{E}}_{\boldsymbol{x}}} \cdot \mathbb{R}_{\boldsymbol{N}\boldsymbol{N}} \right) - \boldsymbol{b} \cdot J_\Delta^* \cdot \boldsymbol{H}^* &= \boldsymbol{1}_\Delta^* \cdot \boldsymbol{H}^* & (3.363) \\ \boldsymbol{w} \cdot \boldsymbol{H} \cdot J_\Delta - \boldsymbol{b} &= 0 \quad . & (3.364) \end{aligned}$$

Then

$$\boldsymbol{b} = \boldsymbol{w} \cdot \boldsymbol{H} \cdot J_\Delta \quad , \tag{3.365}$$

and thus

$$\boldsymbol{w}\left(\boldsymbol{H} \cdot \boldsymbol{H}^* - \boldsymbol{H} \cdot J_\Delta \cdot J_\Delta^* \cdot \boldsymbol{H}^* + \frac{1}{\bar{\mathcal{E}}_{\boldsymbol{x}}} \cdot R_{\boldsymbol{NN}}\right) = \mathbf{1}_\Delta^* \cdot \boldsymbol{H}^* \tag{3.366}$$

or

$$\boldsymbol{w} = \mathbf{1}_\Delta^* \cdot \boldsymbol{H}^* \cdot \left(\boldsymbol{H} \cdot \boldsymbol{H}^* - \boldsymbol{H} \cdot J_\Delta \cdot J_\Delta^* \cdot \boldsymbol{H}^* + \frac{1}{\bar{\mathcal{E}}_{\boldsymbol{x}}} \cdot R_{\boldsymbol{NN}}\right)^{-1} \quad . \tag{3.367}$$

Then

$$\boldsymbol{b} = \mathbf{1}_\Delta^* \cdot \boldsymbol{H}^* \cdot \left(\boldsymbol{H} \cdot \boldsymbol{H}^* - \boldsymbol{H} \cdot J_\Delta \cdot J_\Delta^* \cdot \boldsymbol{H}^* + \frac{1}{\bar{\mathcal{E}}_{\boldsymbol{x}}} \cdot R_{\boldsymbol{NN}}\right)^{-1} \cdot \boldsymbol{H} \cdot J_\Delta \quad . \tag{3.368}$$

The MMSE is then

$$\begin{aligned}
\sigma^2_{MMSE-DFE} &= \bar{\mathcal{E}}_{\boldsymbol{x}} - \tilde{\boldsymbol{w}} \cdot \boldsymbol{R}_{\tilde{\boldsymbol{Y}}_x} && (3.369)\\
&= \bar{\mathcal{E}}_{\boldsymbol{x}} - \boldsymbol{w} \cdot \boldsymbol{R}_{\boldsymbol{Y}_x} && (3.370)\\
&= \bar{\mathcal{E}}_{\boldsymbol{x}} \cdot \left(1 - \mathbf{1}_\Delta^* \cdot \boldsymbol{H}^* \cdot \left(\boldsymbol{H} \cdot \boldsymbol{H}^* - \boldsymbol{H} \cdot J_\Delta \cdot J_\Delta^* \cdot \boldsymbol{H}^* + \frac{1}{\bar{\mathcal{E}}_{\boldsymbol{x}}} R_{\boldsymbol{NN}}\right)^{-1} \cdot \boldsymbol{H} \cdot \mathbf{1}_\Delta\right) \quad ,
\end{aligned}$$

which is a function to be minimized over Δ. Thus, the SNR for the unbiased FIR MMSE-DFE is

$$SNR_{MMSE-DFE,U} = \frac{\bar{\mathcal{E}}_{\boldsymbol{x}}}{\sigma^2_{MMSE-DFE}} - 1 = \frac{\tilde{\boldsymbol{w}} \cdot \boldsymbol{R}_{\tilde{\boldsymbol{Y}}_x}}{\bar{\mathcal{E}}_{\boldsymbol{x}} - \tilde{\boldsymbol{w}} \cdot \boldsymbol{R}_{\tilde{\boldsymbol{Y}}_x}} \quad , \tag{3.371}$$

and the loss is again

$$\gamma_{MMSE-DFE} = \frac{SNR_{MMSE-DFE,U}}{SNR_{MFB}} \quad . \tag{3.372}$$

EXAMPLE 3.7.3 [MMSE-DFEs, PAM and QAM] For the earlier example with $l = 1$, $N_f = 2$, and $N_b = 1$ and $\nu = 1$, we will also choose $\Delta = 1$. Then

$$\boldsymbol{H} = \begin{bmatrix} .9 & 1 & 0 \\ 0 & .9 & 1 \end{bmatrix} \quad , \tag{3.373}$$

$$J_\Delta = \begin{bmatrix} 0 \\ 0 \\ 1 \end{bmatrix} \quad , \tag{3.374}$$

$$\mathbf{1}_\Delta = \begin{bmatrix} 0 \\ 1 \\ 0 \end{bmatrix} \quad , \tag{3.375}$$

and

$$\boldsymbol{R}_{\boldsymbol{YY}} = \begin{bmatrix} 1.991 & .9 \\ .9 & 1.991 \end{bmatrix} \quad . \tag{3.376}$$

Then

$$\begin{aligned}
\boldsymbol{w} &= [0\ 1\ 0] \begin{bmatrix} .9 & 0 \\ 1 & .9 \\ 0 & 1 \end{bmatrix} \left\{ \begin{bmatrix} 1.991 & .9 \\ .9 & 1.991 \end{bmatrix} - \begin{bmatrix} 0 \\ 1 \end{bmatrix} [0\ 1] \right\}^{-1} && (3.377)\\
&= [1\ .9] \begin{bmatrix} 1.991 & .9 \\ .9 & 0.991 \end{bmatrix}^{-1} && (3.378)\\
&= [.1556\ .7668] && (3.379)\\
\boldsymbol{b} &= \boldsymbol{w} \cdot \boldsymbol{H} \cdot J_\Delta && (3.380)\\
&= [.1556\ .7668] \begin{bmatrix} .9 & 1 & 0 \\ 0 & .9 & 1 \end{bmatrix} \begin{bmatrix} 0 \\ 0 \\ 1 \end{bmatrix} && (3.381)\\
&= .7668 \quad . && (3.382)
\end{aligned}$$

Then

$$\sigma^2_{MMSE-DFE} = \left(1 - [.16\ .76]\begin{bmatrix} 1 \\ .9 \end{bmatrix}\right) = .1542 \quad . \tag{3.383}$$

The SNR is computed to be

$$SNR_{MMSE-DFE,U} = \frac{1 - .1542}{.1542} = 5.4\ (7.4\text{dB}) \quad , \tag{3.384}$$

which is 2.7 dB below MFB performance, but 2.8 dB better than the **infinite-length** MMSE-LE for this channel! The loss with respect to the infinite-length MMSE-DFE is 1.1 dB. Figure 3.45 illustrates this FIR MMSE-DFE.

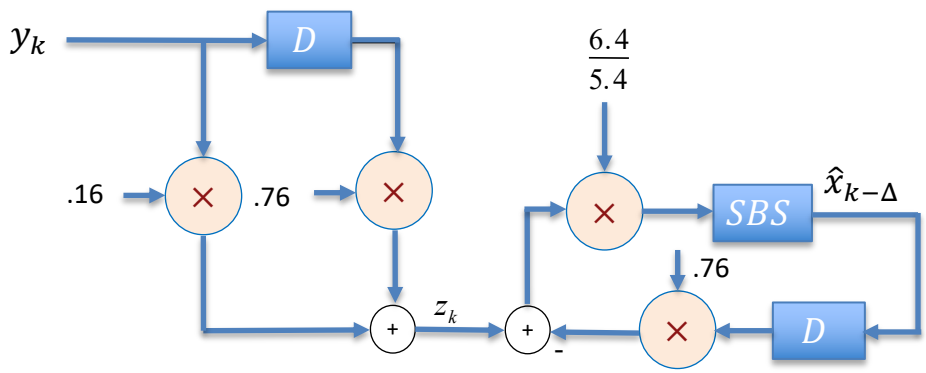

Figure 3.45: FIR MMSE-DFE Example.

With a sufficiently large number of taps, this channel's infinite-length performance level can be attained. Figure 3.46 plots this performance ersus the number of feed-forward taps (this channel requires only one feedback tap is necessary for infinite-length performance). 7 feed-forward and 1 feedback taps essentially infinite-length performance. Thus, the finite-length DFE not only outperforms the finite or infinite-length LE, it also has less complexity. Also here, we briefly review the previous QAM example with $\ell = 1$, $N_f = 2$, $N_b = 2$, and $\nu = 2$ and choose $\Delta = 1$. Tthis channel will need more taps to do well with the DFE structure, but we can still choose these values and proceed. Then

$$\boldsymbol{H} = \begin{bmatrix} -.5 & 1+\jmath/4 & -\jmath/2 & 0 \\ 0 & -.5 & 1+\jmath/4 & -\jmath/2 \end{bmatrix} \quad , \tag{3.385}$$

$$J_\Delta = \begin{bmatrix} 0 & 0 \\ 0 & 0 \\ 1 & 0 \\ 0 & 1 \end{bmatrix} \quad , \tag{3.386}$$

$$\mathbf{1}_\Delta = \begin{bmatrix} 0 \\ 1 \\ 0 \\ 0 \end{bmatrix} \quad , \tag{3.387}$$

and

$$\boldsymbol{R_{YY}} = \begin{bmatrix} 1.7188 & -0.6250 - 0.6250\jmath \\ -0.6250 - 0.6250\jmath & 1.7188 \end{bmatrix} \quad . \tag{3.388}$$

Then

$$\boldsymbol{w} = [0\ 1\ 0\ 0] \begin{bmatrix} -.5 & 0 \\ 1-\jmath/4 & -.5 \\ \jmath/2 & 1-\jmath/4 \\ 0 & \jmath/2 \end{bmatrix} \cdot \tag{3.389}$$

$$\left\{ \begin{bmatrix} 1.7188 & -0.6250-0.6250\jmath \\ -0.6250-0.6250\jmath & 1.7188 \end{bmatrix} - \begin{bmatrix} 1/4 & -1/8-\jmath/2 \\ -1/8+\jmath/2 & 1.3125 \end{bmatrix} \right\}^{-1}$$

$$= [1-\jmath/2\ \ -.5] \begin{bmatrix} 1.2277 & 1.5103+\jmath.3776 \\ 1.5103-\jmath.3776 & 4.4366 \end{bmatrix} \tag{3.390}$$

$$= [.4720-\jmath.1180\quad -.6136] \tag{3.391}$$

$$\boldsymbol{b} = \boldsymbol{w}\cdot\boldsymbol{H}\cdot J_\Delta \tag{3.392}$$

$$= [.4720-\jmath.1180\quad .6136] \begin{bmatrix} -.5 & 1+\jmath/4 & -\jmath/2 & 0 \\ 0 & -.5 & 1+\jmath/4 & -\jmath/2 \end{bmatrix} \begin{bmatrix} 0 & 0 \\ 0 & 0 \\ 1 & 0 \\ 0 & 1 \end{bmatrix} \tag{3.393}$$

$$= [-.6726-\jmath.3894\quad .3608\jmath] \quad . \tag{3.394}$$

Then

$$\sigma^2_{MMSE-DFE} = .1917 \quad . \tag{3.395}$$

The SNR is

$$SNR_{MMSE-DFE,U} = \frac{1-.1917}{.1917} = 6.23\text{dB} \quad , \tag{3.396}$$

which is 3.77 dB below MFB performance, and not very good on this channel! The reader is encouraged to investigate various filter lengths and delays to find a best use of 3, 4, 5, and 6 parameters on this channel (using the Matlab programs shortly to be described).

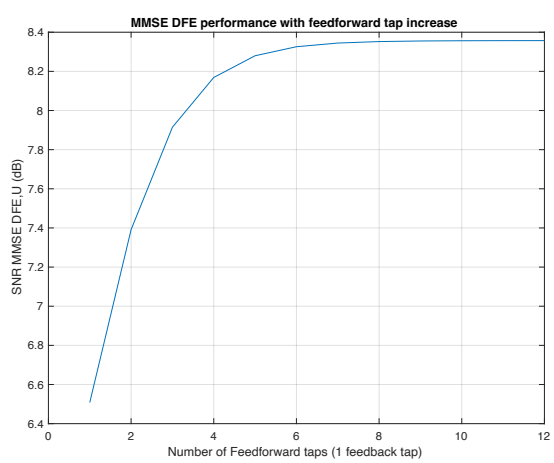

Figure 3.46: FIR MMSE-DFE performance for $1+.9D^{-1}$ versus number of feed-forward equalizer taps.

FIR ZF-DFE One obtains the FIR ZF-DFE by letting the SNR$\rightarrow\infty$ in the FIR MMSE-DFE, which alters $\boldsymbol{R}_{\tilde{\boldsymbol{Y}}\tilde{\boldsymbol{Y}}}$ to

$$\boldsymbol{R}_{\tilde{\boldsymbol{Y}}\tilde{\boldsymbol{Y}}} = \begin{bmatrix} \bar{\mathcal{E}}_{\boldsymbol{x}}\cdot\tilde{\boldsymbol{H}}\cdot\tilde{\boldsymbol{H}}^* & \bar{\mathcal{E}}_{\boldsymbol{x}}\cdot\boldsymbol{H}\cdot J_\Delta \\ \bar{\mathcal{E}}_{\boldsymbol{x}}\cdot J_\Delta^*\cdot\boldsymbol{H}^* & \bar{\mathcal{E}}_{\boldsymbol{x}}\cdot I_{N_b} \end{bmatrix} \tag{3.397}$$

and then $\tilde{\boldsymbol{w}}$ remains as

$$\tilde{\boldsymbol{w}} = \boldsymbol{R}_{x\tilde{\boldsymbol{Y}}}\cdot\boldsymbol{R}^{-1}_{\tilde{\boldsymbol{Y}}\tilde{\boldsymbol{Y}}} \quad . \tag{3.398}$$

Because the FIR equalizer may not be sufficiently long to cancel all ISI, the FIR ZF-DFE may still have nonzero residual ISI. This ISI power is given by

$$\sigma^2_{MMSE-DFE} = \bar{\mathcal{E}}_{\boldsymbol{x}} - \tilde{\boldsymbol{w}} \cdot \boldsymbol{R}_{\tilde{\boldsymbol{Y}}_x} \quad . \tag{3.399}$$

However, (3.399) still ignores the enhanced noise at the $\tilde{\boldsymbol{w}}_k$ filter output. There is again a bias given by

$$1/\omega_{zfe} \triangleq \boldsymbol{w} \cdot \boldsymbol{H} \cdot \boldsymbol{1}_\Delta \quad . \tag{3.400}$$

This noise's energy is

$$\text{FIR ZFDFE noise variance} = \boldsymbol{w} \cdot R_{\boldsymbol{NN}} \cdot \boldsymbol{w}^* \quad , \tag{3.401}$$

making the SNR at the FIR ZF-DFE output

$$SNR_{ZF-DFE} = \frac{\bar{\mathcal{E}}_{\boldsymbol{x}}}{\omega_{zfe} \cdot \left(\bar{\mathcal{E}}_{\boldsymbol{x}} - \tilde{\boldsymbol{w}} \cdot \boldsymbol{R}_{\tilde{\boldsymbol{Y}}_x} + \boldsymbol{w} \cdot R_{\boldsymbol{NN}} \cdot \boldsymbol{w}^*\right)} \quad . \tag{3.402}$$

The filter is $\boldsymbol{w}$ in (3.401) and (3.402), not $\tilde{\boldsymbol{w}}$ because only the feed-forward section processes the noise. The loss is:

$$\gamma_{\text{ZF-DFE}} = \frac{SNR_{ZF-DFE}}{SNR_{MFB}} \quad . \tag{3.403}$$

3.7.5 An Alternative Approach to the DFE

While the above approach directly computes the FIR DFE settings, it yields less insight into the DFE's internal structure than did Section 3.6's infinite-length structures. In particular, there is no explicity spectral (canonical) factorization into causal and anti-causal ISI components. This subsection provides such an alternative caused by the finite-length filters. This is because finite-length filters inherently correspond to non-stationary processing.[14]

The feedforward-section input vector is again $\boldsymbol{Y}_k$, and the corresponding feedforward-filter vector also remains$\boldsymbol{w}$. The feed-forward filter output is $z_k = \boldsymbol{w} \cdot \boldsymbol{Y}_k$. Continuing in the same fashion, the DFE error signal is then

$$e_k = \boldsymbol{b} \cdot \boldsymbol{X}_k(\Delta) - \boldsymbol{w} \cdot \boldsymbol{Y}_k \quad , \tag{3.404}$$

where

$$\boldsymbol{X}_k(\Delta) = \begin{bmatrix} x_{k-\Delta} \\ \vdots \\ x_{k-\Delta-\nu} \end{bmatrix} \tag{3.405}$$

and $\boldsymbol{b}$ remains monic and causal corresponding to the delay Δ

$$\boldsymbol{b} \triangleq [1 \; b_1 \; b_2 \; ... \; b_{N_b}] \quad . \tag{3.406}$$

The MMSE optimizes over both $\boldsymbol{b}$ and $\boldsymbol{w}$. Signals most generally complex, and all developments here simplify to the one-dimensional real case easily. It is important to remember to divide any complex signal's variance by 2 to get the energy per real dimension. The SNR equals $\bar{\mathcal{E}}_{\boldsymbol{x}}/\frac{\mathcal{N}_0}{2} = \mathcal{E}_{\boldsymbol{x}}/\mathcal{N}_0$ in either case.

Optimizing the feed-forward and feedback filters: For any fixed $\boldsymbol{b}$ in (3.404), the cross-correlation between the error and the channel-output vector $\boldsymbol{Y}_k$ should be zero for MMSE,

$$E\left[e_k \cdot \boldsymbol{Y}_k^*\right] = 0 \quad . \tag{3.407}$$

So,

$$\boldsymbol{w} \cdot \boldsymbol{R}_{\boldsymbol{YY}} = \boldsymbol{b} \cdot \boldsymbol{R}_{\boldsymbol{XY}}(\Delta) \quad , \tag{3.408}$$

[14] Chapter 5 provides a more complete analogy between finite-length and infinite-length DFE's, where the best finite-length DFE's are actually periodic over a packet period corresponding to N_f.

and

$$\boldsymbol{R}_{\boldsymbol{XY}}(\Delta) = \mathbb{E}\left\{\boldsymbol{X}_k(\Delta)\cdot\left[x_k^* \; x_{k-1}^* \; ... \; x_{k-N_f-\nu+1}^*\right]\cdot\boldsymbol{H}^*\right\} \tag{3.409}$$

$$= \bar{\mathcal{E}}_{\boldsymbol{x}}\cdot\tilde{J}_\Delta^*\cdot\boldsymbol{H}^* \quad , \tag{3.410}$$

where the $(N_b+1)\times(N_f+\nu)$ matrix $\tilde{J}_\Delta^*$ has the first Δ columns all zeros, then an (up to) $N_b\times N_b$ identity matrix at the top of the up to N_b columns, and zeros in any row entries below that identity, and possibly zeroed columns following the identity if $N_f+\nu-\Delta-2>N_b+1$. The following matlab commands produce $\tilde{J}_\Delta^*$, using for instance $N_f=8$, $N_b=5$, $\Delta=3$, and $\nu=5$,

```
Delta = 3;
Nb=5;
nu=5;
Nf=8;
sizeI=min(Nb,Nf+nu-1-Delta)
= 5
sizerest=max(0,Nf+nu-1-Delta-Nb-1)
= 3
Jdeltastar = [zeros(Nb+1,Delta) [eye(sizeI) ; zeros(Nb+1-sizeI,sizeI)] zeros(Nb+1,sizerest)]

Jdeltastar =

     0     0     0     1     0     0     0     0     0     0     0
     0     0     0     0     1     0     0     0     0     0     0
     0     0     0     0     0     1     0     0     0     0     0
     0     0     0     0     0     0     1     0     0     0     0
     0     0     0     0     0     0     0     1     0     0     0
     0     0     0     0     0     0     0     0     0     0     0

OR FOR Nf=2;

sizeI=min(Nb,Nf+nu-1-Delta)
sizerest=max(0,Nf+nu-1-Delta-Nb-1)
Jdeltastar = [zeros(Nb+1,Delta) [eye(sizeI) ; zeros(Nb+1-sizeI,sizeI)] zeros(Nb+1,sizerest)]

sizeI =  3
sizerest =     0
Jdeltastar =

     0     0     0     1     0     0
     0     0     0     0     1     0
     0     0     0     0     0     1
     0     0     0     0     0     0
     0     0     0     0     0     0
     0     0     0     0     0     0
```

With a shorter feedback section so $N_f=8$, $N_b=2$, $\Delta=3$, and $\nu=5$,

```
sizeI=min(Nb,Nf+nu-1-Delta)
sizerest=max(0,Nf+nu-1-Delta-Nb-1)
Jdeltastar = [zeros(Nb+1,Delta) [eye(sizeI) ; zeros(Nb+1-sizeI,sizeI)] zeros(Nb+1,sizerest)]

sizeI = 2
sizerest =     6
```

```
Jdeltastar =

     0     0     0     1     0     0     0     0     0     0     0
     0     0     0     0     1     0     0     0     0     0     0
     0     0     0     0     0     0     0     0     0     0     0
```

Then with

$$\boldsymbol{R}^{\perp}_{\boldsymbol{X}/\boldsymbol{Y}}(\Delta) \triangleq \bar{\mathcal{E}}_{\boldsymbol{x}} \cdot I - \boldsymbol{R}_{\boldsymbol{XY}}(\Delta) \cdot \boldsymbol{R}^{-1}_{\boldsymbol{YY}} \cdot \boldsymbol{R}_{\boldsymbol{YX}}(\Delta) \ , \tag{3.411}$$

the MSE for this fixed $\boldsymbol{b}$ value becomes

$$\begin{aligned}
\sigma^2_{\epsilon}(\Delta) &= \boldsymbol{b}^* \cdot \boldsymbol{R}^{\perp}_{\boldsymbol{X}/\boldsymbol{Y}}(\Delta) \cdot \boldsymbol{b} && (3.412)\\
&= \boldsymbol{b}^* \cdot \left(\bar{\mathcal{E}}_{\boldsymbol{x}} \cdot I_{N_b} - \bar{\mathcal{E}}_{\boldsymbol{x}} \cdot \tilde{J}^*_{\Delta} \cdot \boldsymbol{H}^* \cdot \left(\boldsymbol{H} \cdot \boldsymbol{H}^* + \frac{1}{\bar{\mathcal{E}}_{\boldsymbol{x}}} \cdot \boldsymbol{R}_{\boldsymbol{nn}} \right)^{-1} \cdot \boldsymbol{H} \cdot \tilde{J}_{\Delta} \right) \cdot \boldsymbol{b} && (3.413)\\
&= \bar{\mathcal{E}}_{\boldsymbol{x}} \cdot \boldsymbol{b}^* \cdot \tilde{J}^*_{\Delta} \cdot \boldsymbol{H} \cdot \left(\bar{\mathcal{E}}_{\boldsymbol{x}} \cdot \boldsymbol{H}^* \cdot \boldsymbol{R}^{-1}_{\boldsymbol{nn}} \cdot \boldsymbol{H} + I \right)^{-1} \boldsymbol{H} \cdot \tilde{J}_{\Delta} \cdot \boldsymbol{b} && (3.414)\\
&= \boldsymbol{b}^* \cdot \tilde{J}^*_{\Delta} \cdot \boldsymbol{H} \cdot \left(\boldsymbol{H}^* \cdot \boldsymbol{R}^{-1}_{\boldsymbol{nn}} \cdot \boldsymbol{H} + \frac{1}{\bar{\mathcal{E}}_{\boldsymbol{x}}} \cdot I \right)^{-1} \boldsymbol{H} \cdot \tilde{J}_{\Delta} \cdot \boldsymbol{b} \quad . && (3.415)
\end{aligned}$$

By rewriting

$$\tilde{\boldsymbol{Q}}(\Delta) = \tilde{J}^*_{\Delta} \cdot \boldsymbol{H} \cdot \left(\boldsymbol{H}^* \cdot \boldsymbol{R}^{-1}_{\boldsymbol{nn}} \cdot \boldsymbol{H} + \frac{1}{\bar{\mathcal{E}}_{\boldsymbol{x}}} \cdot I \right)^{-1} \boldsymbol{H} \cdot \tilde{J}_{\Delta} \quad , \tag{3.416}$$

this matrix now appears similar to (3.226) The simple scaling by channel energy becomes more complex with finite-length filters, but the basic structure is the same. That is $\boldsymbol{R}^{\perp}_{\boldsymbol{X}/\boldsymbol{Y}}(\Delta)$ is the autocorrelation matrix for the error sequence of length N_b that is associated with a "matrix" MMSE-LE in both finite- and infinite-length cases. The solution then requires factorization of the inner matrix into canonical factors, which is executed with Cholesky factorization for finite matrices, according to

$$\sigma^2_{\epsilon}(\Delta) = \boldsymbol{b} \cdot \underbrace{G^{-1}_{\Delta} \cdot S^{-1}_{\Delta} \cdot G^{-*}_{\Delta}}_{\tilde{\boldsymbol{Q}}(\Delta)} \cdot \boldsymbol{b}^* \quad , \tag{3.417}$$

The is minimum occurs when

$$\boldsymbol{b} = \boldsymbol{g}(\Delta) \quad , \tag{3.418}$$

the top row of the upper-triangular matrix G_{Δ}. The MMSE is thus obtained by computing Cholesky factorizations of $\tilde{\boldsymbol{Q}}$ for all reasonable values of Δ and then setting $\boldsymbol{b} = \boldsymbol{g}(\Delta)$. There is a similarity with Chapter 2's MMSE MAC solution also, but because there are no block symbols, the determinant of the multiuser case is replaced by the corresponding Cholesky factor. Then, the minimum is the corresponding Cholesky factor:

$$\sigma^2_{\epsilon}(\Delta) = S^{-1}_0(\Delta) \quad . \tag{3.419}$$

From previous developments, as the lengths of filters go to infinity, any value of Δ works and also $S_0 \to \gamma_0 \cdot \frac{\mathcal{N}_0}{2} / \bar{\mathcal{E}}_{\boldsymbol{x}}$ to ensure the infinite-length MMSE-DFE solution of Section 3.6.

The feed-forward filter then becomes

$$\begin{aligned}
\boldsymbol{w} &= \boldsymbol{b} \cdot \boldsymbol{R}_{\boldsymbol{XY}}(\Delta) \cdot \boldsymbol{R}^{-1}_{\boldsymbol{YY}} && (3.420)\\
&= \boldsymbol{g}(\Delta) \cdot \tilde{J}^*_{\Delta} \cdot \boldsymbol{H}^* \cdot \left(\boldsymbol{H} \cdot \boldsymbol{H}^* + \frac{1}{\bar{\mathcal{E}}_{\boldsymbol{x}}} \cdot \boldsymbol{R}_{\boldsymbol{nn}} \right)^{-1} && (3.421)\\
&= \underbrace{\boldsymbol{g}(\Delta) \cdot \tilde{J}^*_{\Delta} \cdot \left(\boldsymbol{H}^* \cdot \boldsymbol{R}^{-1}_{\boldsymbol{nn}} \cdot \boldsymbol{H} + \frac{1}{\bar{\mathcal{E}}_{\boldsymbol{x}}} \right)^{-1}}_{\text{feedforward filter}} \cdot \underbrace{\boldsymbol{H}^*}_{\text{matched filter}} \quad , && (3.422)
\end{aligned}$$

which can be interpreted as a matched filter followed by a feed-forward filter that becomes $1/G^*(D^{-*})$ as its length goes to infinity. However, the result that the feed-forward filter is an anti-causal factor of

the canonical factorization does not follow for finite length. Chapter 5 finds a situation that is an exact match and for which the feed-forward filter is an inverse of a canonical factor, but this requires the DFE filters to become periodic in a period equal to the number of taps of the feed-forward filter (plus an excess bandwidth factor).

The SNR is as always

$$SNR_{MMSE-DFE,U} = \frac{\bar{\mathcal{E}}_{\boldsymbol{x}}}{S_0(\Delta)} - 1 \quad . \tag{3.423}$$

Bias can be removed by scaling the decision-element input by the ratio of $SNR_{MMSE-DFE}/SNR_{MMSE-DFE,U}$, thus increasing its variance by $(SNR_{MMSE-DFE}/SNR_{MMSE-DFE,U})^2$.

3.7.5.1 Finite-length Noise-Predictive DFE

Figure 3.47 introduces the "noise-predictive" DFE, which is also Problem 3.8's subject.

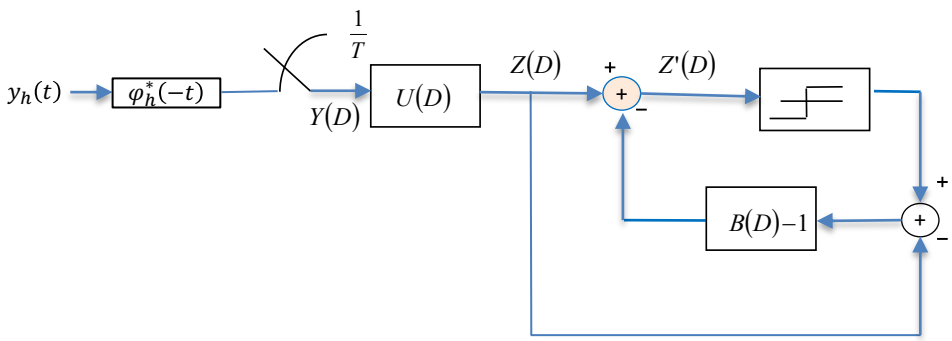

Figure 3.47: Noise-Predictive DFE

This DFE feeds back the error sequence instead of decisions. The feedforward filter output essentially predicts the noise and then the DFE cancels this noise, whence the name "noise-predictive" DFE. Correct solution to the infinite-length MMSE filter Problem 3.8 finds that $B(D)$ remains equal to the same $G(D)$ as the infinite-length MMSE-DFE. The filter $U(D)$ becomes the MMSE-LE so that $Z(D)$ has no ISI, but a strongly correlated (and enhanced) noise. The predictor then reduces the noise to a white error sequence. If $W(D) = \frac{1}{\gamma_0 \cdot \|h\| \cdot G^{-*}(D^{-*})}$ of the normal MMSE-DFE, then (see Problem 3.8)

$$U(D) = \frac{W(D)}{G(D)} \quad . \tag{3.424}$$

The MMSE, all SNR's, and biasing/unbiasing remain the same.

The finite-length noise-predictive DFE follows similarly. It is notationally convenient to say that the number of feedforward taps in $\boldsymbol{u}$ is $(N_f - \nu)\ell$. Clearly if ν is fixed as always, then any number of taps (greater than ν can be investigated without loss of generality with this early notational abuse. Clearly by abusing N_f (which is not the number of taps), ANY positive number of taps in $\boldsymbol{u}$ can be constructed without loss of generality for any value of $\nu \geq 0$. In this case, the error signal can becomes

$$e_k = \boldsymbol{b}_k \cdot \boldsymbol{X}_k(\Delta) - \boldsymbol{b} \cdot \boldsymbol{Z} \tag{3.425}$$

where

$$\boldsymbol{Z}_k = \begin{bmatrix} z_k \\ \vdots \\ z_{k-\nu} \end{bmatrix} \quad . \tag{3.426}$$

Then,

$$\boldsymbol{Z}_k = U \cdot \boldsymbol{Y}_k \tag{3.427}$$

where

$$U = \begin{bmatrix} \boldsymbol{u} & 0 & ... & 0 \\ 0 & \boldsymbol{u} & ... & 0 \\ \vdots & \ddots & \ddots & \vdots \\ 0 & ... & 0 & \boldsymbol{u} \end{bmatrix} \tag{3.428}$$

and

$$\boldsymbol{Y}_k = \begin{bmatrix} y_k \\ \vdots \\ y_{k-N_f+1} \end{bmatrix} \quad . \tag{3.429}$$

By defining the $(N_f)l$-tap filter

$$\boldsymbol{w} \triangleq \boldsymbol{b} \cdot U \quad , \tag{3.430}$$

then the error becomes

$$e_k = \boldsymbol{b}_k \cdot \boldsymbol{X}_k(\Delta) - \boldsymbol{w} \cdot \boldsymbol{Y} \quad , \tag{3.431}$$

which is the same error as in the alternate finite-DFE viewpoint. Thus, solution for the conventional DFE's $\boldsymbol{b}$ and $\boldsymbol{w}$ solves Equation (3.430) for U when $\boldsymbol{b}$ and $\boldsymbol{w}$ are known. However, it follows directly then from Equation (3.408) that

$$\boldsymbol{u} = \boldsymbol{R}_{\boldsymbol{XY}}(\Delta) \cdot \boldsymbol{R}_{\boldsymbol{YY}}^{-1} \quad , \tag{3.432}$$

so following the infinite-case form, $\boldsymbol{u}$ is the finite-length MMSE-LE with $(N_f - \nu)l$ taps. The only difference from the infinite-length case is the change in length.

3.7.6 The Stanford DFE Program

The Stanford DFE matlab program has been created, used, and refined by Stanford students over many years, and appears in Appendix G. The program has the following call command:

function (SNR, wt) = **dfe** (ℓ,h,nff, nbb, delay, Ex, noise);
where the inputs and outputs are listed as

- ℓ = oversampling factor
- h = pulse response, oversampled at l (size)
- nff = number of feed-forward taps, N_f
- nbb = number of feedback taps N_b
- delay $\approx$ delay of system Nff + length of p - nbb ; Δ ; if delay = -1, then choose the best delay
- Ex = average energy of signals $\mathcal{E}_{\boldsymbol{x}}$
- noise = autocorrelation vector (size l*nff) (NOTE: noise is assumed to be stationary). For white noise, this vector is simply [σ^2 0...0].
- SNR = equalizer SNR, unbiased and in dB
- wt = equalizer coefficients, $\boldsymbol{w}$.

```
>> help dfecolor
  ---------------------------------------------------------------
  [dfseSNR,w_t] = dfecolor(l,p,nff,nbb,delay,Ex,noise);

  INPUTS
  l     = oversampling factor
```

```
h     = pulse response, oversampled at l (size)
nff   = number of feed-forward taps
nbb   = number of feedback taps
delay = delay of system <= nff+length of p - 2 - nbb
        if delay = -1, then choose best delay
Ex    = average energy of signals
noise = noise autocorrelation vector (size l*nff)
  so white noise is [1 zeros(l*nff-1)]
NOTE: noise is assumed to be stationary

OUTPUTS
dfseSNR = equalizer SNR, unbiased in dB
w_t = equalizer coefficients [w -b]
opt_delay = optimal delay found if delay =-1 option used.
            otherwise, returns delay value passed to function
-------------------------------------------------------------
```

A complete program listing appears in Appendix G.

The designer may use this program to a substantial advantage in avoiding tedious matrix calculations. The program has also found wide industrial use to compute/project equalizer performance (setting nbb=0 also provides a linear equalizer). The reader is cautioned against the use of a number of rules of thumb (like "DFE SNR is the SNR(f) at the middle of the band") used by various who call themselves experts and often over-estimate the DFE performance using such formulas. Difficult transmission channels may require large numbers of taps and considerable experimentation to find the best settings.

3.7.7 Error Propagation in the DFE

This chapter so far has ignored the effect of feedback-section decision errors. At low error rates, say 10^{-5} or below, this is reasonable. When an error occurs, it can cause another error, and thus create **error propagation**. There is, however, an accurate computation of the DFE errors' performance loss, although enormous amounts of computational power may be necessary (much more than that required to simulate the DFE and measure the error-rate increase).

At high error rates of 10^{-3} and above, error propagation can lead to several dB of loss. In coded systems (see Chapter 2), the inner channel (DFE) may have an error rate that is unacceptably high (for a DFE to avoid error propagation) that theoretically would later reduce in the applied code's decoder. However, error propagation may significantly degrade such a system. Section 3.8's precoders eliminate error propagation, but this requires that the transmitter know the channel, which is not always possible, Transmit channel knowledge can be difficult in transmission systems with significant channel variation, i.e, digital mobile telephony or impossible in broadcast radio or television. An error-propagation analysis for the infinite-length equalizer has not yet been invented, thus the analysis here applies only to FIR DFE's with finite N_b.

If the equalized pulse response is v_k (after removal of any bias), and assuming that any error signal, e_k, in the DFE output is uncorrelated with the symbol of interest, x_k, this error signal can be decomposed into 4 constituent signals

1. precursor ISI - $e_{pr,k} = \sum_{i=-\infty}^{-1} v_i \cdot x_{k-i}$
2. postcursor ISI - $e_{po,k} = \sum_{i=N_b+1}^{\infty} v_i \cdot x_{k-i}$
3. filtered noise - $e_{n,k} = \sum_{i=-\infty}^{\infty} w_i \cdot n_{k-i}$
4. feedback errors - $e_{f,k} = \sum_{i=1}^{N_b} v_i \cdot (x_{k-i} - \hat{x}_{k-i})$

The sum of the first 3 signals constitute the MMSE with energy $\sigma^2_{MMSE-DFE}$. The last signal is

$$e_{f,k} = \sum_{i=1}^{N_b} v_i \cdot \epsilon_{k-i} \tag{3.433}$$

where $\epsilon_k \triangleq x_k - \hat{x}_k$. This last distortion component has a discrete distribution with $(2M-1)^{N_b}$ possible points.

The **error event vector**, $\boldsymbol{\epsilon}_k$, is

$$\boldsymbol{\epsilon}_k \triangleq [\epsilon_{k-N_b+1}\ \epsilon_{k-N_b+2}\ \dots\ \epsilon_k] \tag{3.434}$$

Given $\boldsymbol{\epsilon}_{k-1}$, there are only $2M-1$ possible values for $\boldsymbol{\epsilon}_k$. Equivalently, an error event's evolution has a finite-state-machine description with $(2M-1)^{N_b}$ states, each corresponding to one of the $(2M-1)^{N_b}$ possible length-N_b error events. Figure 3.48 shows such a finite state machine .

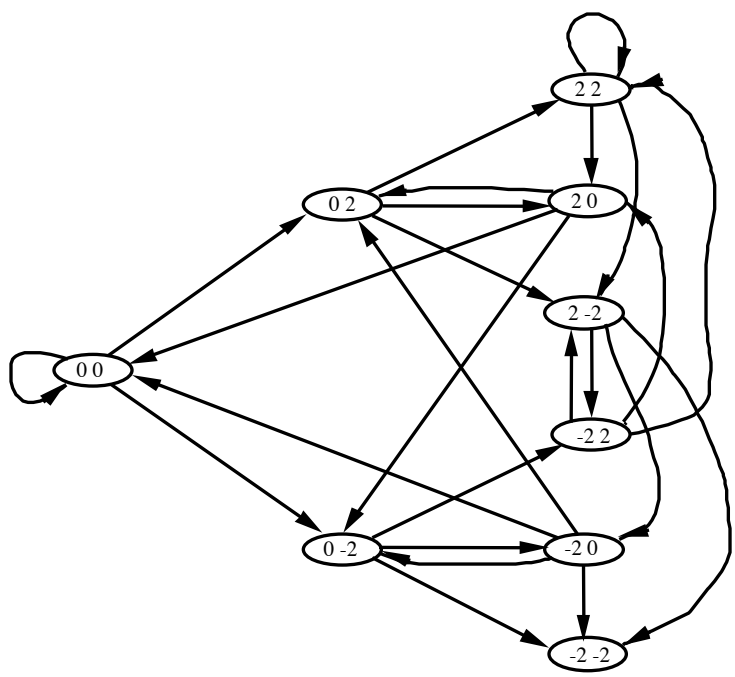

Figure 3.48: Finite State Machine for $N_b = 2$ and $M = 2$ in evaluating DFE Error Propagation

. The probability that $\boldsymbol{\epsilon}_k$ has a specific value, or that the state transition diagram goes to the corresponding state at time k, is (denoting the corresponding new entry in $\boldsymbol{\epsilon}_k$ as ϵ_k)

$$P_{\boldsymbol{\epsilon}_k/\boldsymbol{\epsilon}_{k-1}} \le Q\left[\frac{|\, d_{\min} - e_{f,k}(\boldsymbol{\epsilon}_{k-1})\,|}{2 \cdot \sigma_{\text{MMSE-DFE}}}\right] \quad . \tag{3.435}$$

The reason for (3.435)'s upper bound and absolute value is that even if $e_{f,k}(\boldsymbol{\epsilon}_{k-1})$ is opposite in direction to noise, it could lead to displacement from a constellation symbol value towards another (erroneous-decision) point if M is large and $|e_{f,k}(\boldsymbol{\epsilon}_{k-1})| > d_{\min}/2$. There are $2M-1$ such values for each of the $(2M-1)^{N_b}$ states. Let $\boldsymbol{\Upsilon}$ denote a square $(2M-1)^{N_b} \times (2M-1)^{N_b}$ transition-probability matrix where the i, j^{th} element is the probability of entering state i, given the DFE is in state j. The column sums are thus all unity. For a matrix of non-negative entries, Appendix A's "Peron-Frobenious" lemma states that there is a unique eigenvector $\boldsymbol{\rho}$ of all nonnegative entries that satisfies the equation (under mild conditions that occur in error propagation)

$$\boldsymbol{\rho} = \boldsymbol{\Upsilon} \cdot \boldsymbol{\rho} \quad . \tag{3.436}$$

The solution $\boldsymbol{\rho}$ is called the **stationary state distribution** or **Markov distribution** of the state transition diagram. The ith entry, ρ_i, is the steady-state probability of being in state i. Of course, $\sum_{i=1}^{(2M-1)^{N_b}} \rho_i = 1$. By denoting the set of states for which $\epsilon_k \neq 0$ as $\mathcal{E}$, one determines the error probability as

$$P_e = \sum_{i \in \mathcal{E}} \rho_i \quad . \tag{3.437}$$

This is a more accurate DFE-error-probability estimate that includes error propagation. A larger state-transition diagram, corresponding to the explicit consideration of residual ISI as a discrete probability mass function, would yield a yet more accurate estimate of the error probability for the equalized channel - however, the relatively large magnitude of the error propagation samples usually makes their explicit consideration more important than the (usually) much smaller residual ISI.

The number of states can be very large for reasonable values of M and N_b, so that the calculation of the stationary distribution $\boldsymbol{\rho}$ could exceed the computation required for a direct measurement of SNR with a DFE simulation. There are a number of methods that can be used to reduce the number of states in the finite-state machine, most of which will reduce the accuracy of the error probability estimate.

In the usual case, the constellation for x_k is symmetric with respect to the origin, and there is essentially no difference between $\boldsymbol{\epsilon}_k$ and $-\boldsymbol{\epsilon}_k$, so that the analysis may merge the two corresponding states and only consider one of the error vectors. This can be done for almost half[15] the states in the state transition diagram, leading to a new state transition diagram with M^{N_b} states. Further analysis then proceeds as above, finding the stationary distribution and adding over states in $\mathcal{E}$. There is essentially no difference in this P_e estimate with respect to the one estimated using all $(2M-1)^{N_b}$ states; however, the number of states can remain unacceptably large.

At a loss in P_e accuracy, the designer may ignore error magnitudes and signs, and compute error statistics for binary error event vectors, which we now denote $\boldsymbol{\varepsilon} = [\varepsilon_1 \, , ..., \, \varepsilon_{N_b}]$, of the type (for $N_b = 3$)

$$[\,0\,0\,0\,] \;,\; [\,0\,1\,0\,] \;,\; [\,1\,0\,0\,] \;,\; [\,1\,0\,1\,] \quad . \tag{3.438}$$

This reduces the number of states to 2^{N_b}, but unfortunately the state transition probabilities no longer depend only on the previous state. Thus, analysis must try to find an upper bound on these probabilities that depends only on the previous states. In so doing, the sum of the stationary probabilities corresponding to states in $\mathcal{E}$ will also upper bound the error probability. $\mathcal{E}$ corresponds to those states with a nonzero entry in the first position (the "odd" states, $\varepsilon_1 = 1$). An upperbound on each transition probability is

$$\begin{aligned} P_{\epsilon_{1,k}=1/\boldsymbol{\epsilon}_{k-1}} &= \sum_{\{i \;|\; \epsilon_{1,k}(i) \text{is allowed transition from } \boldsymbol{\epsilon}_{k-1}\}} P_{\epsilon_{1,k}=1/\boldsymbol{\epsilon}_{k-1},\epsilon_{1,k}(i)} \cdot P_{\epsilon_{1,k}(i)} & (3.439) \\ &\leq \sum_{i \;|\; \epsilon_{1,k}(i) \text{is allowed transition from } \boldsymbol{\epsilon}_{k-1}} \max_{\epsilon_{1,k}(i)} P_{\epsilon_{1,k}=1/\boldsymbol{\epsilon}_{k-1},\epsilon_{1,k}(i)} \cdot P_{\epsilon_{1,k}(i)} \\ &= \max_{\epsilon_{1,k}(i)} P_{\epsilon_{1,k}=1/\boldsymbol{\epsilon}_{k-1},\epsilon_{1,k}(i)} \quad . & (3.440) \end{aligned}$$

Explicit computation of (3.440)'s maximum value observes that this error probability corresponds to a worst-case signal offset of

$$\delta_{max}(\boldsymbol{\epsilon}) = (M-1) \cdot d \cdot \sum_{i=1}^{N_b} |v_i| \cdot \epsilon_{1,k-i} \quad , \tag{3.441}$$

which is analogous to peak distortion. This distortion corresponds to the worst of the two QAM dimensions, which are assumed to be rotated so that $d_{\min}$ lies along either or both of the dimensions. As long as this quantity is less than the minimum distance between constellation points, the corresponding error probability has then upper bound

$$P_{e_k/\boldsymbol{\epsilon}_{k-1}} \leq Q\left[\frac{\frac{d_{\min}}{2} - \delta_{max}(\boldsymbol{\epsilon})}{\sqrt{\sigma^2_{MMSE-DFE}}}\right] \quad . \tag{3.442}$$

[15] There is no reduction for zero entries.

Now, with the desired state-dependent (only) transition probabilities, the upper bound for P_e with error propagation is

$$P_e \leq \sum_{\boldsymbol{\varepsilon}} Q \left[\frac{\frac{d_{\min}}{2} - \delta_{max}(\boldsymbol{\varepsilon})}{\sqrt{\sigma^2_{MMSE-DFE}}} \right] \cdot P_{\boldsymbol{\varepsilon}} \quad . \tag{3.443}$$

Even in this case, the number of states 2^{N_b} can be too large.

A further reduction to $N_b + 1$ states is possible, by partitioning the 2^{N_b} states into groups that index only by first i elements of $\boldsymbol{\epsilon}_{k-1}$; thus, state $i = 1$ corresponds to any state of the form $[0\ \epsilon]$, while state $i = 2$ corresponds to $[0\ 0\ \varepsilon\ ...]$, etc. The upper bound on error probability for transitions into any state, i, then uses a $\delta_{max}(i)$ given by

$$\delta_{max}(i) = (M-1) \cdot d \cdot \sum_{i=i+1}^{N_b} |v_i| \quad , \tag{3.444}$$

and $\delta_{max}(N_b) = 0$.

Finally, a trivial bound that corresponds to noting that after an error is made, we have $M^{N_b} - 1$ possible following error event vectors that can correspond to error propagation (only the all zeros error event vector corresponds to no additional errors within the time-span of the feedback path). These error event vectors' probability of occurrence is each no greater than the initial error probability, so they can all be considered as nearest neighbors. Thus adding these to the original probability of the first error,

$$P_e(errorprop) \leq M^{N_b} \cdot P_e(first) \quad . \tag{3.445}$$

It should be obvious that this bound gives useful results only if N_b is small (that is a error probability bound of .5 for i.i.d. input data may be lower than this bound even for reasonable values of M and N_b). That is suppose, the first error probability is 10^{-5}, and $M = 8$ and $N_b = 8$, then this last (easily computed) bound gives $P_e \leq 100$!

3.7.8 Look-Ahead

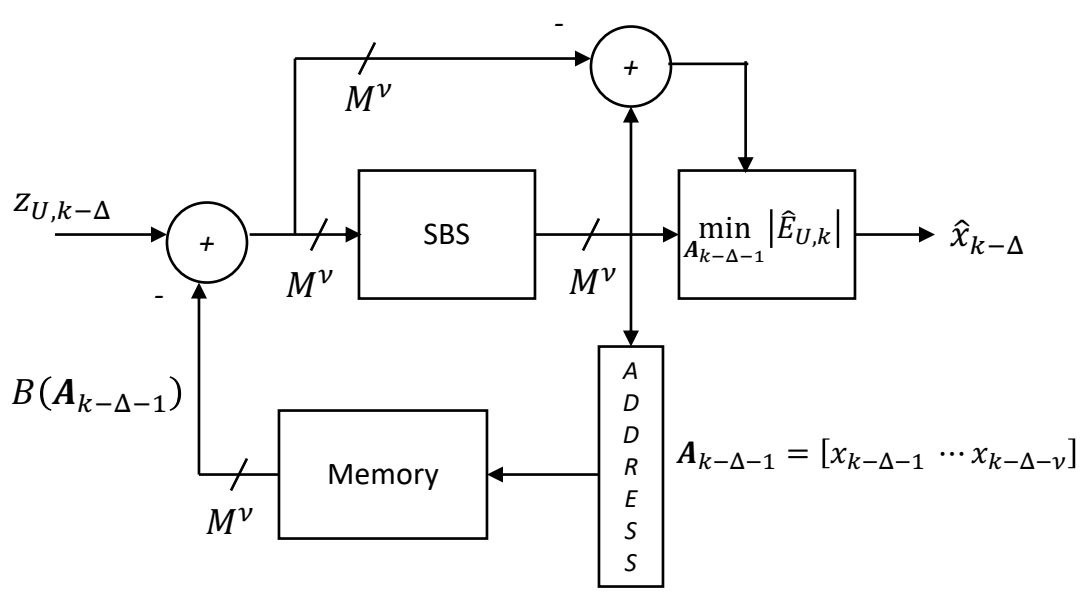

Figure 3.49: Look-Ahead mitigation of error propagation in DFEs.

Figure 3.49 illustrates a "look-ahead" mechanism for reducing error propagation. Instead of using the decision, the decoder retains M^ν possible decision vectors. The vector is of dimension ν and can be

viewed as an address $\boldsymbol{A}_{k-\Delta-1}$ to the memory. The receiver computes the possible output for each of the M^ν and subtracts it from $z_{U,k-\Delta}$. The receiver precomputes M^ν SBS decisions and compares their distances from a potential symbol value, namely smallest $|E_{U,k-\Delta}|$. The decoder selects the $\hat{x}_{k-\Delta}$ that has smallest such distance. This method is called "look-ahead" decoding basically because all possible previous decisions' The receiver essentially precomputes and stores ISI. If M^ν calculations (or memory locations) is too complex, then the largest $\nu' < \nu$ taps can be used (or typically the most recent ν' and the rest subtracted in typical DFE fashion for whatever the decisions previous to the ν'-tap interval in a linear filter. Look-ahead leads to the Maximum Likelihood Sequence detection (MLSD) methods of Chapter 7 that are no longer SBS based. Such look-ahead methods can never exceed $SNR_{MMSE-DFE,U}$ in terms of performance, but can come very close since error propagation can be very small. (MLSD methods can exceed $SNR_{MMSE-DFE,U}$.)

3.7.9 Dummy Guard Periods

To be added, see Lecture 17:8 2024 slide.

3.8 Precoding and Error-Propagation Loss

This section addresses solutions to the DFE error-propagation problem. Subsection 3.8.1 first presents precoding, which essentially moves the DFE's feedback section to the transmitter with a minimal (but nonzero) transmit-power-increase penalty, but with no reduction in DFE SNR. Subsection 3.8.2's second approach of partial response channels (which have trivial precoders) is similar, but with no transmit power penalty. Partial response systems may however have a DFE SNR loss because the feedback section has preset $B(D)$ rather than optimal $B(D)$. This preset value, usually with all integer coefficients, leads to DFE structural simplification.

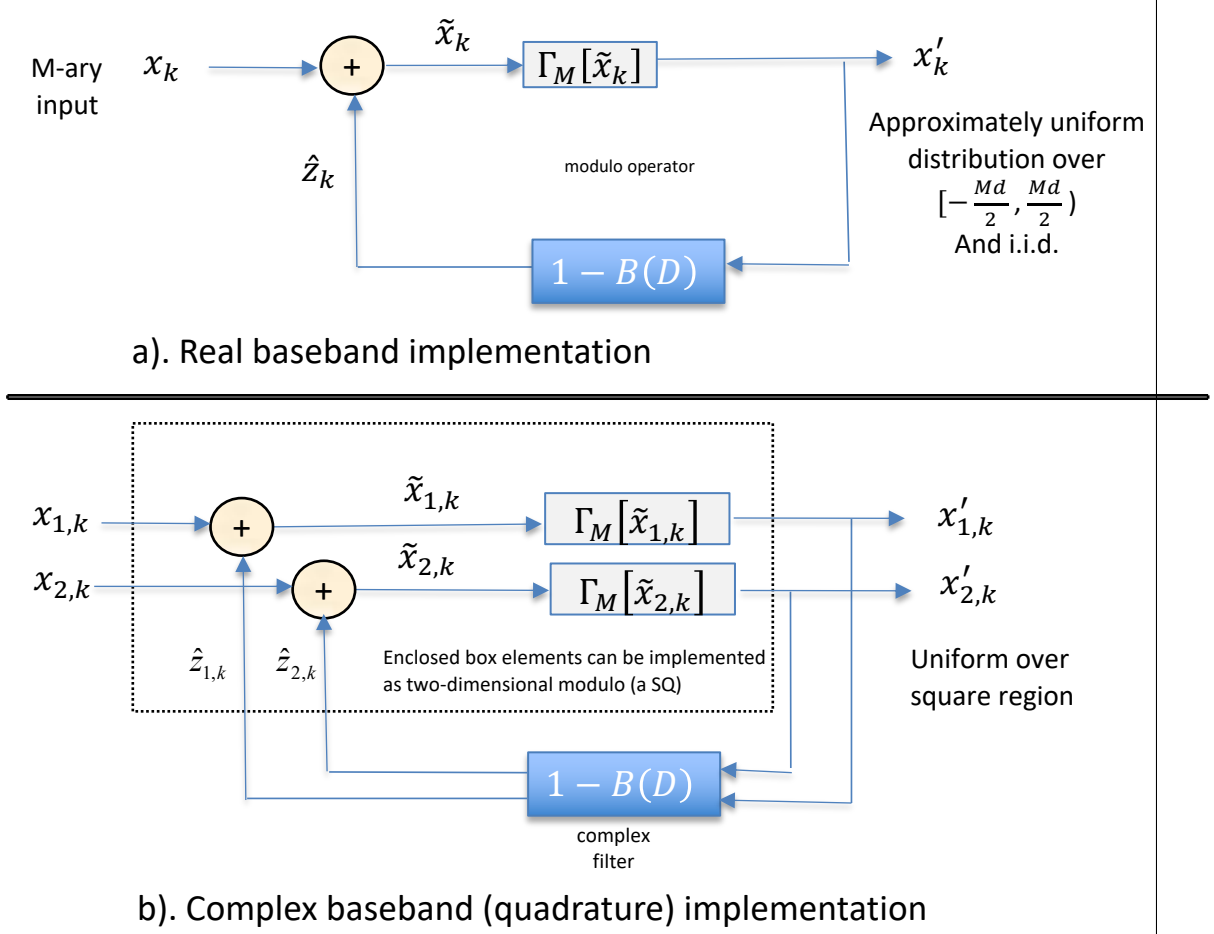

Figure 3.50: The Tomlinson Precoder.

3.8.1 Precoders

Precoders attempt to add the negative ISI at the channel input, with minimal transmit-energy increase.

3.8.1.1 Tomlinson Precoding

The **Tomlinson Precoder (TPC)**, or Tomlinson-Harashima Precoder[16] [5], eliminates error propagation as in Figure 3.50. Figure 3.50(a) illustrates the case for real one-dimensional signals, while Figure 3.50(b) illustrates a generalization to complex-baseband signals. In the second complex case, the two real sums and two one-dimensional modulo operators can be generalized to a two-dimensional modulo where arithmetic is modulo a two-dimensional region that tesselates two-dimensional space (for example, a hexagon, or a square).

The Tomlinson precoder appears in the transmitter before the modulator. The Tomlinson Precoder maps the data symbol x_k into another data symbol x'_k, which is in turn applied to the modulator (not shown in Figure 3.50). The basic idea is to move the DFE feedback section to the transmitter where decision errors are impossible. However, straightforward moving of the filter $1/B(D)$ to the transmitter could result in significant transmit-energy increase. To prevent energy increase, modulo arithmetic bounds the precoder output value x'_k:

Definition 3.8.1 *[Modulo Operator] The* **modulo operator** $\Gamma_M(x)$ *is a nonlinear function, defined on an M-ary (PAM or QAM square) input constellation with uniform spacing d, such that*

$$\Gamma_M(x) = x - M \cdot d \cdot \left\lfloor \frac{x + \frac{M \cdot d}{2}}{M \cdot d} \right\rfloor \tag{3.446}$$

where $\lfloor y \rfloor$ means the largest integer that is less than or equal to y. $\Gamma_M(x)$ **need not be an integer**. *This text denotes modulo M addition and subtraction by $\oplus_M$ and $\ominus_M$ respectively. That is*

$$x \oplus_M y \triangleq \Gamma_M[x + y] \tag{3.447}$$

and

$$x \ominus_M y \triangleq \Gamma_M[x - y] \quad . \tag{3.448}$$

For complex QAM, each dimension is treated modulo $\sqrt{M}$ independently.

Figure 3.51 illustrates modulo arithmetic for $M = 4$ PAM signals with $d = 2$. The following lemma notes that the modulo operation distributes over addition:

Lemma 3.8.1 *[Distribution of $\Gamma_M(x)$ over addition] The modulo operator can be distributed over a sum in the following manner:*

$$\Gamma_M[x + y] = \Gamma_M(x) \oplus_M \Gamma_M(y) \tag{3.449}$$

$$\Gamma_M[x - y] = \Gamma_M(x) \ominus_M \Gamma_M(y) \quad . \tag{3.450}$$

The proof is trivial.

[16] This device was long called "Tomlinson Precoder" before it was discovered a slightly earlier paper by Harashima covered the same topic. The concept is somewhat trivial, so we'll not put significant effort into author description and origins.

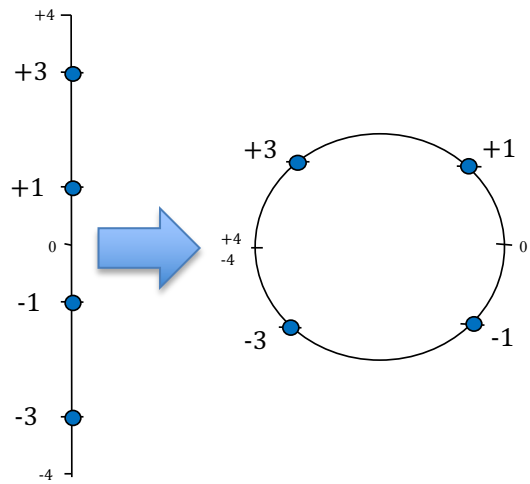

x_k	$\Gamma_4(x_k)$
+3	+3
-3	-3
-4.5	+3.5
-6	+2
+6.1	-1.9

Figure 3.51: Illustration of modulo arithmetic operator.

The Tomlinson Precoder generates an internal signal

$$\tilde{x}_k = x_k - \sum_{i=1}^{\infty} b_i \cdot x'_{k-i} \tag{3.451}$$

where

$$x'_k = \Gamma_M[\tilde{x}_k] = \Gamma_M \left[x_k - \sum_{i=1}^{\infty} b_i \cdot x'_{k-i} \right] \quad . \tag{3.452}$$

The scaled-by-$SNR_{MMSE-DFE}/SNR_{MMSE-DFE,U}$ MS-WMF output in the receiver is an optimal unbiased MMSE approximation to $X(D) \cdot G_U(D)$. That is

$$\mathbb{E}\left[\frac{SNR_{MMSE-DFE}}{SNR_{MMSE-DFE,U}} \cdot z_k / [x_k \; x_{k-1} \; , ...,] \right] = \sum_{i=0}^{\infty} g_{U,i} \cdot x_{k-i} \quad . \tag{3.453}$$

Thus, $B(D) = G_U(D)$. From Equation (3.256) with $x'(D)$ as the new input, the scaled feedforward filter output with the Tomlinson precoder is

$$z_{U,k} = \left(x'_k + \sum_{i=1}^{\infty} g_{U,i} \cdot x'_{k-i} \right) + e_{U,k} \quad . \tag{3.454}$$

$\Gamma_M[z_{U,k}]$ is

$$\begin{aligned}
\Gamma_M\left[z_{U,k}\right] &= \Gamma_M \left[\Gamma_M(x_k - \sum_{i=1}^{\infty} g_{U,i} \cdot x'_{k-i}) + \sum_{i=1}^{\infty} g_{U,i} \cdot x'_{k-i} + e_{U,k} \right] && (3.455)\\
&= \Gamma_M \left[x_k - \sum_{i=1}^{\infty} g_{U,i} x'_{k-i} + \sum_{i=1}^{\infty} g_{U,i} \cdot x'_{k-i} + e_{U,k} \right] && (3.456)\\
&= \Gamma_M\left[x_k + e_{U,k}\right] && (3.457)\\
&= x_k \oplus_M \Gamma_M\left[e_{U,k}\right] && (3.458)\\
&= x_k + e'_{U,k} \quad . && (3.459)
\end{aligned}$$

Since the probability that $|e_{U,k}|$ is larger than $M \cdot d/2$ is small in a well-designed system, the receiver design may assume that the error sequence has the same distribution and correlation properties after

the modulo operation. Thus, the Tomlinson Precoder permits the receiver to reproduce an ISI replica of input sequence at the (scaled) MS-WMF output. The original Tomlinson work was done for the ZF-DFE, which is a special case, with $G_U(D) = P_c(D)$. Figure 3.52 shows the receiver for the Tomlinson precoder.

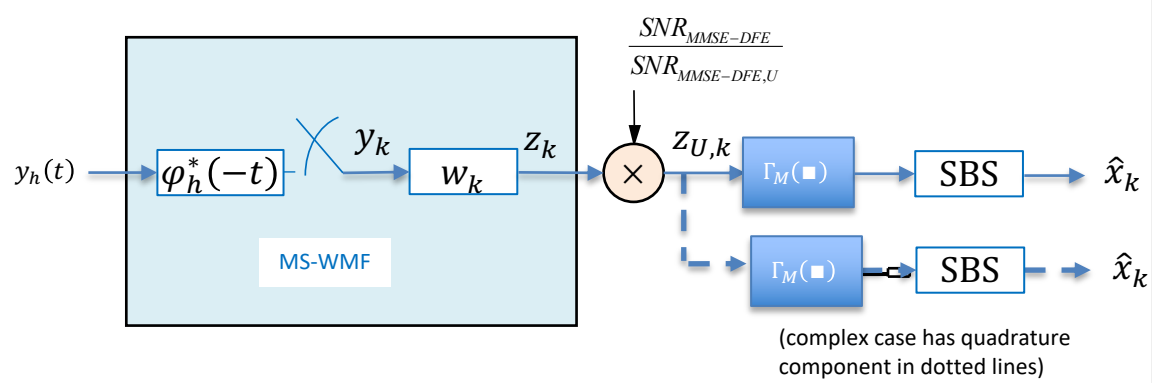

Figure 3.52: Receiver for Tomlinson precoded MMSE-DFE implementation.

The noise power at the feed-forward output is thus almost exactly the same as that of the corresponding MMSE-DFE and with no error progagation because there is no longer any need for the DFE feedback section. As stated here without proof, there is only a small price to pay in increased transmitter power when the TPC is used.

Theorem 3.8.1 [Tomlinson Precoder Output] *The Tomlinson Precoder output, when the input is an i.i.d. sequence, is also approximately i.i.d., and futhermore the output sequence is approximately uniform in distribution over the interval* $[-Md/2, Md/2)$.

There is no explicit proof of this theorem for finite M, although it can be proved exactly as $M \to \infty$. This theorem notes that the unbiased and biased receivers are identical as $M \to \infty$, because the SNR must also be infinite. Then, the modulo element is not really necessary, and the sequence x'_k can be shown to be equivalent to a prediction-error or "innovations" sequence, which is known in the estimation literature to be i.i.d. The i.i.d. part of the theorem appears to be valid for almost any M. The TPC's distribution and autocorrelation properties, in closed form, remain an unsolved problem at time of writing.

Using the uniform distribution assumption, the TPC's transmit-energy increase is the inverse ratio of the nominal value of $\frac{(M^2-1)d^2}{12}$ to the value for a continuous uniform random variable over the output interval $[-Md/2, Md/2)$, which is $\frac{M^2d^2}{12}$, leading to an input energy increase of

$$\frac{M^2}{M^2-1} \tag{3.460}$$

for PAM and correspondingly

$$\frac{M}{M-1} \tag{3.461}$$

for QAM. Ultimately, the designer has to reduce the distance between points to maintain constant energy. When the input is not a square constellation, the Tomlinson Precoder energy loss is usually larger, but never more than a few dB. The number of nearest neighbors also increases to $\bar{N}_e = 2$ for all constellations. These losses can be eliminated (and actually a gain is possible) using techniques called Trellis Precoding and/or shell mapping (See Section 10.6).

3.8.1.2 Laroia or Flexible Precoder

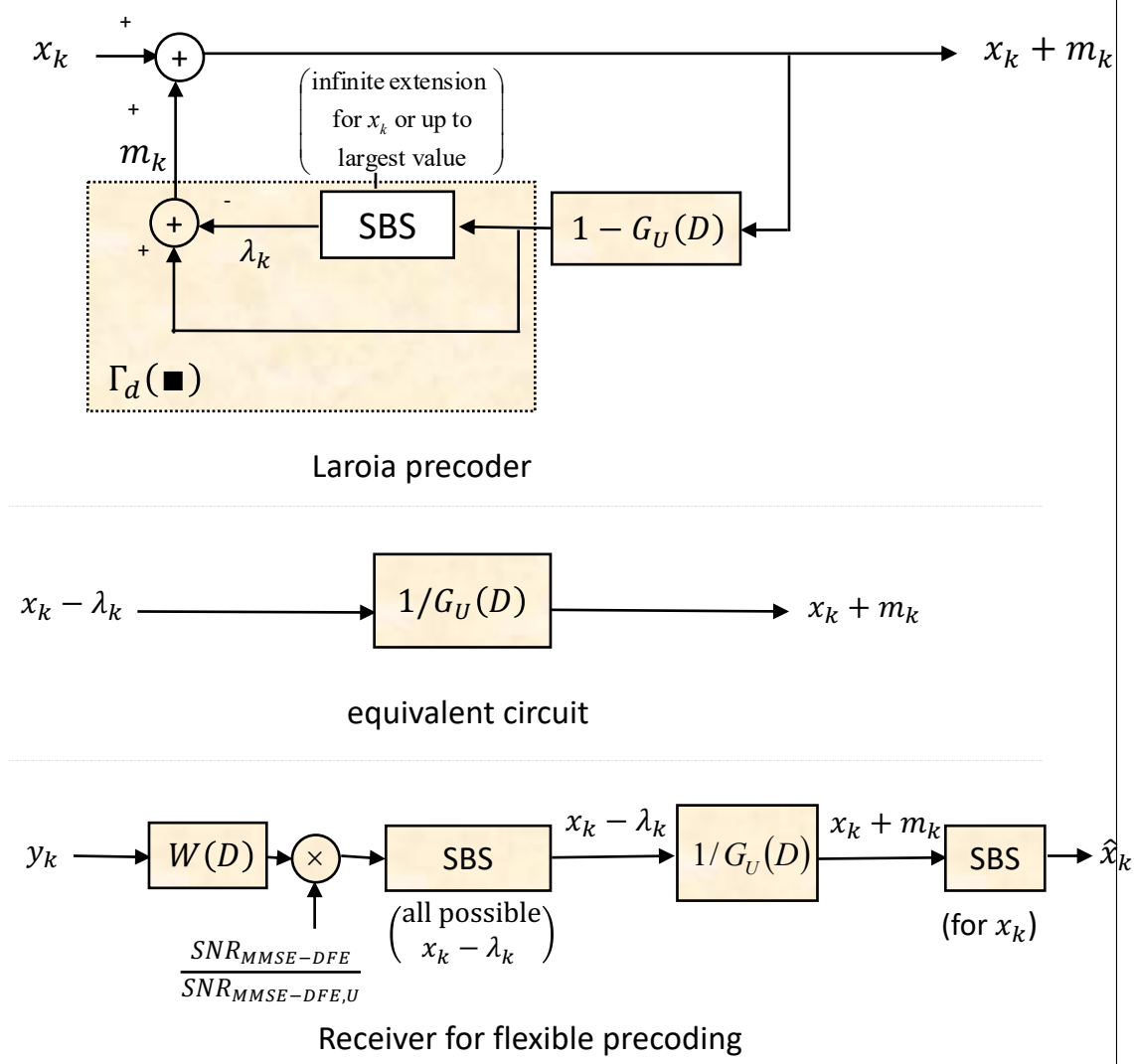

Figure 3.53: Flexible Precoding.

Figure 3.53 shows the Laroia precoder [6], which is a variation on Tomlinson precoding that mainly preserves the transmitted constellation's shape, unlike the Tomlinson precoder that forces a uniform square. The equivalent circuit is also shown in Figure 3.53 where the input is the difference between the actual input symbol value x_k and the "decision" output λ_k. The decision device finds the closest point in the constellation's infinite extension[17]. The constellation's extension is the set of points that continue to be spaced by $d_{\min}$ from the edge points along the same dimensions as the original constellation. This is a simple form of Chapter 2's dirty-paper precoders (which appear unknown to Laroia at time of conception). m_k is therefore a small error signal that is uniform in distribution over $(-d/2, d/2)$, thus having variance $d^2/12 << \mathcal{E}_x$, which follows from Chapter 2's crypto lemma.

[17]Such infinite extension's maximum range is actually the sum $\sum_{i=1}^{\nu} |\Re \; or \; \Im g_{U,i}| \cdot |\bar{R}_{ee}(D)$ or $\Im x_{max}|$.

The energy increase is therefore

$$\frac{\bar{\mathcal{E}}_{\boldsymbol{x}} + \frac{d^2}{12}}{\bar{\mathcal{E}}_{\boldsymbol{x}}} \quad . \tag{3.462}$$

For PAM, this increase would be

$$\frac{\frac{M^2-1}{3}\frac{d^2}{4}}{\frac{M^2-1}{3}\frac{d^2}{4} + \frac{d^2}{4}} = \frac{1}{1 + \frac{3}{M^2-1}} = \frac{M^2-1}{M^2-2} \quad , \tag{3.463}$$

while similarly it would be for SQ QAM:

$$\frac{M-1}{M-2} \quad , \tag{3.464}$$

This is a larger increase than the Tomlinson precoder for square constellations, for instance for binary it is an increase of 3/2 or 1.7 dB instead of the Tomlinson Precoders 4/3 or 1.3 dB. However, for a cross constellations, the flexible precoder is better. Indeed wherever constellation boundary is non-square and presumably shaping gain is positive flexible precoding retains tthat γ_s largely, and perfectly as $|C| \to \infty$, which is typical of systems that provide shaping gain when $\bar{b} > 1$.

Because of the combination of channel and feedforward equalizer filters, the feedforward filter output is

$$Z_U(D) = [X(D) + M(D)] \cdot G_U(D) + E_U(D) = X(D) - \lambda(D) + E_U(D) \quad . \tag{3.465}$$

Processing $Z_U(D)$ by a decision operation leaves $X(D) - \lambda(D)$, which essentially is the decision. However, to recover the input sequence $X(D)$, the receiver forms

$$Z'(D) = \frac{X(D) - \lambda(D)}{G_U(D)} = X(D) + M(D) \quad . \tag{3.466}$$

Since $M(D)$ is uniform and has magnitude always less than $d/2$, then $M(D)$ is removed by a second truncation (which is not really a decision, but operates using essentially the same logic as the first decision).

3.8.1.3 Example and error propagation in flexible precoding

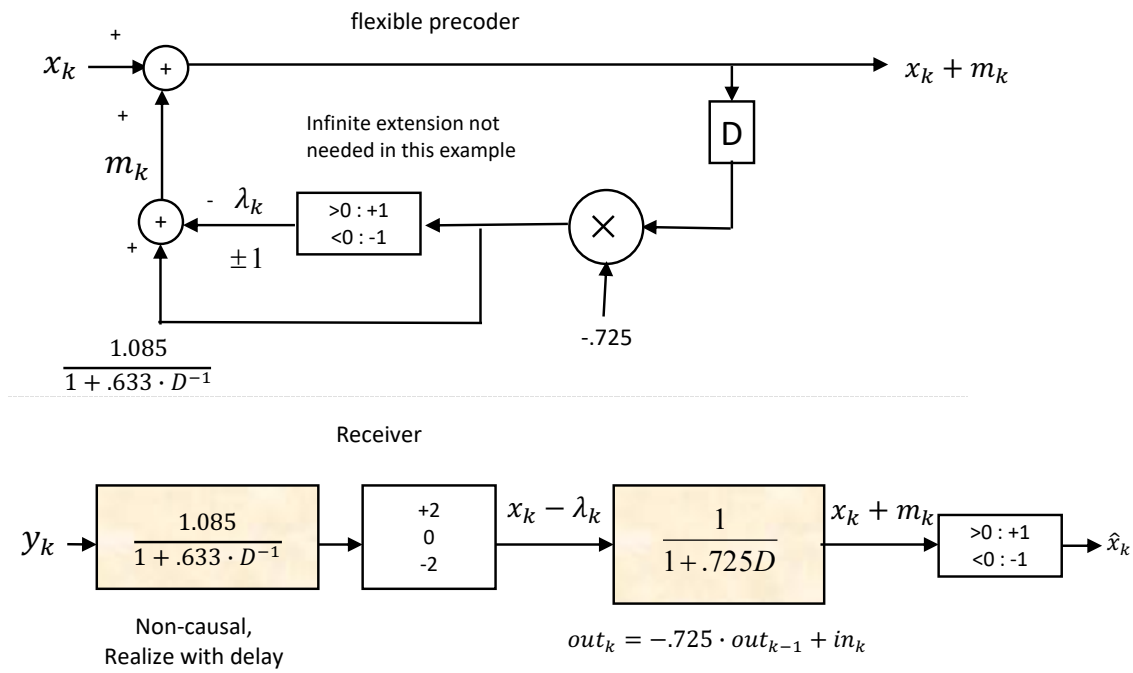

Figure 3.54: Flexible Precoding Example.

EXAMPLE 3.8.1 *[$1 + .9D^{-1}$ system with flexible precoding]* The flexible precoder and corresponding receiver for the $1 + .9 \cdot D^{-1}$ example appear in Figure 3.54. The bias removal factor has been absorbed into all filters (7.85/6.85 multiples .633 to get .725 in feedback section, and multiplies .9469 to get 1.085 in feedforward section). The decision device is binary in this case since binary antipodal transmission is used. Note the IIR filter in the receiver: If the first SBS makes an error, then this error's magnitude is $2 = |+1 - (-1)| = |-1 - (+1)|$. Such an error is like an impulse of magnitude 2 added to the input of the IIR filter, which has impulse response $(-.725)^k \cdot u_k$, producing a contribution to the correct sequence of $2 \cdot (-.725)^k \cdot u_k$. This produces an additional 1 error half the time and an additional 2 errors 1/4 the time. Longer strings of errors will not occur. Thus, the bit and symbol error rate in this case increase by a factor of 1.5. (less than .1 dB loss).

A minor point is that the first decision in the receiver has an increased nearest neighbor coefficient of $N_e = 1.5$.

Generally speaking, when the flexible precoder makes an error,

$$(x_k - \lambda_k) - \text{decision}(x_k - \lambda_k) = \epsilon \cdot \delta_k \tag{3.467}$$

where ϵ could be complex for QAM. Then the designer must compute the probability of each such error's occurence and then investigate the string (with $(1/B(D)$ being the impulse response of the receiver's post-first-decision filter)

$$\left|\epsilon \cdot (1/b)^k\right| << d_{\min}/2 \quad . \tag{3.468}$$

For some k, this relation will hold and that then is the maximum burst length possible for the particular type of error. Given the filter $B(D)$ is monic and minimum phase, this string should not be too long as long as the roots are not too close to the unit circle. The single error may cause additional errors, but

none of these additional errors in turn cause yet more errors (unlike a DFE where second and subsequent errors can lead to some small probability of infinite-length bursts), thus the probability of an infinitely long burst is zero for the flexible precoder situation (or indeed any burst longer than the k that solves the above equation.

3.8.2 Partial Response Channel Models

Partial-response methods are a special case of precoding design where the ISI is forced to some known well-defined pattern. Receiver detectors are then designed for such partial-response channels directly, exploiting the known nature of the ISI rather than attempting to eliminate this ISI.

Classic partial-response-channel uses abound in data transmission. For instance, the earliest data transmission on telephone wires inevitably found large ISI because these "phone lines" isolate DC powering currents from other information-bearing signals (see Prob 3.35). The transformer does not pass low frequencies (i.e., DC), thus inevitably leading to non-Nyquist[18] pulse-response shapes even if the phone line otherwise introduced no signficant ISI. Equalization may be too complex or otherwise undesirable as a solution, so a receiver can use a detector design that instead presumes the presence of a known fixed ISI. Another example is magnetic recording (see Problem 3.36) where only flux changes on a recording surface can be sensed by a read-head, and thus D.C. will not pass through the "read channel," again inevitably leading to ISI. Straightforward equalization is often too expensive at the very high speeds of magnetic-disk recording systems.

Partial-Response (PR) channels have non-Nyquist pulse responses – that is, PR channels allow ISI – over a few (and finite number of) symbol periods, and the sampling rate equals the symbol rate. A unit-valued pulse-response sample occurs at time zero and the remaining non-zero response samples at subsequent sampling times, thus the name "partial response." The study of PR channels tacitly presumes a whitened matched filter, as will be described shortly. Then, a number of common PR channels can be easily addressed.

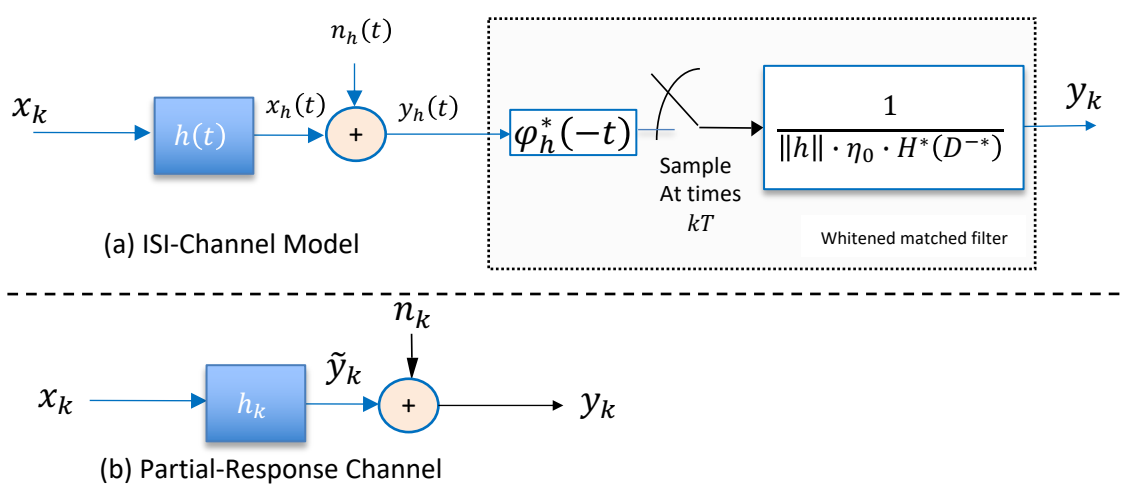

Figure 3.55: Minimum Phase Equivalent Channel.

Figure 3.55(a) illustrates the whitened-matched-filter. The minimum-phase equivalent of Figure 3.55(b) exists if $Q(D) = \eta_0 \cdot H(D) \cdot H^*(D^{-*})$ is factorizable.[19] This chapter focuses on the discrete-time channel and presumes the WMF's presence without explicitly showing or considering it. The discrete-

[18] That is, they do not satisfy Nyquist's condition for nonzero ISI - See Section 3.4.
[19] $H(D) = P_c(D)$ in Section 3.6.3 on ZF-DFE.

time channel output is

$$y_k = \sum_{m=-\infty}^{\infty} h_m \cdot x_{k-m} + n_k \quad , \tag{3.469}$$

or

$$Y(D) = H(D) \cdot X(D) + N(D) \quad , \tag{3.470}$$

where n_k is sampled Gaussian noise with autocorrelation $\bar{r}_{nn,k} = \|h\|^{-2} \cdot \eta_0^{-1} \cdot \frac{\mathcal{N}_0}{2} \cdot \delta_k$ or $\bar{R}_{nn}(D) = \|h\|^{-2} \cdot \eta_0^{-1} \cdot \frac{\mathcal{N}_0}{2}$ when the whitened-matched filter is used, and just denoted σ_{pr}^2 otherwise. In both cases, this noise is exactly AWGN with mean-square sample value σ_{pr}^2, which is conveniently abbreviated σ^2 for this chapter's duration.

Definition 3.8.2 *[Partial-Response Channel] A* **partial-response** *(PR) channel is any discrete-time channel with input/output relation described in (3.469) or (3.470) that also satisfies the following properties:*

1. *h_k is finite-length and causal; $h_k = 0 \;\; \forall\, k < 0$ or $k > \nu$, where $\nu < \infty$ and is the PR channel's* **constraint length**.
2. *h_k is monic; $h_0 = 1$,*
3. *h_k is minimum phase; $H(D)$ has all ν roots on or outside the unit circle,*
4. *h_k has all integer coefficients; $h_k \in \mathbb{Z} \;\forall\, k \neq 0$ (where $\mathbb{Z}$ denotes the set of integers).*

More generally, a discrete finite-length channel satisfying all properties above except the last restriction to all integer coefficients is a **controlled ISI** *channel.*

Controlled ISI and PR channels are a special subcase of all ISI channels, for which $h_k = 0 \;\forall\; k > \nu$. Thus, effectively, the PR channel is an FIR filter, and h_k is the minimum-phase equivalent of that filter's sampled pulse response. The constraint length defines the span in time νT of the PR channel's non-zero samples.

The controlled ISI polynomial (D-transform)[20] for the channel simplifies to

$$H(D) \triangleq \sum_{m=0}^{\nu} h_m \cdot D^m \quad , \tag{3.471}$$

where $H(D)$ is always monic, causal, minimum-phase, and an all-zero (FIR) polynomial. If the receiver processes the ISI channel output with the same whitened-matched filter that occurs in the ZF-DFE of Section 3.7, and if $P_c(D)$ (the resulting discrete-time minimum-phase equivalent channel polynomial when it exists) is of finite degree ν, then the channel is a controlled intersymbol interference channel with $H(D) = P_c(D)$ and $\sigma^2 = \frac{\mathcal{N}_0}{2} \cdot \|h\|^{-2} \cdot \eta_0^{-1}$. Any controlled intersymbol-interference channel is in the form that the Tomlinson Precoder of Section 3.8.1 could be used to implement symbol-by-symbol detection on the channel output. As noted in Section 3.8.1, Tomlinson Precoder use causes a (usually small) transmit symbol energy increase. PR channels will use simple precoders that avoid this loss.

3.8.2.1 Equalizers for the Partial-response channel.

This small subsection serves to simplify and review equalization structure for PR channels.

[20] The D-Transform of FIR channels ($\nu < \infty$) is often called the "channel polynomial," rather than its "D-Transform" in partial-response theory. This text uses these two terms interchangeably.

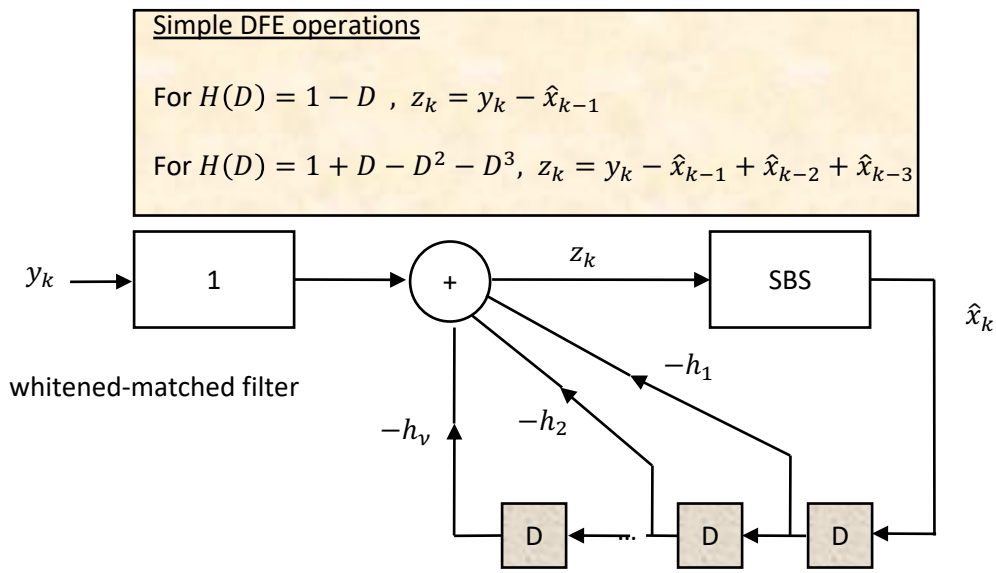

Figure 3.56: Simple DFE for some partial-response channels.

The PR channel's combination of integer coefficients and minimum-phase constraints permits Figure 3.56's very simple ZF-DFE implementation. Since the PR channel is already discrete time, no sampling is necessary and the minimum-phase characteristic of $H(D)$ causes the WMF of the ZF-DFE to simplify to a combined transfer function of 1 (that is, there is no feedforward section because the channel is already minimum phase). The ZF-DFE is then just Figure 3.56's feedback section, which easily consists of the feedback coefficients $-h_m$ for the delayed decisions corresponding to $\hat{x}_{k-m}, m = 1, ..., \nu$. The loss with respect to the matched filter bound is trivially $1/\|h\|^2$, which is easily computed as 3 dB for $H(D) = 1 \pm D^\nu$ (any finite ν) with simple ZF-DFE operation $z_k = y_k - \hat{x}_{k-\nu}$ and 6 dB for $H(D) = 1 + D - D^2 - D^3$ with simple ZF-DFE operation $z_k = y_k - \hat{x}_{k-1} + \hat{x}_{k-2} + \hat{x}_{k-3}$.

The ZF-LE does not exist if the channel has a zero on the unit circle, which all partial-response channels do. A MMSE-LE could be expected to have significant noise enhancement while existing. The MMSE-DFE will perform slightly better than the ZF-DFE, but is not so easy to compute as the simple ZF-DFE. Tomlinson or Flexible precoding could be applied to eliminate error propagation for a small increase in transmit power ($\frac{M^2}{M^2-1}$).

3.8.3 Classes of Partial Response

A widely used class of PR channels are those with $H(D)$ given by

$$H(D) = (1 + D)^l \cdot (1 - D)^n \quad , \tag{3.472}$$

where l and n are nonnegative integers.

For illustration, Let $l = 1$ and $n = 0$ in (3.472), then

$$H(D) = 1 + D \quad , \tag{3.473}$$

which is sometimes called a "duobinary" channel (introduced by Lender[21] in 1963, [7]). The Fourier transform of the duobinary channel is

$$H(e^{-\jmath\omega T}) = H(D)|_{D=e^{-\jmath\omega T}} = 1 + e^{-\jmath\omega T} = 2 \cdot e^{-\jmath\omega T/2} \cdot \cos\left(\frac{\omega T}{2}\right) \quad . \tag{3.474}$$

[21] See Also Weinstein's memorium describing Adam Lender in the July 2003 Issue of IEEE Communications Magazine.

The transfer function in (3.474) has a notch at the Nyquist Frequency and is generally "lowpass" in shape, as is shown in Figure 3.57.

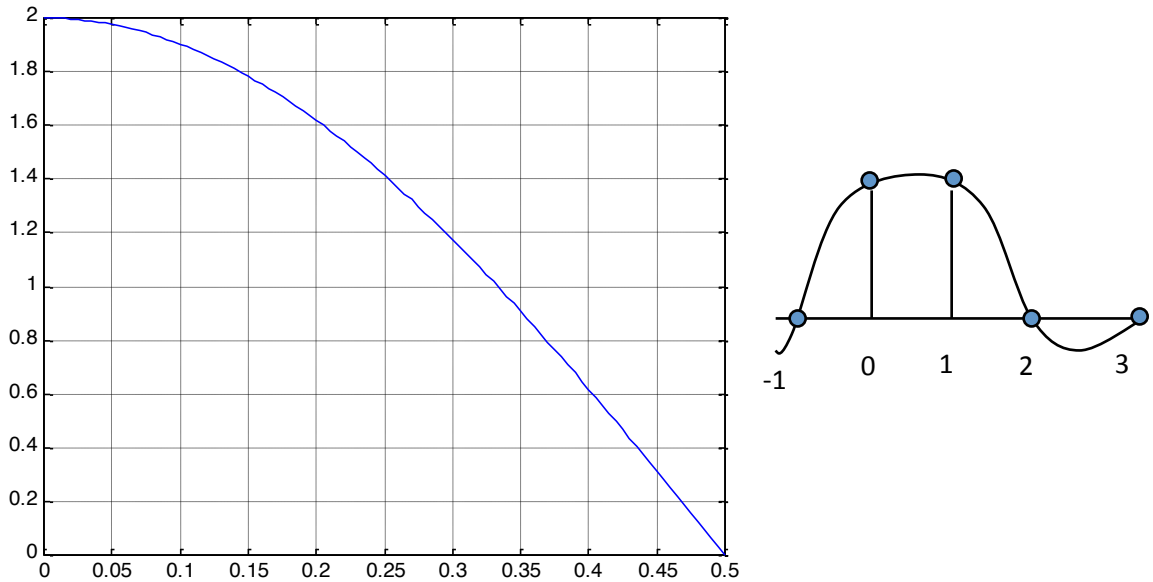

Figure 3.57: Transfer Characteristic for Duobinary signaling.

A discrete-time ZFE operating on this channel has infinite noise enhancement. If $SNR_{MFB} = 16$ dB, then

$$Q(e^{-\jmath\omega T}) + \frac{1}{SNR_{MFB}} = (1 + 1/40) + \cos\omega T \quad . \tag{3.475}$$

The MMSE-LE has performance (observe that $\frac{\mathcal{N}_0}{2} = .05$)

$$\sigma^2_{MMSE-LE} = \frac{\mathcal{N}_0}{2}\frac{T}{2\pi}\int_{-\frac{\pi}{T}}^{\frac{\pi}{T}} \frac{d\omega}{\|h\|^2 \cdot (1.025 + \cos\omega T)} = \frac{\mathcal{N}_0}{2} \cdot \frac{1/2}{\sqrt{1.025^2 - 1^2}} = 2.22 \cdot \frac{\mathcal{N}_0}{2} \quad , \tag{3.476}$$

The $\text{SNR}_{MMSE-LE,U}$ is thus 8 (9 dB), so the equalizer loss is 7 dB in this case. For the MMSE-DFE, $Q(D) + \frac{1}{SNR_{MFB}} = \frac{1.025}{1.64}(1+.8D)(1+.8D^{-1})$, so that $\gamma_0 = 1.025/1.64 = .625$, and thus $\gamma_{\text{MMSE-DFE}} = 2.2$dB. For the ZF-DFE, $\eta_0 = \frac{1}{2}$, and thus $\gamma_{\text{ZF-DFE}} = 3$dB.

It is possible to achieve MFB performance on this PR channel with complexity far less than any equalizer studied earlier, as in Chapter 8's maximum-likelihood sequence detectors. It is also possible to use a precoder with no transmit energy increase to eliminate the error-propagation-prone feedback section of the ZF-DFE, as to be shown shortly.

There are several specific channels that are used in practice for partial-response detection:

EXAMPLE 3.8.2 *[Duobinary $1 + D$]* The duobinary channel (as we have already seen) has

$$H(D) = 1 + D \quad . \tag{3.477}$$

The frequency response was already plotted in Figure 3.57. This response goes to zero at the Nyquist Frequency, thus modeling a lowpass-like channel. For a binary input of $x_k = \pm 1$, the channel output (with zero noise) takes on values ± 2 with probability 1/4 each and 0 with

probability 1/2. In general, for M-level inputs ($\pm 1 \ \pm 3 \ \pm 5 \ldots \ \pm (M-1)$), there are $2M-1$ possible output levels, $-2M+2, \ \ldots, \ 0, \ \ldots, \ 2M-2$. These output values are all possible sums of successive input symbols.

EXAMPLE 3.8.3 *[DC Notch $1-D$]* The DC Notch channel has

$$H(D) = 1 - D \quad , \tag{3.478}$$

so that $l = 0$ and $n = 1$ in (3.472). The frequency response is

$$H(e^{-\jmath\omega T}) = 1 - e^{-\jmath\omega T} = 2\jmath e^{-\jmath\omega\frac{T}{2}} \cdot \sin\frac{\omega T}{2} \quad . \tag{3.479}$$

The response goes to zero at the DC ($\omega = 0$), thus modeling a highpass-like channel. For a binary input of $x_k = \pm 1$, the channel output (with zero noise) takes on values ± 2 with probability 1/4 each and 0 with probability 1/2. In general for M-level inputs ($\pm 1 \ \pm 3 \ \pm 5 \ldots \ \pm (M-1)$), there are $2M-1$ possible output levels, $-2M+2, \ \ldots, \ 0, \ \ldots, \ 2M-2$.

When the modulator imposes the $1-D$ shaping iitself, rather than its cause being the channel, the corresponding modulation is known as **AMI (Alternate Mark Inversion)** if a differential encoder is also used as shown later in this section. AMI modulation prevents "charge" (DC) from accumulating and is sometimes also called "bipolar coding," although the use of the latter term is often confusing because bipolar transmission may have other meanings for some communications engineers. AMI coding, and closely related methods are used in multiplexed T1 (1.544 Mbps DS1 or "ANSI T1.403") and E1 (2.048 Mbps or "ITU-T G.703") speed digital data transmission on twisted pairs or coaxial links. These signals were once prevalent in telephone-company non-fiber central-office transmission of data between switch elements.

EXAMPLE 3.8.4 *[Modified Duobinary $1-D^2$]* The modified duobinary channel has

$$H(D) = 1 - D^2 = (1+D)\cdot(1-D) \quad , \tag{3.480}$$

so $l = n = 1$ in (3.472). Modified Duobinary is sometimes also called "Partial Response Class IV" or PR4 or PRIV in the literature. The frequency response is

$$H(e^{-\jmath\omega T}) = 1 - e^{-\jmath\omega 2T} = 2\jmath \cdot e^{-\jmath\omega T} \cdot \sin(\omega T) \quad . \tag{3.481}$$

The response goes to zero at the DC ($\omega = 0$) and at the Nyquist frequency ($\omega = \pi/T$), thus modeling a bandpass-like channel. For a binary input of $x_k = \pm 1$, the channel output (with zero noise) takes on values ± 2 with probability 1/4 each and 0 with probability 1/2. In general, for M-level inputs ($\pm 1 \ \pm 3 \ \pm 5 \ \ldots \ \pm (M-1)$), there are $2M-1$ possible output levels. Modified duobinary is equivalent to two interleaved $1-D$ channels, each independently acting on the inputs corresponding to even (odd) time samples, respectively. Many commercial disk drives use PR4.

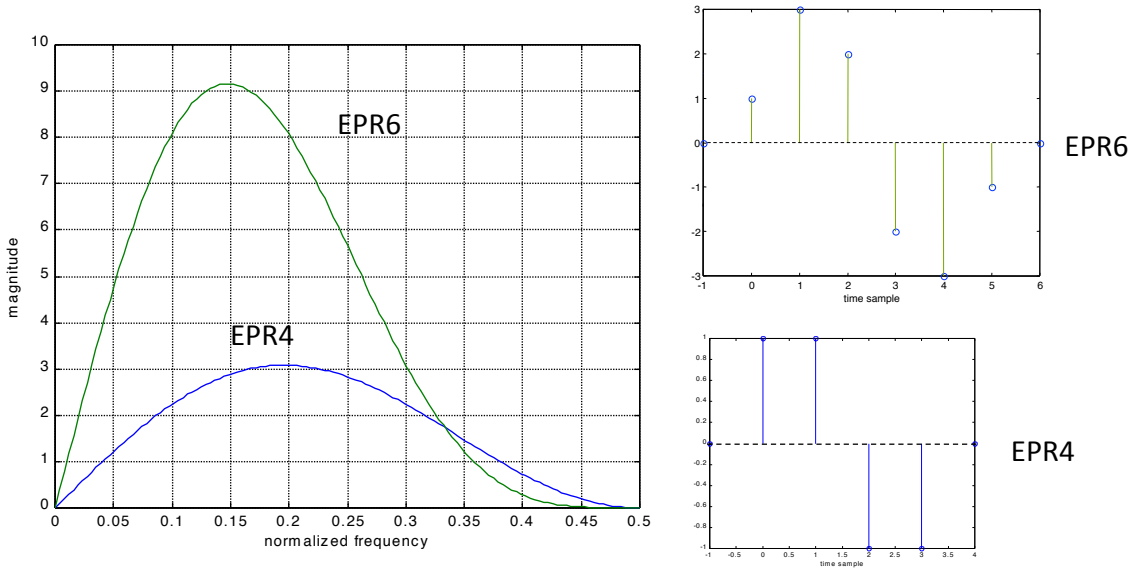

Figure 3.58: Transfer Characteristic for EPR4 and EPR6

EXAMPLE 3.8.5 *[Extended Partial Response 4 and 6 $(1+D)^l(1-D)^n$]* The Extended Partial-Response (EPR) channels were introduced by H. Thapar[22] [8] The EPR4 channel has $l = 2$ and $n = 1$ or

$$H(D) = (1+D)^2 \cdot (1-D) = 1 + D - D^2 - D^3 \quad . \tag{3.482}$$

This channel is called EPR4 because it has 4 non-zero samples. The frequency response is

$$H(e^{-\jmath\omega T}) = (1+e^{-\jmath\omega T})^2 \cdot (1-e^{-\jmath\omega T}) \quad . \tag{3.483}$$

The EPR6 channel has $l = 4$ and $n = 1$ (6 nonzero samples)

$$H(D) = (1+D)^4 \cdot (1-D) = 1 + 3 \cdot D + 2 \cdot D^2 - 2 \cdot D^3 - 3 \cdot D^4 - D^5 \quad . \tag{3.484}$$

The frequency response is

$$H(e^{-\jmath\omega T}) = (1+e^{-\jmath\omega T})^4 (1-e^{-\jmath\omega T}) \quad . \tag{3.485}$$

These 2 channels, along with PR4, are often used to model disk storage channels in magnetic disk or tape recording. The response goes to zero at DC ($\omega = 0$) and at the Nyquist frequency in both EPR4 and EPR6, thus modeling bandpass-like channels. The magnitude of these two frequency characteristics are shown in Figure 3.58. These found wide use in commercial disk storage read detectors.

The higher the l, the more "lowpass" in nature that the EPR channel becomes, and the more appropriate as bit density increases on any given disk.

For partial-response channels, the use of Tomlinson Precoding permits symbol-by-symbol detection, but also incurs an $M^2/(M^2-1)$ signal energy loss for PAM (and $M/(M-1)$ for QAM). A simpler method for PR channels, that also has no transmit energy penalty appears next.

[22] Dr. Hemant Thapar, 09-29-1951 - ; an Indian-born American Engineer and Entrepreneur of significant success.

3.8.4 Simple Precoding

The simplest precoder for the duobinary, DC-notch, and modified duobinary partial-response channels is a "**differential encoder**." The message at time k, m_k, may take values $m = 0, 1, \ldots, M-1$. For $M = 2$, the differential encoder has the simple description as "a device that observes the input bit stream, and changes its output if the input is 1 and repeats the last output if the input is 0." Thus, the differential encoder input, m_k, represents the binary difference (or sum) between adjacent differential encoder output ($\bar{m}_k$ and $\bar{m}_{k-1}$) messages[23]:

Definition 3.8.3 *[Differential Encoder]* **Differential encoders** *for PAM or QAM modulation obey one of the two following relationships:*

$$\bar{m}_k = m_k \ominus \bar{m}_{k-1} \tag{3.486}$$

$$\bar{m}_k = m_k \oplus \bar{m}_{k-1} \quad , \tag{3.487}$$

where $\ominus$ represents subtraction modulo M (and $\oplus$ represents addition modulo M). When $M = 2$, these operations are the same. For SQ QAM, the modulo addition and subtraction are performed independently on each of the two dimensions, with $\sqrt{M}$ replacing M. (A differential phase encoder is also often used for QAM and appears later in this section.)

Figure 3.59's left side illustrates a differential encoder. As an example if $M = 4$ the corresponding inputs and outputs are given in the following table:

m_k	-	3	1	0	2	1	0	3
$\bar{m}_k$	0	3	2	2	0	1	3	0
k	-1	0	1	2	3	4	5	6

With either PAM or QAM constellations, the modulator converts the encoder-output dimensional messages $\bar{m}_k$ symbols ($\pm\frac{d}{2}$, $\pm\frac{3d}{2}$...) according to

$$x_k = [2\bar{m}_k - (M-1)]\,\frac{d}{2} \quad . \tag{3.488}$$

[23] This operation is also very useful even on channels without ISI, as an unknown inversion in the channel (for instance, an odd number of amplifiers) will cause all bits to be in error if (differential) precoding is not used.

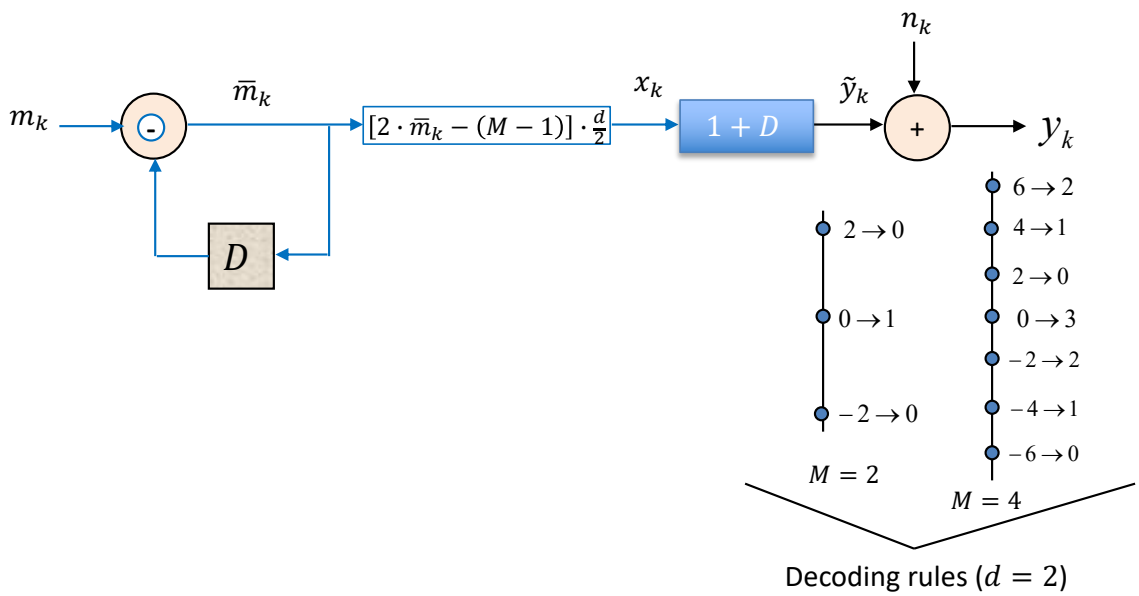

Figure 3.59: Precoded Partial Response Channel.

Figure 3.59 illustrates the precoder for the duobinary channel $H(D) = 1 + D$ as in (3.486). The noiseless minimum-phase-equivalent channel output $\tilde{y}_k$ is

$$\tilde{y}_k = x_k + x_{k-1} = 2 \cdot (\bar{m}_k + \bar{m}_{k-1}) \cdot \frac{d}{2} - 2 \cdot (M-1) \cdot \frac{d}{2} \tag{3.489}$$

so[24]

$$\frac{\tilde{y}_k}{d} + (M-1) = \bar{m}_k + \bar{m}_{k-1} \tag{3.490}$$

$$\left(\left[\frac{\tilde{y}_k}{d} + (M-1)\right]\right)_M = \bar{m}_k \oplus \bar{m}_{k-1} \tag{3.491}$$

$$\left(\left[\frac{\tilde{y}_k}{d} + (M-1)\right]\right)_M = m_k \tag{3.492}$$

where the last relation (3.492) follows from the definition in (3.486). All operations are integer mod-M. Equation (3.492) shows that a decision on $\tilde{y}_k$ about m_k occurs without concern for preceding or succeeding $\tilde{y}_k$, because of the precoder's action. The decision boundaries are simply the obvious regions symmetrically placed around each point for a memoryless ML detector of inputs and the decoding rules for $M = 2$ and $M = 4$ are shown in Figure 3.59. In practice, the decoder observes y_k, not $\tilde{y}_k$, so that the decoder makes a decision on y_k to the closest noise-free level of y_k. That is, the decoder first quantizes $\tilde{y}_k$ to one of the values of $(-2M+2) \cdot (d/2)$, ..., $(2M-2) \cdot (d/2)$. Then, the minimum distance between outputs is $d_{\text{min}} = d$, so that $\frac{d_{\text{min}}}{2\sigma_{pr}} = \frac{d}{2\sigma_{pr}}$, which is 3 dB below the $\sqrt{MFB} = \frac{\sqrt{2}}{\sigma_{pr}}(d/2)$ for the $1 + D$ channel because $\|h\|^2 = 2$. (Again, $\sigma_{pr}^2 = \|h\|^{-2} \cdot \eta_0^{-1} \cdot \frac{\mathcal{N}_0}{2}$ with a WMF and otherwise is just σ_{pr}^2.) This loss is identical to the loss in the ZF-DFE for this channel. The designer may consider the ZF-DFE feedback section as having been pushed through the linear channel back to the transmitter, where it becomes the precoder. With some algebra, one can show that the TPC, while also effective,

[24] $(\bullet)_M$ means the quantity is computed in M-level arithmetic, for instance, $(5)_4 = 1$. Also note that $\Gamma_M(x) \neq (x)_M$, and therefore $\oplus$ is different from the $\oplus_M$ of Section 3.5. The functions $(x)_M$ and $\oplus$ have strictly integer inputs and have possible outputs $0, ..., M-1$ only.

would produce a 4-level output with 1.3 dB higher average transmit symbol energy for binary inputs. The output levels are not equally likely in determining the decision boundaries (half way between the levels) but the two inputs are equally likely and the detector is for the inputs, so the decision regions are half-way between points.

Nearest Neighbors: The precoded partial-response system eliminates error propagation, and thus has lower P_e than the ZF-DFE. This elimination of error propagation can be understood by investigating the nearest neighbor coefficient for the precoded situation in general. For the $1+D$ channel, the (noiseless) channel output levels are $-(2M-2)$ $-(2M-4)$... 0 ... $(2M-4)$ $(2M-2)$ with probabilities of occurrence $\frac{1}{M^2}$ $\frac{2}{M^2}$ ... $\frac{M}{M^2}$ ... $\frac{2}{M^2}$ $\frac{1}{M^2}$, assuming a uniform channel-input distribution. Only the two outer-most levels have one nearest neighbor, all the rest have 2 nearest neighbors. Thus,

$$\bar{N}_e = \frac{2}{M^2}(1) + \frac{M^2-2}{M^2}(2) = 2 \cdot \left(1 - \frac{1}{M^2}\right) \quad . \tag{3.493}$$

For the ZF-DFE, the input to the decision device $\tilde{z}_k$ as

$$\tilde{z}_k = x_k + x_{k-1} + n_k - \hat{x}_{k-1} \quad , \tag{3.494}$$

which can be rewritten

$$\tilde{z}_k = x_k + (x_{k-1} - \hat{x}_{k-1}) + n_k \quad . \tag{3.495}$$

Equation 3.495 becomes $\tilde{z}_k = x_k + n_k$ if the previous symbol decision was correct. However, if the previous decision was incorrect, say $+1$ was decided (binary case) instead of the correct -1, then

$$\tilde{z}_k = x_k - 2 + n_k \quad , \tag{3.496}$$

which will lead to a next-symbol error immediately following the first almost surely if $x_k = 1$ (and no error almost surely if $x_k = -1$). The possibility of $\tilde{z}_k = x_k + 2 + n_k$ is just as likely to occur and follows an identical analysis with signs reversed. For either case, the probability of a second error propagating is 1/2. The other half of the time, only 1 error occurs. Half the times that 2 errors occur, a third error also occurs, and so on, effectively increasing the error coefficient from $N_e = 1$ to

$$N_e = 2 = 1(\frac{1}{2}) + 2(\frac{1}{4}) + 3(\frac{1}{8}) + 4(\frac{1}{16}) + ... = \sum_{k=1}^{\infty} k \cdot (.5)^k = \frac{.5}{(1-.5)^2} \quad . \tag{3.497}$$

(In general, the formula $\sum_{k=1}^{\infty} k \cdot r^k = \frac{r}{(1-r)^2}, r < 1$ may be useful in error-propagation analysis.) The error propagation can be worse in multilevel PAM transmission, when the probability of a second error is $(M-1)/M$, leading to

$$\frac{N_e(\text{error prop})}{N_e(\text{no error prop})} = 1 \cdot \frac{1}{M} + 2 \cdot \frac{M-1}{M} \cdot \frac{1}{M} + 3 \cdot \left(\frac{M-1}{M}\right)^2 \cdot \frac{1}{M} + ... \tag{3.498}$$

$$= \sum_{k=1}^{\infty} k \cdot \left(\frac{M-1}{M}\right)^{k-1} \cdot \frac{1}{M} \tag{3.499}$$

$$= M \quad . \tag{3.500}$$

Precoding eliminates this type of error propagation, although $\bar{N}_e$ increases by a factor[25] of $(1 + 1/M)$ with respect to the case where no error propagation occurred.

For the ZF-DFE system, $\bar{P}_e = 2(M-1)Q(\frac{d}{2\sigma_{pr}})$, while for the precoded partial-response system, $\bar{P}_e = 2\left(1 - \frac{1}{M^2}\right)Q(\frac{d}{2\sigma_{pr}})$. For $M \geq 2$, the precoded system always has the same or fewer nearest neighbors, and the advantage becomes particularly pronounced for large M. Using a rule-of-thumb that a factor of 2 increase in nearest neighbors is equivalent to an SNR loss of .2 dB (which holds at reasonable error rates in the 10^{-5} to 10^{-6} range), the advantage of precoding is almost .2 dB for $M = 4$. For $M = 8$, the advantage is about .6 dB, and for $M = 64$, almost 1.2 dB. Precoding can be simpler to implement than a ZF-DFE because the integer partial-response channel coefficients translate readily into easily realized finite-field operations in the precoder, while they represent full-precision add (and shift) operations in feedback section of the ZF-DFE.

[25] The ratio of $2(1 - 1/M^2)$ with precoding to $2(1 - 1/M)$ for M-ary PAM with no error propagation effects included

3.8.4.1 Precoding the DC Notch or Modified Duobinary Channels

The $\bar{m}_k = m_k \ominus \bar{m}_{k-1}$ differential encoder works for the $1+D$ channel. For the $1-D$ channel, the equivalent precoder is

$$\bar{m}_k = m_k \oplus \bar{m}_{k-1} \quad , \tag{3.501}$$

which is sometimes also called **NRZI** (non-return-to-zero inverted) precoding, especially by storage-channel engineers. In the $1-D$ case, the channel output is

$$\begin{aligned}
\tilde{y}_k &= x_k - x_{k-1} = 2 \cdot (\bar{m}_k - \bar{m}_{k-1}) \cdot \frac{d}{2} && (3.502)\\
\frac{\tilde{y}_k}{d} &= \bar{m}_k - \bar{m}_{k-1} && (3.503)\\
\left(\frac{\tilde{y}_k}{d}\right)_M &= \bar{m}_k \ominus \bar{m}_{k-1} && (3.504)\\
\left(\frac{\tilde{y}_k}{d}\right)_M &= m_k \quad . && (3.505)
\end{aligned}$$

The minimum distance and number of nearest neighbors are otherwise identical to the $1+D$ case just studied, as is the improvement over the ZF-DFE. The $1-D^2$ case is identical to the $1-D$ case, on two interleaved $1-D$ channels at half the rate. The overall precoder for this situation is

$$\bar{m}_k = m_k \oplus \bar{m}_{k-2} \quad , \tag{3.506}$$

and the decision rule is

$$\left(\frac{\tilde{y}_k}{d}\right)_M = m_k \quad . \tag{3.507}$$

The combination of precoding with the $1-D$ channel is often called "alternate mark inversion (AMI)" because each successive transmitted "1" bit value causes a nonzero channel output amplitude of polarity oppositie to the last nonzero channel output amplitude, while a "0" bit always produces a 0 level at the channel output.

3.8.4.2 Precoding EPR4

An example of precoding for the extended Partial Response class is EPR4, which has $l = 2$ and $n = 1$ in (3.482), or EPR4. Then,

$$\begin{aligned}
\tilde{y}_k &= x_k + x_{k-1} - x_{k-2} - x_{k-3} && (3.508)\\
\tilde{y}_k &= d \cdot (\bar{m}_k + \bar{m}_{k-1} - \bar{m}_{k-2} - \bar{m}_{k-3}) && (3.509)\\
\frac{\tilde{y}_k}{d} &= \bar{m}_k + \bar{m}_{k-1} - \bar{m}_{k-2} - \bar{m}_{k-3} && (3.510)\\
\left(\frac{\tilde{y}_k}{d}\right)_M &= \bar{m}_k \oplus \bar{m}_{k-1} \ominus \bar{m}_{k-2} \ominus \bar{m}_{k-3} && (3.511)\\
\left(\frac{\tilde{y}_k}{d}\right)_M &= m_k && (3.512)
\end{aligned}$$

where the precoder, from (3.512) and (3.511), is

$$\bar{m}_k = m_k \ominus \bar{m}_{k-1} \oplus \bar{m}_{k-2} \oplus \bar{m}_{k-3} \quad . \tag{3.513}$$

The channel output's minimum distance thus remains d, so $P_e \leq N_e \cdot Q(\frac{d}{2 \cdot \sigma_{pr}})$, but the MFB $= (\frac{d}{\sigma_{pr}})^2$, which is 6dB higher. The same 6dB loss that would occur with an error-propagation-free ZF-DFE on this EPR4 channel.

For the $1 + D - D^2 - D^3$ channel, the (noiseless) channel output levels are $-(4M-4)$ $-(4M-6)$... 0 ... $(4M-6)$ $(4M-4)$. Only the two outer-most levels have one nearest neighbor, all the rest have 2 nearest neighbors. Thus,

$$\bar{N}_e = \frac{2}{M^4}(1) + \frac{M^4-2}{M^4}(2) = 2\left(1 - \frac{1}{M^4}\right) \quad . \tag{3.514}$$

Thus the precoded system's error probability f is $\bar{P}_e = 2 \cdot \left(1 - \frac{1}{M^4}\right) \cdot Q(\frac{1}{\sigma_{pr}})$. The ZF-DFE's number of nearest neighbors with error propagation is difficult to compute, but clearly will be worse.

3.8.5 General Precoding

The general partial response precoder extrapolates readily from previous results:

Definition 3.8.4 [The Partial-Response Precoder] *The* **partial-response precoder** *for a channel with partial-response polynomial $H(D)$ is defined by*

$$\bar{m}_k = m_k \bigoplus_{i=1}^{\nu} (-h_i) \cdot \bar{m}_{k-i} \quad . \tag{3.515}$$

The notation $\bigoplus$ means a mod-M summation, and the multiplication can be performed without ambiguity because the h_i and $\bar{m}_{k-i}$ are always integers.

The corresponding memoryless decision at the channel output is

$$\hat{m}_k = \left(\frac{\hat{y}_k}{d} + \sum_{i=0}^{\nu} h_i \cdot \left(\frac{M-1}{2}\right)\right)_M \quad . \tag{3.516}$$

The reader should be aware that while the relationship in (3.515) is general for partial-response channels, the relationship can often simplify in specific instances, for instance the precoder for "EPR5," $H(D) = (1+D)^3(1-D)$ simplifies to $\bar{m}_k = m_k \oplus \bar{m}_{k-4}$ when $M = 2$.

In a slight abuse of notation, engineers often simplify the representation of the precoder by simply writing it as

$$\mathcal{P}(D) = \frac{1}{H(D)} \tag{3.517}$$

where $\mathcal{P}(D)$ is a polynomial in D that describes the "modulo-M" filtering in (3.515). Of course, this notation is symbolic. Furthermore, the D means unit delay in a finite field, and is therefore a delay operator only – there is no Fourier transform that inserts $D = e^{-\jmath\omega T}$ into $\mathcal{P}(D)$; Nevertheless, engineers commonly to refer to the NRZI precoder as a $1/(1 \oplus D)$ precoder.

Lemma 3.8.2 [Memoryless Decisions for the Partial-Response Precoder] *The partial-response precoder, often abbreviated by $\mathcal{P}(D) = 1/H(D)$, enables symbol-by-symbol decoding on the partial-response channel $H(D)$. An upper bound on the performance of such SBS decoding is*

$$\bar{P}_e \leq 2 \cdot \left(1 - \frac{1}{M^{\nu+1}}\right) \cdot Q\left[\frac{d}{2\sigma_{pr}}\right] \quad , \tag{3.518}$$

where d is the input constellation's minimum distance, which remains the same at the channel output.

Proof: The proof follows by simply inserting (3.515) into the expression for $\tilde{y}_k$ and simplifying to cancel all terms with h_i, $i > 0$. The nearest-neighbor coefficient and $d/2\sigma_{pr}$ follow trivially from inspection of the output. Adjacent levels can be no closer than d on a partial-response channel, and if all such adjacent levels occur, an upper bound on error probability is the $\bar{P}_e$ bound in (3.518). **QED**.

3.8.6 Quadrature PR

Differential encoding of the type specified earlier is not often used with QAM systems, because QAM constellations usually exhibit 90° symmetry. Thus a 90° offset in carrier recovery would make the constellation appear exactly as the original constellation. To eliminate the ambiguity, the bit assignment for QAM constellations usually uses a precoder that exploits the four possibilities of the most-significant bits that represent each symbol to specify a phase rotation of 0°, 90°, 180°, or 270° with respect to the last symbol transmitted. For instance, the sequence 01, 11, 10, 00 would produce (assuming an initial phase of 0°, the sequence of subsequent phases 90°, 0°, 180°, and 180°. By comparing adjacent decisions and their phase difference, these two bits can be resolved without ambiguity even in the presence of unknown phase shifts of multiples of 90°. This type of encoding is known as **differential phase encoding**. The remaining bits map to points in large M QAM constellations so that they are the same for points that are just 90° rotations of one another. (Similar methods could easily be derived using 3 or more bits for constellations with even greater symmetry, like 8PSK.)

Thus the simple precoder for the $1 + D$ and $1 - D$ (or $1 - D^2$) given earlier really only is practical for PAM systems. Figure 3.60's precoder illustrates an issue for quadarture PR channels:

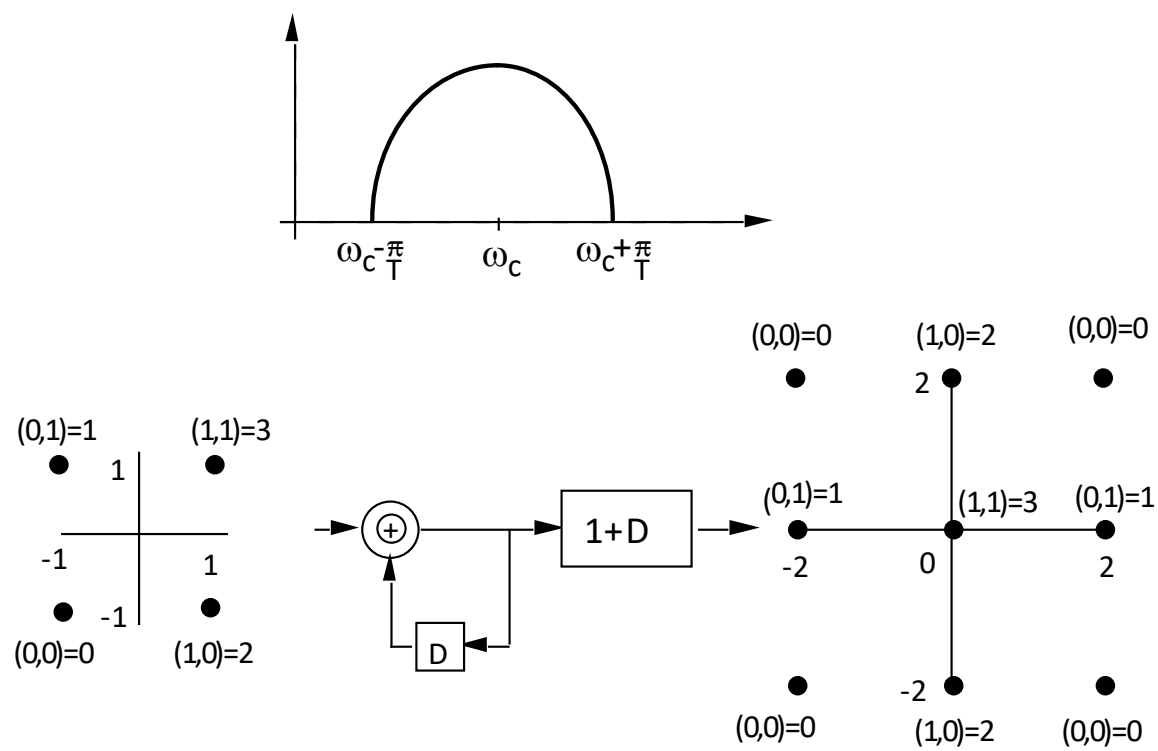

Figure 3.60: Quadrature Partial Response Example with $1 + D$.

The previous differential encoder appiies individually to both inphase and quadrature dimensions of the $1 + D$ channel, and it could be decoded without error. All previous analysis is correct, individually,

for each dimension. There is, however, one practical problem with this approach: If the channel were to somehow rotate the phase by $\pm 90^o$ (that is, the carrier recovery system locked on the wrong phase because of the symmetry in the output), then there would be an ambiguity as to which part was real and which was imaginary. Figure 3.60 illustrates the ambiguity: the two messages $(0,1) = 1$ and $(1,0) = 2$ commute if the channel has an unknown phase shift of $\pm 90^o$. No ambiguity exists for either the message $(0,0) = 0$ or the message $(1,1) = 3$. To eliminate the ambiguity,the precoder encodes the 1 and 2 signals into a difference between the last 1 (or 2) that was transmitted. This precoder thus specifies that an input of 1 (or 2) maps to no change with respect to the last input of 1 (or 2), while an input of 2 maps to a change with respect to the last input of 1 or 2.

A precoding rule that will eliminate the ambiguity is then

Rule 3.8.1 *[Complex Precoding for the 1+D Channel]* **if** $m_k = (m_{i,k}, m_{q,k}) = (0,0)$ *or* $(1,1)$ **then**

$$\bar{m}_{i,k} = m_{i,k} \oplus \bar{m}_{i,k-1} \tag{3.519}$$

$$\bar{m}_{q,k} = m_{q,k} \oplus \bar{m}_{q,k-1} \tag{3.520}$$

else if $m_k = (m_{i,k}, m_{q,k}) = (0,1)$ *or* $(1,0)$*, check the last* $\bar{m} = (0,1)$ *or* $(1,0)$ *transmitted, call it* $\bar{m}_{90}$*, (that is, was* $\bar{m}_{90} = 1$ *or 2 ?). If* $\bar{m}_{90} = 1$*, the precoder leaves* m_k *unchanged prior to differential encoding according to (3.519) and (3.520). The operations* $\oplus$ *and* $\ominus$ *are the same in binary arithmetic.*

If $\bar{m}_{90} = 2$*, then the precoder changes* m_k *from 1 to 2 (or from 2 to 1) prior to encoding according to (3.519) and (3.520).*

The corresponding decoding rule is (keeping a similar state $\hat{y}_{90} = 1, 2$ *at the decoder)*

$$\hat{m}_k = \begin{cases} (0,0) & \hat{y}_k = [\,\pm 2 \;\; \pm 2\,] \\ (1,1) & \hat{y}_k = [\,0\;0\,] \\ (0,1) & (\hat{y}_k = [\,0 \;\; \pm 2\,] \text{ or } \hat{y}_k = [\,\pm 2 \;\; 0\,]) \text{ and } \angle \hat{y}_k - \angle \hat{y}_{90} = 0 \\ (1,0) & (\hat{y}_k = [\,0 \;\; \pm 2\,] \text{ or } \hat{y}_k = [\,\pm 2 \;\; 0\,]) \text{ and } \angle \hat{y}_k - \angle \hat{y}_{90} \neq 0 \end{cases} . \tag{3.521}$$

The error probability and minimum distance are the same as was demonstrated earlier for this precoder, which only resolves the 90° ambiguity, but is otherwise equivalent to a differential encoder. There will however be limited error propagation in that one detection error on the 1 or 2 message points leads to two decoded symbol errors on the decoder output.

3.9 Diversity Equalization

Subsection 3.9.1's **Diversity** in transmission occurs when there are multiple channels from a single message source to several receivers, as in Figure 3.61. Optimally, Chapter 1's principles apply directly where the channel's conditional probability distribution $p_{\boldsymbol{y}/\boldsymbol{x}}$ typically has a larger channel-output dimensionality for $\boldsymbol{y}$ than for the input, $\boldsymbol{x}$, $L_y > L_x$ (or $N_y > N_x$ or both). This diversity often leads to a lower error probability for the same message, mainly because a greater channel-output minimum distance between possible (noiseless) output data symbols can occur with a larger number of channel output dimensions. However, ISI and/or crosstalk between the diversity dimensions can lead to a potentially complex optimum receiver and detector. Thus, equalization again allows SBS detectors' use with diversity channels. The **diversity combiners** or equalizers become matrix equivalents of those in Sections 3.5 - 3.7.

3.9.1 Multiple Received Signals and the RAKE

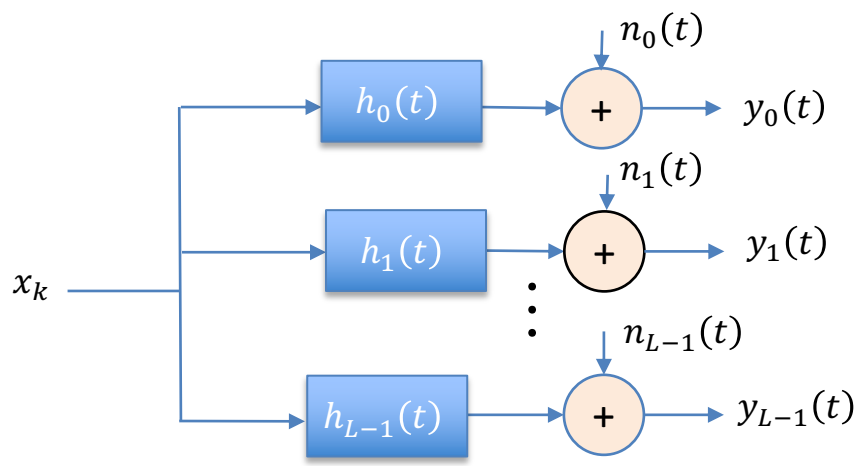

Figure 3.61: Basic diversity channel model.

Figure 3.61 illustrates the basic diversity channel. Channel outputs caused by the same channel input have labels $y_l(t)$, $l = 0, ..., L-1$. These diverse channel outputs may occur intentionally by retransmission of the same data symbols at different times and/or (center) frequencies. Spatial diversity often occurs in wireless transmission where L spatially separated antennas may all receive the same transmitted signal, but possibly with different filtering and with noises that are at least partially independent.

With each channel output following the model

$$y_{p,l}(t) = \sum_k x_k \cdot h_l(t - kT) + n_l(t) \quad , \tag{3.522}$$

a corresponding $L \times 1$ vector channel description is

$$\boldsymbol{y}_h(t) = \sum_k x_k \cdot \boldsymbol{h}(t - kT) + \boldsymbol{n}_h(t) \quad , \tag{3.523}$$

where

$$\boldsymbol{y}_h(t) \triangleq \begin{bmatrix} y_0(t) \\ y_1(t) \\ \vdots \\ y_{L-1}(t) \end{bmatrix} \quad \boldsymbol{h}(t) \triangleq \begin{bmatrix} h_0(t) \\ h_1(t) \\ \vdots \\ h_{L-1}(t) \end{bmatrix} \quad \text{and} \quad \boldsymbol{n}_h(t) \triangleq \begin{bmatrix} n_0(t) \\ n_1(t) \\ \vdots \\ n_{L-1}(t) \end{bmatrix} \quad . \tag{3.524}$$

The inner product is

$$< \boldsymbol{x}(t), \boldsymbol{y}(t) >= \sum_i \int_{-\infty}^{\infty} x_i^*(t) \cdot y_i(t) dt \quad . \tag{3.525}$$

Without loss of generality, the noise can be considered to be white on each of the L diversity channels, independent of the other diversity channels, and with equal power spectral densities $\frac{\mathcal{N}_0}{2}$.[26]

A single transmission of x_0 corresponds to a vector signal

$$\boldsymbol{y}_h(t) = x_0 \cdot \boldsymbol{h}(t) + \boldsymbol{n}(t) = x_0 \cdot \|\boldsymbol{h}\| \cdot \boldsymbol{\varphi}_h(t) + \boldsymbol{n}(t) \quad . \tag{3.526}$$

This situation generalizes slightly that considered in Chapter 1, where matched-filter demodulators there combined all time instants through integration, a generalization of the inner product's usual sum of products. A matched filter in general simply combines the signal components from all dimensions that have independent (pre-whitened if necessary) noise. Here, the inner product includes also the components corresponding to each of the diversity channels so that all signal contributions are summed to create maximum signal-to-noise ratio. The relative weighting of the different diversity channels is thus maintained through L unnormalized parallel matched filters each corresponding to one of the diversity channels. When several copies are combined across several diversity channels or new dimensions (whether created in frequency, long delays in time, or space), the combination is known as the **RAKE** matched filter of Figure 3.62:

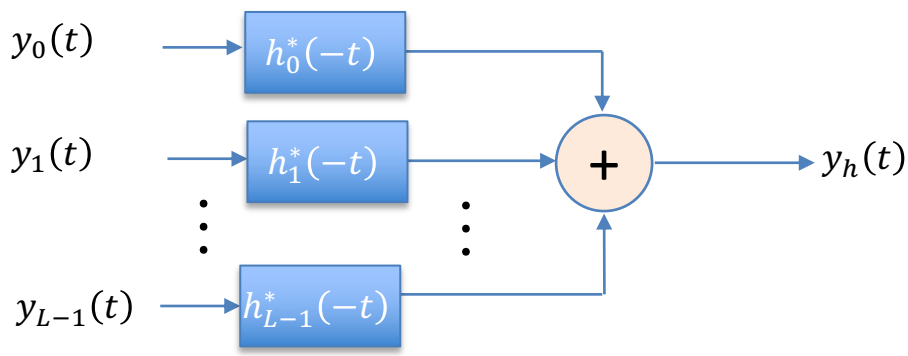

Figure 3.62: The basic RAKE matched filter combiner.

Definition 3.9.1 [RAKE matched filter] *A* **RAKE** *matched filter is a set of parallel matched filters each operating on one of the diversity channels in a diversity transmission system that is followed by a summing device as shown in Figure 3.62. Mathematically, the operation is*

$$y_h(t) = \sum_{l=0}^{L-1} h_l^*(-t) * y_l(t) \quad . \tag{3.527}$$

The RAKE was originally so named by Green[27] and Price[28] in 1958 because of the analogy of the various

[26] In practice, the noises may be correlated with each other on different subchannels and not white with covariance matrix $\mathcal{R}_n(t)$ and power spectral density matrix $R_n(f) = \frac{\mathcal{N}_0}{2} \cdot R_n^{1/2}(f) \cdot R_n^{*/2}(f)$. By prefiltering the vector channel output by the matrix filter $R_n^{-1/2}(f)$, the noise will be whitened and the noise equivalent matrix channel becomes $\boldsymbol{H}(f) \rightarrow R_n^{-1/2}(f) \cdot \boldsymbol{H}(f)$. Anaylsis with the equivalent channel can then proceed as if the noise where white, independent on the diversity channels, and of the same variance $\frac{\mathcal{N}_0}{2}$ on all.

[27] Dr. Paul Green, 1/14/1924 -3/22/2018 was at MIT Lincoln Labs and also Head of IBM research and a pioneer in optical-fiber and radio communiation.

[28] Dr. Robert Price, 7/7/1929 - 12/3/2008, was an electrical engineer at MIT Lincoln Labs and MIT PhD who helped

matched filters being the "fingers" of a garden rake and the sum corresponding to the collection of the fingers at the rake's pole handle. The RAKE is sometimes also called a **diversity combiner**, although the latter term also applies to other lower-performance suboptimal combining methods that do not maximize overall signal-to-noise strength through matched filter. One structure, often called **maximal combining**, applies a matched filter only to the strongest of the L diversity paths to save complexity. The maximal combiner's equivalent channel then corresponds only to this maximum-strength individual path. The original RAKE concept was conceived in connection with a spread-spectrum transmission method that achieves diversity essentially in frequency (but more precisely in a code-division dimension to be discussed in Chapter 5), but the matched filtering implied is easily generalized. Some of those who later studied diversity combining were not aware of the connection to the RAKE and thus the multiple names for the same structure, although diversity combining is a more accurate name for the method.

This text also defines $r_l(t) = h_l(t) * h_l^*(-t)$ and

$$r(t) = \sum_{l=0}^{L-1} r_l(t) \tag{3.528}$$

for an equivalent RAKE-output equivalent channel and the norm

$$\|\boldsymbol{h}\|^2 = \sum_{l=0}^{L-1} \|h_l\|^2 \quad . \tag{3.529}$$

Then, the normalized equivalent channel $q(t)$ is defined through

$$r(t) = \|\boldsymbol{h}\|^2 \cdot q(t) \quad . \tag{3.530}$$

The sampled RAKE output has D-transform

$$Y(D) = X(D) \cdot \|\boldsymbol{h}\|^2 \cdot Q(D) + \boldsymbol{N}(D) \quad , \tag{3.531}$$

which is essentially the same as the early channel models used without diversity except for the additional scale factor of $\|\boldsymbol{h}\|^2$, which also occurs in the noise autocorrelation, which is

$$\bar{R}_{nn}(D) = \frac{\mathcal{N}_0}{2} \cdot \|\boldsymbol{h}\|^2 \cdot Q(D) \quad . \tag{3.532}$$

An $SNR_{MFB} = \frac{\bar{\mathcal{E}}_{\boldsymbol{x}} \cdot \|\boldsymbol{h}\|^2}{\frac{\mathcal{N}_0}{2}}$ and all other detector and receiver principles previously developed in this text now apply directly.

If there were no ISI, or only one-shot transmission, the RAKE plus symbol-by-symbol detection would be an optimum ML/MAP detector. However, from Subsection 3.1.3, the set of samples created by this set of matched filters is sufficient. Thus, a single equalizer can be applied to the sum of the matched filter outputs without loss of generality as in Subsection 3.9.2. However, if the matched filters absorb into a fractionally-spaced and/or FIR equalizer, then the equalizers become distinct set of coefficients for each rail before being summed and input to a symbol-by-symbol detector as in Subsection 3.9.3.

3.9.2 Infinite-length MMSE Equalization Structures

The the receiver may scale the sampled RAKE output by $\|\boldsymbol{h}\|^{-1}$ to obtain a model identical to that of Section 3.1 in Equation (3.26) with $Q(D)$ and $\|\boldsymbol{h}\|$ as in Subsection 3.9.1. Thus, the MMSE-DFE, MMSE-LE, and ZF-LE/DFE all follow exactly as in Sections 3.5 -3.7. The matched-filter bound SNR and each equalization structure usually have higher SNRs with diversity because $\|\boldsymbol{h}\|^2$ is typically larger on the equivalent RAKE channel. Indeed the RAKE will work better than any of the individual channels, or any subset of the diversity channels, with each of the equalizer structures.

Often while one diversity channel has severe characteristics, like an inband notch or poor transmission characteristic, a second channel is better. Thus, diversity systems tend to be more robust.

pioneer spread-spectrum communication.

EXAMPLE 3.9.1 *[Two ISI channels in parallel]* Figure 3.63 illustrates two diversity channels with the same input and different intersymbol interference. The first upper channel has a sampled time equivalent of $1 + .9 \cdot D^{-1}$ with noise variance per sample of .181 (and thus could be the channel consistently examined throughout this Chapter so $\bar{\mathcal{E}}_{\boldsymbol{x}} = 1$). This channel is in effect anti-causal (or in reality, the .9 comes first in time). A second channel has causal response $1 + .8D$ with noise variance .164 per sample and has noise independent of the first channel's noise. The ISI effectively spans 3 symbol periods among the two channels at a common receiver that will decide whether $x_k = \pm 1$ has been transmitted.

The SNR_{MFB} for this channel remains $SNR_{MFB} = \frac{\bar{\mathcal{E}}_{\boldsymbol{x}} \cdot \|\boldsymbol{h}\|^2}{\frac{\mathcal{N}_0}{2}}$, but it remains to compute this quantity correctly. First the noise needs to be whitened. While the two noises are independent, they do not have the same variance per sample, so a pre-whitening matrix is

$$\begin{bmatrix} 1 & 0 \\ 0 & \sqrt{\frac{.181}{.164}} \end{bmatrix} \tag{3.533}$$

and so then the energy quantified by $\|\boldsymbol{h}\|^2$ is

$$\|\boldsymbol{h}\|^2 = \|h_1\|^2 + \|\tilde{h}_2\|^2 = 1.81 + \left(\frac{.181}{.164}\right) 1.64 = 2(1.81) \quad . \tag{3.534}$$

Then

$$SNR_{MFB} = \frac{1 \cdot 2(1.81)}{.181} = 13 \text{ dB} \; . \tag{3.535}$$

Because of diversity, this channel has a higher potential performance than either single channel alone. Clearly having a second look at the input through another channel can't hurt (even if there is more ISI). As always, $Q(D)$ characterizes the ISI:

$$\begin{aligned} Q(D) &= \frac{1}{2(1.81)} \left[(1 + .9D^{-1})(1 + .9D) + \frac{.181}{.164}(1 + .8D)(1 + .8D^{-1}) \right] && (3.536) \\ &= .492D + 1 + .492D^{-1} && (3.537) \\ &= .589 \cdot (1 + .835D) \cdot (1 + .835D^{-1}) && (3.538) \\ \tilde{Q}(D) &= .492D + (1 + 1/20) + .492D^{-1} && (3.539) \\ &= .7082 \cdot (1 + .695D) \cdot (1 + .695D^{-1}) && (3.540) \end{aligned}$$

Thus, the SNR of a MMSE-DFE would be

$$SNR_{MMSE-DFE,U} = .7082(20) - 1 = 13.16 \text{ (11.15 dB)} \quad . \tag{3.541}$$

The diversity improvement with respect to a single channel is about 2.8 dB in this case. The receiver is a MMSE-DFE essentially designed for the 1+.839D ISI channel after adding the matched-filter outputs. The loss with respect to the MFB is about 1.8 dB.

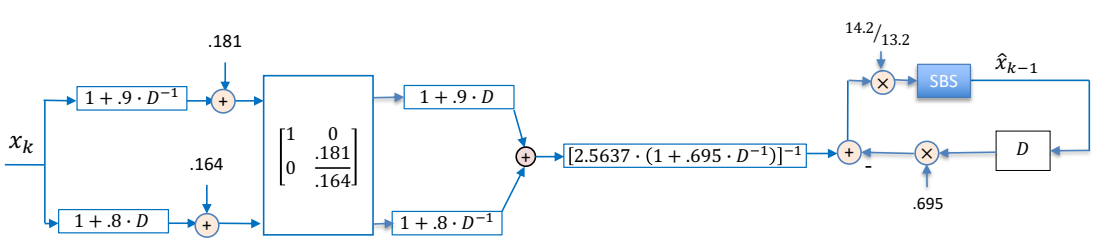

Figure 3.63: Two channel example.

3.9.3 Finite-length Multidimensional Equalizers

Finite-length diversity equalization becomes more complex because the matched filters are implemented within the (possibly fractionally spaced) equalizers associated with each of the diversity subchannels. There may be thus many coefficients in such a diversity equalizer.[29]

Figure 3.64's finite-length equalizers replace each of the RAKE's matched filters by a lowpass filter of wider bandwidth (usually ℓ times wider as in Section 3.7), a sampling device at rate $l\ell T$, and a fractionally spaced equalizer prior to the summing device. With vectors $\boldsymbol{h}_k$ in Equation (3.295) now becoming $\ell \cdot L$-tuples,

$$\boldsymbol{h}_k = \boldsymbol{h}(kT) \quad , \tag{3.542}$$

as do the channel output vectors $\boldsymbol{y}_k$ and the noise vector $\boldsymbol{n}_k$, the channel input/output relationship (in Eq (3.297)) again becomes

$$\boldsymbol{Y}_k \triangleq \begin{bmatrix} \boldsymbol{y}_k \\ \boldsymbol{y}_{k-1} \\ \vdots \\ \boldsymbol{y}_{k-N_f+1} \end{bmatrix} \tag{3.543}$$

$$= \begin{bmatrix} \boldsymbol{h}_0 & \boldsymbol{h}_1 & \dots & \boldsymbol{h}_\nu & 0 & 0 & \dots & 0 \\ 0 & \boldsymbol{h}_0 & \boldsymbol{h}_1 & \dots & \dots & \boldsymbol{h}_\nu & \dots & 0 \\ \vdots & \vdots & \ddots & \ddots & \ddots & \ddots & \vdots & \\ 0 & \dots & 0 & 0 & \boldsymbol{h}_0 & \boldsymbol{h}_1 & \dots & \boldsymbol{h}_\nu \end{bmatrix} \begin{bmatrix} x_k \\ x_{k-1} \\ \vdots \\ \vdots \\ x_{k-N_f-\nu+1} \end{bmatrix}$$

$$+ \begin{bmatrix} \boldsymbol{n}_k \\ \boldsymbol{n}_{k-1} \\ \vdots \\ \boldsymbol{n}_{k-N_f+1} \end{bmatrix} \quad . \tag{3.544}$$

The rest of Section 3.7 then directly applies with the matrix $\boldsymbol{H}$ changing to include the larger $l \cdot L$-tuples corresponding to L diversity channels, and the corresponding equalizer $\boldsymbol{W}$ having its $1 \times L$ coefficients corresponding to $\boldsymbol{w}_0 \dots \boldsymbol{w}_{N_f}$. Each coefficient thus contains ℓ values for each of the L equalizers.

The diversity equalizer is the same in principle as a fractionally spaced equalizer except that the oversampling that creates FSE diversity generalizes to simply any type of additional dimensions per symbol in the diversity equalizer. The dfecolor program can be used where the oversampling factor is simply $\ell \cdot L$ and the vector of the impulse response is appropriately organized to have $\ell \cdot L$ phases per entry. Often, $\ell = 1$, so there are just L antennas or lines of samples per symbol period entry in that input vector.

[29] Maximal combiners that select only one (the best) of the diversity channels for equalization are popular because they reduce the equalization complexity by at least a factor of L – and perhaps more when the best subchannel needs less equalization.

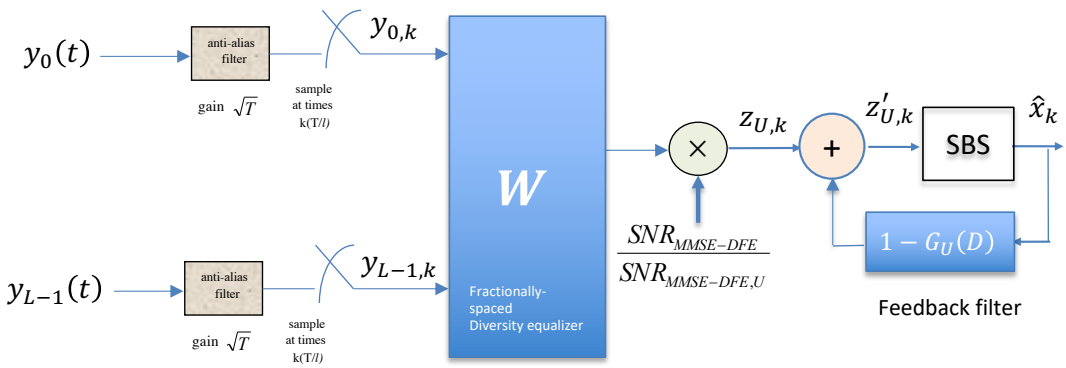

Figure 3.64: Fractionally spaced RAKE MMSE-DFE.

3.9.4 DFE RAKE Program

A Stanford effort by the instructor and many students has created the DFE RAKE program similar to the dfecolor matlab program and is listed in Appendix G.

```
function [dfseSNR,W,b]=dfsecolorsnr(l,h,nff,nbb,delay,Ex,noise);
DFE design program for RAKE receiver


Inputs
l     = oversampling factor
L       = No. of fingers in RAKE
h     = pulse response matrix, oversampled at l (size),
        each row corresponding to a diversity path
nff   = number of feedforward taps for each RAKE finger
nbb   = number of feedback taps
delay = delay of system <= nff+length of p - 2 - nbb
        if delay = -1, then choose best delay
Ex    = average energy of signals
noise = noise autocorrelation vector (size L x l*nff)
NOTE: noise is assumed to be stationary, but may be spatially correlated

outputs:
dfseSNR = equalizer SNR, unbiased in dB
------------------------------
```

For the previous example, some command strings that work are (with whitened-noise equivalent channel first):

```
>> h
h =    0.9000    1.0000         0
         0    1.0500    0.8400
>> [snr,W,b] = dfeRAKE(1,h,6,1,5,1,[.181 zeros(1,5) ; .181 zeros(1,5)])

snr =  11.1465
W = 0.0213   -0.0439    0.0668   -0.0984    0.1430    0.3546
```

```
   -0.0027    0.0124   -0.0237    0.0382    0.4137   -0.0000
b = 0.7022
```

or with unequal-variance noise directly inserted

```
>> h1
h1 =    0.9000    1.0000         0
         0    1.0000    0.8000

>> [snr,W,b] = dfeRAKE(1,h1,6,1,5,1,[.181 zeros(1,5) ; .164 zeros(1,5)])

snr = 11.1486

W = 0.0213   -0.0439    0.0667   -0.0984    0.1430    0.3545
   -0.0028    0.0130   -0.0249    0.0401    0.4347    0.0000

b = 0.7022
```

Two outputs are not quite the same because of the finite number of taps.

3.10 MIMO/Matrix Equalizers

This section extends basic infinite-length equalization designs to single-user MIMO systems. Chapter 2's codes concatenate sets of these $N = \widetilde{N} = 1$-dimensional-real and/or $N = \widetilde{N} = 2$-dimensional-complex subsymbols to form "codewords" of $\overline{N} \geq 1$ subsymbols/codeword or subsymbols/symbol, all selected from the same subsymbol constellation C with size $|C|$. Effectively in this chapter's equalization theory, a symbol is a subsymbol. Thus, the theory developed here in Chapter 3 remains applicable also to coded systems with the constellation points viewed as equally likely, so a presumption essentially that $M = |C|$, allowing separation of Chapter 2's coding and Chapter 3's equalization.

Chapter 1's general MIMO channel is $(L_y \cdot N) \times (L_x \cdot N)$, so even with $N = 1$ there is a multidimensional symbol with MIMO. This chapter continues to address time-domain transmission as symbol sequences of $N = \widetilde{N} = 1$-dimensional real or $N = \widetilde{N} = 2$-dimensional-complex symbols, with $\overline{N} = 1$. However, the transmitted symbol will become L_x dimensional. The index for these **spatial** dimensions will be l, while time indices will be k. The index n will return in Chapter 4 and beyond as a frequency index, and continues to be used as a codeword subsymbol index with codes. That index does not appear in this section.

3.10.1 The MIMO Channel Model

The space-time MIMO channel (without loss of generality) can be viewed as being $L_y \times L_x$ for each symbol. The input is a sequence of $L_x \times 1$ complex-vector-symbol inputs that then modulate the basis-function column vectors of $L_x \times L_x$ matrix $\boldsymbol{\Phi}(t)$:

$$\boldsymbol{\Phi}(t) = \begin{bmatrix} \varphi_{L_x,L_x}(t) & \varphi_{L_x,L_x-1}(t) & \cdots & \varphi_{L_x,1} \\ \varphi_{L_x-1,L_x}(t) & \varphi_{L_x-1,L_x-1}(t) & \cdots & \varphi_{L_x-1,1} \\ \vdots & \vdots & \ddots & \vdots \\ \varphi_{1,L_x} & \varphi_{1,L_x-1} & \cdots & \varphi_{1,1}(t) \end{bmatrix} \tag{3.545}$$

$$= \left[\boldsymbol{\varphi}_{L_x}(t)\ \boldsymbol{\varphi}_{L_x-1}(t)\ \ldots\ \boldsymbol{\varphi}_1(t)\right] \quad \text{with} \tag{3.546}$$

$$\boldsymbol{x}(t) = \boldsymbol{\Phi}(t) \cdot \boldsymbol{x} \quad . \tag{3.547}$$

$\boldsymbol{\Phi}(t)$'s columns in (3.546), $\boldsymbol{\varphi}_l(t)$ for $l = 1, \ldots L_x$, are $L_x \times 1$ basis-vector functions. There is one such basis function for each of $\boldsymbol{x}$'s L_x components. Column basis-vector "orthonormality" passes from the modulator to the demodulator when the channel's spatial dimensions have no crosstalk, the spatial equivalent of no ISI – but more accurately no inter-dimensional interference. Equivalently stated, the design tries to create column vectors need that are non overlapping in "space." Some vector-modulation design methods may lead to such crosstalk-free dimensions. Often, there will be nonzero crosstalk and this subsection's MIMO equalization methods address both reduction of ISI and of crosstalk.

There can thus be ISI between the successive overlapping vector symbols transmitted as well as crosstalk. Each transmit column vector $\boldsymbol{\varphi}_l(t)$ has unit norm. A simple model of such spatially orthogonal basis-function vectors has diagonal $\boldsymbol{\Phi}(t)$, probably with the same unit-norm basis function $\varphi(t)$ along the constant diagonal $\boldsymbol{\Phi}(t) = \boldsymbol{\varphi}(t) \cdot I$. However, as later chapters show, it can be helpful to be non-diagonal if the ensuing channel has crosstalk.

Vector Pulse Response: With $\boldsymbol{\Phi}(t)$ having L_x normalized column basis-vector functions, the vector continuous-time transmit signal is

$$\boldsymbol{x}(t) = \sum_k \boldsymbol{\Phi}(t - kT) \cdot \boldsymbol{x}_k \quad , \tag{3.548}$$

consistent with the scalar successive-transmission development earlier in Section 3.1[30]. The L_x-dimensional modulated signal vector has a (possibly complex) component for each channel-input dimension instead

[30] The use of a "·" in (3.548) simply denotes multiplication. This dot notation is used for appearance of results to separate quantities that might otherwise notationally confused - it can mean matrix multiply or scalar multiply in this text, depending on context.

of being a complex scalar ($L_x = 1$). The L_y-dimensional channel output is

$$\underbrace{\boldsymbol{y}_h(t)}_{L_y \times 1} = \underbrace{H_c(t)}_{L_y \times L_x} * \underbrace{\boldsymbol{x}(t)}_{L_x \times 1} + \underbrace{\boldsymbol{n}_h(t)}_{L_y \times 1} \quad , \tag{3.549}$$

an $L_y \times 1$ random-process vector of noise[31]. Thus, Section 3.9's diversity is a special case with $L_x = 1$ but $L_y > 1$. MIMO is essentially L_x independent diversity channels each of size $L_y \times 1$. In effect, Section 3.9's diversity applies to each spatial dimension independently. However, this section's treatment is more compact and allows some insights into these diversity channels' data-rate sum as a direct calculation and as a direct interpretation of the MIMO-channel performance for a single user. This MIMO system then has matrix pulse response

$$\boldsymbol{H}(t) = H_c(t) * \boldsymbol{\Phi}(t) \quad , \tag{3.550}$$

and so the vector channel output (see Figure 3.66) is

$$\boldsymbol{y}_h(t) = \sum_k \boldsymbol{H}(t - kT) \cdot \boldsymbol{x}_k + \boldsymbol{n}_h(t) \quad . \tag{3.551}$$

Vector One Shot: A MIMO "one-shot" system sends only the single vector symbol $\boldsymbol{x}_0$, so $\boldsymbol{y}_h(t) = H(t) \cdot \boldsymbol{x}_0 + \boldsymbol{n}_h(t)$. However, an L_y-dimensional channel output consequentially occurs with possible crosstalk between the output dimensions. The corresponding ML "MIMO symbol-by-symbol" detector is not a simple slicer on each dimension unless the channel is crosstalk free (or the inputs have been carefully designed, see Chapters 4 and 5). Nonetheless, a constant (operating within the symbol only on crosstalk) MMSE equalizer of $L_x \times L_y$ coefficients could be designed for this one-shot system.

Continuous-Time Vector Noise Whitening: The MIMO stationary noise vector has $L_y \times L_y$ dimensional autocorrelation matrix function $\boldsymbol{R}_n(t)$. Ideally, $R_{\boldsymbol{nn}}(t) = \frac{\mathcal{N}_0}{2} \cdot I \cdot \delta(t)$ so that the noise is white in all time dimensions and also uncorrelated between the different spatial dimensions, with the same variance $\frac{\mathcal{N}_0}{2}$ on all dimensions. Such a noise autocorrelation matrix function will have a matrix Fourier transform $\boldsymbol{S_n}(f) = \frac{\mathcal{N}_0}{2} \cdot I_{L_y}$ (see Appendix D.4). When $\boldsymbol{S_n}(f)$ satisfies the MIMO Paley-Wiener criterion of Appendix D.4 (and all practical noises will),

$$\int_{-\infty}^{\infty} \frac{|\ln[\boldsymbol{S}_n(f)]|}{1 + f^2} \cdot df < \infty \quad , \tag{3.552}$$

then a factorization of $\boldsymbol{S_n}(f)$ into a causal and causally invertible matrix filter exists (through Appendix D.4's matrix spectral factorization):

$$\boldsymbol{S_n}(f) = \frac{\mathcal{N}_0}{2} \cdot \boldsymbol{S}_{\boldsymbol{n}}^{1/2}(f) \cdot \boldsymbol{S}_{\boldsymbol{n}}^{*/2}(-f) \quad . \tag{3.553}$$

$\boldsymbol{S}_n^{-1/2}(f)$ is the causal and causally invertible filter matrix. This $\boldsymbol{S}_n^{-1/2}(f)$ is the causal, MIMO, noise-whitening matrix filter, and the MIMO white-noise equivalent channel becomes

$$\tilde{\boldsymbol{H}}(f) = \boldsymbol{S}_n^{-1/2}(f) \cdot \boldsymbol{H}(f) \quad , \tag{3.554}$$

which has inverse transform $\widetilde{\boldsymbol{H}}(t)$. Then the noise-whitened channel output becomes

$$\boldsymbol{y}_h(t) = \sum_k \widetilde{\boldsymbol{H}}(t - kT) \cdot \boldsymbol{x}_k + \boldsymbol{n}_h(t) \quad , \tag{3.555}$$

where $\boldsymbol{n}_h(t)$ is now the desired white noise with variance $\frac{\mathcal{N}_0}{2}$ in each and every (real) dimension.

[31] AWGN means white Gaussian noise on each dimension, but also of equal power and independent of all other $L_y - 1$ dimensions for every dimension.

Matrix Matched Fiber Bound: The **matched-filter matrix operation** result is

$$\boldsymbol{y}(t) = \widetilde{\boldsymbol{H}}^*(-t) * \boldsymbol{y}_h(t) \quad . \tag{3.556}$$

The unnormalized $L_x \times L_x$ ISI-crosstalk characterizing matrix function is

$$\boldsymbol{R}_h(t) \triangleq \widetilde{\boldsymbol{H}}^*(-t) * \tilde{\boldsymbol{H}}(t) \quad . \tag{3.557}$$

Then, finally the sampled channel output vector is (with $\boldsymbol{R}_{h,k} \triangleq \boldsymbol{R}_h(kT)$ and noting therefore that $\boldsymbol{R}_{h,k} = \boldsymbol{R}^*_{h,-k}$ or $\boldsymbol{R}_h(D) = \boldsymbol{R}^*_h(D^{-*})$)

$$\boldsymbol{y}_k = \sum_m \boldsymbol{R}_{p,k-m} \cdot \boldsymbol{x}_m + \boldsymbol{n}_k \quad . \tag{3.558}$$

The vector D-Transform (see Appendix D.4) is correspondingly

$$\boldsymbol{Y}(D) = \boldsymbol{R}_h(D) \cdot \boldsymbol{X}(D) + \boldsymbol{N}(D) \quad . \tag{3.559}$$

The matched-filter-bound (MFB) measures if a receiver's performance is close to an upper bound (that may not always be attainable). This MFB concept makes more sense for MIMO if each dimension of a simple slicer were used in each output dimension (following a MIMO matched filter of size $L_x \times L_y$). Thus, the MFB is really a concept to be individually applied to each of these L_x dimensions. An $L_x \times L_x$ diagonal matrix with the norms of individual matched-filter-output scalings on the diagonal will also be useful and is

$$\|\widetilde{\boldsymbol{H}}\| \triangleq \begin{bmatrix} \|\widetilde{\boldsymbol{H}}_{L_x}\| & 0 & \dots & 0 \\ 0 & \|\widetilde{\boldsymbol{H}}_{L_x-1}\| & \dots & 0 \\ \vdots & \vdots & \ddots & \vdots \\ 0 & 0 & \dots & \|\widetilde{\boldsymbol{H}}_1\| \end{bmatrix} \quad . \tag{3.560}$$

Each of (3.560)'s diagonal norm elements $\|\boldsymbol{H}_\ell\|$, $\ell = 1, ..., L_x$ is the sum of L_y integrals, each corresponding to one of the pulse-response matrix', $\boldsymbol{H}(t)$'s, L_x columns, so

$$\|\boldsymbol{H}_\ell\|^2 = \sum_{i=1}^{L_y} \int_{-\infty}^{\infty} |h_{i,l}(t)|^2 \cdot dt \quad , \tag{3.561}$$

where

$$\tilde{\boldsymbol{H}}_\ell(t) \triangleq \begin{bmatrix} h_{L_y,\ell}(t) \\ \vdots \\ h_{1,\ell}(t) \end{bmatrix} \quad \ell = 1, ..., L_x \quad . \tag{3.562}$$

There is no intersymbol interference (nor crosstalk) when $R_{h,k} = \|\tilde{\boldsymbol{H}}\|^2 \cdot \delta_k$ or $R_h(D) = \|\tilde{\boldsymbol{H}}\|^2$, basically a MIMO Nyquist criterion. In this Nyquist-satisfying case, the pulse response is such that dimension-by-dimension detection within symbol-by-symbol detection is optimum, and each dimension has a best SNR indexed by ℓ as

$$SNR_{MFB}(\ell) = \|\tilde{\boldsymbol{H}}_\ell\|^2 \cdot \frac{\bar{\mathcal{E}}_\ell}{\frac{\mathcal{N}_0}{2}} \quad \ell = 1, ..., L_x \quad . \tag{3.563}$$

The corresponding diagonal SNR matrix is

$$\mathbf{SNR}_{MFB} = \|\tilde{\boldsymbol{H}}\|^2 \cdot \frac{\bar{\mathcal{E}}_{\boldsymbol{x}}}{\frac{\mathcal{N}_0}{2}} \quad . \tag{3.564}$$

The next subsection explores further matrix SNRs.

3.10.2 Matrix SNRs

The single-user SNR concept for MIMO/vector transmission systems remains a scalar for each dimension,[32] SNR_ℓ, $\ell = 1, ..., L_x$. Unlike the previous subsection's scalar receivers, these different SNR's could lead to different signal constellations C_ℓ on each spatial dimension and thus different dimensional $\tilde{b}_\ell$ or $M_\ell = |C_\ell|$. When the gap $\Gamma = 0$ dB, a single equivalent SNR can replace the set and corresponds to the average $\tilde{b}_{ave} = \frac{1}{L_x} \cdot \sum_{\ell=1}^{L_x} \tilde{b}_\ell$. This single SNR's biased version is the geometric average the (biased) SNR set, $SNR(\boldsymbol{R}) = \left\{\prod_{\ell=1}^{L_x}(1 + SNR_\ell)\right\}^{1/L_x} - 1$, as this subsection develops. The receiver's objective will be to maximize this SNR and thus maximize the data-rate sum (or equivalently $\tilde{b}_{ave}$ over all dimensions. This MIMO equalization appears similar to Chapter 2's vector coding systems for the matrix AWGN, except MIMO equalizers address ISI between successive symbols while those earlier vector coding systems did not.

Figure 3.65 expands Figure 3.14 of Section 3.2 to the MIMO case. The MMSE solution minimizes Figure 3.65's error-vector autocorrelation-matrix determinant $|R_{\boldsymbol{ee}}|$ as proved in Appendix D.4. Appendix D.4 also shows that minimizing this determinant minimizes $trace\{R_{\boldsymbol{ee}}\}$ so corresponds also to minimum sum of mean-squared spatial-dimension errors. As Figure 3.65 shows, an "SNR" can thus correspond to the ratio of the input-autocorrelation-to-error-autocorrelation determinants.

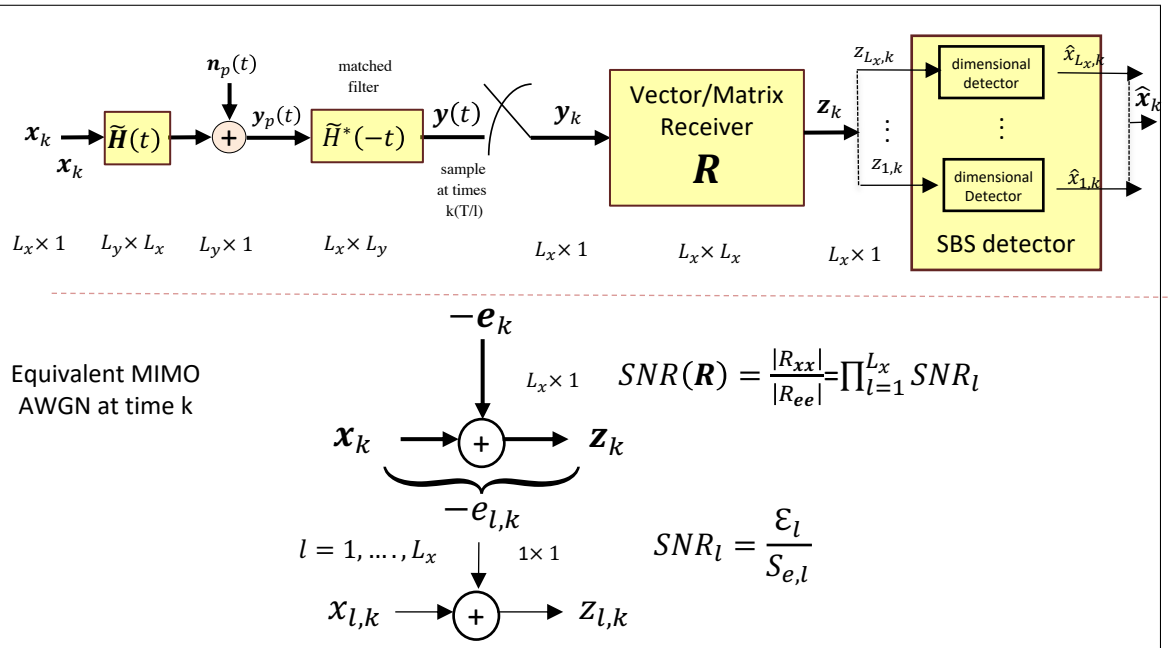

Figure 3.65: Suboptimal MIMO receiver that approximates/creates an equivalent MIMO AWGN.

This chapter's transmit symbol vector has independent and equal energy per spatial dimension $\bar{\mathcal{E}}_{\boldsymbol{x}}$ so that $\bar{R}_{\boldsymbol{xx}}(D) = \bar{\mathcal{E}}_{\boldsymbol{x}} \cdot I$. If $R_{\boldsymbol{ee}}(D) = R_{\boldsymbol{ee}}(0)$ and is also diagonal [33] $R_{\boldsymbol{ee}}(D) = \text{Diag}\{S_{e,L_x}, ..., S_{e,1}\}$, then (with numerator and denominator autocorrelation matrices both normalized consistently to the

[32] It is possible to do an ML L_x-dimensional SBS detector that chooses $\hat{\boldsymbol{x}}_k$ to minimize the quantity $\|\boldsymbol{z}_k - B \cdot \hat{\boldsymbol{x}}_k\|^2$ over all choices for the L_x-dimensional $\boldsymbol{x}$ where B represents the crosstalk within the symbol's spatial dimensions. Such a detector can be complex for $L_x > 1$ so this chapter does not further pursue it because the main focus is simple detectors.

[33] The notation "Diag (R)" with a capital letter "D" for an $N \times N$ square matrix means a square diagonal matrix that has a diagonal matching R and all zeros off-diagonal. The notation, "diag (R)" means an $N \times 1$ vector formed from the diagonal elements of R, so similar to the Matlab command. The notation "Diag $\{a, b, ...\}$" will mean forming a diagonal matrix from the set of elements in the obvious way.

same number of dimensions, 1 for real or 2 for complex):

$$SNR(R) = \frac{|R_{\boldsymbol{xx}}(D)|}{|R_{\boldsymbol{ee}}(D)|} = \frac{\prod_{\ell=1}^{L_x} \bar{\mathcal{E}}_{\boldsymbol{x}}}{\prod_{\ell=1}^{L_x} \bar{S}_{e,l}} = \prod_{\ell=1}^{L_x} SNR_l \quad . \tag{3.565}$$

If $R_{\boldsymbol{ee}}(D)$ is not diagonal, Figure 3.65's SBS detector will still independently detect each of the L_x dimensions, so (3.565) has consistent practical meaning, but then the dimensional SNR's simply use the diagonal elements of $R_{\boldsymbol{ee}}(D=0)$ as the entries of $S_{e,\ell}$, so $\text{Diag}\{R_{\boldsymbol{ee}}(0)\} = S_{e,l}$. As in Appendix D.4, the individual optimization problems are separable if the receiver uses a MMSE criterion, and each dimension is an equalizer with a bias that can be removed, so

$$SNR_{U,\ell} = SNR_\ell - 1 \tag{3.566}$$

define the unbiased SNR's that can be obtained in the usual way with bias removal in MMSE equalization. Each SNR corresponds to one of the L_x MIMO dimensions so the data rate is the sum of the individual data rates for the entire L_x-dimensional symbol[34]. The sum of the spatial dimensions' bits per symbol entries is then (with gap $\Gamma = 0$ dB)

$$\tilde{b} = \sum_{\ell=1}^{L_x} \tilde{b}_\ell \quad , \tag{3.567}$$

recalling that the notation $\tilde{b}$ normalizes to the number of complex (temporal) dimensions when QAM is used and to the number of real temporal dimensions when PAM is used. The quantity $\tilde{b}_{ave}$ then normalizes to the number of spatial dimensions L_x, so $\tilde{b}_{ave} = \frac{\tilde{b}}{L_x}$.

$$\tilde{b} = \sum_{\ell=1}^{L_x} \tilde{b}_l \ell = \sum_{\ell=1}^{L_x} \log_2 (1 + SNR_{U,\ell}) \tag{3.568}$$

$$= \log_2 \prod_{\ell=1}^{L_x} (1 + SNR_{U,\ell}) \tag{3.569}$$

$$= \log_2 \left[\frac{|R_{\boldsymbol{xx}}(D)|}{|R_{\boldsymbol{ee}}(D)|} \right] \quad , \tag{3.570}$$

which also validates the utility of the determinant ratio. Further, the average number of bits per spatial symbol defines a geometric SNR through

$$\tilde{b}_{ave} = \log_2 (1 + SNR_{geo,U}) \quad , \tag{3.571}$$

or

$$SNR_{geo,U} = \left[\prod_{\ell=1}^{L_x} (1 + SNR_{\ell,U}) \right]^{1/L_x} - 1 \quad . \tag{3.572}$$

3.10.3 The MIMO MMSE DFE and Equalizers

Figure 3.66 redraws Figure 3.36 for the case of MIMO filters. All vector processes are shown in boldface, while the matrix filters are also in boldface. Dimensions have been included to facilitate understanding. This section will follow the earlier infinite-length scalar DFE development, starting immediately with MMSE.

The feedback section eliminates intersymbol interference from previous L_x-dimensional symbols, but also eliminates some crosstalk from "earlier" decided spatial dimensions. Thus $\boldsymbol{B}_0$ is monic and upper triangular. $\boldsymbol{B}(D)$ is not generally upper triangular, but is causal. This structure specifically permits a first decision on dimension 1 after all previous ISI corresponding to $\boldsymbol{x}_{k-n}$ for all $n \geq 1$ can be made by subtracting ISI from that sole dimension (since the feedback section is also upper triangular and

[34] Or $2L_x$ real dimensions if the system is complex baseband, but consists of L_x complex dimensional channels.

then has only one non-zero coefficient in the bottom row). That first dimension's current decision, plus all its previous decisions, can be used respectively to subtract current symbol-instance crosstalk and ISI from the bottom dimension into the next dimension up. This process continues up the triangular feedback section where the top row uses the current decisions from all lower dimensions to eliminate current crosstalk along with all previous-decision dimensions' crosstalk and ISI from its dimension.

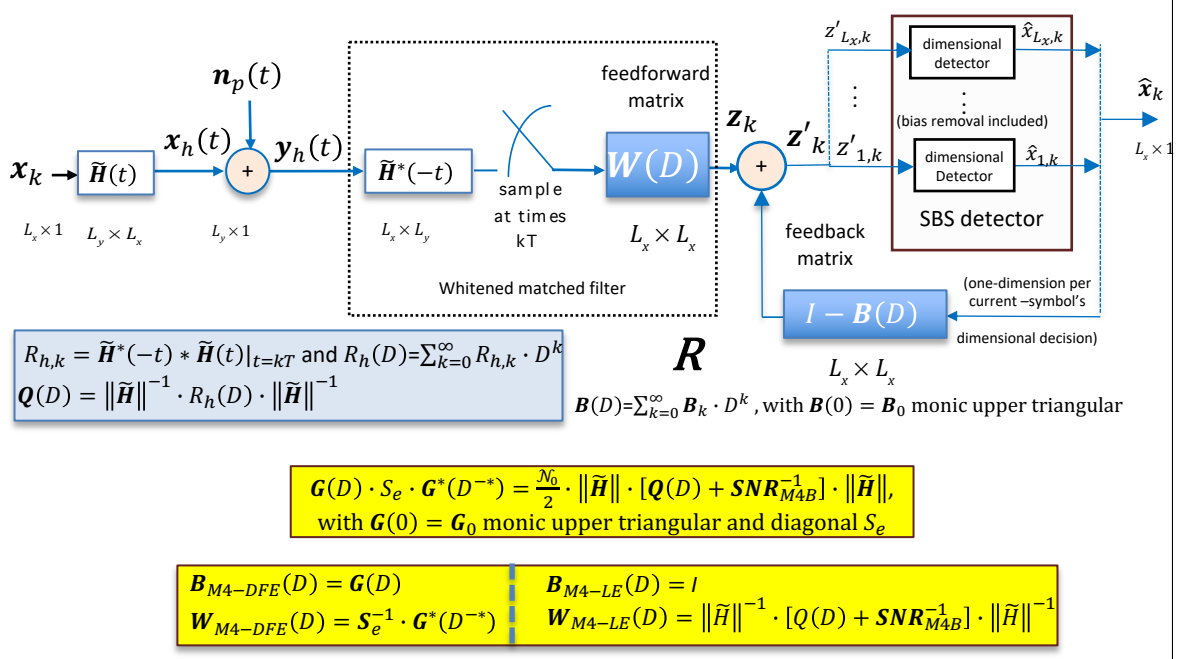

Figure 3.66: **MIMO decision feedback equalization.**

The **MIMO MMSE Decision Feedback Equalizer (M4-DFE)** jointly optimizes the settings of both the infinite-length $L_x \times L_y$ matrix-sequence feedforward filter $\boldsymbol{W}_k$ and the causal infinite-length $L_x \times L_x$ monic ($\boldsymbol{B}_0$ is monic and upper triangular) matrix-sequence feedback filter $\boldsymbol{B}_0 \cdot \delta_k - \boldsymbol{B}_k$ to minimize the MSE. Appendix D.1 develops the orthogonality principal for vector processes and MIMO.

Definition 3.10.1 **[Minimum Mean Square Error Vector (for M4-DFE)]** *The* **M4-DFE error** *signal is*

$$\boldsymbol{e}_k = \boldsymbol{x}_k - \boldsymbol{z}_k^{'} \quad . \tag{3.573}$$

The MMSE *for the* M4-DFE *is*

$$\sigma^2_{MMSE-DFE} \triangleq \min_{\boldsymbol{W}(D),\boldsymbol{B}(D)} E\left\{|R_{\boldsymbol{ee}}(D)|\right\} \quad . \tag{3.574}$$

The $L_x \times 1$ vector error sequence can be written as:

$$\boldsymbol{E}(D) = \boldsymbol{X}(D) - \boldsymbol{W}(D) \cdot \boldsymbol{Y}(D) - [I - \boldsymbol{B}(D)] \cdot \boldsymbol{X}(D) = \boldsymbol{B}(D) \cdot \boldsymbol{X}(D) - \boldsymbol{W}(D) \cdot \boldsymbol{Y}(D) \quad . \tag{3.575}$$

For any fixed $\boldsymbol{B}(D)$, $\mathbb{E}\left[\boldsymbol{E}(D) \cdot \boldsymbol{Y}^*(D^{-*})\right] = 0$ to minimize MSE, which leads to the relation

$$\boldsymbol{B}(D) \cdot R_{\boldsymbol{xy}}(D) - \boldsymbol{W}(D) \cdot R_{\boldsymbol{yy}}(D) = 0 \quad . \tag{3.576}$$

Two correlation matrices of interest are (assuming the input has equal energy in all dimensions, $\bar{\mathcal{E}}_{\boldsymbol{x}}$)

$$R_{\boldsymbol{xy}}(D) = \bar{\mathcal{E}}_{\boldsymbol{x}} \cdot R_h(D) \tag{3.577}$$

$$R_{\boldsymbol{yy}}(D) = \bar{\mathcal{E}}_{\boldsymbol{x}} \cdot R_h^2(D) + \frac{\mathcal{N}_0}{2} \cdot R_p(D) \quad , \tag{3.578}$$

The MMSE-MIMO LE (M4-LE) matrix filter then readily becomes

$$\begin{aligned}
\boldsymbol{W}_{M4-LE}(D) &= R_{\boldsymbol{xy}}(D) \cdot R_{\boldsymbol{yy}}^{-1}(D) && (3.579)\\
&= \bar{\mathcal{E}}_{\boldsymbol{x}} \cdot \boldsymbol{R}_h(D) \cdot \left[\bar{\mathcal{E}}_{\boldsymbol{x}} \cdot \boldsymbol{R}_h^2(D) + \frac{\mathcal{N}_0}{2} \cdot \boldsymbol{R}_h(D)\right]^{-1} && (3.580)\\
&= \bar{\mathcal{E}}_{\boldsymbol{x}} \cdot \boldsymbol{R}_h(D) \cdot \left[\left\{\bar{\mathcal{E}}_{\boldsymbol{x}} \cdot \boldsymbol{R}_h(D) + \frac{\mathcal{N}_0}{2} \cdot I\right\} \cdot \boldsymbol{R}_h(D)\right]^{-1} && (3.581)\\
&= \bar{\mathcal{E}}_{\boldsymbol{x}} \cdot \boldsymbol{R}_h(D) \cdot \boldsymbol{R}_h^{-1}(D) \cdot \left[\bar{\mathcal{E}}_{\boldsymbol{x}} \cdot \boldsymbol{R}_h(D) + \frac{\mathcal{N}_0}{2} \cdot I\right]^{-1} && (3.582)\\
&= \left[\boldsymbol{R}_h(D) + \boldsymbol{SNR}\right]^{-1} \quad , && (3.583)
\end{aligned}$$

where $\boldsymbol{SNR} \triangleq \frac{\bar{\mathcal{E}}_{\boldsymbol{x}}}{\frac{\mathcal{N}_0}{2}} \cdot I$. The corresponding MMSE MIMO (M4-LE) matrix is (with $\boldsymbol{B}(D) = I$)

$$\begin{aligned}
S_{M4-LE}(D) &= \min_{\boldsymbol{W}(D)} \mathbb{E}\left\{R_{\boldsymbol{e}_{M4-LE}\boldsymbol{e}_{M4-LE}}(D)\right\} && (3.584)\\
&= R_{\boldsymbol{xx}}(D) - R_{\boldsymbol{xy}}(D) \cdot R_{\boldsymbol{yy}}(D) \cdot R_{\boldsymbol{yx}}(D) && (3.585)\\
&= \bar{\mathcal{E}}_{\boldsymbol{x}} \cdot I - \bar{\mathcal{E}}_{\boldsymbol{x}} \cdot \boldsymbol{R}_h(D) \left[\bar{\mathcal{E}}_{\boldsymbol{x}} \cdot \boldsymbol{R}_h^2(D) + \frac{\mathcal{N}_0}{2} \cdot \boldsymbol{R}_h\right]^{-1} \cdot \boldsymbol{R}_h(D)\bar{\mathcal{E}}_{\boldsymbol{x}} \cdot && (3.586)\\
&= \bar{\mathcal{E}}_{\boldsymbol{x}} \cdot I - \left[\boldsymbol{R}_h(D) + \boldsymbol{SNR}^{-1}\right]^{-1} \cdot \boldsymbol{R}_h(D) \cdot \bar{\mathcal{E}}_{\boldsymbol{x}} && (3.587)\\
&= \bar{\mathcal{E}}_{\boldsymbol{x}} \cdot \left\{I - \left[\boldsymbol{R}_h(D) + \boldsymbol{SNR}^{-1}\right]^{-1} \cdot \boldsymbol{R}_h(D)\right\} && (3.588)\\
&= \bar{\mathcal{E}}_{\boldsymbol{x}} \cdot \left[\boldsymbol{R}_h(D) + \boldsymbol{SNR}^{-1}\right]^{-1} \cdot \left[\boldsymbol{R}_h(D) + \boldsymbol{SNR}^{-1} - \boldsymbol{R}_h(D)\right] && (3.589)\\
&= \frac{\mathcal{N}_0}{2} \cdot \left[\boldsymbol{R}_p(D) + \boldsymbol{SNR}^{-1}\right]^{-1} && (3.590)\\
R_{M4-LE}(D) &= \frac{\frac{\mathcal{N}_0}{2}}{\left|\boldsymbol{R}_h(D) + \boldsymbol{SNR}^{-1}\right|} \quad . && (3.591)
\end{aligned}$$

A form similar to the scalar MMSE-LE version defines

$$Q(D) \triangleq \|\tilde{\boldsymbol{H}}\|^{-1} \cdot \boldsymbol{R}_h(D) \cdot \|\tilde{\boldsymbol{H}}\|^{-1} \quad , \tag{3.592}$$

and then

$$\boldsymbol{W}_{M4-LE}(D) = \|\tilde{\boldsymbol{H}}\|^{-1} \cdot \left[Q(D) + \mathbf{SNR}_{MFB}^{-1}\right]^{-1} \cdot \|\tilde{\boldsymbol{H}}\|^{-1} \quad , \tag{3.593}$$

where the trailing factor $\|\tilde{\boldsymbol{H}}\|^{-1}$ could be absorbed into the preceding matrix-matched filter to "normalize" it in Figure 3.66, and thus this development would exactly then parallel the scalar result (noting that multiplication by a non-constant diagonal matrix does not in general commute). Similarly,

$$\begin{aligned}
S_{M4-LE}(D) &= \frac{\mathcal{N}_0}{2} \cdot \|\tilde{\boldsymbol{H}}\|^{-1} \cdot \left[Q(D) + \mathbf{SNR}_{MFB}^{-1}\right]^{-1} \cdot \|\tilde{\boldsymbol{H}}\|^{-1} && (3.594)\\
R_{M4-LE}(D) &= \frac{\frac{\mathcal{N}_0}{2}}{\left|\|\tilde{\boldsymbol{H}}\|\right|^2 \cdot \left|Q(D) + \boldsymbol{SNR}^{-1}\right|} \quad . && (3.595)
\end{aligned}$$

The MMSE, as in Appendix D, occurs for either choice of determinant or norm (they are not equal, but both minimized) and the more convenient form for the M4-LE is the determinant:

$$\begin{aligned}
\sigma_{M4-LE}^2 &\triangleq R_{M4-LE}(0) && (3.596)\\
&= \frac{T}{2\pi} \int_{-\pi/T}^{\pi/T} \left|R_{M4-LE}(e^{-\jmath\omega T})\right| d\omega && (3.597)\\
&= \frac{T}{2\pi} \int_{-\pi/T}^{\pi/T} \frac{\frac{\mathcal{N}_0}{2}}{\left|\boldsymbol{R}_p(e^{-\jmath\omega T}) + \boldsymbol{SNR}^{-1}\right|} d\omega && (3.598)\\
&= \frac{\mathcal{N}_0}{2} \cdot \boldsymbol{W}_0^{-1} \quad . && (3.599)
\end{aligned}$$

For dimension-by-dimension detection, $\boldsymbol{W}_0$ is factored as $Q_w \cdot S_w \cdot Q_w^*$ (an eigenvalue decomposition of this symmetric positive definite matrix). Then,

$$\boldsymbol{W}(D) \rightarrow Q_w^* \cdot \boldsymbol{W}(D) \tag{3.600}$$

so as to diagonalize the MMSE and allow each dimension independent decisions (instead of an ML detector for each symbol over L_x dimensions). This orthogonal transformation does not change the MMSE although it may redistribute error energy over the spatial dimensions. The overall SNR per spatial dimension then is

$$SNR_{M4-LE} = \frac{\tilde{\mathcal{E}}_x}{\left(\prod_{\ell=1}^{L_x} S_w(\ell)\right)^{1/L_x}} = \left[\prod_{\ell=1}^{L_x} (1 + SNR_{M4-LE}(\ell))\right]^{1/L_x} \quad . \tag{3.601}$$

and of course $SNR_{M4-LE,U} = SNR_{M4-LE} - 1$. By linearity of MMSE estimates, then the FF filter matrix for any $\boldsymbol{B}(D)$ becomes

$$\begin{aligned} \boldsymbol{W}(D) &= \boldsymbol{B}(D) \cdot R_{\boldsymbol{xy}}(D) \cdot R_{\boldsymbol{yy}}^{-1}(D) & (3.602)\\ &= \boldsymbol{B}(D) \cdot [R_h(D) + \boldsymbol{SNR}]^{-1} & (3.603)\\ &= \boldsymbol{B}(D) \cdot \|\tilde{\boldsymbol{H}}\|^{-1} \cdot \left[Q(D) + \mathbf{SNR}_{MFB}^{-1}\right]^{-1} \cdot \|\tilde{\boldsymbol{H}}\|^{-1} \quad , & (3.604) \end{aligned}$$

for any causal $\boldsymbol{B}(D)$. Again, since the MMSE estimate is linear then

$$\boldsymbol{E}(D) = \boldsymbol{B}(D) \cdot \boldsymbol{E}_{\text{M4-LE}}(D) \quad . \tag{3.605}$$

The error sequence's autocorrelation function for arbitrary monic $B(D)$ is

$$R_{\boldsymbol{ee}}(D) = \boldsymbol{B}(D) \cdot R_{\boldsymbol{e}_{M4-LE}\boldsymbol{e}_{M4-LE}}(D) \cdot \boldsymbol{B}^*(D^{-*}) \quad , \tag{3.606}$$

which has a form very similar to the scalar quantity. The scalar case uses a canonical factorization of the scalar $\tilde{Q}(D)$ that was proportional to the (inverse of the) MMSE-LE's autocorrelation function, but not exactly equal. Here because matrices do not usually commute, the MIMO canonical factorization will be directly of $R_{\boldsymbol{e}_{M4-LE}\boldsymbol{e}_{M4-LE}}^{-1}(D)$, or via (3.594) of $\frac{\mathcal{N}_0}{2}\|\tilde{\boldsymbol{H}}\| \cdot \left[Q(D) + \mathbf{SNR}_{MFB}^{-1}\right] \|\tilde{\boldsymbol{H}}\|$, so

$$\begin{aligned} R_{\boldsymbol{e}_{M4-LE}\boldsymbol{e}_{M4-LE}}(D)^{-1} &= \boldsymbol{G}(D) \cdot \boldsymbol{S}_e \cdot \boldsymbol{G}^*(D^{-*}) \text{ or} & (3.607)\\ \left[Q(D) + \mathbf{SNR}_{MFB}^{-1}\right] &= \|\tilde{\boldsymbol{H}}\|^{-1} \cdot G(D) \cdot \boldsymbol{S}_e \cdot G^*(D^{-*})\|\tilde{\boldsymbol{H}}\|^{-1} \quad , & (3.608) \end{aligned}$$

where $\boldsymbol{G}(D)$ has Diag $\{\boldsymbol{G}(0)\} = I$, and is causal minimum-phase (causally invertible); $\boldsymbol{S}_e$ is diagonal with all positive elements. Such a factorization exists when the MIMO PW Criterion is satisfied (as in Appendix D.4, which will be the case if $R_{\boldsymbol{xx}} = \mathcal{E} \cdot I$ and $\mathcal{E} > 0$ and $\frac{\mathcal{N}_0}{2} > 0$. Substitution of the inverse factorization into (3.606) produces

$$R_{\boldsymbol{ee}}(D) = \frac{\mathcal{N}_0}{2} \cdot \boldsymbol{B}(D) \cdot \boldsymbol{G}^{-1}(D) \cdot \boldsymbol{S}_e^{-1} \cdot \boldsymbol{G}^{-*}(D^{-*}) \cdot \boldsymbol{B}^*(D^{-*}) \quad . \tag{3.609}$$

The determinant $|R_{\boldsymbol{ee}}(D)|$ is the product of $(\frac{\mathcal{N}_0}{2})^{L_x}$ with the determinants of the 5 matrices above, each of which is the product of the elements on the diagonal. Since $\boldsymbol{B}(D)$ and $\boldsymbol{G}(D)$ are both causal and both $\boldsymbol{B}_0$ and $\boldsymbol{G}_0$ are monic upper triangular, their product $F_0 = B_0 \cdot G_0$ shares these same properties. The product $F = \boldsymbol{B}(D) \cdot \boldsymbol{G}(D)$ has a causal monic form $F_0 + F_1 D + F_2 D^2 + ...$ with F_0 monic upeer triangular. The product $F(D) \cdot \boldsymbol{S}_e^{-1} \cdot F^*(D^{-*})$ contains a weighted sum of positive terms with $F_0 \cdot \boldsymbol{S}_e^{-1} \cdot F_0^*$ as one of them (time zero-offset term) and has all other terms as positive definite matrices $F_k \cdot F_k^*$ and thus is minimized when when $F_k = 0 \; \forall \; k > 0$, so $\boldsymbol{B}(D) = \boldsymbol{G}(D)$, and in particular $\boldsymbol{B}_0 = \boldsymbol{G}_0$ for crosstalk elimination, is the MMSE solution. Further the minimum value is $R_{\boldsymbol{ee}}(D) = \boldsymbol{S}_e^{-1}$.

$$\begin{aligned} R_{\boldsymbol{ee}}(D) &= \boldsymbol{S}_e^{-1} & (3.610)\\ \sigma_{M4-DFE}^2 &\triangleq \left|\boldsymbol{S}_e^{-1}\right| \triangleq S_e^{-1} \quad . & (3.611) \end{aligned}$$

Lemma 3.10.1 [MMSE-DFE] *The MMSE-DFE has* **feedforward matrix filter**

$$\boldsymbol{W}(D) = \boldsymbol{W}(D) = \boldsymbol{S}_e^{-1} \cdot \boldsymbol{G}^{-*}(D^{-*}) \tag{3.612}$$

(realized with delay, as it is strictly noncausal) and **feedback section**

$$\boldsymbol{B}(D) = \boldsymbol{G}(D) \tag{3.613}$$

where $\boldsymbol{G}(D)$ is the unique canonical factor of the following equation:

$$\frac{\mathcal{N}_0}{2} \cdot \|\tilde{\boldsymbol{H}}\| \cdot \left[Q(D) + \mathbf{SNR}_{MFB}^{-1}\right] \cdot \|\tilde{\boldsymbol{H}}\| = \boldsymbol{G}(D) \cdot \boldsymbol{S}_e \cdot \boldsymbol{G}^*(D^{-*}) \quad . \tag{3.614}$$

*This text also calls the joint matched-filter/sampler/$\boldsymbol{W}(D)$ combination in the forward path of the DFE the "***MIMO Mean-Square Whitened Matched Filter (M4-WMF)***". These settings for the M4-DFE minimize the MSE as was shown above in (3.611).*

The matrix signal to noise ratio is

$$\begin{aligned}
\boldsymbol{SNR}_{M4-DFE} &= \frac{|R_{\boldsymbol{xx}}|}{|\boldsymbol{S}_e^{-1}|} && (3.615)\\
&= \frac{(\bar{\mathcal{E}}_{\boldsymbol{x}})^{L_x}}{\prod_{\ell=1}^{L_x} S_{e,\ell}} && (3.616)\\
&= \prod_{\ell=1}^{L_x} SNR_{M4-DFE}(\ell) && (3.617)
\end{aligned}$$

and correspondingly each such individual SNR is biased and can be written as

$$SNR_{M4-DFE}(\ell) = SNR_{M4-DFE,U}(\ell) + 1 \quad , \tag{3.618}$$

while also

$$\boldsymbol{SNR}_{M4-DFE} = \boldsymbol{SNR}_{M4-DFE,U} + I \quad . \tag{3.619}$$

The overall bits per symbol (with zero-dB gap) is written as (with $\bar{\ell} = 2$ when the signals are real baseband, and $\bar{\ell} = 1$ when complex baseband)

$$\begin{aligned}
b &= \frac{1}{\bar{\ell}} \cdot \log_2 \left\{ \frac{|R_{\boldsymbol{xx}}|}{|\boldsymbol{S}_e^{-1}|} \right\} && (3.620)\\
b &= \frac{1}{\bar{\ell}} \cdot \sum_{l=1}^{L_x} \cdot \log_2 \left[1 + SNR_{M4-DFE,U}(\ell)\right] && (3.621)
\end{aligned}$$

and with non-zero gap,

$$\tilde{b} = \sum_{\ell=1}^{L_x} \cdot \log_2 \left[1 + \frac{SNR_{M4-DFE,U}(\ell)}{\Gamma}\right] \quad . \tag{3.622}$$

Equal energy on each dimension probably is not optimum for transmission. Chapter 4 studies such optimization or **loading**.

The process of current symbol previous-order crosstalk subtraction can be explicitly written by defining the ISI-free (but not current crosstalk-free) output

$$\boldsymbol{z}_k' = \boldsymbol{z}_k - \sum_{l=1}^{\infty} \boldsymbol{G}_l \cdot \hat{\boldsymbol{x}}_{k-l} \quad . \tag{3.623}$$

Any coefficient matrix of $\boldsymbol{G}(D)$ can be written $\boldsymbol{G}_k$ with its $(m,n)^{th}$ element counting up and to the left from the bottom right corner where m is the row index and n is the column index, and $m = 0, ..., L_x$

and also $n = 0, ..., L_x$. Then, the current decisions can be written as (with sbs denoting simple one- (or two- if complex) dimensional slicing detection):

$$\hat{x}_{0,k} = \text{sbs}_0\left(z'_{0,k}\right) \tag{3.624}$$

$$\hat{x}_{1,k} = \text{sbs}_1\left(z'_{1,k} - \boldsymbol{G}_0(1,0)\cdot\hat{x}_{0,k}\right) \tag{3.625}$$

$$\hat{x}_{2,k} = \text{sbs}_2\left(z'_{2,k} - \boldsymbol{G}_0(2,1)\cdot\hat{x}_{1,k} - \boldsymbol{G}_0(2,0)\cdot\hat{x}_{0,k}\right) \tag{3.626}$$

$$\vdots = \vdots \tag{3.627}$$

$$\hat{x}_{L_x-1,k} = \text{sbs}_{L_x-1}\left(z'_{L_x-1,k} - \sum_{l=0}^{L_x-2}\boldsymbol{G}_0(L_x-1,l)\cdot\hat{x}_{l,k}\right) \quad . \tag{3.628}$$

3.10.4 MIMO Precoding

Tomlinson Precoders follow exactly as they did in the scalar case with the sbs above in Equations (3.624) - (3.628) being replaced by the modulo element in the transmitter. The signal constellation on each dimension may vary so the modulo device corresponding to that dimension corresponds to the signal constellation used. Similar Laroia/Flexible precoders also operate in the same way with each spatial dimension have the correct constellation. To form these systems, an unbiased feedback matrix filter is necessary, which is found by computing the new unbiased feedback matrix filter

$$\boldsymbol{G}_U(D) = \left[\boldsymbol{SNR}_{M4-DFE} - I\right]^{-1}\cdot\boldsymbol{SNR}_{M4-DFE}\left[\boldsymbol{G}(D) - \boldsymbol{SNR}^{-1}_{M4-DFE}\right] \quad . \tag{3.629}$$

$\boldsymbol{G}_U(D)$ may then replace $\boldsymbol{G}(D)$ in feedback section with the feedforward matrix-filter output in Figure 3.66 scaled up by $\left[\boldsymbol{SNR}_{M4-DFE} - I\right]^{-1}\cdot\boldsymbol{SNR}_{M4-DFE}$. However, the precoder will move the feedback section using $\boldsymbol{G}_U(D)$ to the transmitter in the same way as the scalar case, just for each dimension.

3.10.5 MIMO Zero-Forcing

The MIMO-ZF equalizers arise from the M4 Equalizers by letting $SNR \to \infty$ in all formulas and figures. However, this may lead to infinite noise enhancement for the MIMO-ZFE or to a unfactorable $R_{\boldsymbol{ee}}(D)$ in the ZF-DFE cases. When these events occur, ZF solutions do not exist as they correspond to channel and/or input singularity. Singularity is otherwise handed more carefully in Chapter 5. In effect the MIMO Channel must be "factorizable" for these solutions to exist, or equivalently the factorization

$$|\tilde{\boldsymbol{H}}\|\cdot Q(D)\cdot\|\tilde{\boldsymbol{H}}\| = \boldsymbol{P}_c(D)\cdot\boldsymbol{S}_c\cdot\boldsymbol{P}^*_c(D^{-*}) \quad , \tag{3.630}$$

exists. This means basically that $Q(D)$ satisfies Appendix D.4's MIMO Paley-Weiner Criterion.

3.11 Information Theoretic Approach to Decision Feedback

Subsection 3.2.1's signal-to-noise ratio and Section 3.6's filter settings for the MMSE-Decision Feedback Equalizer also follow from some basic information-theoretic results for Gaussian sequences. Chapter 2 defines information measures that this section uses to establish an information-theoretic approach canonical equalization. Subsection 3.11.1 revisits the basic information measures of entropy and mutual information for Gaussian sequences, particularly that MMSE estimation is fundamentally related to conditional entropy for jointly Gaussian stationary sequences.

Combination of the MMSE results with the information measures then simply relate the "CDEF" result of decision feedback equalization in Section 3.11.2, which suggests that good codes in combination with an appropriate (set of) DFE(s) can reliably allow the highest possible transmission rates, even though the receiver is not MAP/ML. Such a result is surprising as equalization methods as originally conceived are decidely suboptimal, but with care of the input spectrum choice can be made to perform at effectively optimum, or "canonical" levels. CDEF is a special case of Chapter 4's Separation Theorem.

3.11.1 MMSE Estimation and Conditional Entropy

Given two complex jointly Gaussian random variables, x and y, the conditional probability density $p_{x/y}$ is also a Gaussian density and has mean $\mathbb{E}[x/y]$ equal to the MMSE estimate[35] of x given y. The (complex) Gaussian vector distribution is $1/(\pi^N|R_{\boldsymbol{xx}}|)\cdot e^{-(\boldsymbol{x}-\boldsymbol{u}_x)R_{\boldsymbol{xx}}{}^{-1}(\boldsymbol{x}^*-\boldsymbol{u}_x^*)}$, where $R_{\boldsymbol{xx}}$ is the covariance matrix and $\boldsymbol{u}_x$ is the mean.) The entropy (see Chapter 2) of a complex Gaussian random variable is

$$H_x = \log_2(\pi\cdot e\cdot \mathcal{E}_x) \quad , \tag{3.631}$$

where $\mathcal{E}_x$ is the mean-square value of x. Thus, the conditional entropy of x given y is

$$H_{x/y} = \log_2(\pi\cdot e\cdot \sigma^2_{x/y}) \quad , \tag{3.632}$$

where $\sigma^2_{x/y}$ is the mean-square error value of for the estimate of x given y because $p_{x/y}$ is also a Gaussian distribution. Entropy can be normalized to the number of real dimensions, and complex random variables in passband transmission have the same variance in both real and imaginary dimensions, which is 1/2 the two-dimensional value or the "complex variance." Thus, $\overline{H}_x = \frac{1}{2}\cdot\log_2(2\cdot\pi\ dote\cdot\bar{\mathcal{E}}_x)$ whether x is real or complex. These results generalize to jointly $\overline{N}$-complex-dimensional non-singular[36] Gaussian random vectors (so $N = 2\overline{N}$ real dimensions) as

$$H_{\boldsymbol{x}} = \log_2\{(\pi\cdot e)^{\overline{N}}\cdot|R_{\boldsymbol{xx}}|\} \tag{3.633}$$

and

$$H_{\boldsymbol{x}/\boldsymbol{y}} = \log_2\{(\pi\cdot e)^{\overline{N}}\cdot|R^{\perp}_{\boldsymbol{x}/\boldsymbol{y}}|\} \tag{3.634}$$

respectively, where $R^{\perp}_{\boldsymbol{x}/\boldsymbol{y}} = R_{\boldsymbol{xx}} - R_{\boldsymbol{xy}}\cdot R^{-1}_{\boldsymbol{yy}}\cdot R_{\boldsymbol{yx}}$ is the error autocorrelation matrix associated with the vector MMSE estimate of $\boldsymbol{x}$ from $\boldsymbol{y}$. As always $\bar{R}_{\boldsymbol{xx}} = \frac{1}{N}\cdot R_{\boldsymbol{xx}}$. Again, per-dimensional quantities normalize by the number of real dimensions $N = 2\overline{N}$: $\bar{H}_{\boldsymbol{x}} = \frac{1}{2}\log_2\{(\pi\cdot e)|R_{\boldsymbol{xx}}|^{1/\overline{N}}\}$. If $\boldsymbol{x} = x$, i.e., a scalar, then $R_{\boldsymbol{xx}} = 2\cdot\bar{\mathcal{E}}_x$ in the entropy formula with $\overline{N} = 1$ and all per-dimensional results are consistent.[37]

[35] This result is easily proved as an exercise by simply taking the ratio of $p_{x,y}$ to p_y, which are both Gaussian with the general N-complex-dimensional ($2N$ real dimension, See Section 2.3 and Appendix D also.

[36] The Guassian probability distribution for any singular dimension would essentially be independent with probability 1 and thus eliminate itself from the overall probability density in practical terms [factoring out 1], leaving only those dimensions that are random, so the entropy in the singular case would simply be the entropy of the non-singular dimensions or products of the non-zero eigenvalues of the matrix $R_{\boldsymbol{xx}}$, which here is simply denoted as $|R_{\boldsymbol{xx}}|$.

[37] For those interested in alternative expressions (that provide the same entropy): If $\boldsymbol{x}$ is real, then $H_{\boldsymbol{x}} = \frac{1}{2}\cdot\log_2\left[(2\cdot\pi\cdot e)^N\cdot|R_{\boldsymbol{xx}}|\right]$ or

$$\bar{H}_{\boldsymbol{x}} = \frac{1}{2N}\log_2\left[(2\cdot\pi\cdot e)^N\cdot|N\cdot\bar{R}_{\boldsymbol{xx}}|\right] \tag{3.635}$$

$$= \frac{1}{2}\log_2\left[(2\cdot N\cdot\pi\cdot e)\cdot|\bar{R}_{\boldsymbol{xx}}|^{1/N}\right] \quad , \tag{3.636}$$

Chapter 2's chain rule for a Gaussian random vector $\boldsymbol{x} = [x_k, x_{k-1}, ..., x_0]$ is

$$H_{\boldsymbol{x}} = H_{x_k/[x_{k-1},...,x_0]} + H_{x_{k-1}/[x_{k-2},...,x_0]} + ... + H_{x_1/x_0} + H_{x_0} = \sum_{n=0}^{k} H_{x_n/[x_{n-1},...,x_0]} \quad . \tag{3.640}$$

($Hx_{0/-1} \triangleq H_{x_0}$.) The first k terms in the sum above are conditional entropies that each equal the logarithm of πe times the MMSE associated with prediction of a component of $\boldsymbol{x}$ based on its past values. A stationary Gaussian sequence's entropy is the time-averaged limit of the vector $[x_k, ..., x_0]$'s entropy, normalized to the number of dimensions:

$$H_{X(D)} = \lim_{k\to\infty} \frac{1}{k+1} \cdot \sum_{n=0}^{k} H_{x_n/[x_{n-1},...,x_0]} \quad \text{bits/complex dimension.} \tag{3.641}$$

For an infinite-length stationary sequency, essentially all the terms in the sum above must be the same, so

$$H_{X(D)} = \log_2 \left[(\pi \cdot e) \cdot S_x\right] \quad , \tag{3.642}$$

where S_x is the MMSE associated with computing x_k from its past, which MMSE linear prediction implements through a monic causal filter:

$$V(D) = A(D) \cdot X(D) \;\; \text{where } A(D) = 1 + a_1 \cdot D + a_2 \cdot D^2 + ... \tag{3.643}$$

so the product corresponds to

$$v_k = x_k + a_1 \cdot x_{k-1} + a_2 \cdot x_{k-2} + ... \tag{3.644}$$

Then, the mean-square prediction error is $E[|v_k|^2]$, which is the time-zero value of the autocorrelation function

$$R_{vv}(D) = A(D) \cdot R_{xx}(D) \cdot A^*(D^{-*}) \quad . \tag{3.645}$$

For Gaussian processes, the MMSE estimate is linear, and is best found by canonical factorization[38] of its autocorrelation function:

$$R_x(D) = S_x \cdot G_x(D) \cdot G_x^*(D^{-*}) \quad , \tag{3.646}$$

where S_x is a positive constant and $G_x(D)$ is causal, monic, and minimum phase. The time-zero value of $R_{vv}(D)$ is then found as

$$E[|v_k|^2] = S_x \cdot \|A/G_x\|^2 \quad , \tag{3.647}$$

which is minimized for monic causal choice of A when $A(D) = 1/G_x(D)$. Figure 3.67 illustrates this MMSE linear prediction . S_x is the MMSE.

---

which checks with one-dimensional formule. If $\boldsymbol{x}$ is complex, then $H_{\boldsymbol{x}} = \log_2 \left[(\pi e)^{\overline{N}} \cdot |R_{\boldsymbol{xx}}|\right]$ or

$$\bar{H}_{\boldsymbol{x}} = \frac{1}{2\overline{N}} \cdot \log_2 \left[(\pi \cdot e)^{\overline{N}} \cdot |2 \cdot \overline{N} \cdot \bar{R}_{\boldsymbol{xx}}|\right] \tag{3.637}$$

$$= \frac{1}{2 \cdot \overline{N}} \log_2 \left[(\pi \cdot e)^{\bar{N}} \cdot (2\bar{N})^{\bar{N}} \cdot |\bar{R}_{\boldsymbol{xx}}|\right] \tag{3.638}$$

$$= \frac{1}{2} \log_2 \left[(2 \cdot \bar{N} \cdot \pi \cdot e) \cdot |\bar{R}_{\boldsymbol{xx}}|^{1/\overline{N}}\right] \tag{3.639}$$

which also checks with the one dimensional formula. When a complex vector is modeled as a doubly-dimensional real vector, the two normalized-entropy formulas are the same, as they should be.

[38] presuming Appendix D.3's Paley-Wiener Criterion is satisfied for the process

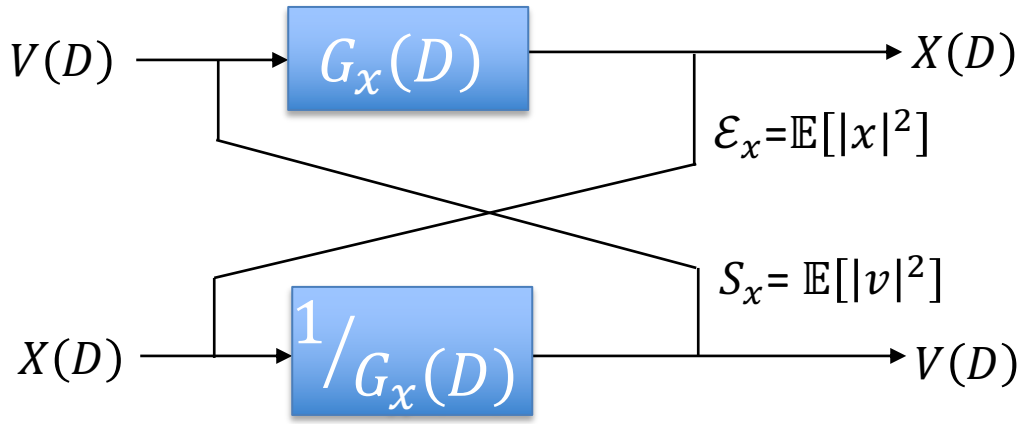

Figure 3.67: Stationary process' linear-prediction illustration.

The output process $V(D)$ is generated by linear prediction, and is also Gaussian and sometimes called the **innovations sequence.** This process carries the essential information for the process $X(D)$, and $X(D)$ can be generated causally from $V(D)$ by processing with $G_x(D)$ to shape the power spectrum, alter the power/energy, but not change the information content of the process, as in Figure 3.67. When $X(D)$ is white (independent and identically distributed over all time samples k), it equals its innovations.

From Chapter 2, the **mutual information** between two random variables x and y is

$$\begin{aligned} I(x;y) &\triangleq H_x - H_{x/y} && (3.648)\\ &= \log_2\left(\frac{S_x}{\sigma^2_{x/y}}\right) = \log_2(1+SNR_{mmse,u}) && (3.649)\\ &= H_y - H_{y/x} && (3.650)\\ &= \log_2\left(\frac{S_y}{\sigma^2_{y/x}}\right) \quad , && (3.651)\end{aligned}$$

showing a symmetry between x and y in estimation, related through the common SNR that characterizes MMSE estimation,

$$1+SNR_{mmse,u} = \frac{S_x}{\sigma^2_{x/y}} = \frac{S_y}{\sigma^2_{y/x}} \quad . \tag{3.652}$$

Equation 3.649 uses the unbiased SNR. For an AWGN, $y = x + n$, $S_y = \mathcal{E}_x + \sigma^2 = \mathcal{E}_x + \sigma^2_{y/x}$. Since $SNR \triangleq \bar{\mathcal{E}}_x/\sigma^2$, then Equation 3.652 relates that

$$1+SNR_{mmse,u} = 1+SNR \quad , \tag{3.653}$$

and thus

$$SNR_{mmse,u} = SNR \quad . \tag{3.654}$$

Thus the unbiased SNR characterizing the forward direction of this AWGN channel is thus also equal to the unbiased SNR ($SNR_{mmse,u}$) in estimating the backward channel of x given y, a fact well established in Subsection 3.2.2. The result will extend to random vectors where the variance quantities are replaced by determinants of covariance matrices as in the next subsection.

3.11.2 The relationship of the MMSE-DFE to mutual information

In data transmission, the largest reliably transmitted data rate for a given input sequence covariance/spectrum is the mutual information between the sequence and the channel output sequence (see Chapter 2). This result's derivation presumes maximum-likelihood detection after observing the entire output sequence $Y(D)$ for the entire input sequence $X(D)$. For the ISI channel, this mutual information is

$$\bar{I}(X(D);Y(D)) = \bar{H}_{X(D)} - \bar{H}_{X(D)/Y(D)} \quad . \tag{3.655}$$

The entropy of a stationary Gaussian sequence is determined by the innovations process, or equivalently its MMSE estimate given its past, thus (3.655) becomes

$$\begin{aligned}
\bar{I}(X(D);Y(D)) &= \bar{H}_{x_k/[x_{k-1},\ldots]} - \bar{H}_{x_k/Y(D),[x_{k-1},\ldots]} && (3.656)\\
&= \frac{1}{2}\cdot\log_2(\pi\cdot e\cdot S_x) - \frac{1}{2}\cdot\log_x(\pi\cdot e\cdot\sigma^2_{MMSE-DFE}) && (3.657)\\
&= \frac{1}{2}\cdot\log_2(SNR_{MMSE-DFE}) && (3.658)\\
&= \frac{1}{2}\cdot\log_2(1+SNR_{MMSE-DFE,U}) \quad . && (3.659)
\end{aligned}$$

The main observation used in the last 3 equations above is that the conditional entropy of x_k, given the entire sequence $Y(D)$ and the past of the sequence x_k exactly depends upon the MMSE estimation problem that the MMSE-DFE solves. Thus the variance associated with the conditional entropy is then the MMSE of the MMSE-DFE. This result was originally noted by four authors[39] and is known as the **CDEF** result (the CDEF result was actually proved by a more circuitous route than in this chapter, with the shorter proof being first shown to the author by Dr. Charles Rohrs of Tellabs Research, Notre Dame, IN).

Lemma 3.11.1 [CDEF Result] *The unbiased SNR of a MMSE-DFE is related to mutual information for a linear ISI channel with additive white Gaussian noise in exactly the same formula as the SNR of an ISI-free channel is related to the mutual information of that channel:*

$$SNR_{MMSE-DFE,U} = 2^{2\bar{I}} - 1 \quad , \tag{3.660}$$

where the mutual information I is computed assuming jointly Gaussian stationary $X(D)$ and $Y(D)$, and only when the MMSE-DFE exists.
Proof: *Follows development above in Equations (3.656)-(3.659).* **QED.**

The CDEF result has stunning implications for transmission on the AWGN channel with linear ISI: It essentially states that the suboptimum MMSE-DFE detector, when combined with the same good codes that allow transmission at or near the highest data rates on the ISI-free channel, will attain the highest possible data rates reliably. This result will be the same as Shannon's infinite-dimensional MT result of Subsection 3.12.2. In all cases, the form of the mutual information used depends on Gaussian $X(D)$. Since a Gaussian $X(D)$ never quite occurs in practice, all analysis is approximate to within the constraints of a finite non-zero gap, $\Gamma > 0$ dB as always in this Chapter, and one could write $\bar{b} = \frac{1}{2}\log_2\left(1+\frac{SNR_{MMSE-DFE,U}}{\Gamma}\right) \leq \bar{I}$ when the DFE exists. Equality holds when the gap is 0 dB[40].

Figure 3.68 depicts the estimation problem associated with $I(X(D);Y(D))$.

[39] "MMSE DFE and Coding: Parts I and II," *IEEE Transactions on Communications*, October 1995, pp. 2582-2604.
[40] Error propagation for non-zero gap codes can cause deviation

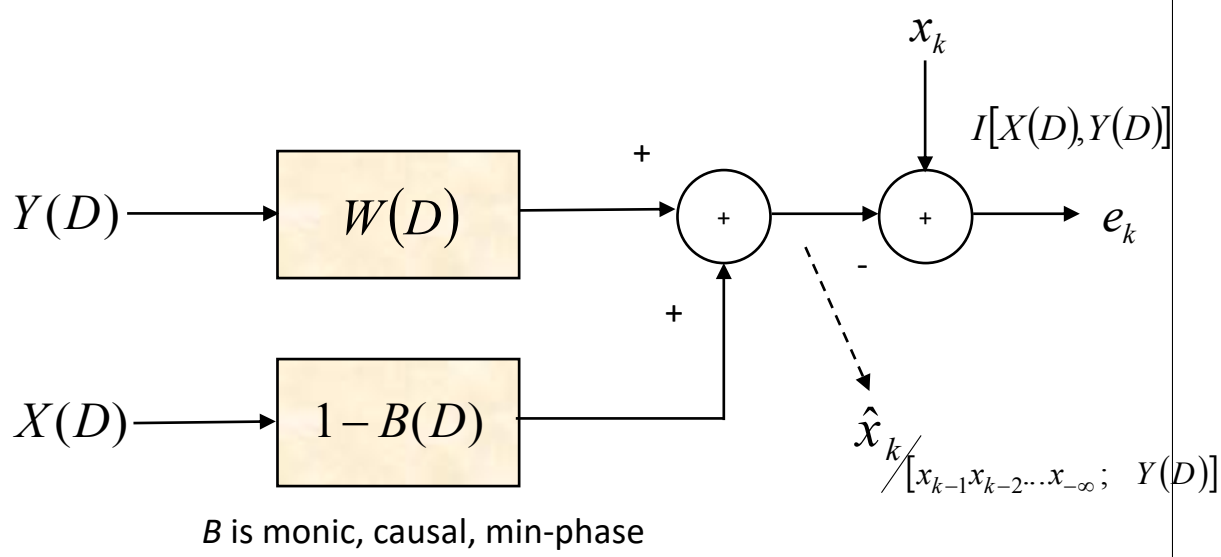

Figure 3.68: MMSE estimation problem associated with $I(X(D);Y(D))$ – the same as the MMSE-DFE.

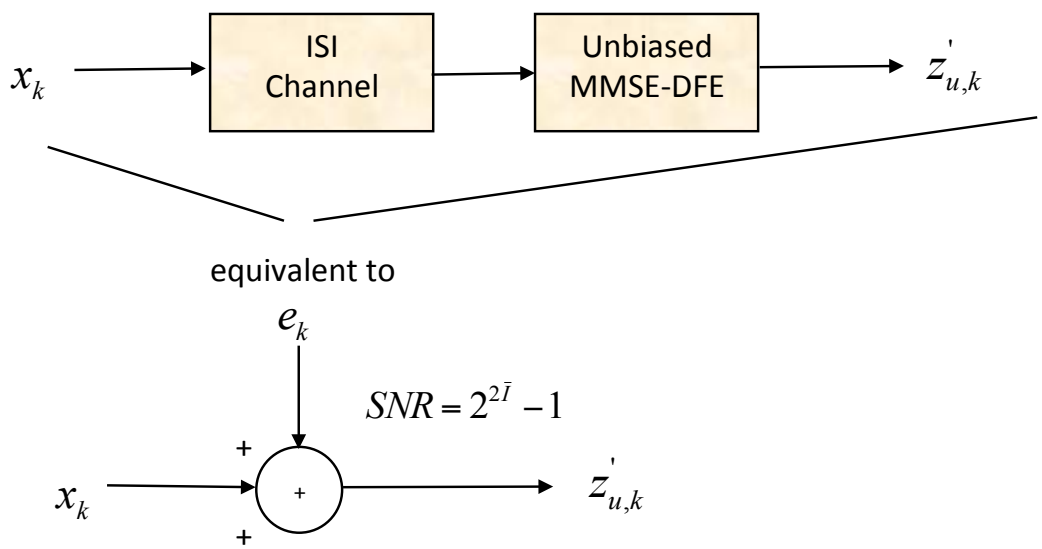

Figure 3.69: CDEF canonical equivalent AWGN channel to MMSE-DFE where codes with gap Γ from capacity on the AWGN channel can be re-used to have the same gap to capacity on the ISI channel.

This particular interpretation shows that the MMSE-DFE structure, when it exists, can be used to approach capacity with $\Gamma \to 0$ dB with the same codes that are used to approach capacity on the AWGN. This implies the MMSE-DFE could then be canonical, especially if the transmitter uses the optimum power spectral density that maximizes $\bar{I}(X(D);Y(D))$ to capacity.

Definition 3.11.1 [Canonical Performance] *The performance of a transmission design is said to be* **canonical** *if the signal-to-noise ratio of the equivalent AWGN characterizing the system is* $2^{2\bar{I}} - 1$ *when the gap is* $\Gamma = 0$ *dB.*

However, there are restrictions on the above CDEF result that were not made explicit to simplify the development. In particular, the designer must optimize the transmit filter for the MMSE-DFE to get the highest mutual information. This process can, and almost always does, lead to unrealizable filters. Happily, there are solutions, but the resulting structures are not the traditional MMSE-DFE except in special cases. Subsections 3.12.2 and 3.12.3 study the necessary modifications of the DFE structure.

3.11.3 Canonical Channel Models

The mutual-information symmetry between $X(D)$ and $Y(D)$ suggest two interpretations of the relationship between $X(D)$ and $Y(D)$, in as Figure 3.70's canonical channel models. The channel autocorrelation is $r(t) \triangleq h(t) * h^*(-t)$ (where any minor transmit and receive analog filtering has been absorbed into the channel impulse/pulse response, while any innovations filtering remains separate), and $R(D) = \sum_k r(kT) \cdot D^k$. $Y(D)$ again corresponds to the overall channel shaping at the sampled matched-filter output.

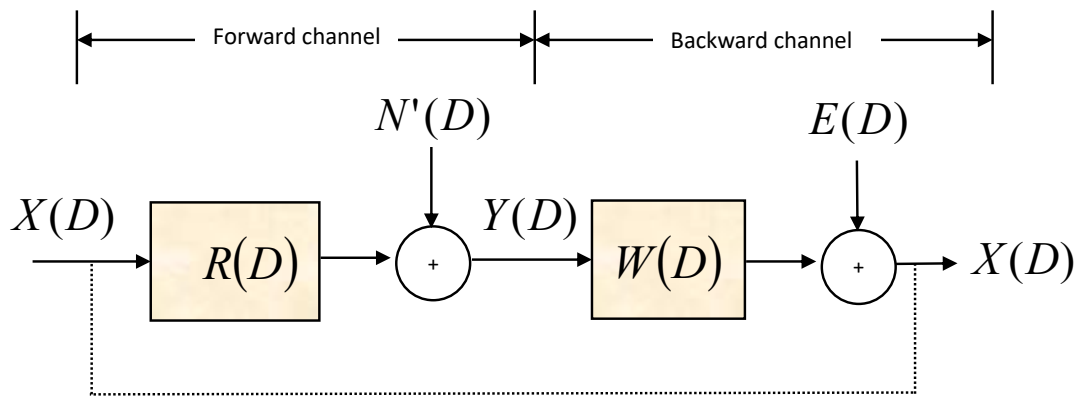

Figure 3.70: Canonical Channel models for same mutual information.

Definition 3.11.2 [Canonical Channel] *A* **canonical channel** *is one in which the linear function or matrix characterizing ISI (or more generally cross-dimensional interference as occurs from Sections 3.11.3 onward) is equal to the autocorrelation function (or matrix) of the additive independent interference. Interference can be Gaussian noise, or some combination of additive Gaussian noise and residual ISI.*

Canonical channels can lead to canonical performance with proper receiver design. This chapter has two canonical channels of interest:

The **forward canonical model** has

$$Y(D) = R(D) \cdot X(D) + N'(D) \quad , \tag{3.661}$$

where $N'(D)$ is the Gaussian noise at the matched-filter output and has autocorrelation function $\frac{\mathcal{N}_0}{2}R(D)$. Thus the noise power spectral density and the channel filtering have the same shape $R(e^{-\jmath\omega T})$. The first term on the right in (3.661) is the MMSE estimate of $Y(D)$ given $X(D)$ and $N'(D)$, the MMSE, and $X(D) = \mathcal{E}_{\boldsymbol{x}}$ so input symbols are independent. The **backward canonical model** is

$$X(D) = W(D) \cdot Y(D) + E(D) \quad . \tag{3.662}$$

where (modulo scaling by $\|h\|^{-1}$) $W(D)$ is the MMSE-LE, and where $E(D)$ is the MMSE-LE's error sequence. Equation (3.662)'s first term on the right is the MMSE estimate of $X(D)$ given $Y(D)$. The equalizer-filter shape and the error-sequence's power spectral density are both $R_{ee}(e^{-\jmath\omega T})$, since $\bar{R}_{ee}(D) = \frac{\mathcal{N}_0}{2}/\{\|h\|^2 \cdot Q(D) + \frac{\mathcal{N}_0}{2}/(\mathcal{E}_{\boldsymbol{x}} \cdot \|h\|^2)\} = \frac{\mathcal{N}_0}{2} \cdot W(D)$.

It is relatively simple to construct DFE's from canonical models: For the forward model, the receiver processes $Y(D)$ by the inverse of the anticausal spectral factor of $R(D) = (S_r \cdot G_r(D) \cdot G_r^*(D^{-*})$ to obtain

$$\frac{Y(D)}{S_r \cdot G_r^*(D^{-*})} = G_r(D) \cdot X(D) + N''(D) \tag{3.663}$$

where $N''(D)$ is white Gaussian noise with energy per dimension $\frac{\mathcal{N}_0}{2}/S_r$. Since $G_r(D)$ is monic, causal, and minimum-phase, a DFE can be readily implemented. This DFE is the ZF-DFE. A forward canonical model will always produce a ZF-DFE. The receiver is not optimum in general mainly because the DFE is not optimum – furthermore, the suboptimum DFE implied is not of highest SNR because the DFE is based on a model that is for the problem of estimating $Y(D)$ from $X(D)$. The DFE from the backward model is the MMSE-DFE. Noting that

$$R(D) + \frac{1}{SNR} = \|h\|^2 \cdot \left[Q(D) + \frac{1}{SNR_{MFB}}\right] = \gamma_0 \cdot \|h\|^2 \cdot G(D) \cdot G^*(D^{-*}) \ , \tag{3.664}$$

with $S_0 = \gamma_0 \cdot \|h\|^2$, then

$$W(D) = \frac{1}{S_0 \cdot G^*(D^{-*})} \quad . \tag{3.665}$$

Then also the action of the feedforward filter $W(D)$ on the sampled matched-filter output $Y(D)$ is

$$\frac{Y(D)}{S_0 \cdot G^*(D^{-*})} = G(D) \cdot X(D) - G(D) \cdot E(D) = G(D) \cdot X(D) - E'(D) \quad . \tag{3.666}$$

where $E'(D)$ is the MMSE sequence associated with the MMSE-DFE and is white (and Gaussian when $X(D)$ is Gaussian) and has energy per dimension $\frac{\mathcal{N}_0}{2}/S_0$.

The forward and backward canonical channel models have the same mutual information between input and output. In the backward model, $Y(D)$ is considered the input, and $X(D)$ is the corresponding output, with $E(D)$ as the noise. Both channels have the same maximum $\bar{b}$ of $\bar{I}(X(D);Y(D))$, and it is the backward channel that describes the MMSE-DFE receiver's action. The DFE receiver's slicing or SBS operation that uses previous decisions to remove the effect of the causal monic $G_r(D)$'s ISI (or $G(D)$'s ISI) in (3.665) or (3.666) is information lossy in general, confirming that DFE's are not optimum ML detectors. However, for the backward channel only, the $SNR_{MMSE-DFE,U}$ is equal to $2^{2\bar{I}(X(D);Y(D))} - 1$, which is the maximum SNR value for the additive white noise/distortion channel created by the MMSE-DFE. Thus, the information loss in the MMSE-DFE does not cause a reduction in achievable data rate and indeed a code with a given gap to capacity on the AWGN channel would be just as close to the corresponding capacity for a bandlimited channel, even with the suboptimum-detector MMSE-DFE's use; as long as decisions are correct, which they would be when $\Gamma = 0$ dB.

3.12 Construction of the Optimized DFE Input

The CDEF result relates mutual information $\bar{I}(X(D);Y(D))$ to $SNR_{MMSE-DFE,U}$ for an AWGN equivalent of the ISI-channel. That relationship is the same as the relationship between $\bar{I}(x;y)$ and SNR as for the (ISI-free) AWGN channel. Thus, the same good codes that bring performance to within gap Γ of capacity on the AWGN channel then do the same for applied (ignoring error propagation[41]) to a MMSE-DFE system because it too looks is an AWGN with the capacity-achieving SNR. A subtlety is the decisions are always correct only for a AWGN-capacity-achieving code that requires infinite delay to decode, so the decisions are not available. Nonetheless, real codes with very low P_e at rates just below capacity can be effective on the DFE system, allowing canonical (but not quite optimum) approach of capacity.

To this point, the MMSE-DFE has used an i.i.d. input sequence x_k, which does not usually maximize $\bar{I}(X(D);Y(D))$. Maximization of $\bar{I}(X(D);Y(D))$ in Subection 3.12.2 develops a best "water-filling (WF)" spectrum that is the same as Chapter 2's multitone transmission system. This WF power spectrum maximizes $\bar{I}(X(D);Y(D))$. A designer might then assume that MMSE-DFE transmit-filter construction with the optimum power-spectral density would then maximize $SNR_{MMSE-DFE,U} = 2^{2\bar{I}(X(D);Y(D))} - 1$. This is correct if the optimum-spectrum-band's measure equals the Nyquist bandwidth, i.e. $|\Omega^{opt}| = 1/T$, or transmit energy must be nonzero at all frequencies except a countable number of infinitesimally narrow notches). This rarely occurs by accident[42], and so the designer must carefully select the symbol rates and carrier frequencies of a at least a minimum-size MMSE-DFE set of energized bands.

It is important to distinguish **coding**, which here means the use of AWGN codes like trellis codes, block codes, turbo codes, etc. (see Chapters 10 and 11 for detailed coding development) from **spectrum design** (sometimes often also confusingly called "coding" in the literature in a more broad use of the term "coding"). This section focuses on spectrum design and presumes use of good known AWGN-channel codes along with the designed spectrum. The two effects are here made independent for the infinite-length MMSE-DFE. This is an instance of Chapter 4's more general **separation theorem** that separates coding from modulation (spectrum choice here in this chapter). This study correspondingly finds best settings for the transmit filter(s), symbol rate(s), and carrier frequency(ies).

Subsection 3.12.1 begins with a discrete-time Paley-Wiener (PW) criterion review (see also Appendix D.3). The PW states when a canonical factorization exists for a random sequence's as a function of its power spectral density. With this PW criterion in mind, Subsection 3.12.2 maximizes $SNR_{MMSE-DFE,U}$ over the transmit filter to find a desired transmit power spectral density, which has a "water-fill shape" when it exists. Subsections 3.12.3 then studies the choice of symbol rates, and possibly carrier frequencies, for a continuous-time channel so that the PW criterion will always be satisfied. Such optimization in these 3 subsections for different increasingly more general cases enables implementation of a countable set realizable transmit filters in each disjoint continuous-time/frequency water-filling band of nonzero measure. Subsection 3.12.5 culminates in the definition of the transmit-optimized MMSE-DFE, as a set of MMSE-DFEs that achieve canonical performance.

3.12.1 The Discrete-Time Paley-Wiener Criterion (PWC) and Filter Synthesis

From Appendix D.3, the discrete-time PWC is"

[41] To ensure avoidance of error-propagation with a code having $\Gamma > 0$ dB, a full maximum-likelihood detector on the entire sequence that would compare the channel-output sequences against all possible noise-free channel-filtered versions of the known possible transmitted codeword sequences. This would ensure the same performance as no error propagation and thus achieve the gap-reduced capacity for this channel at the target P_e.

[42] Some designers of single-carrier QAM systems often err in assuming the full-spectrum-measure use does occur by accident only to find their system does not perform as expected.

Theorem 3.12.1 (Discrete-Time Paley Wiener) *The canonical factorization $R_{xx}(D) = S_x \cdot G_x(D) \cdot G_x^*(D^{-*})$ of the power spectral density of a stationary random sequence x_k exists if and only if*

$$\int_{-\pi/T}^{\pi/T} |\ln R_{xx}(e^{-\jmath\omega T})| \cdot d\omega < \infty \quad . \tag{3.667}$$

Proof: The proof appears in Appendix D.2.

From Section 3.11, the factor $G_x(D)$ is monic, causal, and minimum phase, and there exists a white **innovations** process v_k with energy per sample $\mathcal{E}_v = S_x$ and autocorrelation function $R_{vv}(D) = S_x$, such that the process $X(D)$ can be constructed from $V(D)$ according to Figure 3.67 as

$$X(D) = V(D) \cdot G_x(D) \quad . \tag{3.668}$$

Any process so constructed can be inverted to get the innovations process as also shown in Figure 3.67 as (even when $G_x(D)$ has zeros on the unit circle or equivalently the spectrum has a countable number of "notches")

$$V(D) = \frac{X(D)}{G_x(D)} \tag{3.669}$$

as also shown in Figure 3.67. There is a causal and causually invertible relationship between $X(D)$ and $V(D)$ that allows realizable synthesis or filter implementation relating the two random sequences. Random sequences with power spectra that do not satisfy the PW criterion can not be so constructed from a white innovations sequence. As shown in Subsection 3.11.1, the innovations sequence determines the information content of the sequence. **In data transmission, the innovations sequence is the message sequence to be transmitted.**

For the MMSE-DFE, the sequence $X(D)$ was white, and so equals its innovations, $X(D) = V(D)$.

EXAMPLE 3.12.1 [White Sequence] A real random sequence taking equiprobable values ± 1 with $R_{xx}(D) = \bar{\mathcal{E}}_{\boldsymbol{x}} = 1$ satisfies the discrete-time Paley Wiener Criterion trivially and has innovations equal to itself $X(D) = V(D)$, $G_x(D) = 1$. The entropy is $\bar{H}_x = 1$ for this binary sequence. As in Chapter 2, if this sequence instead has a Gaussian distribution, then the factorizations remain the same, but this entropy is $\bar{H}_x = .5 \log_2(2 \cdot \pi \cdot e)$ bits/dimension. Figure 3.71(a) shows this spectrum.

EXAMPLE 3.12.2 [AMI Sequence] Subsection 3.8.3 presented the AMI sequence as a (real-baseband) partial-response channel. The AMI encoder transmits successive differences of the actual channel inputs (this "encoder" can happen naturally on channels that block DC so the encoder is in effect the channel prior to the addition of WGN). This action can be described or approximated by the D-transform $1 - D$. The consequent AMI sequence then has $R_{xx}(D) = -1D^{-1} + 2 - D$ clearly factors into $R_{xx}(D) = 1 \cdot (1 - D)(1 - D^{-1})$ and thus must satisfy the Paley Wiener Criterion. The innovations sequence is $V(D) = X(D)/(1 - D)$ and has unit energy per sample.[43] The energy per sample of $X(D)$ is $r_{xx,0} = 2$. For the binary case, the entropy is that of the input $v(D)$, which is 1 bit/dimension if $v_k = \pm 1$. For the Gaussian case, the entropy is $\bar{H}_x = .5 \log_2(2\pi \cdot e \cdot \bar{\mathcal{E}}_{\boldsymbol{x}})$ bits/dimension – the same entropy as in Example 3.12.1, even though the spectrum in Figure 3.71(b) is different from Figure 3.71(a).

The last example illustrates that the innovations never has energy/sample greater than the sequence from which it is derived.

[43] This filter is marginally stable in that a pole is on the unit circle - however, the input to it, $X(D)$, has zero energy at this location (DC).

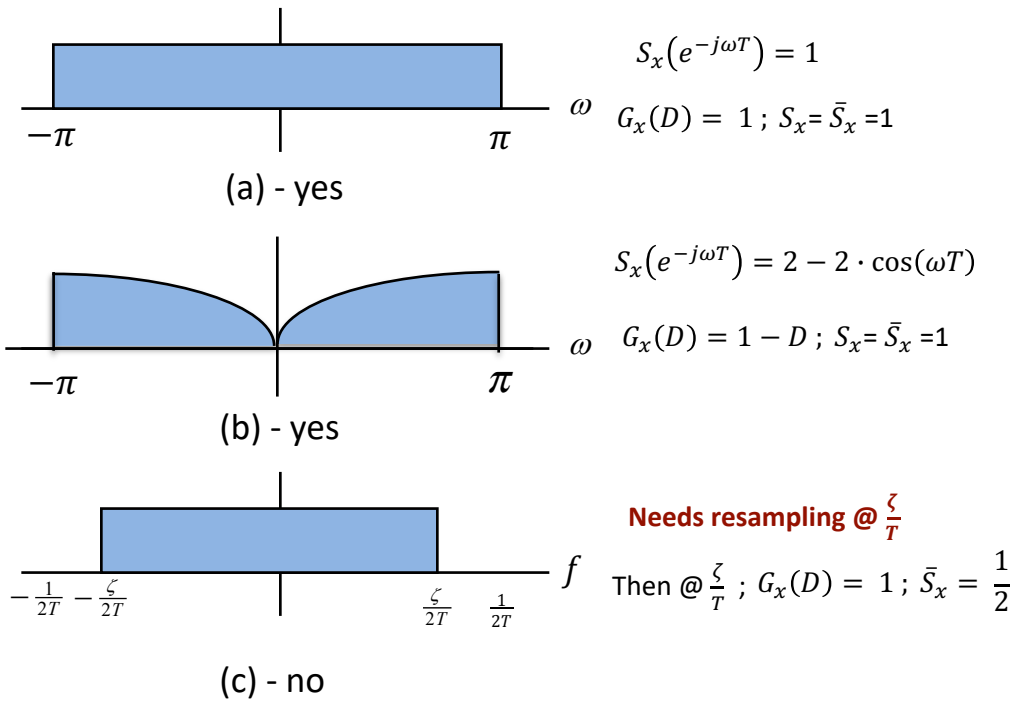

Figure 3.71: Illustration of two spectra that satisfy discrete PW in (a) and (b) while (c) does not satisfy the PW criterion.

EXAMPLE 3.12.3 [Ideal Lowpass Process] Figure 3.71(c)'s complex baseband sequence has power spectral density ($\zeta < 1$ is a positive constant)

$$R_{xx}(e^{-\jmath\omega T}) = \begin{cases} 1 & |\omega| < \zeta\frac{\pi}{T} \\ 0 & |\omega| \geq \zeta\frac{\pi}{T} \end{cases} \quad . \tag{3.670}$$

It does NOT satisfy the PW criterion. This process cannot be implemented causally by passing a white information sequence through a "brickwall lowpass filter" because that filter has infinite (two-sided) delay. An causal-filter approximation would lead to a slightly different power spectral density and could satisfy the PW criterion. The designer might better consider a new sampling rate of ζ/T, and the resulting new sampled random sequence would then truly satisfy the PW criterion trivially as in Example 3.12.1, rather than incur the complexity of such a lowpass filter.

When optimizing a transmit complex transmit filter, an adjustment to the real basis function of Chapter 1 must occur. Chapter 1's QAM basis functions are:

$$\varphi_1(t) = \sqrt{\frac{2}{T}} \cdot \varphi(t) \cdot \cos(\omega_c t) \tag{3.671}$$

$$\varphi_2(t) = -\sqrt{\frac{2}{T}} \cdot \varphi(t) \cdot \sin(\omega_c t) \quad , \tag{3.672}$$

where $\varphi(t)$ was real. Spectrum optimization consequently reduces to optimization of $\left|\Phi(e^{-\jmath\omega T})\right|^2 = \mathcal{F}\left\{\varphi(t) * \varphi^*(-t)\right|_{t=kT}$ and remains insensitive to carrier phase as far as performance; so while complex basis functions with unequal imaginary and real parts might appear an alternative, there is always one basis function with constant amplitude on both inphase and quadrature and has the desired optimum magnitude at any carrier phase.

3.12.2 Theoretical multi-tone system tool for transmit optimization

Chapter 4 develops Multi-Tone (MT) transmission systems in more detail, including the heavily used and optimum Discrete MulitTone (DMT) for stationary channels and Coded-OFDM methods for statistically model channels (statistically modeled channels being more completely addressed also in Chapter 1). To progress transmit-spectrum optimization in equalized system, it is convenient here to review ad eexpand slightly the theoretically optimum MT system of Chapter 2. Chapter 4's DMT approximates very closely this theoretical MT system in practical implementations.

MT Review: Chapter 2 Section 5's MT system uses a set of $N \to \infty$ infinitesimally narrow QAM channels (and one PAM channel at baseband/DC if a real-baseband system). The MT system independently excites each tone as if it were its own isolated AWGN channel with the gain being the channel gain

$$H_n \triangleq H_c(\omega)|_{\omega=2\pi\frac{n}{T}} \quad \forall\, n = -\infty, ... -1, 0, 1 ... \infty \quad , \tag{3.673}$$

where T is the symbol rate and n/T is the carrier frequency where $T \to \infty$. The nth QAM system uses the band $f \in \frac{n}{T} + \left[-\frac{1}{2T}, \frac{1}{2T}\right]$. The limit means that the carriers get infinitesimally narrow and the symbol length becomes all time. Also $g(\omega) \triangleq H_c(\omega)/\sigma^2$. The transmit filter gain at any frequency is

$$\Phi_n \triangleq \Phi(\omega)|_{\omega=2\pi\frac{n}{T}} \quad . \tag{3.674}$$

The noise power spectral density is $\sigma^2 = \mathcal{N}_0/2$ at all frequencies (or the equivalently white-noise channel can replace H). The transmit filter has no energy outside its band, so

$$\Phi_n(\omega) = \begin{cases} 0 & \omega \notin 2\pi \cdot \left(\frac{n}{T} + \left[-\frac{1}{2T}, \frac{1}{2T}\right]\right) \\ \Phi_n \neq 0 & \omega \in 2\pi \cdot \left(\frac{n}{T} + \left[-\frac{1}{2T}, \frac{1}{2T}\right]\right) \end{cases} \quad , \tag{3.675}$$

so that all the tones' subchannels are independent.

The interval or "band" of non-zero-energized frequencies is a set of contiguous tones' frequencies, or several such sets, and is denoted by Ω. The measure of Ω is the total used bandwidth

$$|\Omega| = \int_\Omega d\omega \quad . \tag{3.676}$$

An optimum bandwidth Ω^{opt} includes all the energized tones that correspond to the optimization as $T \to \infty$. The data rate is

$$R = \lim_{T\to\infty} \frac{b}{T} \quad . \tag{3.677}$$

Continuous frequency can then replace the frequency index n according to

$$\omega = 2\pi \cdot \lim_{T\to\infty} \frac{n}{T} \;, \quad n = -\infty, ... -1, 0, 1 ... \infty \quad , \tag{3.678}$$

and the width of a tone becomes

$$d\omega = \lim_{N\to\infty} \frac{2\pi}{NT'} \tag{3.679}$$

If $1/T'$ is sufficiently large to be at least twice the highest frequency that could be conceived of for use on any given band-limited channel, then Ω^{opt} becomes the true optimum band for use on the continuous channel. The two-sided power spectral density at frequency ω corresponding to $\frac{n}{NT}$ then is

$$S_x(\omega) = \lim_{T\to\infty} \bar{\mathcal{E}}_n \quad . \tag{3.680}$$

When using infinite positive **and negative** time and frequency as here, there is no need for complex baseband equivalents, and thus all dimensions are considered real (and QAM is just then one real

dimension at positive frequency and one real dimension at that the negative image of that frequency). The data rate then becomes

$$R = \frac{1}{2\pi} \int_{\Omega^{opt}} \frac{1}{2} \log_2 \left(1 + \frac{S_x(\omega) \cdot g(\omega)}{\Gamma} \right) d\omega \quad . \tag{3.681}$$

The input power constraint is

$$P_x = \frac{1}{2\pi} \cdot \int_{\Omega^{opt}} S_x(\omega) d\omega \quad . \tag{3.682}$$

Calculus of variations (see Section 2.5) produces Shannon's famous water-filling equation for continuous frequency with discrete time as:

$$\bar{\mathcal{E}}_n + \frac{\Gamma}{g(\omega)} \to S_x(\omega) + \frac{\Gamma}{g(\omega)} = \lambda \text{ (a constant)} \tag{3.683}$$

where the the value λ is chosen to meet the total power constraint in (3.682), recalling that $S_x(\omega) > 0$ for all $\omega \in \Omega^{opt}$ and $S_x(\omega) = 0$ at all other frequencies. The data rate then can be also written

$$R = \frac{1}{2\pi} \int_{\Omega^{opt}} \frac{1}{2} \log_2 \left(\frac{\lambda \cdot g(\omega)}{\Gamma} \right) d\omega \quad , \tag{3.684}$$

These results do extend to MIMO, but require some notational effort that will be facilitated by Chapter 4's more detailed developments.

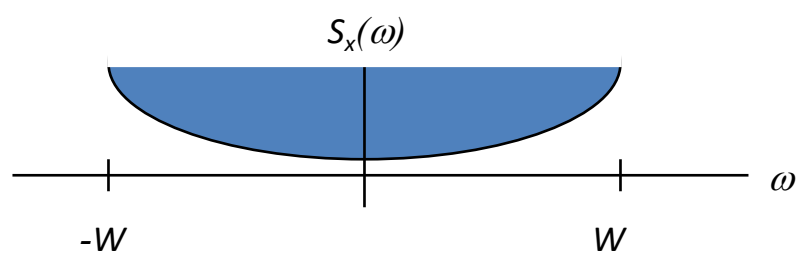

Figure 3.72: Capacity frequency interval for $1 + .9D^{-1}$ channel.

EXAMPLE 3.12.4 **[1+.9·D channel]** The channel with impulse response $h(t) = \text{sinc}(t) + .9 \cdot \text{sinc}(t-1)$ has the same performance as the $1 + .9 \cdot D^{-1}$ channel studied throughout this book, if the analog transmit filter (without spectrum shaping included as it will be optimized) is $\frac{1}{\sqrt{T}}\text{sinc}(t/T)$. A system with optimized MT basis functions of infinite length (as $T \to \infty$) would have an optimum bandwidth $\Omega^{opt} = [-W, W]$ as in Figure 3.72 Then, continuous water-filling with $\Gamma = 1$ produces

$$P_x = \int_{-W}^{W} \left(\lambda' - \frac{.181}{1.81 + 1.8\cos(\omega)} \right) \frac{d\omega}{2\pi} \tag{3.685}$$

where W is implicitly in radians/second for this example. If $P_x = 1$ with $\frac{\mathcal{N}_0}{2} = .181$, the integral in (3.685) simplifies to

$$\pi = \int_0^W \left(\lambda' - \frac{.181}{1.81 + 1.8\cos(\omega)} \right) d\omega \tag{3.686}$$

$$= \lambda' W - .181 \left\{ \frac{2}{\sqrt{1.81^2 - 1.8^2}} \arctan \left[\frac{\sqrt{1.81^2 - 1.8^2}}{1.81 + 1.8} \tan\left(\frac{W}{2}\right) \right] \right\} \tag{3.687}$$

At the bandedge W,

$$\lambda' = \frac{.181}{1.81 + 1.8\cos(W)} \quad . \tag{3.688}$$

leaving the following transcendental equation to solve by trial and error:

$$\pi = \frac{.181W}{1.81 + 1.8\cos(W)} - 1.9053 \arctan\left(.0526 \tan(W/2)\right) \tag{3.689}$$

$W = .88\pi$ approximately solves (3.689), and the corresponding value of λ is $\lambda = 1.33$.

The highest data rate with $1/T' = 1$ is then

$$\begin{aligned}
\mathcal{C} &= \frac{2}{2\pi}\int_0^{.88\pi} \frac{1}{2}\log_2\left(\frac{1.33}{.181}(1.81 + 1.8\cos\omega)\right) d\omega && (3.690)\\
&= \frac{1}{2\pi}\int_0^{.88\pi} \log_2 7.35 d\omega + \frac{1}{2\pi}\int_0^{.88\pi} \log_2\left(1.81 + 1.8\cos\omega\right) d\omega && (3.691)\\
&= 1.266 + .284 && (3.692)\\
&\approx 1.55\text{bits/second} \quad . && (3.693)
\end{aligned}$$

This exceeds the 1 bit/second transmitted on this channel in this chapter's earlier examples where $T = T' = 1$. The MT system has no error propagation, and is also an ML detector.

3.12.3 Discrete-Time Water-filling and the Paley-Wiener Citerion

As in Subsection 3.12.1, transmission analysis and design often is in discrete time. The mutual information $\bar{I}(X(D);Y(D))$ is a function only of the discrete-time processes' power spectral densities if $X(D)$ and $Y(D)$ are Gaussian. Thus maximization of $\bar{I}(X(D);Y(D))$ over the power spectral density of $X(D)$ will produce a symbol-rate-dependent waterfill spectrum for the transmit filter, which in turn has as input a white (and "near-Gaussian") message sequence ν_k

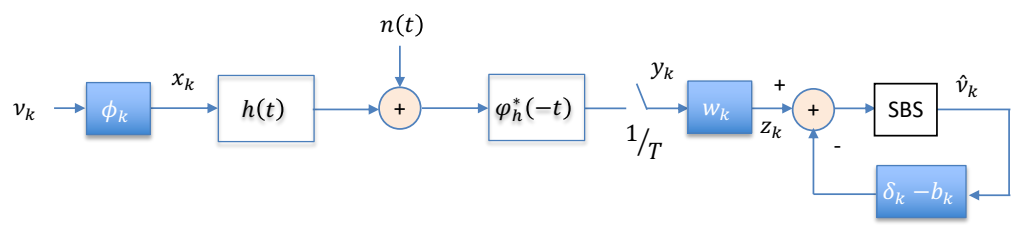

Figure 3.73: MMSE-DFE system with digital transmit filter.

Figure 3.73 shows the implementation of a transmitter that includes a digital filter ϕ_k (with transform $\Phi(D)$). This filter preceeds the modulator that converts the symbols at its output x_k into the modulated waveform $x(t)$, typically QAM or PAM. The discrete-time filter input is ν_k, which now becomes the message sequence. Recalling that $q(t) \triangleq h(t) * h^*(-t)/\|h\|^2$, the mutual information or maximum data rate from Section 4.4.3 is

$$\bar{I}(X(D);Y(D)) = \frac{T}{2\pi}\int_{-\pi/T}^{\pi/T} \log_2\left(\frac{\|h\|^2 \cdot \bar{\mathcal{E}}_\nu}{\frac{\mathcal{N}_0}{2}} \cdot |\Phi(e^{-\jmath\omega T})|^2 \cdot Q(e^{-\jmath\omega T}) + 1\right) \cdot d\omega \quad . \tag{3.694}$$

The transmit energy constraint is the ($\Gamma = 0$ dB)-sum of data rates on an infinite number of infinitessimally small tones:

$$\frac{T}{2\pi}\int_{-\pi/T}^{\pi/T} \bar{\mathcal{E}}_\nu \cdot |\Phi(e^{-\jmath\omega T})|^2 \cdot d\omega = \bar{\mathcal{E}}_x \quad . \tag{3.695}$$

The maximization of $\bar{I}(X(D);Y(D))$ is then achieved by classic water fill solution in

$$|\Phi(e^{-\jmath\omega T})|^2 + \frac{\frac{\mathcal{N}_0}{2}}{\bar{\mathcal{E}}_\nu \cdot \|h\|^2 \cdot Q(e^{-\jmath\omega T})} = K \quad . \tag{3.696}$$

As always, energy at any frequency ω must be nonnegative, so

$$|\Phi(e^{-\jmath\omega T})|^2 \geq 0 \quad . \tag{3.697}$$

There is a set of frequencies Ω^{opt} for which transmit energy is nonzero and for which the discrete-time transmit filter output energy satisfies water-filling. The corresponding capacity is then

$$\bar{C} = \max_{\|\Phi(e^{-\jmath\omega T})\|^2=1} \bar{I}(X(D);Y(D)) \quad . \tag{3.698}$$

The **measure** of Ω^{opt} for the discrete-time case is similarly

$$|\Omega^{opt}| = \frac{T}{2\pi}\int_{\Omega^{opt}} d\omega \quad . \tag{3.699}$$

If $|\Omega^{opt}| = 1$, then a realizable transmit filter exists by the PW criterion. In this case, $SNR_{MMSE-DFE,U} = 2^{2\bar{C}} - 1$ and the MMSE-DFE transmission system with water-fill transmit power spectral density can reliably achieve, with powerful known AWGN-channel codes, the highest possible rates, so the MMSE-DFE in this case only is effectively optimal or "canonical." **If the water-fill band does not have unit measure, the transmitter is not realizable, and the MMSE-DFE is not optimal.** The non-unit-measure case is very unlikely to occur unless the sampling rate has been judiciously chosen. This is the single most commonly encountered mistake of QAM/PAM designers who attempt to match the performance of MT systems - only in the rare case of $|\Omega^{opt}| = 1$ can this design work.

3.12.4 The baseband lowpass channel with a single contiguous water-fill band

The baseband lowpass channel has Figure 3.74's transfer characteristic. The continuous-time waterfill band Ω^{opt} also appears. Clearly sampling of this channel at any rate exceeding $1/T^{opt} = |\Omega^{opt}|$ should produce a discrete-time channel with capacity in bits/dimension

$$\bar{\mathcal{C}}(T < T^{opt}) = \mathcal{C} \cdot T \quad , \tag{3.700}$$

where the explicit dependency of $\bar{\mathcal{C}}(T)$ on choice of symbol period T appears in the argument $\bar{\mathcal{C}}(T)$. $\mathcal{C}$ with no argument is the continuous time (highest possible) capacity in bits/ second. The capacity in bits/second remains constant while the capacity in bits per symbol decreases with increasing symbol rate to maintain the constant value $\mathcal{C} = \bar{\mathcal{C}}(T)/T$. At symbol rates below $1/T < 1/T^{opt} = |\Omega^{opt}|$, capacity $\mathcal{C}$ may not be (and usually is not) achieved so

$$\bar{\mathcal{C}}(T > T^{opt}) \leq \mathcal{C} \cdot T \quad . \tag{3.701}$$

To achieve the highest data rates on this lowpass channel with good codes, the designer would like to choose $1/T \geq 1/T^{opt}$. However, the transmit filter is not realizable unless $1/T = 1/T^{opt}$, so there is an optimum symbol rate $1/T^{opt}$ for which

$$SNR_{MMSE-DFE,U}(T^{opt}) = 2^{2\mathcal{C}\cdot T^{opt}} - 1 \quad . \tag{3.702}$$

At this symbol rate **only** can the MMSE-DFE can achieve the best possible performance for the lowpass channel and indeed canonically achieve the MT performance levels, see also Chapter 4. This example correctly suggests that an ideal symbol rate exists for each channel with "PAM/QAM-like" transmission and a MMSE-DFE receiver.

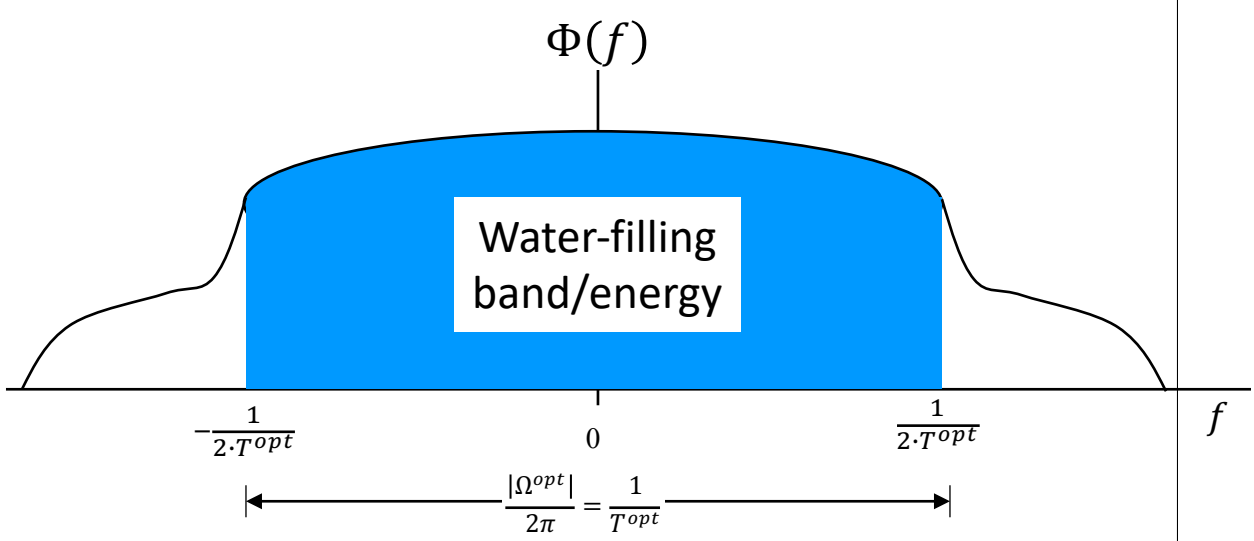

Figure 3.74: llustration of water-filling and transmit optimization for real baseband lowpass channel.

For rates below capacity using codes with gap $\Gamma > 1$, the continuous-time water-filling applies with the reduced transmit power P_x/Γ. This new water-filling solution has a lower[44] optimum symbol rate $1/T_\Gamma^{opt} \leq 1/T^{opt}$. Designs then use this lower symbol rate with the code of gap Γ, and the corresponding MMSE-DFE data rate is then

$$R = \frac{\bar{b}}{T_\Gamma^{opt}} = \frac{1}{2 \cdot T_\Gamma^{opt}} \cdot \log_2 \left(1 + \frac{SNR_{MMSE-DFE,U}(T_\Gamma^{opt})}{\Gamma} \right) \quad . \tag{3.703}$$

Two examples illustrate the effects and terminology of symbol-rate optimization:

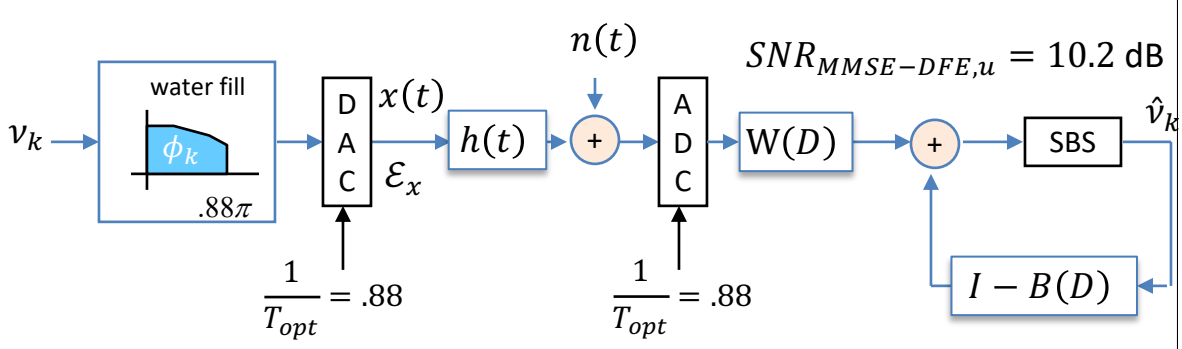

Figure 3.75: Block diagram of optimized DFE system for the $1 + .9D^{-1}$ channel.

EXAMPLE 3.12.5 ($1 + .9 \cdot D^{-1}$ channel) The $1 + .9 \cdot D^{-1}$ ISI-channel has been revisited often, and is again revisted here with $\bar{\mathcal{E}}_x \|h\|^2 / \frac{\mathcal{N}_0}{2}$=10 dB. This channel corresponds to the real baseband lowpass channel discussed above. The capacity in bits per real sample/dimension has been previously found in Example 4.4.1 to be $C(T = 1) = 1.55$ bits/dimension,

[44] Less water to pour means more, or same, narrow water-fill band always.

so that $\mathcal{C} = 1.55$ bits/second with $T = 1$. This capacity corresponds to an overall best SNR of 8.8 dB with $T = 1$, but could not be directly realized with a MMSE-DFE, which instead had an $SNR_{MMSE-DFE,U} = 8.4$ dB at the symbol rate of $1/T = 1$ and a causally realizable transmit filter. The optimum water-fill band has width $|\Omega^{opt}| = .88\pi$ (positive frequencies). Then, the optimum symbol rate is

$$1/T^{opt} = .88 \quad . \tag{3.704}$$

Thus, the capacity in bits/dimension for the system with optimum symbol rate is

$$\bar{\mathcal{C}}(T^{opt}) = \frac{1.55}{.88} = 1.76 \text{ bits/dimension} \quad . \tag{3.705}$$

The resultant SNR is then

$$SNR_{MMSE-DFE,U}(T^{opt}) = SNR^{opt}_{MMSE-DFE,U} = 2^{2\cdot 1.76} - 1 = 10.2 \text{ dB} \quad . \tag{3.706}$$

This optimum MMSE-DFE at this new symbol rate is the only MMSE-DFE that can match the MT system in performance (if there is no loss from error propagation or precoding). The SNR_{MFB} of 10 dB in this example's previous invocations is only a bound for the symbol rate is $1/T = 1$; this bound needs recalculation at another symbol rate. For verification, the capacity in bits/second is consistently the same at both sampling rates, but only $1/T^{opt} = .88$ can be used with a MMSE-DFE[45]. The capacity in bits/second remains

$$\mathcal{C} = \frac{.88}{2} \cdot \log_2(1 + 10^{1.02}) = \frac{1}{2} \cdot \log_2(1 + 10^{.88}) = 1.55 \text{ bits/second} \quad . \tag{3.707}$$

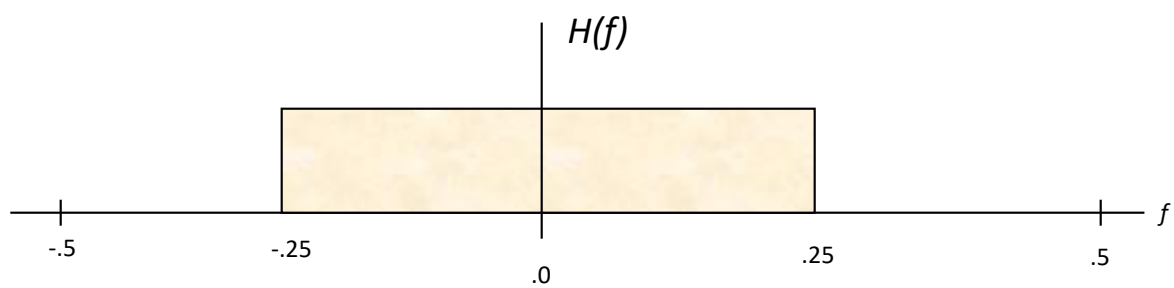

Figure 3.76: Example channel.

EXAMPLE 3.12.6 [The "half-band" ideal lowpass channel] Figure 3.76's "brickwall "lowpass channel has cut-off frequency .25 Hz. The corresponding water-filling bandwidth is $\Omega^{opt} = 2\pi(-.25, .25)$. This channel's capacity is $\mathcal{C} = 2$ bits per second. Thus, at $T^{opt} = 2$, then $\bar{C}(T^{opt}) = 4$ bits/dimension. By the CDEF result, a MMSE-DFE with this symbol rate has $SNR_{MMSE-DFE,U}(T^{opt} = 2) = 2^{2\cdot 4} - 1 \approx 24$ dB. This MMSE-DFE is clearly trivial and the equalized channel is equivalent to the original ISI-free channel at this symbol rate.

Suppose instead, a designer not knowing (or not being able to know for instance in broadcast or one-directional transmission) the channel's Fourier transform or shape instead uses $T = 1$ for a MMSE-DFE with flat transmit energy. While clearly this is a poor choice, this can happen when there is channel variability that the designer cannot anticipate. An immediate obvious loss is the 3 dB loss in received energy that is outside the channel's passband, which

[45] At the optimum symbol rate, $\bar{\mathcal{E}}_{\boldsymbol{x}} = 1/.88$, $\|p\|^2 = 1.81/.88$, and the noise per sample increases by $1/.88$. Thus, $SNR_{MFB}(.88) = 10.6$ dB.

in PAM/QAM is equivalent to roughly to .5 bit/dimension loss. This represents an upper bound SNR for the MMSE-DFE performance.[46] The mutual information (which is now less than capacity) is approximately then

$$\bar{I}(T=1) \approx \frac{\bar{I}(T^{opt}=2)-.5}{2} = \frac{3.5}{2} = 1.75 \text{ bits/dimension} \quad . \tag{3.708}$$

The .5 bit/dimension loss in the numerator $\bar{I}(T^{opt}=2)-.5 = \frac{1}{2}\cdot\log_2(1+\frac{SNR}{2}) = 3.5$ approximates the 3 dB loss of channel-output energy caused by the channel response. Clearly, the channel has severe ISI when $T=1$, but the CDEF result easily provides the MMSE-DFE SNR according to

$$SNR_{MMSE-DFE,U}(T=1) = 2^{2\cdot 1.75}-1 = 10.1 \text{ dB} \quad . \tag{3.709}$$

The equalized system with $T=1$ is equivalent to an AWGN with SNR=10.1 dB, although not so trivially and with long equalization filters in this $T=1$ case, because ISI will be severe.

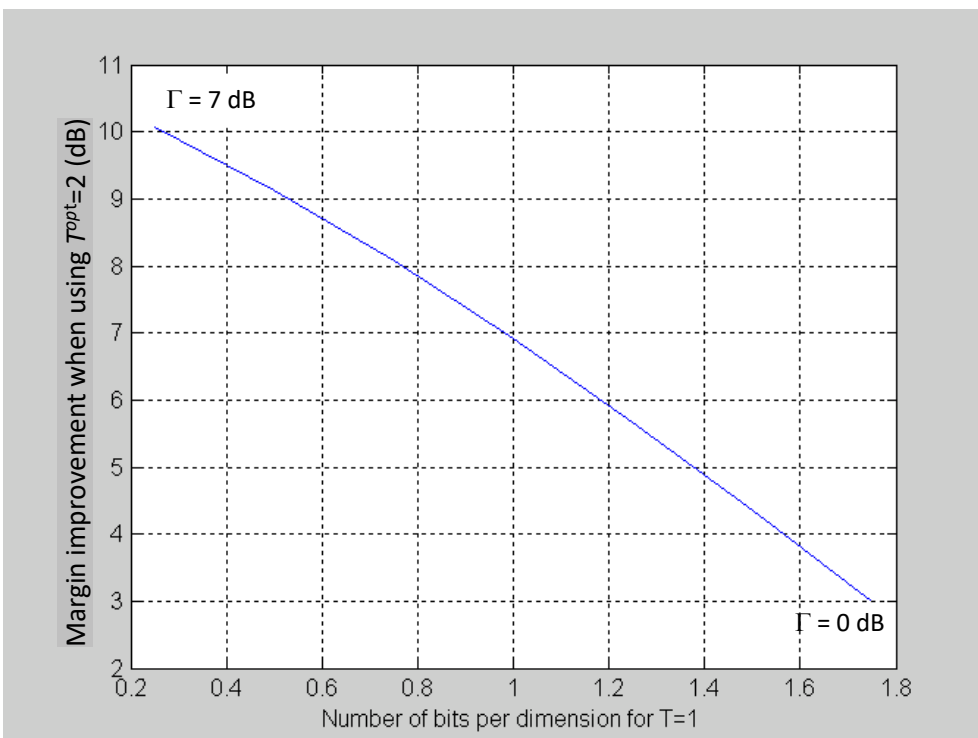

Figure 3.77: Margin difference (improvement) for optimized transmission over unoptimized MMSE-DFE on a "half-band" channel.

The system with $T=1$ then attempts to transmit at $\bar{b}(T=1)$ with $SNR = 10.1$ dB, while the optimized system transmits $\bar{b}(T^{opt}=2) = 2\cdot\bar{b}(T=1)$ with $SNR = 24$ dB. The margin as a function of $\bar{b}(T=1)$ is then

$$\gamma_m(T=1) = 10\cdot\log_{10}\left(\frac{2^{2\cdot 1.75}-1}{2^{2\cdot\bar{b}(T=1)}-1}\right) = 10.1 \text{ dB} - 10\cdot\log_{10}\left[2^{2\cdot\bar{b}(T=1)}-1\right] \quad . \tag{3.710}$$

[46] In fact, this upper bound can be very closely achieved for very long filters in MMSE-DFE design, which could be verified by DFE design for instance according to the DFE program in Section 3.7.6.

For $T^{opt} = 2$, the corresponding margin (basically against an increase in the flat AWGN noise level) is

$$\gamma_m(T^{opt} = 2) = 10 \cdot \log_{10}\left(\frac{2^{2\cdot 4} - 1}{2^{2\bar{b}(T^{opt}=2)} - 1}\right) = 24 \text{ dB} - 10 \cdot \log_{10}\left[2^{4\bar{b}(T=1)} - 1\right] \quad . \quad (3.711)$$

Figure 3.77 plots the margin difference for $T = 1$ and $T^{opt} = 2$ versus the design's attempted number of bits per dimension. The difference decreases as the systems approach capacity, meaning use of smaller-gap codes, but is always nonzero in this case because the system with $T = 1$ essentially "wastes 3 dB (a factor of 2) of bandwidth." Indeed, it is not possible for the $T = 1$ system to transmit beyond 1.75 bits/second and is thus at best 3 dB worse than the $T^{opt} = 2$ system because half the energy is wasted on a channel band that cannot pass signal energy. One could infer that at fixed P_e, the gap decreases with increasing $\bar{b}(T = 1)$ on the horizontal access until the $\Gamma = 0$ dB limit is reached at 1.75 bps.

Some designers might attempt transmission with ϕ_k as a low-pass filter (with gain 3 dB) to correct the situation, thus regaining some of the minimum 3 dB energy loss when $\Gamma = 0$ dB. As the transmit filter becomes more tight, it becomes difficult to implement; in the limit, such a filter is not realizable because it does not meet the PW criterion. Further, the receiver MMSE-DFE consequently also becomes very complex. Concisely, leaving $T = 1$, forces ISI and makes both transmitter and receiver very complex with respect to using the optimum $T^{opt} = 2$. As the gap increases, the performance difference also magnifies between $T = 1$ and $T^{opt} = 2$, so even a very good brickwall transmit filter at $T = 1$ loses performance when $\Gamma > 0$. Any implementable system must have a non-zero gap. By contrast, the optimum transmit filter is simple flat passband at $T^{opt} = 2$, and the MMSE-DFE receiver filters are trivial. Also as the capacity/SNR increases, the curve in Figure 3.77 shows larger difference at reasonable data rates, but more rapidly falls to again 3 dB at the point where the $T = 1$ system achieves capacity with $\Gamma = 0$ dB. It is thus very inadvisable design to use the incorrect symbol rate from the perspectives of performance and/or complexity.

3.12.5 The single-band bandpass case

The previous subsection (3.12.3)'s channels were baseband (i.e., real one-dimensional) lowpass channels. A complex lowpass channel tacitly includes the effect of a carrier frequency. Figure 3.78 illustrates the passband channel and the choice of best carrier (or really "center") frequency f_c and then consequently the best symbol rate $1/T^{opt}$. Clearly, to select the optimum symbol rate, the QAM carrier frequency must be in the center of the water-filling band. Any other carrier-frequency choice results in an asymmetric use of water-filling band frequencies around DC, which does not satisfy the PW criterion.[47] Thus, for the MMSE-DFE on a passband channel, the carrier frequency must be centered in the water-filling band and the symbol rate is chosen to be the measure of the resulting (postive-frequency for passband case) continuous-time water-filling band. Again, a gap $\Gamma > 0$ dB causes a slight decrease in the water-fill band's measure and will alter the carrier/center frequency slightly (unless the band is conjugate symmetric with respect to the choice of carrier/center frequency) along with the best symbol rate.

EXAMPLE 3.12.7 [V.34 Voiceband Modems] Chapter 4's multitone-like systems have come into wide use, so examples of optimized single-carrier systems are few. However, a historical and informative example of carrier/symbol-rate optimization from the last century is the voiceband modem. Voiceband modems once were heavily used for data transmission over the 4kHz-wide end-to-end channels that originally, at the dawn of telecommunications, carried analog voice signals. This application motivated and ignited modern data-transmission fundamentals. The pioneering voiceband modem designers did not yet comprehend that simplicity and utility of MT systems, seeing them instead as a theoretical abstraction based on

[47] Note Carrierless AMPM (CAP) systems of Chapter 1 do not use a carrier, but have a "center" frequency. The optimum center frequency equals the optimum carrier frequency in this subsection.

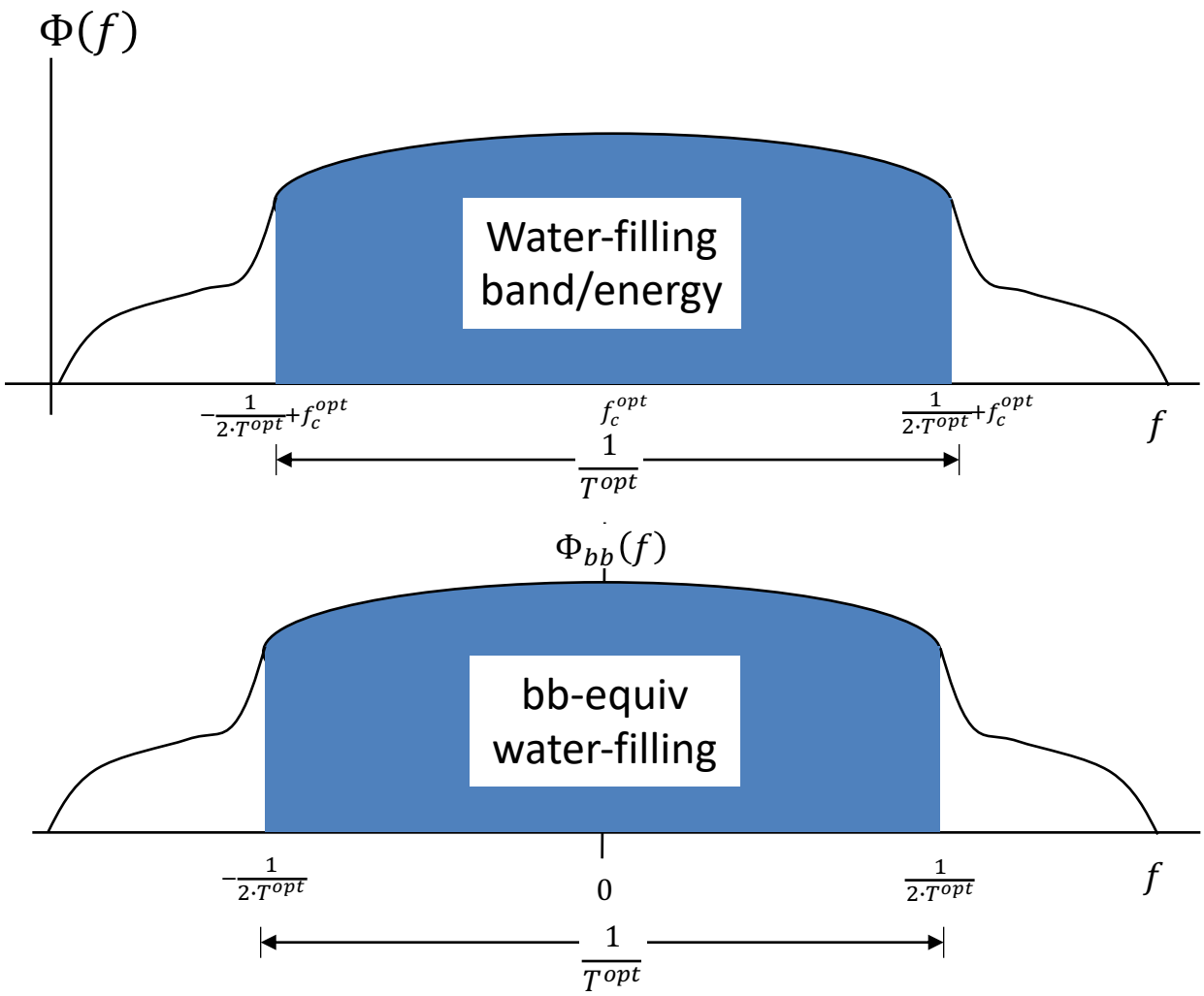

Figure 3.78: Illustration of water-filling and transmit optimization for ("complex") passband channel.

Shannon's early work in system bounds. Chapter 4 provides more information on the MT systems and their various forms of easy practical implementation.

An early International Telecommunications Union (ITU) standard was v.34 modem, better known as the "28.8 kbps" voiceband modem; this standard presumed use of optimized decision feedback equalization with variable symbol rates and carrier frequenciess. These older modems initially trained by using rudimentary MT transmission technology, specifically 25 equally spaced tones are sent with fixed amplitude and phase at the frequencies $n(150Hz)$ where $n = 1...25$. The frequencies 900, 1200, 1800, and 2400 are silenced, leaving 21 active tones for which the SNR's are measured (and interpolated for 900, 1200, 1800, and 2400) Water-filling or other spectrum-setting procedures determine an optimum bandwidth, that reduces to a choice of symbol rate and carrier frequency for QAM. The v.34 choices for symbol rate and carrier must be from the attached table:

$1/T^{opt}$	f_{c1}	f_{c2}
2400	1600	1800
2743	1646	1829
2800	1680	1867
3000	1800	2000
3200	1829	1920
3429	1959	1959

The receiver communicated its v.34 choice through a reverse control channel present as the system initializes. The receiver may only select from the table's symbol rates; the receiver then selects one of two carrier frequencies that correspond to the selected symbol rate. V.34 does not permit the choice of more than one disjoint waterfilling band. This is because examination of the choices with respect to optimum has revealed a loss of less than 1 dB. (Voiceband modems rarely needed $M > 1$). This special case of a single band being sufficient does not usually extend to other wireline applications, see Chapter 4. However, the variability of symbol rate and carrier frequency allowed these systems to double previous data rates with respect to earlier voiceband modem systems that simply fixed a single carrier and symbol rate.

3.12.6 The general multiple band case and the Optimum MMSE-DFE

Examples 3.74 and 3.78 are overly simple in that a single continuous transmission band is optimum. On ISI channels that exhibit notches (i.e., multipath fading or bridged-taps, multiple antennas, etc.) and/or band-selective noise (crosstalk, RF noise, etc.), Ω^{opt} may consist of many bands. This subsection addresses these more practical cases to find a minimal set of MMSE-DFEs that can be analyzed as a single system.

Practical ISI-channels often have waterfilling solutions that consist of a countable number of bandpass (and perhaps one lowpass) water-fill frequency bands, which have nonzero transmit energy over each band's continuous set of frequencies. To satisfy the PW criterion, the MMSE-DFE then must become multiple MMSE-DFE's, each with its own independent waterfilling-band solution. Figure 3.79 illustrates this situation for 3 disjoint water-fill regions. Correspondingly, there would be 3 MMSE-DFE's, each operating at an $SNR_{MMSE-DFE,U}$ and data rate R_i.

An optimum multi-band symbol rate sums the individual bands' optimum symbol rates and is

$$\frac{1}{T^{opt}} \triangleq \sum_{i=1}^{M} \frac{1}{\bar{T}_i^{opt}} \quad , \tag{3.712}$$

where $\bar{T}_i^{opt} = (1 \text{ or } 2) \cdot T_i^{opt}$ for complex passband or real baseband respectively. The SNR in each band

is $SNR_i(T_i^{opt})$. Each band has data rate

$$R_i = \frac{1}{\bar{T}_i^{opt}} \cdot \log_2 \left(1 + \frac{SNR_i(T_i^{opt})}{\Gamma} \right) \quad . \tag{3.713}$$

Then, the overall data rate is in bits per second is

$$\begin{aligned}
R &= \sum_{i=1}^{M} R_i & (3.714)\\
&= \sum_{i=1}^{M} R_i = \sum_{i=1}^{M} \frac{1}{\bar{T}_i^{opt}} \cdot \log_2 \left(1 + \frac{SNR_i(T_i^{opt})}{\Gamma} \right) & (3.715)\\
&= \frac{T^{opt}}{T^{opt}} \log_2 \prod_{i=1}^{M} \left(1 + \frac{SNR_i(T_i^{opt})}{\Gamma} \right)^{1/\bar{T}_i^{opt}} & (3.716)\\
&= \frac{1}{T^{opt}} \log_2 \prod_{i=1}^{M} \left(1 + \frac{SNR_i(T_i^{opt})}{\Gamma} \right)^{T^{opt}/\bar{T}_i^{opt}} & (3.717)\\
&= \frac{1}{T^{opt}} \log_2 \left(1 + \frac{SNR_{MMSE-DFE,U}^{opt}(T^{opt})}{\Gamma} \right) & (3.718)\\
&= \frac{b^{opt}}{T^{opt}} \quad , & (3.719)
\end{aligned}$$

where

$$SNR_{MMSE-DFE,U}^{opt} \triangleq \Gamma \cdot \left\{ \left[\prod_{i=1}^{M} \left(1 + \frac{SNR_i(T_i^{opt})}{\Gamma} \right)^{T^{opt}/\bar{T}_i^{opt}} \right] - 1 \right\} \tag{3.720}$$

and

$$\bar{b}^{opt} \triangleq \frac{1}{2} \cdot \log_2 \left(1 + \frac{SNR_{MMSE-DFE,U}^{opt}}{\Gamma} \right) \quad \text{bits/dimension} \quad . \tag{3.721}$$

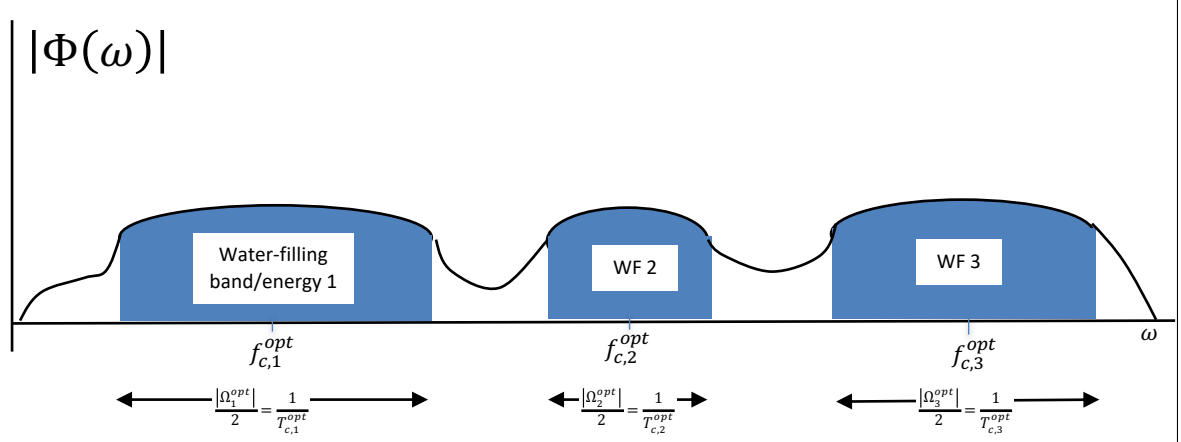

Figure 3.79: Illustration water-filling transmit optimization for more than one passband.

When all symbol rates and carrier frequencies are optimal, clearly this SNR is equivalent to Subsection 3.12.2's MT system because the rates/capacities for each water-filling band are the same. However, the

MMSE-DFE now is often many MMSE-DFE's, and each has a distinct variable carrier frequency and symbol rate. Readers should not misinterpret the CDEF result to mean that a "single-carrier system performs the same as a multi-carrier system" – misquoting the CDEF result. Such a statement is only true in the simplest cases where a single water-fill band is optimum, and the symbol rate and carrier frequencies have been precisely chosen as a function of the specific channel's water-filling solution and coding gap. Otherwise, multicarrier will outperform single carrier – and further, single carrier can never outperform multicarrier (with codes of the same gap Γ). Chapter 4 develops more sophisticated DMT systems for realistic MT implementation.

Lemma 3.12.1 [The Optimum MMSE-DFE] *The optimum MMSE-DFE is a set of M independent DFE's with M equal to the number of disjoint water-filling bands. Each of the MMSE-DFE's must have a symbol rate equal to the measure of a continuous water-fill band $1/T_m^{opt} = |\Omega_m^{opt}|$ and a carrier frequency where appropriate set exactly in the middle of this band ($f_{c,m} = [f_{max,m} + f_{min,m}/2]\ \forall\ m = 1, ..., M$). The number of bits per dimension for each such MMSE-DFE is*

$$\bar{b}_m = \frac{1}{2} \cdot \log_2 \left(1 + \frac{SNR_m(T_m^{opt})}{\Gamma} \right) \quad . \tag{3.722}$$

The overall SNR is provided in (3.720) and the (3.721). **Proof:** *See preceding paragraphs.***QED.**

A final simplified VDSL example provided to illustrate both proper design and a performance loss that might be incurred when designers try "to simplify" by only using one fixed band.

EXAMPLE 3.12.8 [Simple Lost "Dead" Bands] Figure 3.80 illustrates equivalent transmitters based on a simplistic variation of Chapter 2's multitone design, which has 8 equal-bandwidth modulators[48]. All tones carry passband uncoded QAM with gap $\Gamma = 8.8$ dB (so design $P_e = 10^{-6}$). This system choses symbol rates to approximate what might happen on a notched channel that might correspond to multipath ISI. The two band's transmit filters have labels A for the lower frequencies and B for the higher frequencies. The table below provides channel gains g_n's within these example subchannels. This channel's gains cause waterfill design to use only 6 of the 8 tones or QAM systems. Set A's 4 tones are adjacent while Set B's 2 tones are also adjacent. Sets A and B, however, are separated by an unused band. That unused band might be for example by notching from a second reflected and delayed channel path, or alternately a noise-equivalent channel's narrowband ("colored") radio-interference. Figure 3.81 shows the corresponding two MMSE-DFE receivers.

Application of waterfilling with 11 units of energy produces that table's energies for a Gap of $\Gamma = 8.8$ dB and a water-filling level of 2:

n	g_n	$\mathcal{E}_n$	b_n
1	15.2	1.50	2
2	30.3	1.75	3
3	121.4	1.9375	5
4	242.7	1.97	6
5	2	0	0
6	60.7	1.875	4
7	242.7	1.97	6
8	2	0	0

[48] Chapter 4 addresses implementation details that include that it is not practical to adjoin without some frequency separation the tones.

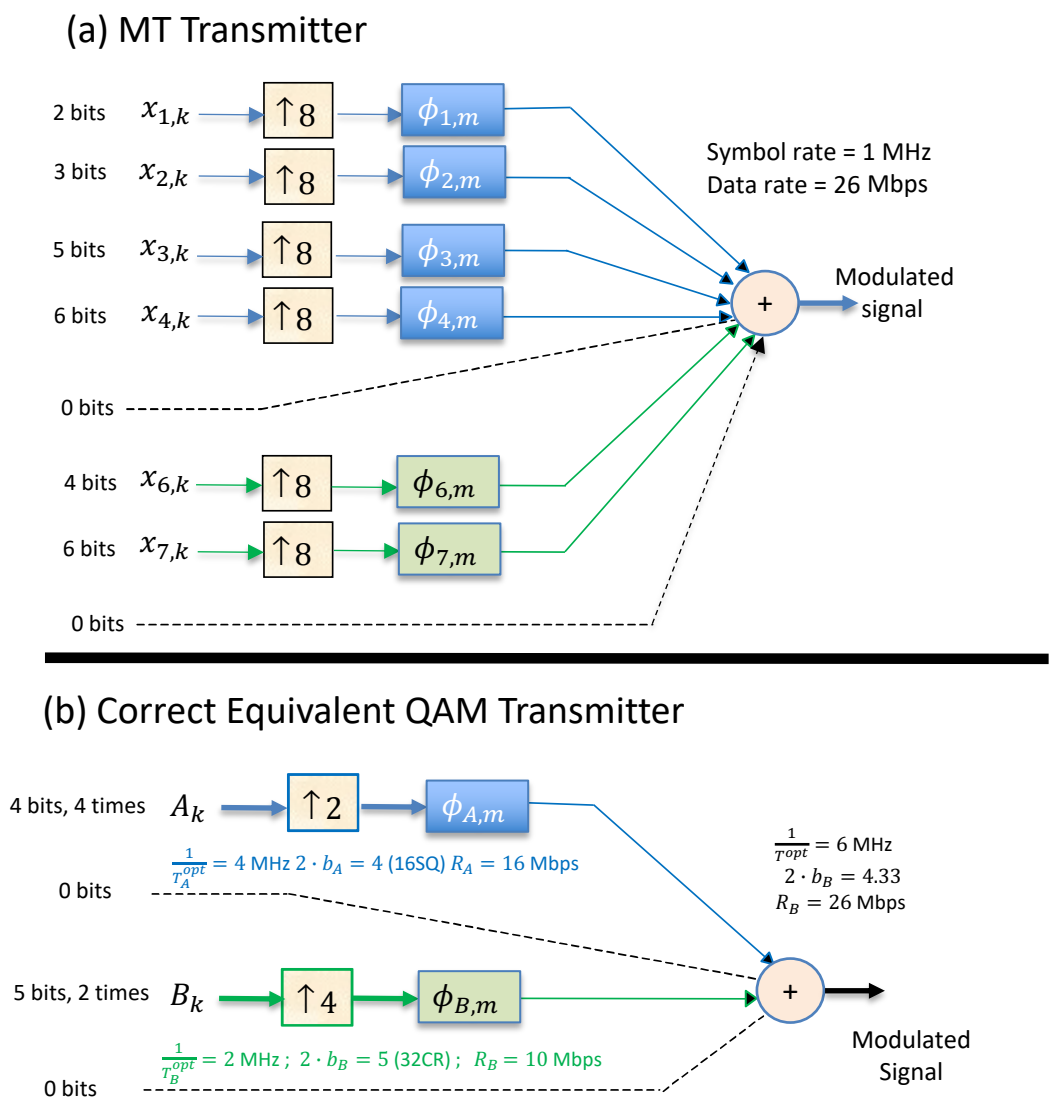

Figure 3.80: Simplified VDSL example multitone and equivalent 2-channel transmitters.

Comparison of 8-tone and 2-tone designs: Figure 3.80(a)'s set-A tones can carry $(2 \cdot \bar{b}_n =)$ 2, 3, 5, and 6 bits respectively corresponding to increasing signal-to-noise ratios in the corresponding channel, while set-B's two tones can carry 4 and 6 bits respectively. Again, this design uses $\Gamma = 8.8$ dB. The unused tones carry 0 bits. Set A's average number of bits per tone is 4 while Set B's average number is 5 bits/tone. If each subchannel's symbol rate is 1 MHz, then the data rate is (2+3+5+6+4+6) bits transmitted one million times per second for a total data rate of 26 Mbps. Equivalently, from Equation (3.712), the overall symbol rate is $1/T^{opt} = 6$ MHz, and there are thus $\bar{b}(1/T^{opt} = 6\text{MHz}) = \frac{26 \text{ Mbps}}{2(1/T^{opt})} = 26/[2(6)] = 2.16$ bits/dim or an average 4.33 bits per equivalent tone. Each of the individual tones could be viewed as the equivalent of a DFE system if there were ISI on the individual tones' channels. Or, these 8 channels could be sufficiently narrow that there is no ISI on any, and a simple QAM detector is ML for each without need for a DFE. In either case, Figure 3.81(a) shows

such an 8-receiver group. Both the 8-tone design and the 2-tone MMSE-DFE design have the same gap-reduced capacity, which relates to a set of (8 or 2) MMSE-DFE designs according to the CDEF result.

Yet another equivalent view measures data rate over the total 8 MHz bandwidth and has $\bar{b}(1/T' = 8\text{MHz}) = 26/16 = 1.625$. The SNR at this new symbol rate of $1/T = 8$ MHz follows from the CDEF result for an aggregate of MMSE-DFE's as

$$SNR_{mt}(1/T' = 8\text{MHz}) = 10 \cdot \log_{10} \left\{ \Gamma \cdot \left[2^{2(1.625)} - 1 \right] \right\} = 18.1\text{dB} \quad . \tag{3.723}$$

The SNR at a symbol rate of $1/T^{opt} = 6$ MHz is

$$SNR^{opt}_{MMSE-DFE,U}(1/T* = 6\text{MHz}) = 10 \cdot \log_{10} \Gamma \cdot \left(2^{4.33} - 1\right) = 21.6\text{dB} \tag{3.724}$$

The two SNRs are different because the symbol rates are different, but both correspond to a $P_e = 10^{-6}$ at the data rate of 26 Mbps with gap 8.8 dB (same code) and $P_e = 10^{-6}$.

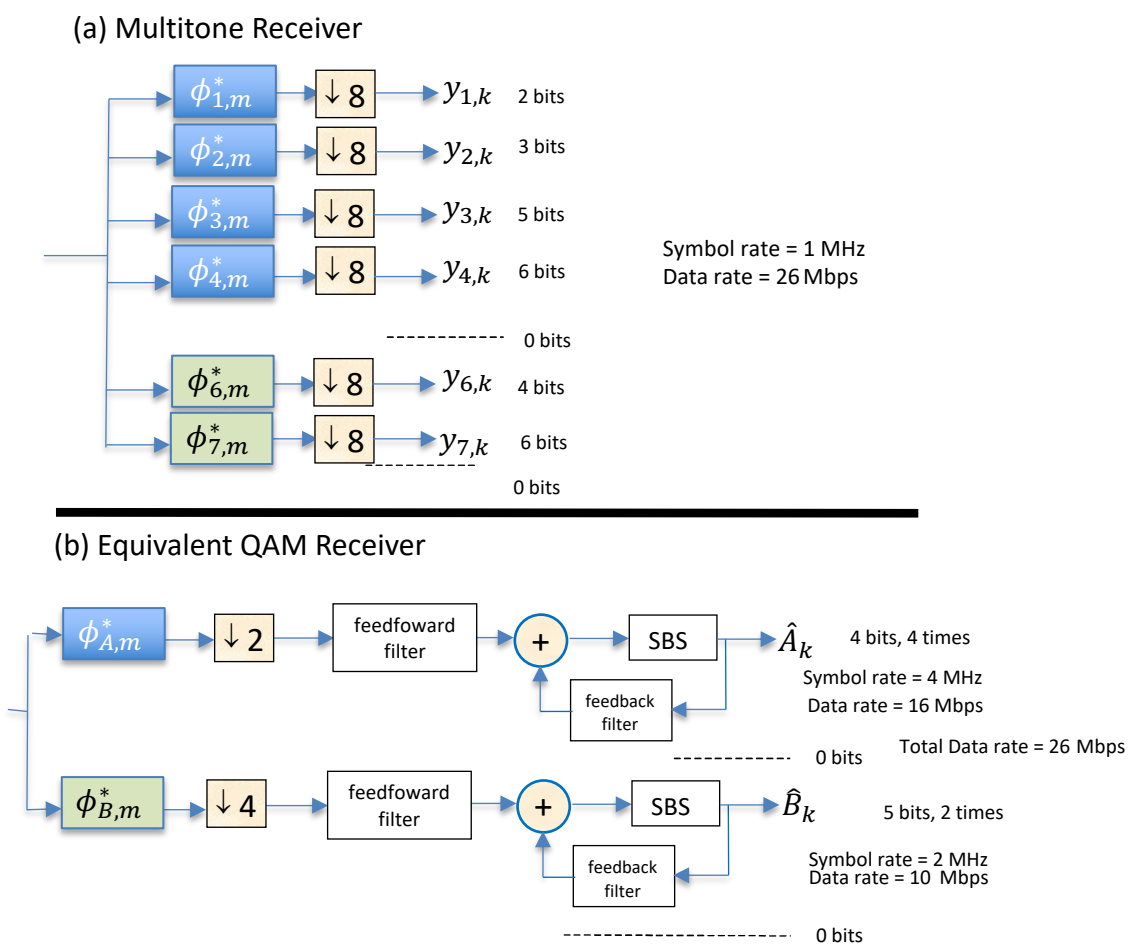

Figure 3.81: Simplified VDSL example multi-tone and equivalent 2-channel receivers.

Further examination of the two-DFE QAM Design: The corresponding best QAM receiver uses the same energized bands and is actually 2 QAM systems, very similar to the

two-tone MT system except now the DFE is more explicit, as per Figure 3.81(b). System A has a symbol rate of $1/T_1^{opt} = 4$ MHz and carries 4 bits per QAM symbol (16 QAM) for a data rate of 16 Mbps. By the CDEF result, the MMSE-DFE receiver has an SNR of $SNR_{dfe,1}(1/T_1^{opt} = 4\text{MHz}) = \Gamma \cdot (2^4 - 1)$=20.6 dB. System B has symbol rate $1/T_2^{opt} = 2$ MHz, and 5 bits per QAM symbol, which corresponds to 10 Mbps and $SNR_{dfe,2}(1/T_2^{opt} = 2\text{MHz}) = \Gamma \cdot (2^5 - 1)$=23.7 dB. The total data rate of 26 Mbps is the same as the first design's MT system. The two systems (DMT or two-tone QAM) carry the same data rate of 26 Mbps with a $P_e = 10^{-6}$. The key here for the same data rate and performance is the use of the same transmit spectra on both designs.

Correct design thus finds a 2-band equivalent of the original 8-tone MT system, but absolutely depends on the use of the 2 separate QAM signals in the lower portions of Figures 3.80 and 3.81.

3rd Design - single-tone QAM designer's paradox: Some designers might instead desire to see the loss of the single-band DFE system. The single-band (with $1/T = 8$ MHz) QAM system with MMSE-DFE then uses $2\bar{\mathcal{E}}_{\boldsymbol{x}} = 11/8 = 1.375$ at all frequencies and thus has

$$SNR_{dfe,flat} = \Gamma \cdot \left\{ \left[\prod_{n=1}^{8} \left(1 + \frac{1.375 \cdot g_n}{\Gamma} \right) \right]^{1/8} - 1 \right\} \tag{3.725}$$

$$= 17\text{dB} \tag{3.726}$$

which is about 1.1 dB below the multitone result. If Tomlinson Precoding was used at the $\bar{b} = 1.625$, the loss is another .4 dB, so this is about 1.5 dB below the MT result in practice. This $1/T = 8$ MHz single-tone QAM does then perform below best design because two separate QAM/DFE systems are required to match MT performance; one is simply insufficient on this channel. Use of a band-reject transmit filter might attempt to approximate the best transmit spectra, but would with the channel create very large intersymbol interference, requiring a very complex DFE structure, which inevitably would still miss best performance. Further it would have any miss magnified by the gap, as was evident in the half-band example's discussion above. Chapter 5's "circulant DFE (CDFE)" will essentially show how to implement such a filter-transmit system, but also shows better designs that are less complex and gain the same performance.

Channel variation: Systems in practice often hope that the loss to a single band is "small enough" that simple flat energy transmission at one symbol rate is sufficient. To examine this, such a flat-transmit-band now faces a more severely attenuated channel for which the upper frequencies are more greatly attenuated and $g_6 = g_7 \leq 2$, essentially zeroing Band B's water-fill energy. The first 8-band system might attempt 16 Mbps data rate. However, such a system could reload the 1.875+1.97 units of energy on tones 6 and 7 to the lower-frequency tones, and the new SNR_{mt} will be 22.5 dB, which is a margin of 1 dB with respect to 16 Mbps ($2\bar{b} = 2$ requires 21.5 dB). A new computation of the single-tone ($1/T = 8$ MHz) SNR according to (3.725), which now has only 4 terms in the product provides $SNR_{DFE}(1/T = 8\text{MHz}) = 12.8$ dB that is nearly 10 dB loss or corresponds to a lower data rate of 8 Mbps with 4QAM. The optimum-spectrum system is much dB better. Furthermore, precoder loss for 4QAM would be 1.3 dB for a Tomlinson or Laroia precoder, leading to yet more degradation. Thus the single band system always has some loss (at least error propagation or precoder loss) and the amount of loss increases with the inaccuracy of the symbol-rate with respect to best symbol rate, and with the gap as in Figure 3.77.

Since the QAM system's margin is negative (or needs lower data rate) on the more severely attenuated channel, a practicing engineer might "design for the worst-case" channel, which means a better symbol rate choice would be 4 MHz. In this case, on the channel, both 4-tones

and 1 tone at 16 Mbps would have the SNR of the A band, 22.5 dB and a margin of 1 dB at $P_e = 10^{-6}$ with $\Gamma = 8.8$ dB. However, if the short line with bands A AND ALSO B now restores, the 4 MHz-worst-case-designed QAM system will remain at at 16 Mbps, while the channel could support about 60% higher data rate.

As the used-bandwidth error grows, the of a single-band DFE loss increases. Used bandwidth ratios can easily vary by a factor of 10 on different channels, increasing the deviation (but not easily depicted with a few tones) between MT systems and DFE systems that use a fixed bandwidth (or single tone). For instance, if only tone 4 were able to carry data, then the best rate-adaptive solution is about 8.5 Mbps, while the full-band single-QAM DFE would attain only 420 kbps.

For real channels with large numbers of narrow tones, independent test laboratories hosted a "VDSL" Olympics in 2003 for comparing MT systems with variable-symbol-rate QAM systems. The test laboratories were neutral and wanted to ascertain whether a single-carrier system (so only one contiguous band that could be optimized and placed anywhere) really could "get the same performance as MT" – an abuse of the CDEF result then misunderstood and promulgated by single-carrier proponents). The results and channels appear in Figures 3.82 and 3.83 respectively. Clearly these fixed-margin (6 dB) tests for length of copper twisted pair at the data rate shown indicate that over a wider range of difficult channels as in DSL, the differences between DMT and single-carrier can be quite large. Generally speaking, the more difficult the channel, the greater the difference. These MT systems used a discrete multitone or DMT as in Chapter 4.

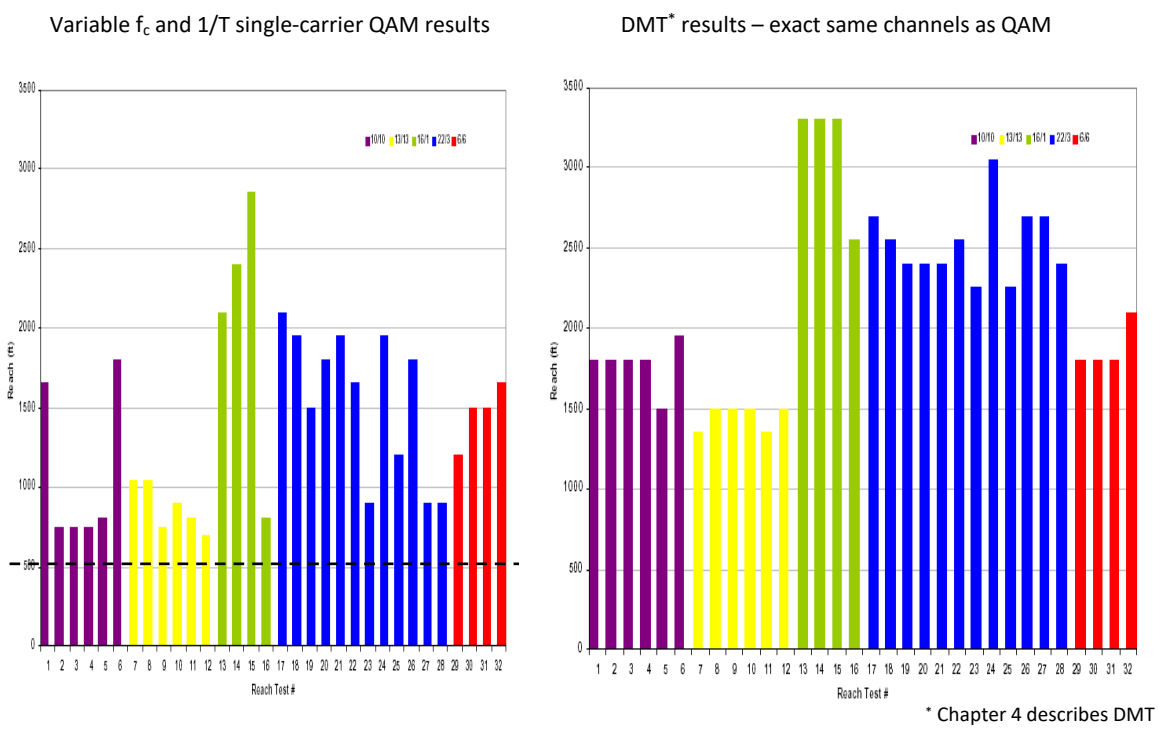

Figure 3.82: Illustration of 2003 VDSL Olympics results.

This section has shown that proper optimization of the MMSE-DFE may lead to several MMSE-DFEs on channels with severe ISI, but that with such a minimum-size set, and properly optimized symbol rate and carrier frequency for the corresponding transmitter of each such MMSE-DFE, determines a canonical transmission system, then matching the MT system.

Config	Test	Service (Mbit/s) (Down/Up)	Reach (ft)
1	1	10/10	1800
2	2	10/10	1800
	3	10/10	1800
	4	10/10	1800
	5	10/10	1500
3	6	10/10	1950
4	7	13/13	1350
	8	13/13	1500
5	9	13/13	1500
6	10	13/13	1500
7	11	13/13	1350
	12	13/13	1500
8	13	16/1	3300
	14	16/1	3300
9	15	16/1	3300
	16	16/1	2550
10	17	22/3	2700
	18	22/3	2550
	19	22/3	2400
	20	22/3	2400
	21	22/3	2400
11	22	22/3	2550
	23	22/3	2250
12	24	22/3	3150
	25	22/3	2250
	26	22/3	2700
13	27	22/3	2700
	28	22/3	2400
14	29	6/6	1800
	30	6/6	1800
	31	6/6	1800
15	32	6/6	2100

Figure 3.83: Channel types and speeds for 2003 VDSL Olympics.

3.12.7 Relations between Zero-Forcing and MMSE DFE receivers

In some special situations, the ZF-DFE and the MMSE-DFE can induce the same equivalent channel, although the performance will not be the same. Some caution needs to be exercised for equivalent channels. Some authors [49] have made some serious errors in interpreting results like CDEF for the ZF-DFE.

[49] One somewhat incorrectly derived result is due to MIT's Professor Robert Price in early 70's where he tacitly assumed zero noise, and then water-filling uses the entire band of transmission. Thus Price accidentally considered only one transmission band that was the entire band. Of course, trivially, ZF and MMSE are the same when there is no noise – this is hardly surprising, and Price erroneously arrived at a result resembling CDFE that is correct only when there is zero noise. This is sometimes referred to as "Price's result," but it is clearly Price at the time did not understand his small-equal-zero noise assumption would completely miss the important need for realizable filters.

Theorem 3.12.2 [CDEF Derivative] Over any of the continuous energized water-filling bands, *if the used spectra are waterfill, then the ZF-DFE and MMSE-DFE produce the same channel shaping before bias removal.*

proof: This proof uses continuous time/frequency, presuming the condition for choice of optimum sampling rate(s) and carrier frequencies have already been made so that these bands energize all frequencies within them (except possibly for countable set of infinitesimally narrow notches) and so satisfy the PW criterion. An ISI channel's input power spectrum, for which the symbol/sampling rate exactly matches to one (any) water-filling band $1/T^{opt}$, must satisfy

$$\bar{\mathcal{E}}_{\boldsymbol{x}} \cdot |\Phi(\omega)|^2 + \frac{\sigma^2}{|\tilde{H}(\omega)|^2} = K \tag{3.727}$$

for all frequencies ω in the band (zeros are only allowed at infinitesimally narrow notch points, so earlier resampling may have necessarily occurred to avoid singularity). $\tilde{H}$ represents the equivalent-white-noise channel $\tilde{H}(\omega) = \frac{H(\omega)}{\sqrt{\bar{S}_n(\omega)}}$. The MMSE-DFE fundamentally has canonical factorization with Fourier Transform

$$\bar{\mathcal{E}}_{\boldsymbol{x}} \cdot |\Phi(\omega)|^2 \cdot |\tilde{H}(\omega)|^2 + 1 = \frac{\gamma_0}{\|\tilde{h}\|^2} \cdot |G(\omega)|^2 \quad . \tag{3.728}$$

Insertion of (3.727) into (3.728) yields

$$K \cdot |\tilde{H}(\omega)|^2 = \frac{\gamma_0}{\|\tilde{h}\|^2} \cdot |G(\omega)|^2 \quad , \tag{3.729}$$

illustrating a very unusual event that the overall equivalent equalized channel has the same shape as the channel itself. This happens when the input is water-filling. Thus, since the shape of H and G are the same, they differ only by an all-pass (phase-only) filter. Equivalently, the receiver's MS-WMF is essentially Φ^{opt} times an all-pass filter. Such an all-pass can be implemented at the transmitter without increasing the transmit energy, leaving only the filter $\bar{S}_n^{-1/2} \cdot \Phi^{opt}$ in the receiver. Such an all-pass phase shift never changes the DFE performance (or any infinite-length equalizer). The receiver's remaining noise whitening filter and matched-filter-to-transmit-water-fill filter constitute the entire MS-WMF, perhaps resulting in an opportunity to reduce receiver complexity. The MMSE-DFE has slightly non-unity gain through the feed-forward filter and the overall channel gain is $\frac{SNR_{MMSE-DFE,U}}{SNR_{MMSE-DFE,U}+1}$, which the receiver removes with anti-bias scaling. However, ignoring the bias removal and consequent effect on signal and error sequence, water-filling creates an equivalent overall channel that has the same shaping of signal as the original channel would have had. That is the MS-WMF-output signal (ignoring bias in error) has the same minimum-phase equivalent ISI as the original channel would have, or equivalently as a ZF-DFE would have generated. **QED.**

The MMSE-DFE however does have a lower MMSE and better SNR, even after bias removal. The difference in SNR is solely a function of the error signal and scaling. The ZF-DFE has white noise and no bias. The MMSE-DFE with water-filling has the same minimum-phase shaping, that is achieved by filtering the signal, reducing noise energy, but then ensuring that the error components (including bias) add in a way that the original channel reappears as a result of all the filtering.

The minimum-phase equivalent of the channel alone $\tilde{H}$ is equal to G via Equation (3.729). However $P_c(D)$, the canonical equivalent of the pulse response $\Phi \cdot H$ (which includes the water-filling shaping) is not the same unless water-filling shape is the special case of being flat. The precoder settings or equivalently unbiased feedback-section settings are not necessarily determined by G, but by G_u. G_u

differs from the minimum-phase channel equivalent.

Thus, the MMSE-DFE results in same equivalent channel as ZF-DFE under water-filling, but still performs slightly better unless water-filling is flat (essentially meaning the channel is flat). Often water-filling is very close to flat in practical situations or there is very little loss. Thus, it may be convenient to implement directly a ZF-DFE once the exact water-filling band of frequencies is known.

Theorem 3.12.3 [Worst-Case Noise Equivalence] Over any of the continuous bands for which the PW Criterion holds, *if the noise power spectral density is the worst possible choice that minimizes channel mutual information as with Chapter 2's worst-case noise, then ZF and MMSE are the same even if the noise is not zero.*

proof: Mutual information's minimization addresses

$$I = \frac{1}{2\pi} \int_{\Omega} \log_2 \left(1 + \frac{S_x(\omega) \cdot |H(\omega)|^2}{S_n(\omega)} \right) d\omega \tag{3.730}$$

with noise power constrained at

$$\sigma^2 = \frac{1}{2\pi} \int_{\Omega} S_n(\omega) \cdot d\omega \tag{3.731}$$

leads easily by differentiation with LaGrange (calculus of variations) constraint to the equation/solution

$$\frac{1}{S_x(\omega) \cdot |H(\omega)|^2 + S_n(\omega)} - \frac{1}{S_n(\omega)} = K \; \forall \; \omega \in \Omega \quad . \tag{3.732}$$

The magnitude of the MS-WMF with noise whitening included is

$$|FF|^2 = \frac{|H(\omega)|^2 \cdot \frac{S_x(\omega)}{\mathcal{E}_{\boldsymbol{x}}}}{S_n^2(\omega) \cdot \gamma_0^2 \cdot \|h\|^2 |G(\omega)|^2} \tag{3.733}$$

$$= \frac{|H(\omega)|^2 \cdot S_x(\omega)}{(S_x(\omega) \cdot |H(\omega)|^2 + S_n(\omega)) \cdot S_n(\omega)} \tag{3.734}$$

$$= \frac{1}{S_n(\omega)} - \frac{1}{S_x(\omega) \cdot |H(\omega)|^2 + S_n(\omega)} = -K \tag{3.735}$$

Thus, the MS-WMF section is exactly an all pass filter, meaning then ZF and MMSE-DFEs (the latter with bias-removal scaling) are the same. **QED.**

The generalization to MIMO follows Chapter 2's worst case noise and leads to

$$R_{\boldsymbol{nn}}^{-1}(\omega) - \left[R_{\boldsymbol{nn}}(\omega) + H(\omega) \cdot R_{\boldsymbol{xx}}(\omega) \cdot H^*(\omega) \right]^{-1} = S_{wcn}(\omega) \tag{3.736}$$

where $S_{wcn}(\omega)$ is (block) diagonal.

The above result holds for any input spectrum $S_x(\omega)$ (and clearly the worst-case noise may vary with this input spectrum choice). In particular, this result does hold for the water-filling spectrum also. It suggests that if the noise is chosen to be the worst possible spectrum (for a given power), receiver processing is unnecessary (as the all-pass could be implemented at the transmitter without loss and a precoder could also be used). Chapter 2 readers recognize this as a multiuser broadcast channel where receiver processing (over all the receivers) cannot occur. Worst-case noise (unlike water-filling transmit spectra) is not good – it means that receiver filtering is essentially useless.

3.12.8 Optimized Transmit Filter with Linear Equalization

Linear equalization is suboptimal and not canonical (on all but trivial channels), but an optimized transmit filter can be found nonetheless, and will improve MMSE-LE performance. Thus subsection develops that optimized transmit filter. The PWC must still apply to any optimized transmit filter, thus there is an associated optimum symbol rate(s) and carrier frequency(ies). For the LE case, the MMSE is revisited without the receiver matched-filter normalization to simplify the mathematical development[50]. Again the transmit-filter input data input isν_k with toutput x_k; this development assumes tacitly that the symbol rate(s) (and carrier frequency(ies) when complex passband) will be set to exactly match the derived optimized transmit filter. This subsumes all the previous development for MMSE-DFE where continuous time was initially assumed to position discrete time. All that will happen together here in one step because in view of previous subsections. Thus we will momentarily drop frequency, continuous ω or discrete $e^{-\jmath\omega T}$, from the frequency-transform notation.

The error signal will be

$$E = V - W \cdot Y \ , \tag{3.737}$$

where the MMSE-LE (including any matched filter an sampling) W in (3.737) is

$$W = R_{VY} \cdot R_{YY}^{-1} \ . \tag{3.738}$$

The channel output is

$$Y = H \cdot \Phi \cdot V + N \ \ . \tag{3.739}$$

The input/ouput cross-correlation is

$$R_{VY} = \bar{\mathcal{E}}_{\boldsymbol{x}} \cdot H \cdot \Phi \ \ , \tag{3.740}$$

while the channel output autocorelation is

$$R_{YY} = \bar{\mathcal{E}}_{\boldsymbol{x}} \cdot |H|^2 \cdot |\Phi|^2 + \frac{\mathcal{N}_0}{2} \ \ . \tag{3.741}$$

The MMSE power spectral density is (recalling that $SNR \triangleq \bar{\mathcal{E}}_{\boldsymbol{x}}/\sigma^2$)

$$\begin{aligned} R_{EE} &= \bar{\mathcal{E}}_{\boldsymbol{x}} - W \cdot R_{VY} && (3.742)\\ &= \bar{\mathcal{E}}_{\boldsymbol{x}} - \frac{\bar{\mathcal{E}}_{\boldsymbol{x}}^2 \cdot |H|^2 \cdot |\Phi|^2}{\bar{\mathcal{E}}_{\boldsymbol{x}} \cdot |H|^2 \cdot |\Phi|^2 + \frac{\mathcal{N}_0}{2}} && (3.743)\\ &= \frac{\bar{\mathcal{E}}_{\boldsymbol{x}}}{1 + SNR \cdot |H|^2 \cdot |\Phi|^2} && (3.744)\\ &= \frac{\frac{\mathcal{N}_0}{2}}{|H|^2 \cdot |\Phi|^2 + \frac{1}{SNR}} \ \ . && (3.745) \end{aligned}$$

The MMSE in (3.745) can be minimized over the squared magnitude of the input filter $|\Phi|^2 \geq 0$ subject to the energy (basis-function normalization) constraint:

$$\frac{1}{2\pi} \int |\Phi(\omega)|^2 d\omega = 1 \ \ . \tag{3.746}$$

[50]The normalization factor $\|h\|$ depends on the transmit filter to be optimized, so it is simpler to avoid that normalization in the development.

Calculus of variations with respect to the squared transmit spectrum $|\Phi|^2$ provides ($\lambda' = \lambda^{-1}$)

$$0 = \frac{-\frac{\mathcal{N}_0}{2} \cdot |H|^2}{\left(|H|^2 \cdot |\Phi|^2 + \frac{1}{SNR}\right)^2} + \lambda \tag{3.747}$$

$$\lambda' \cdot \frac{\mathcal{N}_0}{2} \cdot |H|^2 = \left(|H|^2 \cdot |\Phi|^2 + \frac{1}{SNR}\right)^2 \tag{3.748}$$

$$0 = |H|^4 \cdot |\Phi|^4 + \frac{2}{SNR} \cdot |H|^2 \cdot |\Phi|^2 + \frac{1}{SNR^2} - \lambda' \cdot \frac{\mathcal{N}_0}{2} \cdot |H|^2 \tag{3.749}$$

$$|\Phi|^2 = \frac{1}{|H|^2} \cdot \left[\sqrt{\lambda' \cdot \frac{\mathcal{N}_0}{2} \cdot |H|^2} - \frac{1}{SNR}\right] \tag{3.750}$$

$$= c \cdot |H| - \frac{1}{SNR \cdot |H|^2} \quad , \tag{3.751}$$

where the value of the Lagrange multiplier-related-constant c and the optimum symbol period T^{opt} are found from from the energy constraint in (3.746), along with the need for non-negative power spectral density, as

$$c = \left[\frac{\mathcal{N}_0}{2} \cdot \frac{T^{opt}}{2\pi} \int_{-\frac{2\pi}{T^{opt}}}^{\frac{2\pi}{T^{opt}}} |H(\omega)| \cdot d\omega\right]^{-1} \left[1 + \frac{T^{opt}}{2\pi \cdot SNR} \int_{-\frac{2\pi}{T^{opt}}}^{\frac{2\pi}{T^{opt}}} |H(\omega)|^2 d\omega\right] . \tag{3.752}$$

The optimized transmit filter has some interesting interpretations. Basically the optimum transmit filter shape is the difference between a scaled $1/|H|$ and $\frac{1}{SNR} \cdot |H|^2$ where the scale constant c is chosen so that the transmit filter has unit norm. Figure 3.84 also illustrates there is again an optimum symbol rate and carrier frequency (center frequency).

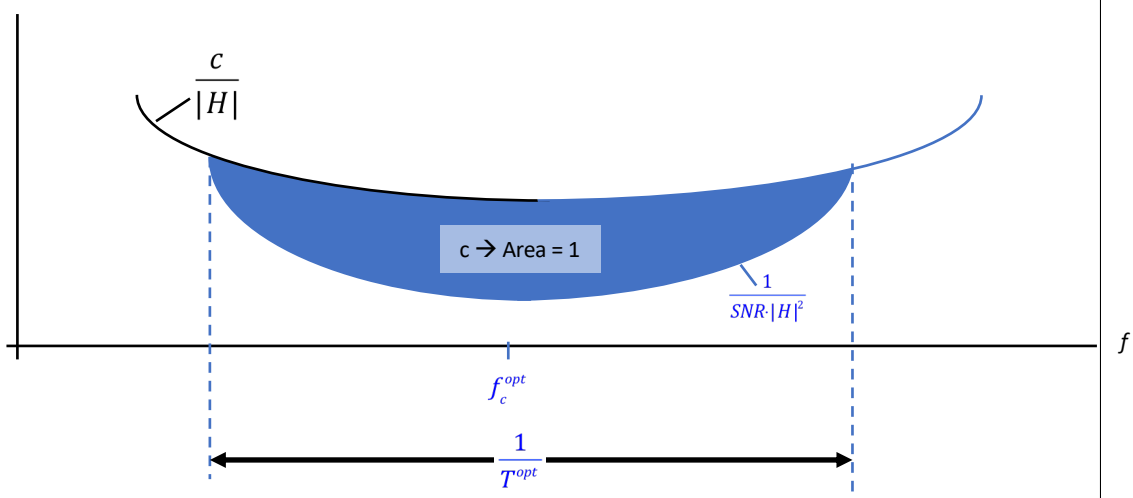

Figure 3.84: Illustration of optimum MMSE-LE transmit filter for the single-band case ("slush packing").

Slush Packing: This joint solution for c and T^{opt} partitions, for a particular initial guess of c, frequency into narrow MT spectra and computing (3.751) for each of these small tones or bands, then retaining and

sorting those with non-negative spectra and then summing (computing the integrals) them to test the power constraint. If too much power, then c is reduced and the process repeated until the first situation where c is exactly achieved. If too little power, then c is increased and the process repeated until the power constraint is met. The author has humorously referred to this process as "slush packing" instead of "water-filling" on numerous ocaissions. The idea being that slush ice (think "icee" for movie/carnival goers) can be molded as shown in Figure 3.84. There can of course be multiple bands when the sorting is undone, but only one band is shown in Figure 3.84. The optimized transmit energy band is clearly not water-filling, although it does tend to favor bands with higher channel gain and to avoid bands with low channel gain (essentially attempting to avoid large noise enhancement by inverting a poor band) in the MMSE-LE.

The corresponding power spectrum is

$$R_{EE} = \frac{\frac{\mathcal{N}_0}{2}}{|H|^2 \cdot |\Phi|^2 + \frac{1}{}SNR} \tag{3.753}$$

$$= \frac{\frac{\mathcal{N}_0}{2}}{c \cdot |H| - \frac{1}{SNR} + \frac{1}{SNR}} \tag{3.754}$$

$$= \frac{\frac{\mathcal{N}_0}{2}}{c \cdot |H|} \tag{3.755}$$

$$\left(\sigma^2_{MMSE-LE}\right)^{opt} = \frac{T^{opt} \cdot \frac{\mathcal{N}_0}{2}}{2\pi c} \int_{-\frac{2\pi}{T^{opt}}}^{\frac{2\pi}{T^{opt}}} \frac{d\omega}{|H(e^{-\jmath\omega T})|} \tag{3.756}$$

$$\left(\mathrm{SNR}_{MMSE-LE,U}\right)^{opt} = \frac{\bar{\mathcal{E}}_{\boldsymbol{x}}}{\left(\sigma^2_{MMSE-LE}\right)^{opt}} - 1 \quad , \tag{3.757}$$

which implies the channel-dependent noise enhancement with optimized transmit spectrum grows only as the square-root of the noise enhancement that occurred with fixed-transmitter MMSE-LE systems. The frequency-dependent SNR can also be found as

$$SNR(\omega) = SNR \cdot |H(\omega)| \cdot c - 1 \tag{3.758}$$

on those frequencies in the used optimum band (and zero elsewhere). The equalized channel output can be found as

$$W \cdot Y = \frac{c \cdot SNR \cdot |H| - 1}{c \cdot SNR \cdot |H|} \cdot V + W \cdot N \quad , \tag{3.759}$$

basically showing the input V with the MMSE bias well known at this point of this chapter and the filtered noise at each frequency going into the SBS detector.

For the zero-forcing case, the equalizer SNR tends to infinity, and the transmit filter becomes a scaled square-root pre-inverse of the channel H, essentially splitting the equalizer's channel inversion between the transmit filter and the receiver's MMSE-LE filter that also will be a scaled square-root inverse of the channel H. The symbol rate will be that corresponding to the measure of the frequency band between the two points shown in Figure 3.84 except that the lower curve will be the horizontal axis line (and the symbol rate is chosen to make the transmit basis-function filter unit norm).

Another situation of interest is when the the receiver has no ability to equalize, but the transmitter can alter the transmit filter. This case readily resolves into the MMSE-LE moving to the transmitter with a scaling constant that prevents transmit energy increase above the constraint (or equivalently the transmit filter has a scaled MMSE-LE shape where the scaling causes the filter to have unit norm).

Chapter 4 continues with a more complete discussion of many transmit-optimization forms, while Chapter 5 develops further the equivalent of finite-length transmit filter optimization in what is called **generalized decision feedback equalization (GDFE)**.

3.13 Equalization for Partial Response

Just as practical channels are often not ISI free, such channels are rarely equal to some desirable partial-response (or even controlled-ISI) polynomial. Thus, an equalizer may adjust the channel's shape to that of the desired partial-response polynomial. This equalizer then enables the receiver to use a partial-response sequence detector or a SBS detector on the equalizer's output (with partial-response precoder). Both detectors' performance is particularly sensitive to channel-estimation errors, and so equalization can be crucial to achieve the highest partial-response performance levels. This section introduces some equalization methods for partial-response signaling.

Chapter 8 studies sequence detection so terms related to it like MLSD (maximum likelihood sequence detection) and Viterbi detectors/algorithm are pertinent to readers already familiar with Chapter 8 contents. Otherwise these terms can be viewed simply as finite-real-time-complexity methods to implement a full maximum-likelihood detector for an ISI channel.

3.13.1 Controlled ISI with the DFE

Section 3.8.2 shows that a minimum-phase channel polynomial $H(D)$ may arise from a DFE feedback section. The polynomial $H(D)$ is often a good controlled intersymbol-interference model when $H(D)$ has finite degree ν. When $H(D)$ is of larger degree or infinite degree, the first ν coefficients of $H(D)$ form a controlled intersymbol-interference channel. Thus, a detector for a DFE 's linear filter output applies then to controlled ISI polynomial $H(D)$.

3.13.1.1 ZF-DFE and the Optimum Sequence Detector

Section 3.1 shows that the sampled outputs, y_k, of the receiver matched filter form a sufficient statistic for the underlying symbol sequence. Thus a maximum likelihood (or MAP) detector can optimally apply to the sequence y_k to detect the input symbol sequence x_k without performance loss. The ZF-DFE feedforward filter $1/(\eta_0 \cdot \|h\| \cdot H^*(D^{-*}))$ is causally invertible when $Q(D)$ is factorizable. Chapter 1's reversibility theorem then states that a maximum likelihood detector that processes this invertible ZF-DFE-feedforward filter's output optimally detects the sequence x_k. The feedforward filter output has D-transform

$$Z(D) = X(D) \cdot H(D) + N'(D) \quad . \tag{3.760}$$

The ZF-DFE's noise sequence n'_k is exactly white Gaussian, so the ZF-DFE produces an equivalent filtered AWGN channel $H(D)$. If $H(D)$ has finite degree $\nu < \infty$, then a maximum-likelihood[51] detector for the controlled-ISI polynomial $H(D)$ has finite real-time comlexity; this detector also has minimum error probability. Figure 3.85 shows such an optimum receiver.

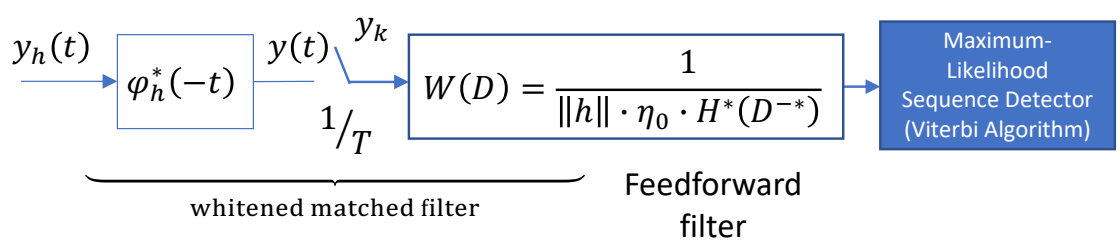

Figure 3.85: The partial response ZF equalizer, decomposed as the cascade of the WMF (the feedforward section of the ZF-DFE) and the desired partial response channel $B(D)$.

[51] The full transmit symbol sequence is a single codeword, which would nominally require infinite delay and complexity; Chapter 9 shows how to implement such a detector recursively with finite delay and finite-real-time complexity.

When $H(D)$ has larger degree than some desired ν determined by complexity constraints, then the first ν feedback taps of $H(D)$ determine

$$H'(D) = 1 + h_1 \cdot D^1 + ... + h_\nu \cdot D^\nu \quad , \tag{3.761}$$

a controlled-ISI channel.

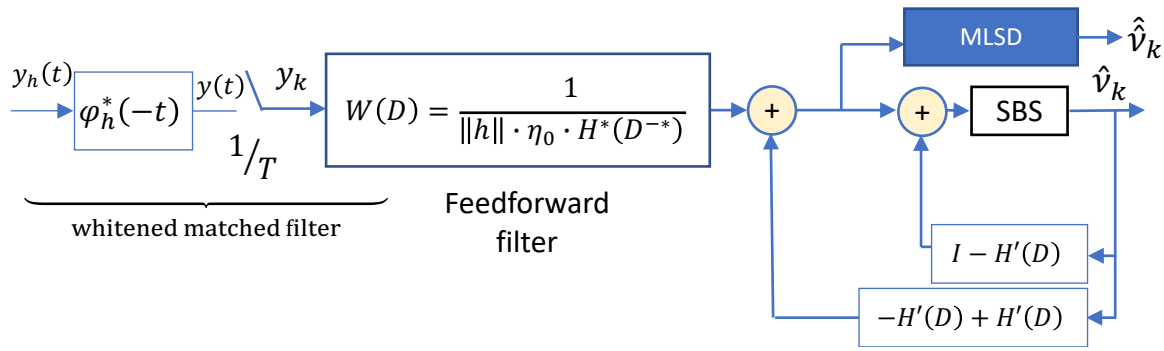

Figure 3.86: Limiting the number of states with ZF-DFE and MLSD.

Figure 3.86 illustrates the receiver's ZF-DFE and a corresponding maximum-likelihood sequence detector (MLSD). The second feedback section contains all the channel coefficients that are not used by the MLSD (see Chapter 8) detector. These coefficients have delay greater than ν. When this second feedback section has zero coefficients, then the configuration shown in Figure 3.86 is an optimum detector. When the additional feedback section is not zero, then this structure is intermediate in performance between optimum and the ZF-DFE with SBS detection. An SBS-modulo combination replaces the inner feedback section with transmitter precoding.

Increase of ν causes the minimum distance to increase, or at worst, remain the same. Thus, Figure 3.86's ZF-DFE with MLSD defines a series of increasingly complex receivers whose performance approach optimum as $\nu \to \infty$. A property of a minimum-phase $H(D)$ is that

$$\sum_{i=0}^{\nu'} |h_i|^2 = \|h'\|^2 \tag{3.762}$$

is maximum for all $\nu' \geq 0$. No other polynomial (that also preserves the AWGN at the feedforward filter output) can have greater energy. Thus the SNR of the signal entering the Viterbi Detector in Figure 3.86, $\frac{\bar{\mathcal{E}}_{\boldsymbol{x}} \|h'\|^2}{\frac{N_0}{2}}$, also increases SNR (nondecreasing) with ν. This SNR must be less than or equal to SNR_{MFB}.

3.13.1.2 MMSE-DFE and MLSD

An SBS-based receiver maximizes an unbiased detector's SNR (see Section 3.3), which leads to the MMSE-DFE. The receiver removes MMSE-induced bias to minimize SBS-detector error probability. Section 3.6. denotes the corresponding monic, causal, minimum-phase, and unbiased feedback polynomial $G_U(D)$. A sequence detector can use Figure 3.85's and/or Figure 3.86's structures with $H(D) \to G_U(D)$. For instance, Figure 3.88 is the same as Figure 3.86, with an unbiased MMSE-DFE's MS-WMF replacing the WMF of the ZF-DFE. A truncated version of $G_U(D)$ corresponding to $H'(D)$ is denoted $G'_U(D)$. The error sequence associated with the unbiased MMSE-DFE is not quite white, nor is it Gaussian. So, a sequence detector based on squared distance is not quite optimum, but it is nevertheless commonly used because the exact optimum detector could be much more complex (and probably not perform noticeably better). As ν increases, the error probability decreases from the unbiased MMSE-DFE's level,

$SNR_{MMSE-DFE,U}$ when $\nu = 0$, to that of the optimum detector when $\nu \to \infty$. The matched filter bound, as always, remains unchanged and is not necessarily obtained. However, minimum distance does increase with ν in the sequence detectors based on a increasing-degree series of $G_U(D)$. With non-trival codes, the detector complexity as well as the difficulty to compute d_{min} can be high. More often, a preferred approach uses the transmit-optimized MMSE-DFE structure, which largely separates decoder complexity of a good code from the receiver demodulation signal processing (although multiple feedback sections for different "survivor" input sequence possibilities may be necessary, see Chapter 8's iterative decoding methods).

3.13.2 Equalization with Fixed Partial Response $B(D)$

Section 3.6's MMSE-DFE derivations include the case where $B(D) \neq G'(D)$, which this subsection reuses.

3.13.2.1 The Partial Response Linear Equalization Case

In the linear equalizer case, the equalization error sequence becomes

$$E_{pr}(D) = B(D) \cdot X(D) - W(D) \cdot Y(D) \quad . \tag{3.763}$$

Section 3.6's theory first minimizes MSE for any $B(D)$ over the coefficients in $W(D)$. The corresponding solution set $\mathbb{E}\left[E_{pr}(D) \cdot y^*(D^{-1})\right] = 0$, to obtain

$$W(D) = B(D) \cdot \frac{\bar{R}_{xy}(D)}{\bar{R}_{yy}(D)} = \frac{B(D)}{\|h\| \cdot (Q(D) + 1/SNR_{MFB})} \quad , \tag{3.764}$$

which is just the MMSE-LE cascaded with $B(D)$.

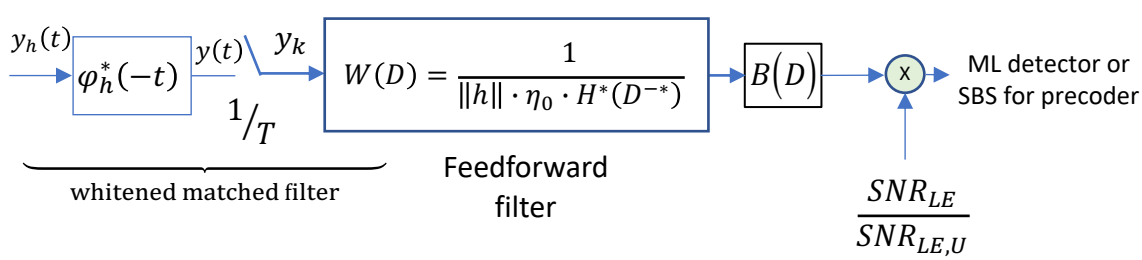

Figure 3.87: Partial-response linear equalization.

Figure 3.87 shows the MMSE-PREQ (MMSE - "Partial Response Equalizer"). This PREQ design realizes Section 3.5's MMSE-LE and follows it by a filter of the desired partial-response (or controlled-ISI) polynomial $B(D)$.[52] For this choice of $W(D)$, the error sequence is

$$E_{pr}(D) = B(D) \cdot X(D) - B(D) \cdot Z(D) = B(D) \cdot [E(D)] \tag{3.765}$$

where $E(D)$ is the MMSE-LE error sequence. From (3.765),

$$\bar{R}_{e_{pr},e_{pr}}(D) = B(D) \cdot \bar{R}_{ee}(D) \cdot B^*(D^{-1}) = \frac{B(D) \cdot \frac{\mathcal{N}_0}{2} \cdot B^*(D^{-1})}{\|h\|^2 \cdot (Q(D) + 1/SNR_{MFB})} \quad . \tag{3.766}$$

Thus, the MMSE for the PREQ is

$$\sigma^2_{MMSE-PREQ} = \frac{T}{2\pi} \int_{-\frac{\pi}{T}}^{\frac{\pi}{T}} \frac{|B(e^{-\jmath\omega T})|^2 \cdot \frac{\mathcal{N}_0}{2}}{\|h\|^2 \cdot (Q(e^{-\jmath\omega T}) + 1/SNR_{MFB})} d\omega \quad . \tag{3.767}$$

[52] This also follows from the linearity of the MMSE estimator.

The SBS detector is equivalent to subtracting $(B(D)-1)\cdot X(D)$ before detection based on decision regions determined by x_k. The $\text{SNR}_{\text{MMSE-PREQ}}$ becomes

$$\text{SNR}_{\text{MMSE-PREQ}} = \frac{\bar{\mathcal{E}}_{\boldsymbol{x}}}{\sigma^2_{MMSE-PREQ}} \quad . \tag{3.768}$$

This performance can be better or worse than the MMSE-LE, depending on the choice of $B(D)$; the designer usually selects $B(D)$ so that $\text{SNR}_{\text{MMSE-PREQ}} > \text{SNR}_{MMSE-LE}$. This receiver also has a bias, but it is usually ignored when (as often) $B(D)$ has integer coefficients – any bias removal could cause the coefficients to be noninteger. There is a consequent (hopefully small) performance loss.

The MMSE-PREQ's error sequence $E_{pr} = B(D)\cdot E(D)$ is not white noise sequence (nor is $E(D)$ for the MMSE-LE), so that Chapter 8's Viterbi Detector, when designed for AWGN on the channel $B(D)$, would not be the optimum detector for the MMSE-PREQ (even with scaling to remove bias). In this case, the ZF-PREQ, obtained by setting $SNR_{MFB}\to\infty$ in the above formulas, would also not have a white error sequence. Thus a linear equalizer for a partial response channel $B(D)$ that is followed by a Viterbi Detector designed for AWGN may not be very close to an optimum detection combination, unless the channel pulse response were already very close to $B(D)$, so that equalization was not initially necessary. While this is a seemingly simple observation made here, there are a number of systems proposed for use in disk-storage detection that overlook this basic observation, and do equalize to partial response, "color" the noise spectrum, and then use a WGN Viterbi Detector. The means by which to correct this situation is the PR-DFE of the next subsection.

3.13.2.2 The Partial-Response Decision Feedback Equalizer

If $B(D)\neq G(D)$ and the design of the detector mandates a partial-response channel with polynomial $B(D)$, then the optimal MMSE-PRDFE is shown in Figure

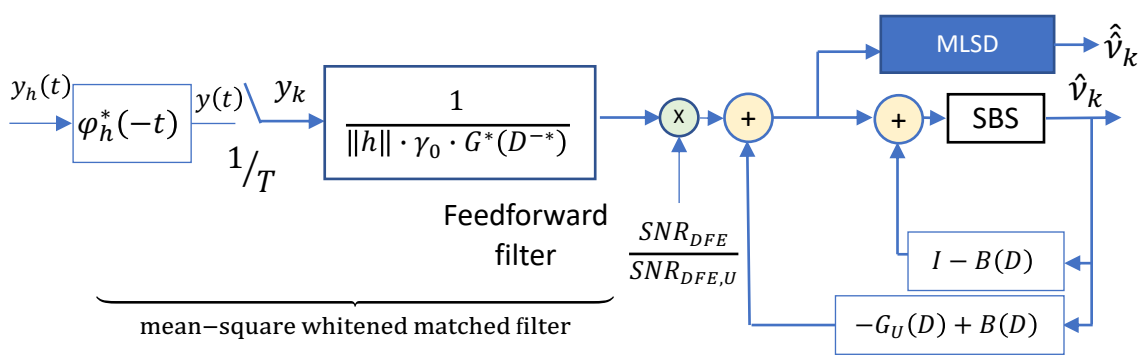

Figure 3.88: Partial-response DFE with $B(D)$.

For any feedback section $B(D)$ such that $G_U(D)=B(D)+\tilde{B}(D)$, with $\tilde{B}(D)$ the feedback-section error with respect to best feedback $G_U(D)$. The error sequence $E(D)$ is the same as that for the MMSE-DFE, and is therefore a white sequence. The signal between the the two feedback sections in Figure 3.88 is input to both the MLSD and the SBSl detectors. This partial-response DFE system processes on an SBS basis with transmit precoding (and also scaling is used to remove the bias - the scaling is again the same scaling as used in the MMSE-DFE), and $\tilde{B}_U(D)=G_U(D)-B_U(D)$, where

$$B_U(D) = \frac{SNR_{MMSE-DFE}}{SNR_{MMSE-DFE,U}}\cdot\left[B(D)-\frac{1}{SNR_{MMSE-DFE}}\right] \quad . \tag{3.769}$$

However, since the MMSE-PRDFE error sequence is white, and because the bias is usually small so that the error sequence in the unbiased case is also almost white, the designer can reasonably use an ML (Viterbi Sequence Detector) designed for $B(D)$ with white noise.

If the bias is negligible, then a ZF-PRDFE should be used, which is illustrated in Figure 3.86, and the filter settings are obtained by setting $SNR_{MFB} \to \infty$ in the above formulas.

3.14 Adaptive Vector Learning algorithms for linear channels

In practice, digital receivers that use equalizers, or linear combiners for MIMO, are usually adaptive. An adaptive equalizer automatically adjusts its internal settings (the values for $\boldsymbol{w}$ so as to realize the MMSE settings as closely as possible. Adaptive equalizers and/or linear combiners perform this self optimization by measuring their own performance and then recursively in time incrementing the vector settings so as to improve their average performance. They find use when the designer does not know the channel response, which prevents predesign of a precise linear filter, and/or that this channel response may vary with time or use.

Equalization and linear-combiners often use one of several adaptive algorithms . By far, the most commonly used is (a variant of) the well-known Widrow-Hoff (1960) LMS (Least Mean Square) algorithm [10], which is an example of the engineering use of what is known in statistics as a "stochastic-gradient" algorithm, see Robbins-Monro (1951) [11]. For numerical reasons, this algorithm is altered slightly in practice. Other algorithms in use are Lucky's Zero-Forcing algorithm (1966), Recursive Least-Squares methods (Godard), and frequency-domain algorithms.

3.14.1 The LMS algorithm for Adaptive Equalization

The Least Mean Square (LMS) algorithm is used with both $\boldsymbol{w}$ (LE or FF of DFE) and FB of DFE $\boldsymbol{b}$ (or $\boldsymbol{G}$ in Chapter 5's upcoming GDFEs) as slowly time-varying FIR filters. The adaptive filter includes any matched filtering and so samples at a rate sufficiently high (so twice the highest baseband-equivalent frequency). For instance, Section 3.6's fractionally spaced equalizers incorporate this sampling. The LMS algorithm attempts to minimize the MSE by incrementing the equalizer parameters in the direction of the MSE's negative gradient with respect to $\boldsymbol{w}$ (and also $\boldsymbol{b}$ or $\boldsymbol{G}$ for the DFE). This direction is the direction of steepest descent (or most MSE reduction). Recall the scalar MSE is $\mathbb{E}\left[|e_k|^2\right]$, so the adaptive algorithm updates the filter parameters $\boldsymbol{w}$ by

$$\boldsymbol{w}_{k+1} = \boldsymbol{w}_k - \frac{\mu}{2} \cdot \nabla_{\boldsymbol{w}_k} \mathbb{E}\left[|e_k|^2\right] \quad , \tag{3.770}$$

where $\nabla_{\boldsymbol{w}_k} \mathbb{E}\left[|e_k|^2\right]$ is the gradient of the MSE with respect to the filter coefficient vector $\boldsymbol{w}_k$. In practice, the channel statistics are not (exactly) known so that the gradient term,$\nabla_{\boldsymbol{w}_k} \mathbb{E}\left[|e_k|^2\right]$, in (3.770) is unknown. It is, instead, estimated by the **stochastic gradient** $\nabla_{\boldsymbol{w}_k} |e_k|^2$, which is implemented as

$$\nabla_{\boldsymbol{w}_k} |e_k|^2 = -2 \cdot e_k^* \cdot \boldsymbol{y}_k \tag{3.771}$$

where $\boldsymbol{y}_k$ is (again) the vector of inputs to the FIR filter(s) in the adaptive equalizer or linear combiner[53]. The LMS algorithm then becomes

$$e_k = x_k - \boldsymbol{w}_k^* \cdot \boldsymbol{y}_k \tag{3.772}$$

$$\boldsymbol{w}_{k+1} = \boldsymbol{w}_k + \mu \cdot e_k^* \cdot \boldsymbol{y}_k \quad . \tag{3.773}$$

There are a variety of proofs, under various mild assumptions and approximations, that the LMS algorithm converges to the MMSE settings if μ is sufficiently small and numerical precision is adequate. Thus the exact channel pulse response and noise statistics need not be known in advance. Usually, the input sequence x_k is known to the receiver for a short training time in advance of unknown data transmission, so that (3.772) can be computed in the receiver, and updating allowed. After training for a time period sufficient for the adaptive filter to converge, the known data sequence must be replaced by the decisions in the receiver for adaptation to continue with **decision directed** equalization.

For stable operation of the LMS adaptive algorithm, with N_{ff} feedforward taps and N_{fb} feedback taps,

$$0 \le \mu \le \frac{1}{N_{ff} \cdot \mathcal{E}_{\boldsymbol{y}} + N_{fb} \cdot \mathcal{E}_{\boldsymbol{x}}} \quad . \tag{3.774}$$

[53] Similarly, the algorithm could use $-2 \cdot e_k^* \cdot \boldsymbol{y}_k^{*t}$, which is the conjugate - both work because this term averages to zero in both cases when MSE is minimum.

Typically, the upper limit is avoided and the step-size μ is usually several orders of magnitude below the upper stability limit, to ensure good noise averaging and performance close to the MMSE level.

In practice, the LMS update must be implemented in finite-precision, and a variant of it, known as the Tap-Leakage Algorithm, or as Leaky LMS, must be used:

$$\boldsymbol{w}_{k+1} = \beta \cdot \boldsymbol{w}_k + \mu \cdot e_k^* \cdot \boldsymbol{y}_k \tag{3.775}$$

where β is close to, but slightly less than unity. This is equivalent to minimizing (via stochastic gradient) the sum of the MSE and $(1-\beta)\cdot\|\boldsymbol{w}_k\|^2$, thus preventing an arbitrary growth of $\boldsymbol{w}$ caused by accumulated round-off error in practical implementation. Essentially $1-\beta$ is a fixed Lagrange multiplier for a finite-norm-squared constraint on the filter.

3.14.1.1 Zero-Forcing Algorithm

A lesser used, but simpler, adaptive algorithm is the zero-forcing algorithm, which converges to the zero forcing solution. This algorithm follows by noting that the equalizer error, and the input data vector should be uncorrelated when the receiver has the zero-forcing setting. This algorithm is written

$$\boldsymbol{w}_{k+1} = \boldsymbol{w}_k + \mu \cdot e_k^* \cdot \boldsymbol{x}_k \tag{3.776}$$

where $\boldsymbol{x}_k$ is a vector of training (or decision-directed-estimated) data-symbol values. Integer/discrete symbol values simplify the (3.776)'s multiply implementation to addition and possible minor shifting, thus making the zero-forcing algorithm somewhat simpler than the LMS.[54] In practice, this simplification can be significant at very high-speeds, where multiplication can be difficult to implement cost effectively.

3.14.1.2 Signed LMS Algorithm

Perhaps, more common than the zero-forcing algorithm is the **signed LMS algorithm**

$$\boldsymbol{w}_{k+1} = \boldsymbol{w}_k + \mu \cdot e_k^* \cdot \operatorname{sgn}[\boldsymbol{y}_k] \tag{3.777}$$

where the sgn function eliminates the need for multiplication.

This algorithm also converges to the MMSE solution in practice, although usually more slowly than the LMS.

3.14.2 Vector-MIMO Generalization of LMS

When the error is a vector, LMS generalizes in the obvious way to (with $\tilde{\boldsymbol{W}} = [\boldsymbol{W} \;\; \boldsymbol{B}]$)

$$\boldsymbol{e}_k = \boldsymbol{x}_k - \tilde{\boldsymbol{W}}_k^* \cdot \boldsymbol{Y}_k \tag{3.778}$$

$$\tilde{\boldsymbol{W}}_{k+1} = \tilde{\boldsymbol{W}}_k + \mu \cdot \boldsymbol{e}_k^* \cdot \boldsymbol{Y}_k \quad . \tag{3.779}$$

Different μ values may apply to different dimensions (as well as for feedback and feedforward components within $\tilde{\boldsymbol{W}}$. The ZF and Signed LMS both also generalize in exactly the same way for the MIMO case.

[54] The step-size μ is usually implemented as a power of 2, and thus also corresponds only to minor shifting.

3.14.3 Gain-Estimation Training

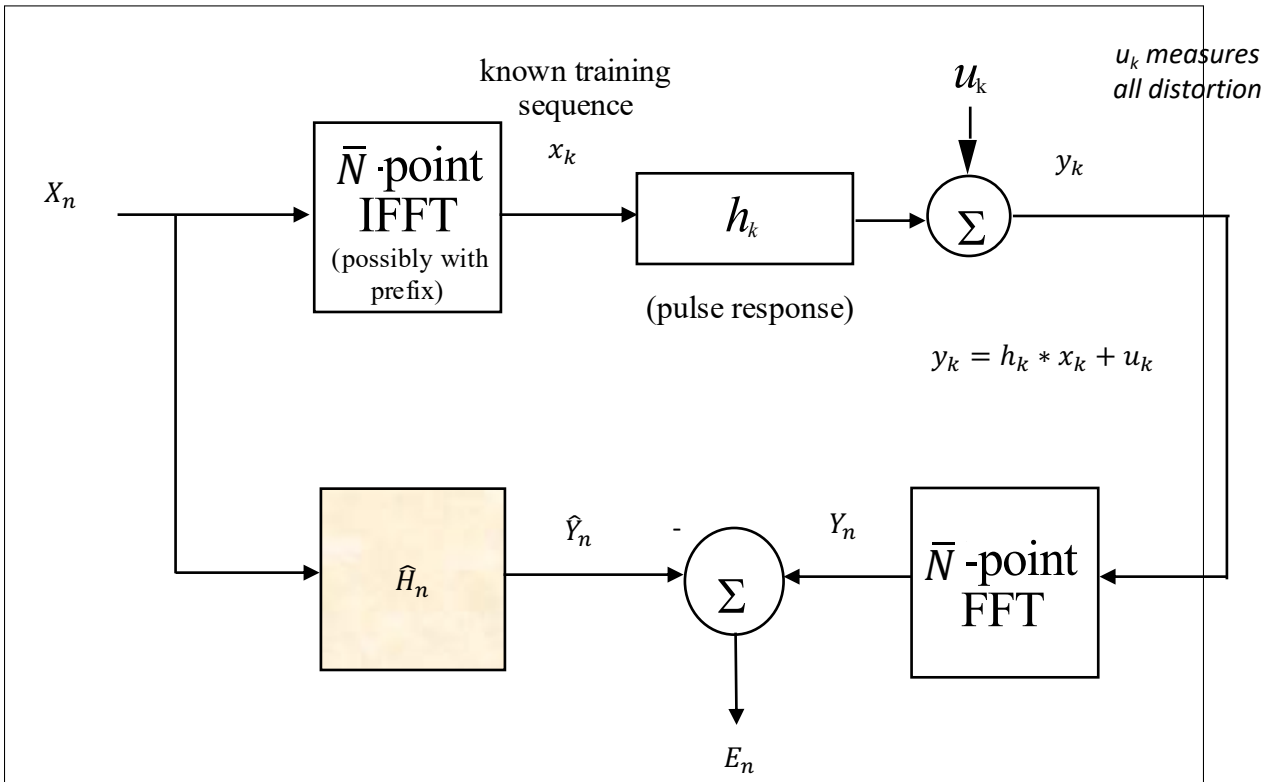

Figure 3.89: Channel-identification basics and terminology.

Figure 3.89 illustrates gain estimation during initialization. An initial known training sequence, x_k, is periodic with period $\bar{N}$ equal to[55] or greater than the number of significant coefficients in the unknown channel pulse response h_k ("periodic" can mean use of the cyclic prefix of Section 4.6). The channel output sequence is

$$y_k = x_k * h_k + u_k \tag{3.780}$$

where u_k is an additive noise signal assumed to be uncorrelated with x_k. The channel distortion sequence is denoted by u_k, instead of n_k, to avoid confusion of the frequency index n with the noise sequence and because practical implementations may have some residual signal elements in the distortion sequence u_k (even though independence from x_k is assumed for simplification of mathematics).

Gain estimation constructs an estimate of the channel pulse response, $\hat{h}_k$, by minimizing the mean square of the error

$$e_k = y_k - \hat{h}_k * x_k \quad . \tag{3.781}$$

Ideally, $\hat{h}_k = h_k$.

The Discrete Fourier Transform, DFT, of x_k is again

$$X_n = \frac{1}{\sqrt{\bar{N}}} \cdot \sum_{k=0}^{N-1} x_k \cdot e^{-\jmath \frac{2\pi}{\bar{N}} kn} \quad . \tag{3.782}$$

[55] Recall from Chapter 5 that to avoid confusion

$$\bar{N} \triangleq \begin{cases} N & \text{real basedband systems} \\ \frac{N}{2} & \text{complex baseband-equivalent systems} \end{cases}$$

and N remains the number of real dimensions.

When x_k is periodic[56] with period $\bar{N}$ samples, the DFT samples X_n are also periodic with period $\bar{N}$ and constitute a complete representation for the periodic time sequence x_k over all time. The N-point DFT's of y_k, u_k, $\hat{h}_k$, h_k, and e_k are Y_n, U_n, $\hat{H}_n$, H_n, and E_n, respectively.

Since x_k is periodic, then

$$Y_n = H_n \cdot X_n + U_n \quad . \tag{3.783}$$

The corresponding frequency-domain error is then

$$E_n = Y_n - \hat{H}_n \cdot X_n \;\; n = 0, ..., \bar{N} \quad . \tag{3.784}$$

(Recall that subchannels 0 and $N/2$ are one-dimensional in a real baseband system, while complex – 2 real-dimensions – in a complex baseband system with FFT size $\bar{N}$.) A vector of samples will contain one period of samples of any of the periodic sequences in question, for instance

$$\boldsymbol{x} = \begin{bmatrix} x_{N-1} \\ \vdots \\ x_1 \\ x_0 \end{bmatrix} \quad . \tag{3.785}$$

Then the FFT relations

$$\boldsymbol{X} = \mathcal{Q}\boldsymbol{x} \quad \boldsymbol{x} = \mathcal{Q}^* \boldsymbol{X} \tag{3.786}$$

follow easily, where Q is the matrix describing the DFT ($q_{\bar{N}-1-i,\bar{N}-1-k} = e^{-\jmath \frac{2\pi}{\bar{N}} ki}$) and $QQ^* = Q^*Q = I$. Similarly, $\boldsymbol{y}$, $\boldsymbol{Y}$, $\boldsymbol{e}$, $\boldsymbol{E}$, $\boldsymbol{h}$, $\boldsymbol{H}$, $\hat{\boldsymbol{h}}$, $\hat{\boldsymbol{H}}$, $\boldsymbol{u}$ and $\boldsymbol{U}$ as corresponding time-domain (lower case) and frequency-domain (upper case) vectors. For aperiodic sequences u_k, and thus aperiodic y_k and e_k, a block-time index l differentiates between different channel-output blocks (symbols) of $\bar{N}$ samples, i.e. $\boldsymbol{y}_l$.

The MSE for any estimate $\boldsymbol{h}$ is then

$$\begin{aligned} {}_{MSE} &= E\left\{|e_k|^2\right\} && (3.787) \\ &= \frac{1}{\bar{N}} E\left\{\|\boldsymbol{e}\|^2\right\} = \frac{1}{\bar{N}} \sum_{k=0}^{\bar{N}-1} E\left\{|e_k|^2\right\} && (3.788) \\ &= \frac{1}{\bar{N}} E\left\{\|\boldsymbol{E}\|^2\right\} = \frac{1}{\bar{N}} \sum_{n=0}^{\bar{N}} E\left\{|E_n|^2\right\} \quad . && (3.789) \end{aligned}$$

The tap error is $\delta_k \triangleq h_k - \hat{h}_k$ in the time domain and $\Delta_n \triangleq H_n - \hat{H}_n$ in the frequency domain. The autocorrelation sequence for any discrete-time sequence x_k is defined by

$$r_{xx,k} = E\left\{x_m x_{m-k}^*\right\} \tag{3.790}$$

with corresponding discrete power spectrum

$$R_{xx,n} = \mathcal{Q} \cdot r_{xx,k} \quad . \tag{3.791}$$

The norm tap error (NTE) is defined as

$$\begin{aligned} \text{NTE} &\triangleq E\left\{\|\boldsymbol{h} - \hat{\boldsymbol{h}}\|^2\right\} = E\left\{\|\boldsymbol{\delta}\|^2\right\} && (3.792) \\ &= E\left\{\|\boldsymbol{H} - \hat{\boldsymbol{H}}\|^2\right\} = E\left\{\|\boldsymbol{\Delta}\|^2\right\} && (3.793) \\ &= \sum_{n=0}^{\bar{N}-1} |H_n - \hat{H}_n|^2 = \sum_{k=0}^{\bar{N}-1} |h_k - \hat{h}_k|^2 \quad . && (3.794) \end{aligned}$$

[56] The periodicity can also be emulated by a cyclic prefix of length ν samples at the beginning of each transmitted block.

When the estimate $\hat{\boldsymbol{h}}$ equals the channel pulse response $\boldsymbol{h}$, then

$$e_k = u_k \tag{3.795}$$

and

$$r_{ee,k} \triangleq E\left[e_m \cdot e^*_{m-k}\right] = r_{uu,k} \;\; \forall\, k = 0, ..., \bar{N}-1 \quad , \tag{3.796}$$

where $r_{ee,k}$ is the autocorrelation function of e_k, and $r_{uu,k}$ is the autocorrelation function of u_k. The MMSE is then

$$MMSE = r_{ee,0} = \sigma_u^2 \quad , \tag{3.797}$$

the mean-square value of the channel noise samples, or $\sigma_u^2 = \frac{\mathcal{N}_0}{2}$ per dimension for the AWGN channel. In practice, $\hat{h}_k \neq h_k$, MSE > MMSE, and the excess MSE[57] is

$$\text{EMSE} \triangleq_{MSE-\sigma_u^2} \quad . \tag{3.798}$$

The overall channel SNR is

$$SNR = \frac{r_{xx,0} \cdot \|\boldsymbol{h}\|^2}{r_{uu,0}} \tag{3.799}$$

and the SNR of the nth channel is

$$SNR_n = \frac{R_{xx,n} \cdot |H_n|^2}{R_{uu,n}} \quad . \tag{3.800}$$

Definition 3.14.1 [Gain-Estimation SNR] The gain-estimation SNR is a measure of the true channel-output signal power on any subchannel to the excess MSE in that same channel (which is caused by $\hat{\boldsymbol{h}} \neq \boldsymbol{h}$), and is

$$SNR_{\hat{H},n} \triangleq \frac{R_{xx,n} \cdot |H_n|^2}{R_{ee,n} - R_{uu,n}} \quad . \tag{3.801}$$

EXAMPLE 3.14.1 [Accuracy] $SNR_{\hat{H},n}$ should be 30-60 dB for good gain estimation. To understand this requirement on $SNR_{\hat{H},n}$, consider the case on a subchannel in DMT with $SNR_n = \frac{R_{xx,n}|H_n|^2}{R_{uu,n}} = 44$ dB, permitting uncoded 2048 QAM to be transmitted at $P_e = 10^{-6}$ on this subchannel. The noise is then 44 dB below the signal on this subchannel. To estimate this noise power to within .1 dB of its true value, any residual gain estimation error on this subchannel, $R_{ee,n} - R_{uu,n}$, should be well below this mean-square noise level. That is

$$R_{ee,n} < 10^{.1/10} \cdot R_{uu,n} \approx (1 + 1/40) \cdot R_{uu,n} \tag{3.802}$$

Then,

$$SNR_{\hat{H},n} = \frac{R_{xx,n}|H_n|^2}{R_{ee,n} - R_{uu,n}} = \frac{SNR_n}{(1/40)} = 40 \cdot SNR \tag{3.803}$$

is then 60 dB (= 16 + 44 dB). Similarly, on a comparatively weak subchannel with SNR_i=14 dB for 4-point QAM, the $SNR_{\hat{H},n}$ should be at least 30 dB (= 14+16).

In general, for x dB accuracy

$$SNR_{\hat{H},n} \geq \left(10^{x/10} - 1\right)^{-1} \cdot SNR_n \quad . \tag{3.804}$$

[57] Toeplitz distribution applies if $\bar{N}$ is large or the input and noise are periodic, and thus the error E_n and noise/distribution U_n are uncorrelated so EMSE> 0. Aberrations lead to EMSE < 0 would occur only if N is too small and the noise is highly correlated.

3.14.3.1 An Accurate Gain Estimation method for Training

A particularly accurate gain-estimation method uses a cyclically prefixed training sequence x_k with number of symbol dimensions, N, equal to or slightly longer than ν, the length of the equalized channel pulse response. Typically, N is the same as in the DMT transmission system. The receiver measures (and possibly averages over the last L of $L+1$ cycles) the corresponding channel output, and then divides the DFT of the channel output by the DFT of the known training sequence.

The channel estimate in the frequency domain is

$$\hat{H}_n = \frac{1}{L}\sum_{l=1}^{L}\frac{Y_{l,n}}{X_{l,n}} \quad . \tag{3.805}$$

3.14.3.2 Training Performance Analysis

The output of the nth dimension on the lth symbol produced by the receiver DFT is $Y_{l,n} = H_n \cdot X_{l,n} + U_{l,n}$. The estimated value for $\hat{H}_n$ is

$$\hat{H}_n = H_n + \sum_{l=1}^{L}\frac{U_{l,n}}{L \cdot X_{l,n}} \quad , \tag{3.806}$$

so

$$\Delta_n = -\sum_{l=1}^{L}\frac{U_{l,n}}{L \cdot X_{l,n}} \quad . \tag{3.807}$$

By selecting the training sequence, $X_{l,n}$, with constant magnitude, the training sequence becomes $X_n = |X|e^{\jmath\theta_{l,n}}$.

The error signal on this dimension after $\hat{H}_n$ has been computed is

$$E_n = Y_n - \hat{H}_n \cdot X_n = \Delta_n \cdot X_n + U_n \tag{3.808}$$

$$= U_n + \frac{1}{L}\cdot\sum_{l=1}^{L} U_{l,n}\cdot e^{\jmath(\theta_n - \theta_{l,n})} \quad . \tag{3.809}$$

The phase term on the noise will not contribute to its mean-square value. U_n corresponds to a block that is not used in training, so that U_n and each of $U_{l,n}$ are independent, and

$$E\left\{|E_n|^2\right\} = R_{ee,n} = R_{uu,n} + \frac{1}{L}\cdot R_{uu,n} = (1+\frac{1}{L})\cdot R_{uu,n} \quad . \tag{3.810}$$

The excess MSE on the ith dimension then has variance $(1/\cdot L)\cdot R_{uu,n}$ that is reduced by a factor equal to the the number of symbol lengths that fit into the entire training interval length, with respect to the mean-square noise in that dimension. Thus the gain-estimation SNR is

$$SNR_{\hat{H},n} = L\cdot\frac{R_{xx,n}\cdot|H_n|^2}{R_{uu,n}} = L\cdot SNR_n \quad , \tag{3.811}$$

which means that the performance of the recommended gain estimation method improves linearly with L on all dimensions. Thus, while noise may be relatively higher (low SNR_n) on some subchannels than on others, the extra noise caused by miss-estimation is a constant factor below the relative signal power on that same dimension. In general then for x dB of accuracy

$$L \geq \left(10^{x/10} - 1\right)^{-1} \quad . \tag{3.812}$$

For an improvement in $SNR_{\hat{H},n}$ of 16 dB, Example 3.14.1 showed that SNR_n degrades by 0.1 dB. This 0.1 dB does not depend on the dimension's SNR_n; gain estimation requires $L = 40$ symbols of training on any dimension for 0.1 dB error.

For instance, the previous ADSL and VDSL examples of Section 4.6 used symbol periods of 250μs. Thus, gain estimation to within .1 dB accuracy is possible (on average) within 10 ms using this simple method.

Windowing: When the FFT size is much larger than the number of significant channel taps, as is usually the case, it is possible to significantly shorten the training period. This is accomplished by transforming (DFT) the final channel estimate to the time domain, windowing to $\nu+1$ samples and then returning to the frequency domain. Essentially, all the noise on sample times $\nu+2...N$ is thus removed without disturbing the channel estimate. The noise on all estimates, or equivalently the residual error in the SNR, improves by the factor N/ν with windowing. For the ADSL/VDSL Examples in Section 4.6, if the channel were limited to 32 nonzero successive samples in duration, then windowing would provide a factor of (32/512) reduction or 12 dB of improvement, possibly allowing just a few DMT symbols to estimate the channel to within an (on average) accuracy of .1 dB, and accurate gain estimation in a few ms.

3.14.3.3 Suggested Training Sequences

One training sequence for the gain estimation phase is a random or white sequence.[58] L blocks are used to create $\hat{H}_n$, which is computed for each dimension, one at a time. The L blocks can be periodic, or a cyclic prefix can be used to make the training sequence appear periodic. For reasons of small unidentified channel aberrations, like small nonlinearities caused by drivers, converters, amplifiers, it is better to use a cyclic prefix with non-periodic training because any such aberrations will appear as noise in the noise estimation to be subsequently described. (A purely periodic training signal might otherwise disguise these abberations.)

In complex baseband channels a "chirp" training sequence can also be used.

$$x_k = e^{J\frac{2\pi}{N}k^2} \quad . \tag{3.813}$$

This chirp has a theoretical minimum peak-to-average (one-dimensional) power ratio of 2 and is a "white sequence," with $r_{xx,k} = \delta_k$, where δ_k is the Kronecker delta (not the norm tap error). While "white" is good for identifying an unknown channel, a chirp's low PAR can leave certain small nonlinear "noise" distortion unidentified, which ultimately might cause the identified SNR_n's to be too optimistic.

3.14.3.4 Gain Estimation in Tracking

The value for μ in the FEQ The EMSE for the first-order zero-forcing update algorithm in Section 4.3 can be found with some algebra and approximations to be

$$\text{EMSE} \approx \frac{\mu_n \cdot \mathcal{E}_n \cdot |H_n|^2}{2 - \mu_n \cdot \mathcal{E}_n \cdot |H_n|^2} \cdot R_{\tilde{u}\tilde{u},n} \quad , \tag{3.814}$$

where $\tilde{U}_n$ is the noise scaled by the inverse of the channel. This scaling is part of both gain and noise and does not affect the achievable SNR. Thus, for the multichannel normalizer to maintain the same accuracy as the initial gain estimation in Equation (3.810)

$$\frac{1}{L} = \frac{\mu_n \cdot \mathcal{E}_n \cdot |H_n|^2}{2 - \mu_n \cdot \mathcal{E}_n \cdot |H_n|^2} \tag{3.815}$$

or

$$\mu_n = \frac{2}{(L+1) \cdot \mathcal{E}_n \cdot |H_n|^2} \quad , \tag{3.816}$$

so for $L = 40$, $|H_n|^2 = 1$, and $\mathcal{E}_n = 1$, the value would be $\mu_n = 2/41$.

Gear shifting occurs when μ_n is set at a large value and then reduced with time as the FEQ nears convergence, allowing smaller excess mean square error with each shift, but faster convergence with each shift compared to using the final μ_n value in (3.816) throughout training.

[58] Say the PRBS of Chapter 10 with polynomial $(1 + D + D^{16})$ with $b_n = 2$ on channels $n = 1, ..., N-1$ and $b_n = 1$ on the DC and Nyquist dimensions. The designer should ensure that the seed for the PRBS is such that no peaks occur that would exceed the dynamic range of channel elements during gain estimation. Such peaks are usually compensated by a variety of other mechanisms when they occur in normal transmission (rarely) and would cause unnecessarily conservative loading if their effects were allowed to dominate measured SNRs.

3.14.4 Noise Spectral Estimation in Training

Training also estimates the discrete-time noise power spectrum[59], or equivalently the mean-square noise at each of the demodulator DFT outputs for SNR_n computation. Noise estimation computes a spectral estimate of the error sequence, E_n, that remains after the channel response has been removed. The training sequence used for gain estimation is usually continued for noise estimation.

3.14.4.1 Analysis of Variance

The variance of L noise samples on the nth dimension is:

$$\hat{\sigma_n^2} = \frac{1}{L} \cdot \sum_{l=1}^{L} |E_{l,n}|^2 \quad . \tag{3.817}$$

For stationary noise on any tone, the mean of this expression is the variance of the (zero-mean) noise. The "variance of this variance estimate" is computed as

$$\text{var}\left(\hat{\sigma_n^2}\right) = \frac{1}{L^2}\left(3 \cdot L \cdot \sigma_n^4 - L \cdot (\sigma_n^2)^2\right) = \frac{2}{L}\sigma_n^4 \tag{3.818}$$

for Gaussian noise.[60] Thus Equation (3.817)'s excess noise estimate is $\sqrt{2/L} \cdot \sigma_n^2$ and this excess noise decreases with the square-root of the number of averaged noise terms. To make this extra noise .1 dB or less, $L = 3200$. Recalling that the actual computed value for the noise estimate will have a standard deviation on average that leads to less than .1 dB error, there is still a 10% chance that the statistics of the noise will lead to deviation greater than 1 standard deviation (assuming Gaussian distribution, or approximating the more exact Chi-square with a Gaussian). Thus, sometimes a yet larger value of L is used. 98% confidence occurs at $L = 12,800$ and 99.9% confidence at $L = 28,800$. If the equivalent noise autocorrelation response is short, windowing could again be used to reduce this training time.

3.14.4.2 Noise Variance Estimate Tracking

The value for μ' in the FEQ The standard deviation for the first-order noise update in the FEQ can be found to be

$$\text{std}(\tilde{\hat{\sigma}}_n^2) = \sqrt{\frac{\mu'}{2-\mu'}} \cdot \tilde{\sigma}_n^2 \quad . \tag{3.819}$$

Thus, to maintain a constant noise accuracy, the step size should satisfy

$$\frac{2}{L} = \frac{\mu'}{2-\mu'} \tag{3.820}$$

or

$$\mu' = \frac{4}{L+2} \tag{3.821}$$

so when $L = 6400$, then $\mu' \approx 6.25 \times 10^{-4}$. In reality, the designer might want high confidence (not just an average confidence) that the accuracy is .1 dB, in which case a μ of perhaps 10^{-4} would suggest the chance of missing would be the same as noise occuring with 4 times the standard deviation (pretty small in Gaussian and Xi-square distributions).

From Section 4.6, gain normalizers in general, – and thus the FEQ – update the noise in the proportion:

$$\frac{1}{g_n} \propto \tilde{\sigma}_n^2 \quad . \tag{3.822}$$

[59] Clearly the noise can not have been whitened if it is unknown and so this step precedes any noise whitening that might occur with later data transmission.

[60] A Gaussian has fourth moment $E(n^4) = 3\sigma^2$.

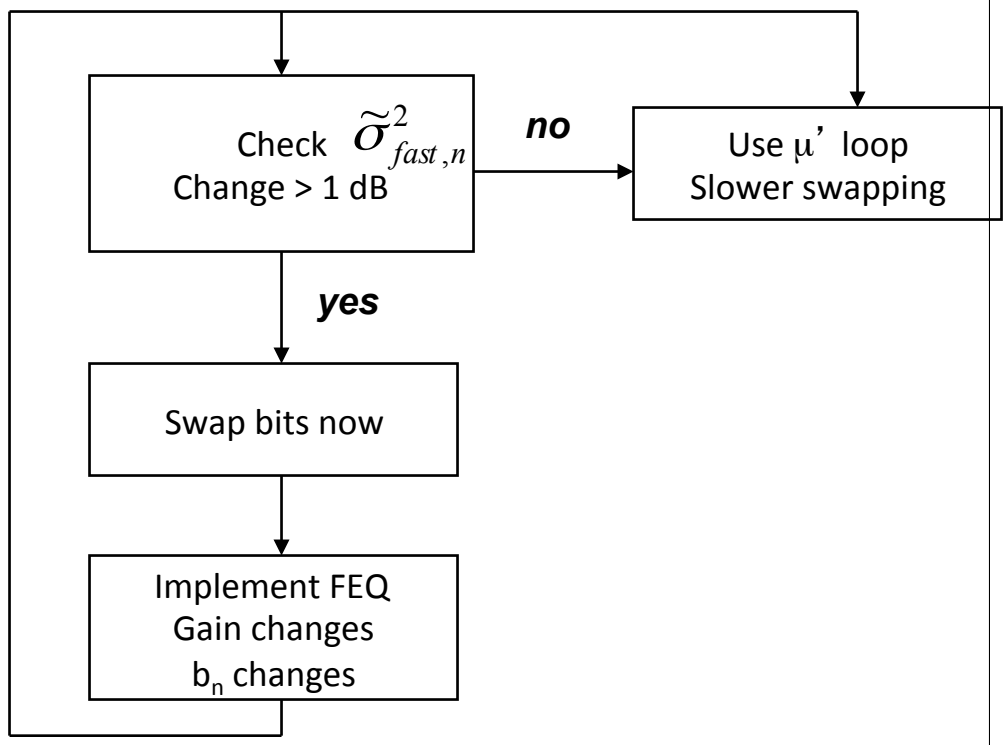

Figure 3.90: Flow chart for fast-swap augmentation of noise calculation.

Effectively, the normalizer then tracks the ratio

$$\text{gain} = \frac{\tilde{\sigma}^2_{n,current}}{\tilde{\sigma}^2_{init,n}} \quad . \tag{3.823}$$

While it may take a long averaging time to introduce .1 dB accuracy, clearly an abrupt change in noise of several dB or more on any (or many) single tones can be detected rapidly.

A simple gear-shifting mechanism would be to introduce a second noise loop as in Section 4.3 with a μ'' replacing μ' where $\mu'' >> \mu'$. This faster update the noise variance estimate would be much less accurate. However, to discern whether the noise has changed rapidly, it provides an early indication. Basically, this faster tracking exploits the fact that the bit distribution is near converged in steady-state operation just before a large noise change on some tones might occur. Thus, the bit-swap controller is looking only for a gross change to initiate more rapid swapping. The following example illustrates.

Figure 3.90 illustrates the basic concept of faster swapping. It is possible to use the FEQ initially with the known training sequence and thereby avoid separate estimation of first gain and then noise, and simply directly compute the g_n values. This is feasible with gear-shifting allowing successive refinements of the g_n estimates, again as implied in Figure 3.90.

3.14.5 SNR Computation in Training

The signal to noise ratio is then estimated for each dimension independently as

$$SNR_n = \mathcal{E}_n \frac{|\hat{H}_n|^2}{\hat{\sigma}^2_n} \quad . \tag{3.824}$$

Loading can then be executed on the g_n to determined the $\mathcal{E}_n$ and b_n at the receiver and sent to the transmitter through a secure feedback channel during training. This step is often called "the exchange"

in DMT modems and occurs as a last significant step prior to live transmission of data, often called "showtime!"

Using the FEQ, the SNR is given by (3.823). Loading can be executed in the receiver (or after passing SNR values, in the transmitter) and then the resulting b_n and $\mathcal{E}_n$ (or relatively increase/decrease in $\mathcal{E}_n$ with respect to what was used last) are sent to the transmitter via the reverse link always necessary in DMT. This was discussed at length in Section 4.3 on bit swapping.

Exercises - Chapter 3

3.1 *Single Sideband (SSB) Data Transmission with no ISI - 8 pts*
Consider the quadrature modulator shown in Figure 3.91,

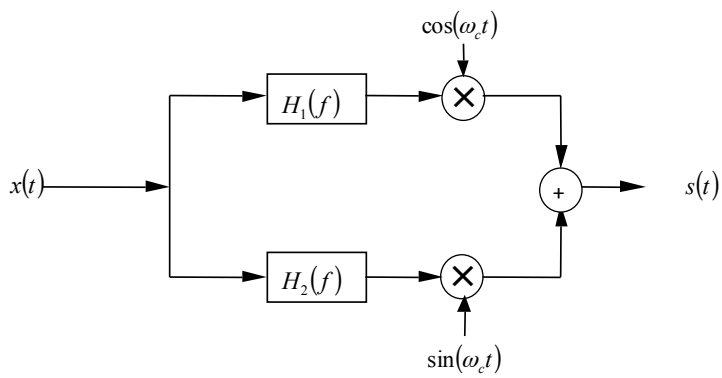

Figure 3.91: Quadrature modulator.

a. What conditions must be imposed on $H_1(f)$ and $H_2(f)$ for the output signal $s(t)$ to have no spectral components between $-f_c$ and f_c? Assume that f_c is larger than the bandwidth of $H_1(f)$ and $H_2(f)$. (2 pts.)

b. With the input signal in the form,

$$x(t) = \sum_{n=-\infty}^{\infty} a_n \cdot \phi(t - nT) \ ,$$

what conditions must be imposed on $H_1(f)$ and $H_2(f)$ if the real part of the demodulated signal is to have no ISI? (3 pts.)

c. Find the impulse responses $h_1(t)$ and $h_2(t)$ corresponding to the minimum bandwidth $H_1(f)$ and $H_2(f)$ that simultaneously satisfy Parts a and b. The answer can be in terms of $\phi(t)$. (3 pts.)

3.2 *Sampling Time and Eye Patterns - 9 pts*
The received signal for a binary transmission system is,

$$y(t) = \sum_{n=-\infty}^{\infty} a_n \cdot q(t - nT) + n(t)$$

where $a_n \in \{-1, +1\}$ and $Q(f)$ is a triangular, i.e. $q(t) = sinc^2(\frac{t}{T})$. The received signal is sampled at $t = kT + t_0$, where k is an integer and t_0 is the sampling phase, $|t_0| < \frac{T}{2}$.

a. Neglecting the noise for this part, find the peak distortion as a function of t_0. *Hint:* Use Parseval's relation. (3 pts.)

b. For the following four binary sequences $\{u_n\}_{-\infty}^{\infty}, \{v_n\}_{-\infty}^{\infty}, \{w_n\}_{-\infty}^{\infty}, \{x_n\}_{-\infty}^{\infty}$:

$$\begin{aligned} u_n &= -1 \qquad \forall n \ , \\ v_n &= +1 \qquad \forall n \ , \\ w_n &= \begin{cases} +1, & for \text{n=0} \\ -1, & otherwise \end{cases} \ , \text{ and} \\ x_n &= \begin{cases} -1, & for \text{n=0} \\ +1, & otherwise \end{cases} \ , \end{aligned}$$

use the result of (a) to find expressions for the 4 outlines of the corresponding binary eye pattern. Sketch the eye pattern for these four sequences over two symbol periods $-T \leq t \leq T$. (2 pts.)

c. Find the eye pattern's width (horizontal) at its widest opening. (2 pts.)

d. If the noise variance is σ^2, find a worst-case bound (using peak distortion) on the error probability as a function of t_0. (2 pts.)

3.3 *The Stanford EE379 Channel Model - 12 pts*

For Figure 3.9's ISI-model with PAM and symbol period T, $\varphi(t) = \frac{1}{\sqrt{T}} \cdot \text{sinc}(\frac{t}{T})$ and $h_c(t) = \delta(t) - \frac{1}{2} \cdot \delta(t-T)$:

a. Determine $h(t)$, the pulse response. (1 pt)

b. Find $\|h\|$ and $\varphi_h(t)$. (2 pts.)

c. (2 pts.) Find $q(t)$, the function that characterizes how one symbol interferes with other symbols. Confirm that $q(0) = 1$ and that $q(t)$ is hermitian (conjugate symmetric). A useful observation is

$$\text{sinc}\left(\frac{t+mT}{T}\right) * \text{sinc}\left(\frac{t+nT}{T}\right) = T \cdot \text{sinc}\left(\frac{t+(m+n)T}{T}\right).$$

d. Use Matlab to plot $q(t)$. This plot may use $T = 10$ and show $q(t)$ for integer values of t. With $y(t)$ sampled at $t = kT$ for some integer k, how many symbols are distorted by a given symbol? How will a given positive symbol affect the distorted symbols? Specifically, will they be increased or decreased? (2 pts.)

The remainder of this problem considers 8 PAM with $d = 1$.

e. Determine the peak distortion, $\mathcal{D}_p$. (2 pts.)

f. Determine the MSE distortion, $\mathcal{D}_{mse}$ and compare with the peak distortion. (2 pts.)

g. Find an approximation to the error probability (using the MSE distortion). The answer will be in terms of σ.(1 pt.)

3.4 *Bias and SNR - 8 pts*

This problem uses the results and specifications of Problem 3.3 with 8 PAM and $d = 1$ and sets

$$\frac{\mathcal{N}_0}{2} = \sigma^2 = 0.1 \ .$$

The detector first scales the sampled output y_k by α and chooses the closest x to $y_k \cdot \alpha$ as illustrated in Figure 3.15. **Express your SNR's below both as a ratio of powers and in dB.**

a. For which value of α is the receiver unbiased? (1 pt.)

b. For the value of α found in Part a, find the receiver signal-to-noise ratio, $SNR(R)$ that is the ratio of the output signal energy before bias removal to the corresponding MSE. (2 pts.)

c. Find the value of α that maximizes SNR_R and the corresponding $SNR(R)$. (2 pts.)

d. Show that the receiver found in the previous part is biased. (1 pt.)

e. Find the matched filter bound on signal-to-noise ratio, SNR_{MFB}. (1 pt.)

f. Discuss the ordering of the three SNR's you have found in this problem. Which inequalities will always be true? (1 pt.)

3.5 *Raised Cosine Pulses with Matlab - 8 pts*

This problem uses the .m files from the instructors EE379A web page at http://web.stanford.edu/group/cioffi/ee379a/homework.html .

a. The formula for the raised cosine pulse is in Equation (3.79) and repeated here as:

$$q(t) = sinc\left(\frac{t}{T}\right) \cdot \left[\frac{\cos\left(\frac{\alpha\pi t}{T}\right)}{1-\left(\frac{2\alpha t}{T}\right)^2}\right]$$

There are three values of t that would cause a program, such as Matlab, difficulty because of a division by zero. Identify these trouble spots and evaluate what $q(t)$ should be for these values. (2 pts)

b. Having identified those three trouble spots, a function to generate raised-cosine pulses is a straightforward implementation of the above equation and is in **mk_rcpulse.m** from the web site. Executing **q = mk_rcpulse(a)** will generate a raised-cosine pulse with $\alpha = \mathbf{a}$. The pulses generated by **mk_rcpulse** assume $T = 10$ and are truncated to 751 points. (2 pts)

Use **mk_rcpulse** to generate raised cosine pulses with 0%, 50%, and 100% excess bandwith and plot them with **plt_pls_lin**. The syntax is **plt_pls_lin(q_50, 'title')** where **q_50** is the vector of pulse samples generated by **mk_rcpulse(0.5)** (50% excess bandwidth). Show results and discuss any deviations from the ideal expected frequency-domain behavior.

c. Use **plt_pls_dB(q, 'title')** to plot the same three raised cosine pulses as in part (b). Show the results. Which of these three pulses would you provides the smallest band of frequencies with energy above -40dB? Explain this unexpected result. (3 pts)

d. The function **plt_qk (q, 'title')** plots $q(k)$ for sampling at the optimal time and for sampling that is off by 4 samples (i.e., $q(kT)$ and $q(kT+4)$ where $T = 10$). Use **plt_qk** to plot **q_k** for 0%, 50%, and 100% excess bandwidth raised cosine pulses. Discuss how excess bandwidth affects sensitivity of ISI performance to sampling at the correct instant. (3 pts)

3.6 *Noise Enhancement: MMSE-LE vs ZFE - 23 pts*

This problem explores the channel with

$$\begin{aligned}
&\|h\|^2 = 1 + aa^* = 1 + |a|^2 \\
&Q(D) = \frac{a^* \cdot D^{-1} + \|h\|^2 + a \cdot D}{\|h\|^2} \\
&0 \le |a| < 1 \ .
\end{aligned}$$

a. (2 pts) Find the zero forcing and minimum mean square error linear equalizers $W_{\text{ZFE}}(D)$ and $W_{\text{MMSE-LE}}(D)$. Use the variable $b = \|h\|^2 \cdot \left(1 + \frac{1}{SNR_{MFB}}\right)$ in your expression for $W_{\text{MMSE-LE}}(D)$.

b. (6 pts) By substituting $e^{-jwT} = D$ (with $T = 1$) and using $SNR_{MFB} = 10 \cdot \|p\|^2$, use Matlab to plot (lots of samples of) $W(e^{jw})$ for both ZFE and MMSE-LE for $a = .5$ and $a = .9$. Discuss the differences between the plots.

c. (3 pts) Find the roots r_1, r_2 of the polynomial

$$a \cdot D^2 + b \cdot D + a^*.$$

Show that $b^2 - 4|a|^2$ is always a real positive number (for $|a| \neq 1$). *Hint:* Consider the case where $\frac{1}{SNR_{MFB}} = 0$. Let r_2 be the root for which $|r_2| < |r_1|$. Show that $r_1 r_2^* = 1$.

d. (2 pts) Use the previous results to show that for the MMSE-LE

$$W(D) = \frac{\|h\|}{a} \cdot \frac{D}{(D-r_1)\cdot(D-r_2)} = \frac{\|h\|}{a\cdot(r_1-r_2)} \cdot \left(\frac{r_1}{D-r_1} - \frac{r_2}{D-r_2}\right). \tag{3.825}$$

e. (2 pts) Show that for the MMSE-LE, $w_0 = \frac{\|h\|}{\sqrt{b^2-4|a|^2}}$. By taking $\frac{1}{SNR_{MFB}} = 0$, show that for the ZFE, $w_0 = \frac{\|h\|}{1-|a|^2}$.

f. (4 pts) For $\bar{\mathcal{E}}_x = 1$ and $\sigma^2 = 0.1$ find expressions for σ^2_{ZFE}, $\sigma^2_{MMSE-LE}$, γ_{ZFE}, and $\gamma_{\text{MMSE-LE}}$.

g. (4 pts) Find γ_{ZFE} and $\gamma_{\text{MMSE-LE}}$ in terms of the parameter a and calculate for $a = 0, 0.5, 1$. Sketch γ_{ZFE} and $\gamma_{\text{MMSE-LE}}$ for $0 \le a < 1$.

3.7 *DFE is Even Better - 8 pts*

a. (2 pts) For the channel of Problem 3.6, show that the canonical factorization is

$$Q(D) + \frac{1}{SNR_{MFB}} = \gamma_0 \cdot (1 - r_2 \cdot D^{-1}) \cdot (1 - r_2^* \cdot D).$$

What is γ_0 in terms of a and b? *Please* don't do this from scratch; use results of Problem 3.6.

b. (2 pts) Find $B(D)$ and $W(D)$ for the MMSE DFE.

c. (4 pts) Give an expression for $\gamma_{\text{MMSE-DFE}}$. Compute its values for $a = 0, .5, 1$ for the $\bar{\mathcal{E}}_x$ and σ^2 of Problem 3.6. Sketch $\gamma_{\text{MMSE-DFE}}$ as in Problem 3.6. Compare with your sketches from Problem 3.6.

3.8 *Noise Predictive DFE - 11 pts*

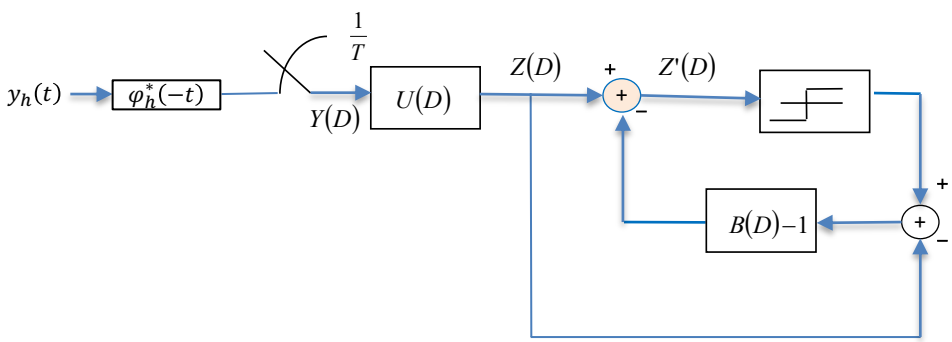

Figure 3.92: Noise-Predictive DFE

Figure 3.92's equalizer restricts $B(D)$ to be causal and monic and presumes all decisions are correct. Use a MMSE criterion to choose $U(D)$ and $B(D)$ to minimize $\mathbb{E}[|x_k - z_k'|^2]$. ($x_k$ is the channel input.)

a. (5 pts) Show this equalizer is equivalent to a MMSE-DFE and find $U(D)$ and $B(D)$ in terms of $G(D)$, $Q(D)$, $\|h\|$, $\bar{\mathcal{E}}_{\boldsymbol{x}}$, SNR_{MFB} and γ_0.

b. (2 pts) Relate $U_{\text{NPDFE}}(D)$ to $W_{\text{MMSE-LE}}(D)$ and to $W_{\text{MMSE-DFE}}(D)$.

c. (1 pt) Without feedback ($B(D) = 1$), what does this equalizer become?

d. (1 pt) Interpret the name "noise-predictive" DFE by explaining what the feedback section is doing.

e. (2 pts) Is the NPDFE biased? If so, show how to remove the bias.

3.9 *Receiver SNR Relationships - 11 pts*

a. (3 pts) Recall that:

$$Q(D) + \frac{1}{\text{SNR}_{\text{MFB}}} = \gamma_0 \cdot G(D) \cdot G^*(D^{-*})$$

Show that:

$$1 + \frac{1}{\text{SNR}_{\text{MFB}}} = \gamma_0 \cdot \|g\|^2$$

b. (3 pts) Show that:

$$\|g\| \geq 1$$

with equality if and only if $Q(D) = 1$ (i.e. if the channel is flat) and therefore:

$$\gamma_0 \leq 1 + \frac{1}{\text{SNR}_{\text{MFB}}}$$

c. (3 pts) Let x_0 denote the time-zero value of the sequence X. Show that:

$$\left[\frac{1}{Q(D) + \frac{1}{\text{SNR}_{\text{MFB}}}}\right]_0 \geq \frac{1}{\gamma_0}$$

and therefore:

$$\text{SNR}_{\text{MMSE-LE,U}} \leq \text{SNR}_{\text{MMSE-DFE,U}}$$

(with equality if and only if $Q(D) = 1$, that is $Q(\omega)$ has vestigial symmetry.)

d. (2 pts) Use the results of parts b) and c) to show:

$$\text{SNR}_{\text{MMSE-LE,U}} \leq \text{SNR}_{\text{DFE,U}} \leq \text{SNR}_{\text{MFB}}$$

3.10 *Bias and Error Probability - 7 pts*

This problem illustrates that the best unbiased receiver has a lower P_e than the (biased) MMSE receiver using the 3-point PAM constellation in Figure 3.93.

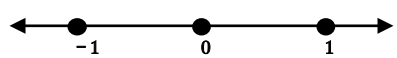

Figure 3.93: A three point PAM constellation.

The AWGN n_k has

$$\frac{\mathcal{N}_0}{2} = \sigma^2 = 0.1.$$

The inputs are independent and identically distributed uniformly over the three possible values. Also, n_k has zero mean and is independent of x_k.

a. (1 pt) Find the mean square error between $y_k = x_k + n_k$ and x_k. (easy)

b. (1 pt) Find the exact P_e for the ML detector of the unbiased values y_k.

c. (2 pts) Find the scale factor α that will minimize the mean square error

$$\mathbb{E}[e_k^2] = \mathbb{E}[(x_k - \alpha \cdot y_k)^2].$$

Prove that this α does in fact provide a minimum by taking the appropriate second derivative.

d. (2 pts) Find $\mathbb{E}[e_k^2]$ and P_e for the scaled output $\alpha \cdot y_k$. When computing P_e, use the decision regions for the unbiased ML detector of Part b. The biased receiver of part (c) has a P_e that is higher than the (unbiased) ML detector of Part b, even though it has a smaller squared error.

e. (1 pt) Where are the optimal decision boundaries for detecting x_k from $\alpha \cdot y_k$ (for the MMSE α) in Part c? What is the error probability for these decision boundaries?

3.11 *Bias and the DFE - 4 pts*

For the DFE of Problem 3.7, the canonical factorization's scale factor was found as:

$$\gamma_0 = \frac{b + \sqrt{b^2 - 4|a|^2}}{2(1 + |a|^2)} \quad .$$

a. (2 pts) Find G_u in terms of a, b, and r_2. Use the same SNR_{MFB} as in Prob 3.7.

b. (1 pt) Draw a DFE block diagram with scaling after the feedback summation.

c. (1 pt) Draw a DFE block diagram with scaling before the feedback summation.

3.12 *Zero-Forcing DFE - 7 pts*

This problem again uses the general channel model of Problems 3.6 and 3.7 with $\bar{\mathcal{E}}_x = 1$ and $\sigma^2 = 0.1$.

a. (2 pts) Find η_0 and $P_c(D)$ so that

$$Q(D) = \eta_0 \cdot P_c(D) P_c^*(D^{-*}).$$

b. (2 pts) Find $B(D)$ and $W(D)$ for the ZF-DFE.

c. (1 pt) Find σ^2_{ZF-DFE}

d. (2 pts) Find the loss with respect to SNR_{MFB} for $a = 0$, .5, 1. Sketch the loss for $0 \le a < 1$.

3.13 *Complex Baseband Channel - 6 pts*

The pulse response of a channel is band-limited to $\frac{\pi}{T}$ and has

$$\begin{aligned} h_0 &= \frac{1}{\sqrt{T}} \cdot (1 + 1.1j) \\ h_1 &= \frac{1}{\sqrt{T}} \cdot (0.95 + 0.5j) \\ h_k &= 0 \quad \text{for } k \neq 0, 1 \end{aligned}$$

where $h_k = h(kT)$ and $SNR_{MFB} = 15$ dB.

a. (2 pts) Find $\|h\|^2$ and a so that

$$Q(D) = \frac{a^* D^{-1} + \|h\|^2 + aD}{\|h\|^2}$$

b. (2 pts) Find $\text{SNR}_{MMSE-LE,U}$ and $\text{SNR}_{MMSE-DFE,U}$ for this channel. Use the results of Problems 3.6 and 3.7 wherever appropriate. Since $\|h\|^2 \neq 1 + |a|^2$, some care should be exercised in using the results of Problems 3.6 and 3.7.

c. (2 pts) Use the SNR's from Part b to compute the NNUB on P_e for 4-QAM with the MMSE-LE and the MMSE-DFE.

3.14 *Tomlinson Precoding - 13 pts*

This problem uses a $1 + 0.9 \cdot D$ channel (i.e. the $1 + aD$ channel that we have been exploring at length with $a = 0.9$) with $\sigma^2 = 0$ and with the 4-PAM constellation having $x_k \in \{-3, -1, 1, 3\}$.

a. (5 pts) Design a Tomlinson precoder and its associated receiver for this system. This system will be fairly simple. How would your design change if noise were present in the system?

b. (5 points) Implement the ZF-DFE's equivalent precoder and its associated receiver for the following input sequence:

$$\{3, -3, 1, -1, 3, -3, -1\}$$

Also compute the corresponding output of the receiver, assuming that the symbol $\boldsymbol{x}' = -3$ was sent just prior to the input sequence.

c. (3 pts) Again with zero noise, remove the modulo operations from the precoder and the receiver. For this modified system, compute the output of the precoder, the output of the channel, and the output of your receiver for the same inputs as in the previous part.

Did the system still work? What changed? What purpose do the modulo operators serve?

3.15 *Flexible Precoding - 13 pts*

This problem uses a $1 + 0.9 \cdot D$ channel (i.e. the $1 + a \cdot D$ channel that we have been exploring at length with $a = 0.9$) with $\sigma^2 = 0$ and with the 4-PAM constellation having $x_k \in \{-3, -1, 1, 3\}$.

a. (5 pts) Design a Flexible precoder and its associated receiver for this system. This system will be fairly simple. How would your design change if noise were present in the system?

b. (5 points) Implement the precoder and its associated receiver using any method you would like with no noise for the following input sequence:

$$\{3, -3, 1, -1, 3, -3, -1\}$$

Also compute the corresponding output of the receiver, assuming that the symbol $\boldsymbol{x}' = -3$ was sent just prior to the input sequence.

c. (3 pts) Again with zero noise, remove the modulo operations from the precoder and the receiver. For this modified system, compute the output of the precoder, the output of the channel, and the output of your receiver for the same inputs as in the previous part.

Did the system still work? What changed? What purpose do the modulo operators serve?

3.16 *Finite-Length Equalization and Matched Filtering - 5 pts*

This problem explores the optimal FIR MMSE-LE without assuming an explicit matched filter. However, there will be a "matched filter" anyway as a result pf this problem. This problem uses a system whose pulse response is band limited to $|\omega| < \frac{\pi}{T}$ that is sampled at the symbol rate T after passing through an anti-alias filter with gain $\sqrt{T}$.

a. (3 pts)

Show that

$$w = R_{xY} \cdot R_{YY}^{-1} = (0, \ldots, 0, 1, 0, \ldots, 0) \cdot {\Phi_h}^* \cdot \left(\|h\| \cdot \left(\hat{\mathbf{Q}} + l \frac{1}{SNR_{MFB}} \mathbf{I} \right) \right)^{-1}.$$

where

$$\hat{Q} = \frac{H \cdot H^*}{\|h\|^2}$$

b. (2 pts) Which terms in Part a correspond to the matched filter? Which terms correspond to the infinite length $W_{MMSE-LE}$?

3.17 *Finite-Length Equalization and MATLAB - 5 pts*

The $1 + 0.25 \cdot D$ channel with $\sigma^2 = .1$ has an input with $\bar{\mathcal{E}}_x = 1$.

a. (1 pt) Find $\text{SNR}_{MMSE-LE,U}$ for the infinite-length filter.

b. (2 pts) This problem uses the MATLAB program **mmsele**. This program is interactive, so just type **mmsele** and answer the questions. When it asks for the pulse response, you can type **[1 0.25]** or **h** if you have defined **h = [1 0.25]**.

Use **mmsele** to find the best Δ and the associated $\text{SNR}_{MMSE-LE,U}$ for a 5-tap linear equalizer . Compare with the value from Part a. How sensitive is performance to Δ for this system?

c. (2 pts) Plot $|H(e^{(jwT)}|$ and $|H(e^{(jwT)} \cdot W(e^{(jwT)}|$ for $w \in [0, \frac{\pi}{T}]$. Discuss the plots briefly.

3.18 *Computing Finite-Length equalizers - 11 pts*

This problem uses the following system description:

$$\bar{\mathcal{E}}_x = 1 \qquad \frac{\mathcal{N}_0}{2} = \frac{1}{8} \qquad \varphi(t) = \frac{1}{\sqrt{T}} \cdot \text{sinc}(\frac{t}{T}) \qquad h(t) = \delta(t) - 0.5\delta(t-T) \qquad l = 1$$

Matlab may assist any matrix manipulations in completing this problem. Answers may be validated with **dfecolor.m**. However, this problem's objective is to explore the calculations in detail.

a. (2 pts) The anti-alias filter is perfect (flat) with gain $\sqrt{T}$. Find $h(t) = (\varphi(t) * h_c(t))$ and $\|h\|^2$, corresponding to the discrete-time channel

$$y_k = x_k - .5 \cdot x_{k-1} + n_k \quad . \tag{3.826}$$

Also, find $\|H(D)\|^2 = \sum_k |h_k|^2$.

b. (1 pt) Compute SNR_{MFB} for this channel.

c. (2 pts) Design a 3 tap FIR MMSE-LE for $\Delta = 0$.

d. (1 pt) Find the σ^2_{LE} for the equalizer of the previous part.

e. (2 pts) Design a 3 tap FIR ZF-LE for $\Delta = 0$.

f. (1 pt) Find the associated σ^2_{ZFE}.

g. (2 pts) Design an MMSE-DFE which has 2 feedforward taps and 1 feedback tap. Again, assume that $\Delta = 0$.

h. (2 pts) Compute the unbiased SNR's for the MMSE-LE and MMSE-DFE. Compare these two SNR's with each other and the SNR_{MFB}.

3.19 *Equalizer for Two-Band Channel with Notch - 10 pts*

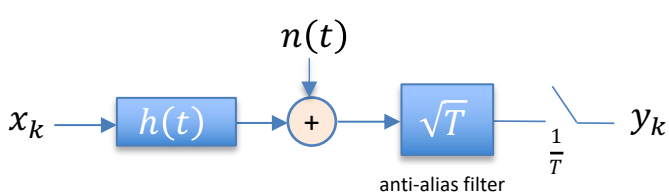

Figure 3.94: Channel for Problem 3.19.

Figure 3.94 has AWGN channel with pulse response $h(t) = \frac{1}{\sqrt{T}} \cdot \left[\text{sinc}\left(\frac{t}{T}\right) - \text{sinc}\left(\frac{t-4T}{T}\right)\right]$. The receiver anti-alias filter has gain $\sqrt{T}$ over the entire Nyquist frequency band, $-1/2T < f < 1/2T$, and

zero outside this band. The filter is followed by a $1/T$ rate sampler so that the sampled output has D-Transform

$$y(D) = (1 - D^4) \cdot x(D) + n(D) \quad . \tag{3.827}$$

$x(D)$ is the D-Transform of the sequence of M-ary PAM input symbols, and $n(D)$ is the D-Transform of the Gaussian noise sample sequence. The noise autocorrelation function is $R_{nn}(D) = \frac{\mathcal{N}_0}{2}$. Further equalization of $y(D)$ is in discrete time where (in this case) the matched filter and equalizer discrete responses (i.e., D-Transforms) can be combined into a single discrete-time response. The target P_e is 10^{-3}.

Let $\frac{\mathcal{N}_0}{2}$ = -100 dBm/Hz (0 dBm = 1 milliwatt = .001 Watt) and let $1/T = 2$ MHz.

a. Sketch $|H(e^{-\jmath\omega T})|^2$. (2 pts)

b. What kind of equalizer should be used on this channel? (2 pts)

c. For a ZF-DFE, find the transmit symbol mean-square value (i.e., the transmit energy) necessary to achieve a data rate of 6 Mbps using PAM and assuming a probability of symbol error equal to 10^{-3}. (4 pts)

d. For the transmit energy in Part c, how would a MMSE-DFE perform on this channel? (2 pts)

3.20 *FIR Equalizer Design - 14 pts*

A symbol-spaced FIR equalizer ($l = 1$) is applied to a stationary sequence y_k at the sampled output of an anti-alias filter, which produces a discrete-time IIR channel with response given by

$$y_k = a \cdot y_{k-1} + b \cdot x_k + n_k \quad , \tag{3.828}$$

where n_k is white Gaussian noise.

The SNR (ratio of mean square x to mean square n) is $\frac{\bar{\mathcal{E}}_{\boldsymbol{x}}}{\frac{\mathcal{N}_0}{2}} = 20$ dB. $|a| < 1$, and both a and b are real. For all parts of this question, choose the best Δ where appropriate.

a. Design a 2-tap FIR ZFE. (3 pts)

b. Compute the SNR_{zfe} for Part a. (2 pts)

c. Compare the answer in Part b with that of the infinite-length ZFE. (1 pt)

d. Let $a = .9$ and $b = 1$. Find the 2-tap FIR MMSE-LE. (4 pts)

e. Find the $\text{SNR}_{MMSE-LE,U}$ for Part d. (2 pts)

f. Find the SNR_{ZFE} for an infinite-length ZF-DFE. How does the SNR compare to the matched-filter bound if there is no information loss incurred in the symbol-spaced anti-alias filter? Use $a = .9$ and $b = 1$. (2 pts)

3.21 *ISI quantification - 8 pts*

For the channel $H(\omega) = \sqrt{T} \cdot (1 + .9 \cdot e^{\jmath\omega T})\ \forall |\omega| < \pi/T$ studied repeatedly in this chapter, use binary PAM with $\bar{\mathcal{E}}_{\boldsymbol{x}} = 1$ and $SNR_{MFB} = 10$ dB. Remember that $q_0 = 1$.

a. Find the peak distortion, $\mathcal{D}_p$. (1 pt)

b. Find the peak-distortion bound on P_e. (2 pts)

c. Find the mean-square distortion, $\mathcal{D}_{MS}$. (1 pt)

d. Approximate P_e using the $\mathcal{D}_{MS}$ of Part c. (2 pts)

e. ZFE: Compare P_e in part d with the P_e for the ZFE. Compute SNR difference in dB between the SNR based on mean-square distortion implied in Parts c and d and SNR_{ZFE}. (hint, see example in this chapter for SNR_{ZFE}) (2 pts)

3.22 *Precoding - 12 pts*

For an ISI channel with

$$Q(D) + \frac{1}{SNR_{MFB}} = .82 \cdot \left[\frac{\jmath}{2} \cdot D^{-1} + 1.25 - \frac{\jmath}{2} \cdot D\right] \quad ,$$

and $\frac{\bar{\mathcal{E}}_{\boldsymbol{x}}}{\sigma^2} = 100$.

a. Find SNR_{MFB}, $\|h\|^2$, and $SNR_{MMSE-DFE}$. (2 pts)

b. Find $G(D)$ and $G_U(D)$ for the MMSE-DFE. (1 pt)

c. Draw a Tomlinson-Harashima precoder, showing from x_k through the decision device in the receiver in your diagram (any M). (2 pts)

d. Let $M = 4$ in the precoder of Part c. Find P_e. (2 pts)

e. Design (show/draw) a Flexible precoder, showing from x_k through the decision device in the receiver in your diagram (any M). (2 pts)

f. Let $M = 4$ the precoder of Part e. Find P_e. (2 pts)

3.23 *Finite-Delay Tree Search - 17 pts*

A channel with multipath fading has one reflecting path with gain (voltage) 90% of the main path with binary input. The relative delay on this path is approximately T seconds, but the carrier sees a phase-shift of -60° that is constant on the second path.

Use the model

$$H(\omega) = \begin{cases} \sqrt{T} \cdot \left(1 + a \cdot e^{-\jmath\omega T}\right) & |\omega| < \pi/T \\ 0 & \text{elsewhere} \end{cases}$$

to approximate this channel with $\frac{\mathcal{N}_0}{2} = .0181$ and $\bar{\mathcal{E}}_{\boldsymbol{x}} = 1$.

a. Find a. (1 pt)

b. Find SNR_{MFB}. (1 pt)

c. Find $W(D)$ and $\text{SNR}_{MMSE-LE,U}$ for the MMSE-LE. (3 pts)

d. Find $W(D)$, $B(D)$, and $\text{SNR}_{MMSE-DFE,U}$ for the MMSE-DFE. (3 pts)

e. Design a simple method to compute $SNR_{\text{ZF-DFE}}$ (2 pts).

f. A finite-delay tree search detector at time k decides $\hat{x}_{k-1}$ is shown in Figure 3.95 and chooses $\hat{x}_{k-1}$ to minimize

$$\min_{\hat{x}_k, \hat{x}_{k-1}} |z_k - \hat{x}_k - a \cdot \hat{x}_{k-1}|^2 + |z_{k-1} - \hat{x}_{k-1} - a \cdot \hat{x}_{k-2}|^2 \quad ,$$

where $\hat{x}_{k-2} = x_{k-2}$ by assumption.

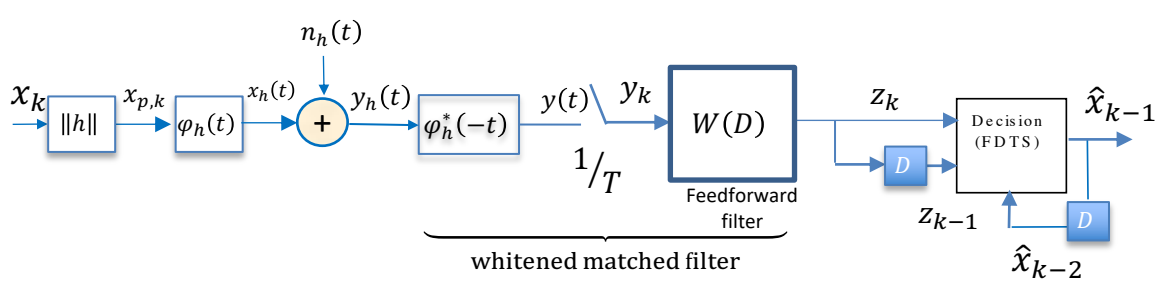

Figure 3.95: Finite-delay tree search.

How does this FDTS compare with the ZF-DFE (better or worse)? (1 pt)

g. Find an SNR_{fdts} for this channel. (3 pts)

h. Could you generalize SNR in part g for FIR channels with ν taps? (3 pts)

3.24 *Peak Distortion - 5 pts*

Peak distortion generalizes to channels without reciever matched filtering (that is $\varphi_p(-t)$ is a lowpass anti-alias filter). A channel has

$$y(D) = x(D) \cdot (1 - .5 \cdot D) + N(D)$$

after sampling, where $N(D)$ is discrete AWGN. $H(D) = 1 - .5 \cdot D$.

a. Write y_k in terms of x_k, x_{k-1} and n_k. (hint, this is easy. 1 pt)

b. The peak distortion for such a channel is $\mathcal{D}_p \triangleq |x_{max}| \cdot \sum_{m \neq 0} |h_m|$. Find this channel's $\mathcal{D}_p$ if $|x_{max}| = 1$. (2 pts)

c. Suppose $\frac{\mathcal{N}_0}{2}$, the mean-square of the sample noise, is .05 and $\bar{\mathcal{E}}_{\boldsymbol{x}} = 1$. What is P_e for symbol-by-symbol detection on y_k with PAM and $M = 2$? (2 pts)

3.25 *Equalization of Phase Distortion - 13 pts*

An ISI channel has $h(t) = 1/\sqrt{T} \cdot [\text{sinc}(t/T) - \jmath \cdot \text{sinc}[(t-T)/T]]$, $\bar{\mathcal{E}}_{\boldsymbol{x}} = 1$, and $\frac{\mathcal{N}_0}{2} = .05$.

a. What is SNR_{MFB}? (1 pt)

b. Find the ZFE. (2 pts)

c. Find the MMSE-LE. (2 pts)

d. Find the ZF-DFE. (2 pts)

e. Find the MMSE-DFE. (2 pts)

f. Draw a diagram illustrating the MMSE-DFE implementation with Tomlinson precoding. (2 pts)

g. For $P_e < 10^{-6}$ and using square or cross QAM, choose a design and find the largest data rate you can transmit using one of the equalizers above. (2 pts)

3.26 *Basic QAM Systems Revisted with Equalization Background - 6 pts*

An AWGN channel has $\bar{\mathcal{E}}_{\boldsymbol{x}} = -40$ dBm/Hz and $\frac{\mathcal{N}_0}{2} = -66$ dBm/Hz. The symbol rate is initially fixed at 5 MHz, and the desired $\bar{P}_e = 10^{-6}$. Only QAM CR or SQ constellations may be used.

a. What is the maximum data rate? (1 pt)

b. What is the maximum data rate if the desired $\bar{P}_e < 10^{-7}$? (1 pt)

c. What is the maximum data rate if the symbol rate can be varied (but transmit power is fixed at the same level as was used with a 5 MHz symbol rate)? (1 pt)

d. Suppose the pulse response of the channel changes from $h(t) = \frac{1}{\sqrt{T}} \cdot \text{sinc}\left(\frac{t}{T}\right)$ to $\frac{1}{\sqrt{T}} \cdot \text{sinc}\left(\frac{t}{T}\right) + .9 \cdot \frac{1}{\sqrt{T}} \cdot \text{sinc}\left(\frac{t+T}{T}\right)$, and Part a is revisited. With respect to your answer in Part a, compare the data rate for a ZF-DFE applied to this channel where $1/T = 5$ MHz. (1 pt)

e. Under the exact same change of Part d, compare the data rate with respect to your answer in Part c. (1 pt)

f. Suppose an optimum ML detector is used (observes all transmissions and makes one large decision on the entire transmitted message) with any pulse response that is a one-to-one transformation on all possible QAM inputs with $\|h\|^2 = 1$. Compare the error probability with respect to that of the correct response to Part a. (1 pt)

3.27 *Expert Understanding - 10 pts*

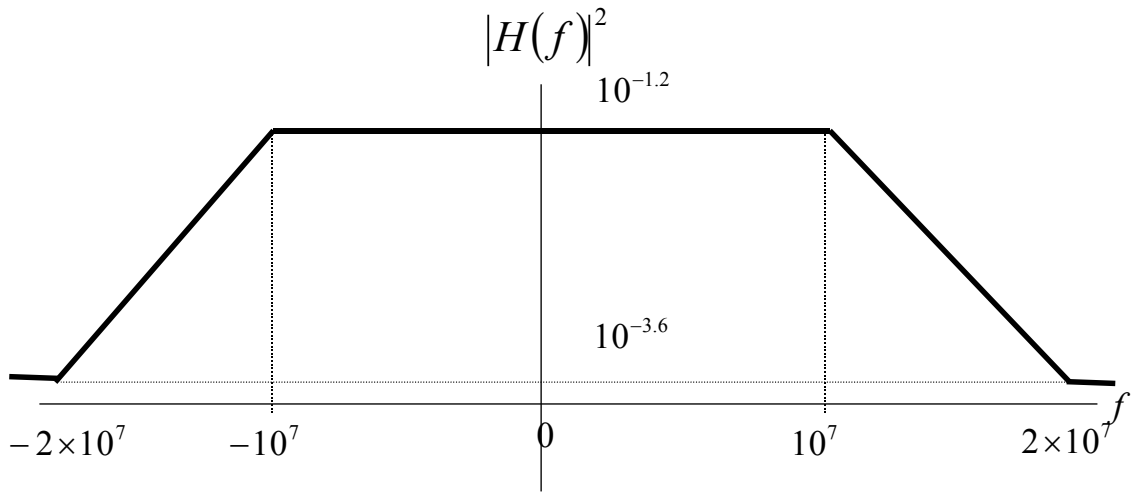

Figure 3.96: Channel for Problem 3.27.

A channel baseband transfer function for PAM transmission is shown in Figure 3.96. PAM transmission with sinc basis function is used on this channel with a transmit power level of 10 mW $=\mathcal{E}_x/T$. The one-sided AWGN psd is -100 dBm/Hz.

a. Let the symbol rate be 20 MHz - find SNR_{MFB}.(1 pt)

b. For the same symbol rate as Part a, what is $\text{SNR}_{MMSE-LE}$? (1 pt)

c. For the equalizer in Part b, what is the data rate for PAM if $P_e \leq 10^{-6}$? (1 pt)

d. Let the symbol rate be 40 MHz - find the new SNR_{MFB}.(2 pts)

e. Draw a the combined shape of the matched-filter and feedforward filter for a ZF-DFE corresponding to the new symbol rate of Part d. (1 pt)

f. Estimate $SNR_{MMSE-DFE,U}$ for the new symbol rate, assuming a MMSE-DFE receiver is used. (2 pts) (Hint: ythe relationship of this transfer function to the channel is often used as an example in Chapter 3).

g. What is the new data rate for this system at the same error probability P_e as Part c - compare with the data rate of part c. (1 pt)

h. What can you conclude about incurring ISI if the transmitter is allowed to vary its bandwidth? (2 pts)

3.28 *Infinite-Length EQ - 10 pts*

An ISI channel with PAM transmission has channel correlation function given by

$$Q(D) = \frac{.19}{(1+.9D)\cdot(1+.9D^{-1})} \quad ,$$

with SNR_{MFB} =10 dB, $\mathcal{E}_{\boldsymbol{x}} = 1$, and $\|p\|^2 = \frac{1}{.19}$.

a. (3 pts) Find $W_{ZFE}(D)$, σ^2_{ZFE}, and SNR_{ZFE}.

b. (1 pt) Find $W_{MMSE-LE}(D)$

c. (3 pts) Find $W_{ZF-DFE}(D)$, $B_{ZF-DFE}(D)$, and SNR_{ZF-DFE}.

d. (3 pts) Find $W_{MMSE-DFE}(D)$, $B_{MMSE-DFE}(D)$, and $SNR_{MMSE-DFE,U}$.

3.29 *Finite-Length EQ - 9 pts*

A baseband channel is given by

$$H(f) = \begin{cases} \sqrt{T} \cdot \left(1 - .7 \cdot e^{j2\pi f T}\right) & |f| < \frac{.5}{T} \\ 0 & |f| \geq \frac{.5}{T} \end{cases} \tag{3.829}$$

and finite-length equalization is used with anti-alias perfect LPR with gain $\sqrt{T}$ followed by symbol-rate sampling. After the sampling, a maximum complexity of 3 taps TOTAL over a feedforward filter and a feedback filter can be used. $\mathcal{E}_{\boldsymbol{x}} = 2$ and $\frac{\mathcal{N}_0}{2} = .01$ for a symbol rate of $1/T = 100$kHz is used with PAM transmission. Given the complexity constraint, find the highest data rate achievable with PAM transmission when the corresponding symbol-error probability P_e must be less than 10^{-5}.

3.30 *Infinite-length Channel and Equalizer - 10 pts*

The pulse response on a channel with additive white Gaussian noise is $h(t) = e^{-at} \cdot u(t)$, where $u(t)$ is the unit step response. $a > 0$ and the two symbol inputs per dimension are ± 1. Only QAM CR or SQ constellations allowed.

a. What is the argument to the Q-function in $\bar{P}_e = Q(x)$ at very low symbol rates ? (1 pt)

b. For $\bar{P}_e \approx 10^{-6}$, $\frac{\mathcal{N}_0}{2} = .05$, and very low symbol period, what is the value of $a =$? (1 pt)

For the remainder of this problem, let $T = 1$.

c. Find $Q(D)$. (1 pt)

d. Find $\mathcal{D}_{ms}$. (1 pt)

e. Find the receiver normalized matched filter prior to any symbol-rate sampling device. (1 pt)

f. Find SNR_{MFB}. Let $SNR = \bar{\mathcal{E}}_{\boldsymbol{x}} / \frac{\mathcal{N}_0}{2}$. (1 pt)

g. Find the loss of the ZF-DFE with respect to the MFB. (1 pt)

h. Find $SNR_{MMSE-DFE,U}$ for $a = 1$ and $SNR = 20$ dB. (3 pts)

i. What would an increase in $a > 1$ with respect to Part h do to the gap in performance between the ZF-DFE and the MMSE-DFE? (2 pts)

3.31 *Diversity Channel - 6 pts*

This problem compares the channel studied throughout this text with the same input energy $\bar{\mathcal{E}}_{\boldsymbol{x}} = 1$ and noise PSD of $\frac{\mathcal{N}_0}{2} = .181$ versus almost the same channel except that two receivers independently receive:

- an undistorted delayed-by-T signal (that is $H(D) = D$), and
- a signal that is not delayed, but reduced to 90% of its amplitude (that is $H(D) = .9$).

On both paths, the channel passes nonzero energy only between zero frequency and the Nyquist frequency.

a. Find $Q(D)$, $\|\boldsymbol{h}\|$, and SNR_{MFB} for the later diversity channel. (3 pts)

b. Find the bit-error rate $\bar{P}_b$ on the diversity channel for the case of 1 bit/dimension transmission. (1 pt)

3.32 *Do we understand basic detection - 9 pts*

A filtered AWGN channel with $T = 1$ has pulse response $h(t) = \text{sinc}(t) + \text{sinc}(t-1)$ with $SNR_{MFB} =$ 14.2 dB.

a. Find the probability of error for a ZF-DFE if a binary symbol is transmitted (2 pts).

b. The Tomlinson precoder in this special case of a monic pulse response with all unity coefficients can be replaced by a simpler precoder whose output is

$$x'_k = \begin{cases} x'_{k-1} & \text{if } x_k = 1 \\ -x'_{k-1} & \text{if } x_k = -1 \end{cases} \tag{3.830}$$

Find the possible (noise-free) channel outputs and determine an SBS decoder rule. What is the performance (probability of error) for this decoder? (2 pts)

c. Suppose this channel (without precoder) is used one time for the transmission of one of the 8 4-dimensional messages that are defined by $[+ \ \pm \ \pm \ \pm]$, which produce 8 possible 5-dimensional outputs. The decoder will use the assumption that the last symbol transmitted before these 4 was -1. ML detection is now used for this multidimensional 1-shot channel. What are the new minimum distance and number of nearest neighbors at this minimum distance, and how do they relate to those for the system in part a? What is the new number of bits per output dimension? (3 pts)

d. Does the error-probability P_e change significantly if the input is extended to arbitrarily long block length N with now the first sample fixed at $+$ and the last sample fixed at $-$, and all other inputs being equally likely $+$ or $-$ in between? What happens to the number of bits per output dimension in this case? (2 pts).

3.33 *Equalization of a 3-tap channel - 10 pts*

PAM transmission wiht $\bar{\mathcal{E}}_{\boldsymbol{x}} = 1$ is used on a filtered AWGN channel with $\frac{\mathcal{N}_0}{2} = .01$, $T = 1$, and pulse repsonse $h(t) = \text{sinc}(t) + 1.8\text{sinc}(t-1) + .81\text{sinc}(t-2)$. The desired symbol-error probability is $P_e = 10^{-6}$.

a. Find $\|h\|^2$, SNR_{MFB}, AND $Q(D)$ for this channel. (2 pts)

b. Find the MMSE-LE and corresponding unbiased $\text{SNR}_{MMSE-LE,U}$ for this channel. (2 pts)

c. Find the ZF-DFE detection SNR and loss with respect to SNR_{MFB}. (1 pt)

d. Find the MMSE-DFE. Also compute the MMSE-DFE SNR and maximum data rate in bits/dimension using the gap approximation. (3 pts)

e. Draw the flexible (Laroia) precoder for the MMSE-DFE and draw the system from transmit symbol to detector in the receiver using this precoder. Implement this precoder for the largest number of integer bits that can be transmitted according to your answer in Part d. (2 pts)

3.34 *Finite-Length Equalizer Design - Lorentzian Pulse Shape- 12 pts*

A filtered AWGN channel has the Lorentzian impulse response

$$h_c(t) = \frac{1}{T} \cdot \frac{1}{1 + \left(\frac{10^7 t}{3}\right)^2} \ , \tag{3.831}$$

with Fourier Transform

$$H_c(f) = \frac{3\pi}{10} e^{-6\pi \cdot 10^{-7} \cdot |f|} \ . \tag{3.832}$$

This channel is used in the transmission system of Figure 3.97. QAM transmission with $1/T = 1$ MHz and carrier frequency $f_c = 600$kHz are used on this channel. The AWGN psd is $\frac{\mathcal{N}_0}{2} = -86.5$ dBm/Hz. The transmit power is $\frac{\mathcal{E}_{\boldsymbol{x}}}{T}$=1 mW. The oversampling factor for the equalizer design is chosen as $l = 2$.

Square-root raised cosine filtering with 10% excess bandwidth is applied as a transmit filter, and an ideal filter is used for anti-alias filtering at the receiver.

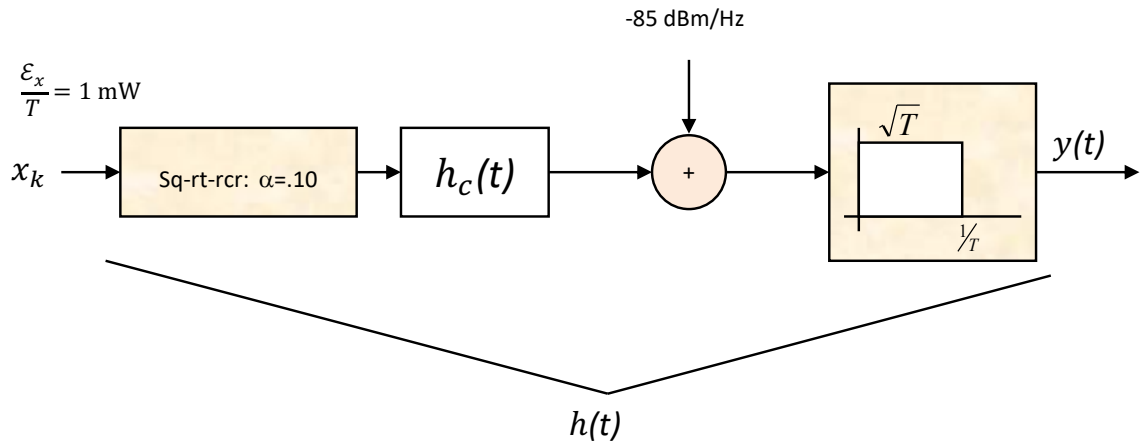

Figure 3.97: Transmission system for Problem 3.34.

A matlab subroutine at the course web site may be useful in computing responses in the frequency domain.

a. Find ν so that an FIR pulse response approximates this pulse response so that less than 5% error[61] in $\|h\|^2$. (3 pts)

b. Calculate SNR_{MFB}. Determine a reasonable set of parameters and settings for an FIR MMSE-LE and the corresponding data rate at $P_e = 10^{-7}$. Calculate the data rate using both an integer and a possibly non-integer number of bits/symbol. (4 pts)

c. Repeat Part b for an FIR MMSE-DFE design and draw receiver. Calculate the data rate using both an integer and a possibly non-integer number of bits/symbol. (3 pts)

d. Can you find a way to improve the data rate on this channel by changing the symbol rate and or carrier frequency? (2 pts)

3.35 *Telephone-Line Transmission with "T1" - 14 pts*

Digital transmission on telephone lines necessarily must pass through two "isolation transformers" as illustrated in Figure 3.98. These transformers prevent large D.C. voltages accidentally placed on the line from unintentionally harming the telephone line or the internet equipment attached to it, and they provide immunity to earth currents, noises, and ground loops. These transformers also introduce ISI.

a. The "derivative taking" combined characteristic of the transformers can be approximately modeled at a sampling rate of $1/T = 1.544$ MHz as successive differences between channel input symbols. For sufficiently short transmission lines, the rest of the line can be modeled as distortionless. What is a reasonable partial-response model for the channel $H(D)$? Sketch the channel transfer function. Is there ISI? (3 pts)

[61] 5% error in approximation does not mean the SNR is limited to 1/20 or 13 dB. 5% error in modeling a type of pulse response for analysis simply means that the designer is estimating the performance of an eventual adaptive system that will adjust its equalizer parameters to the best MMSE settings for whatever channel. Thus, 5% modeling error is often sufficient for the analysis step to get basic estimates of the SNR performance and consequent achievable data rates.

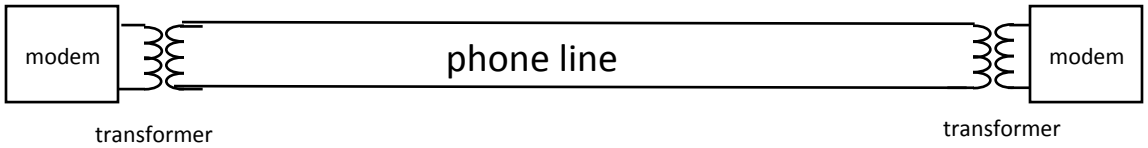

Figure 3.98: Illustration of a telephone-line data transmission for Problem 3.35.

b. How would a zero-forcing decision-feedback equalizer generally perform on this channel with respect to the case where channel output energy was the same but there are no transformers? (2 pts)

c. What are some of the drawbacks of a ZF-DFE on this channel? (2 pts)

d. Suppose a Tomlinson precoder were used on the channel with $M = 2$, how much is transmit energy increased generally? Can you reduce this increase by good choice of initial condition for the Tomlinson Precoder? (3 pts)

e. Show how a binary precoder and corresponding decoder can significantly simplify the implementation of a detector. What is the loss with respect to optimum MFB performance on this channel with your precoder and detector? (3 pts)

f. Suppose the channel were not exactly a PR channel as in Part a, but were relatively close. Characterize the loss in performance that you would expect to see for your detector. (1 pt)

3.36 *Magnetic Recording Channel - 14 pts*

Digital magnetic information storage (i.e., disks) and retrieval makes use of the storage of magnetic fluexes on a magnetic disk. The disk spins under a "read head" and by Maxwell's laws the read-head wire senses flus changes in the moving magnetic field. This read head thus generates a read current that is translated into a voltage through amplifiers succeeding the read head. Change in flux is often encoded to mean a "1" was stored and no change means a "0" was stored. The read head also has finite-band limitations.

a. Pick a partial-resonse channel with $\nu = 2$ that models the read-back channel. Sketch the magnitude characteristic (versus frequency) for your channel and justify its use. (2 pts)

b. How would a zero-forcing decision-feedback equalizer generally perform on this channel with respect to the best case where all read-head channel output energy conveyed either a positive or negative polarity for each pulse? (1 pt)

c. What are some of the drawbacks of a ZF-DFE on this channel? (2 pts)

d. Suppose a Tomlinson Precoder were used on the channel (ignore the practical fact that magnetic saturation might not allow a Tomlinson nor any type of precoder) with $M = 2$, how much is transmit energy increased generally? Can you reduce this increase by good choice of initial condition for the Tomlinson Precoder? (2 pts)

e. Show how a binary precoder and corresponding decoder can significantly simplify the implementation of a detector. What is the loss with respect to optimum MFB performance on this channel with your precoder and detector? (3 pts)

f. Suppose the channel were not exactly a PR channel as in Part a, but were relatively close. Characterize the loss in performance that you would expect to see for your detector. (1 pt)

g. Suppose the density (bits per linear inch) of a disk is to be increased so one can store more files on it. What new partial response might apply with the same read-channel electronics, but with a correspondingly faster symbol rate? (3 pts)

3.37 *Tomlinson Preocoding and Simple Precoding - 8 pts*
Section 3.8 derives a simple precoder for $H(D) = 1 + D$.

a. Design the Tomlinson precoder corresponding to a ZF-DFE for this channel with the possible binary inputs to the precoder being ± 1. (4 pts)

b. How many distinct outputs are produced by the Tomlinson Precoder assuming an initial state (feedback D element contents) of zero for the precoder. (1 pt)

c. Compute the average energy of the Tomlinson precoder output. (1 pt)

d. How many possible outputs are produced by the simple precoder with binary inputs? (1 pt)

e. Compute the average energy of the channel input for the simple precoder with the input constellation of Part a. (1 pt)

3.38 *Flexible Precoding and Simple Precoding - 8 pts*
Section 3.8 derives a simple precoder for $H(D) = 1 + D$.

a. Design the Flexible precoder corresponding to a ZF-DFE for this channel with the possible binary inputs to the precoder being ± 1. (4 pts)

b. How many distinct outputs are produced by the Flexible Precoder assuming an initial state (feedback D element contents) of zero for the precoder. (1 pt)

c. Compute the average energy of the Flexible precoder output. (1 pt)

d. How many possible outputs are produced by the simple precoder with binary inputs? (1 pt)

e. Compute the average energy of the channel input for the simple precoder with the input constellation of Part a. (1 pt)

3.39 *Partial Response Precoding and the ZF-DFE - 10 pts*
An AWGN has response $H(D) = (1 - D)^2$ with noise variance σ^2 and one-dimensional real input $x_k = \pm 1$.

a. Determine a partial-response (PR) precoder for the channel, as well as the decoding rule for the noiseless channel output. (2 pts)

b. What are the possible noiseless outputs and their probabilities? From these, determine the P_e for the precoded channel. (4 pts)

c. If the partial-response precoder is used with symbol-by-symbol detection, what is the loss with respect to the MFB? Ignore nearest neighbor terms for this calculation since the MFB concerns only the argument of the Q-function. (1 pt)

d. If a ZF-DFE is used instead of a precoder for this channel, so that $P_c(D) = 1 - 2D + D^2$, what is η_0? Determine also the SNR loss with respect to the SNR_{MFB} (2 pts)

e. Compare this with the performance of the precoder, ignoring nearest neighbor calculations. (1 pt)

3.40 *Error propagation and nearest neighbors - 10 pts*
A partial-response channel has $H(D) = 1 - D^2$ channel with AWGN noise variance σ^2 and $d = 2$ and 4-level PAM transmission.

a. State the precoding rule and the noiseless decoding rule. (1 pts)

b. Find the possible noiseless outputs and their probabilities. Find also N_e and P_e with the use of precoding. (4 pts)

c. Suppose a ZF-DFE is used on this system and that at time $k = 0$ an incorrect decision $x_0 - \hat{x}_0 = 2$ occurs. This incorrect decision affects z_k at time $k = 2$. Find the N_e (taking the error at $k = 0$ into account) for the ZF-DFE. From this, determine the P_e with the effect of error propagation included. (4 pts)

d. Compare the P_e in part (c) with that of the use of the precoder in Part a. (1 pt)

3.41 *Forcing Partial Response - 6 pts*

Consider a $H(D) = 1 + .9D$ channel with AWGN noise variance σ^2. The objective is to convert this to a $1 + D$ channel

a. Design an equalizer that will convert the channel to a $1 + D$ channel. (2 pts)

b. The received signal is $y_k = x_k + .9 \cdot x_{k-1} + n_k$ where n_k is the AWGN. Find the autocorrelation of the noise after going through the receiver designed in Part a. Evaluate r_0, $r_{\pm 1}$, and $r_{\pm 2}$. Is the noise white? (3 pts)

c. Would the noise terms would be more or less correlated if the conversion were instead of a $1 + .1D$ channel to a $1 + D$ channel? You need only discuss briefly. (1 pt)

3.42 *Equalization of a General Single-Pole Channel - 11 pts*

PAM transmission on a filtered AWGN channel uses basis function $\varphi(t) = \frac{1}{\sqrt{T}} \cdot \text{sinc}\left(\frac{t}{T}\right)$ with $T = 1$ and undergoes channel impulse response with Fourier transform ($|\alpha| < 1$)

$$H(\omega) = \begin{cases} \frac{1}{1+a \cdot e^{\jmath\omega}} & |\omega| \leq \pi \\ 0 & |\omega| > \pi \end{cases} \tag{3.833}$$

and $SNR = \frac{\bar{\mathcal{E}}_{\boldsymbol{x}}}{\sigma^2} = 28$ dB.

a. Find the Fourier Transform of the pulse response,$P(\omega) =$? (1 pt)

b. Find $\|h\|^2$. (1 pt)

c. Find $Q(D)$, the function characterizing ISI. (2 pts)

d. Find the filters and sketch the block diagram of receiver for the MMSE-DFE on this channel for $a = .9$. (3 pts)

e. Estimate the data rate for uncoded PAM transmission and $P_e < 10^{-6}$ that is achievable with your answer in part d. (2 pts)

f. Draw a diagram of the better precoder's (Tomlinson or Laroia), transmitter and receiver, implementations with $d = 2$ in the transmitted constellation. (2 pts)

3.43 *Finite Equalization of a "causal" complex channel – 15 pts*

A channel sampled at symbol rate $T = 1$ (after anti-alias filtering) has output samples given by

$$y_k = h_k * x_k + n_k \ ,$$

where $h_k = \delta_k + (-2 + 0.25\jmath) \cdot \delta_{k+1}$, $E[n_k \cdot n_{k-l}] = \frac{\delta_l}{50}$ and $\mathcal{E}_{\boldsymbol{x}} = 2$.

a. Compute SNR_{MFB}. (1 pt)

b. For a channel equalizer with 3 feedforward taps and no feedback, write the H convolution matrix. Is this channel causal? If not, is it somehow equivalent to causal for the use of equalization programs like DFE color? (2 pts)

c. For the re-indexing of time to correspond to your answer in Part b, find the best delay for an MMSE-LE when $N_f = 3$. (1 pt)

d. Find $W_{MMSE-LE}$ for $N_{ff} = 3$ for the delay in Part c. (1 pt)

e. Convolve the equalizer for Part d with the channel and show the result. (1 pt).

f. Compute $\text{SNR}_{MMSE-LE,U}$ and the corresponding MMSE. (both per-dimension and per symbol). (2 pts).

g. Compute the loss w.r.t. MFB for the 3-tap linear equalizer. (1 pt).

h. Find a better linear equalizer using up to 10 taps and corresponding $\text{SNR}_{MMSE-LE,U}$ improvement. (2 pts)

i. For your answer in Part h, what is $\bar{P}_e$ for 16 QAM transmission? (1 pt)

j. Design an MMSE-DFE with no more than 3 total taps that performs better than anything above. (3 pts)

3.44 *Diversity Concept and COFDM - 7 pts*

An additive white Gaussian noise channel supports QAM transmission with a symbol rate of $1/T =$ 100 kHz (with 0 % excess bandwidth) anywhere in a total baseband-equivalent bandwidth of 10 MHz transmission. Each 100 kHz wide QAM signal can be nominally received with an SNR of 14.5 dB without equalization. However, this 10 MHz wide channel has a 100 kHz wide band that is attenuated by 20 dB with respect to the rest of the band, but the location of the frequency of this notch is not known in advance to the designer. The transmitters are collocated.

a. What is the data rate sustainable at probability of bit error $\bar{P}_b \leq 10^{-7}$ in the nominal condition? (1 pt)

b. What is the maximum number of simultaneous QAM users can share this channel at the performance level of Part a if the notch does not exist? (1 pt)

c. What is the worst-case error probability P_e for the number of users in Part b if the notch does exist? (1 pt)

d. Suppose now (unlike Part b) that the notch does exist, and the designer decides to send each QAM signal in two distinct frequency bands. (This is a simple example of what is often called Coded Orthogonal Frequency Division Modulation or COFDM.) What is the worst-case probability of error for a diversity-equalization system applied to this channel? (1 pt)

e. For the same system as Part d, what is the best SNR that a diversity equalizer system can achieve? (1 pt)

f. For the system of Part d, how many users can now share the band all with bit error rate $\bar{P}_b$ less than 10^{-7}? Can you think of a way to improve this number closer to the level of the Part b? (2 pts)

3.45 *Hybrid ARQ (HARQ) Diversity - 12 pts*

A time-varying wireless channel sends long packets of binary information that are decoded by a receiver that uses a symbol-by-symbol decision device. The channel has pulse response in the familiar form:

$$H(\omega) = \begin{cases} \sqrt{T} \cdot \left(1 + a_i \cdot e^{-\jmath\omega T}\right) & |\omega| \leq \frac{\pi}{T} \\ 0 & |\omega| > \frac{\pi}{T} \end{cases} \tag{3.834}$$

where a_i may vary from packet to packet (but not within a packet). There is also AWGN with constant power spectral density $\frac{\mathcal{N}_0}{2} = .1$. QPSK (4QAM) is sent on this channel with symbol energy 2.

a. Find the best DFE SNR and corresponding probability of symbol error for the two cases or "states" when $a_1 = .9$ and $a_2 = .5$. Which is better and why? (2 pts)

Now, suppose the transmitter can resend the same packet of symbols to the receiver, which can delay the channel output packet from the first transmission until the symbols from the new packet arrive. Further suppose that the second transmission occurs at a time when the channel state is known to have changed. However, a symbol-by-symbol detector is still to be used by the receiver jointly on both outputs. This is a variant of what is called "Automatic Repeat reQuest" or ARQ. (Usually ARQ only resends when it is determined by the receiver that the decision made on the first transmission is unreliable and discarded. Hybrid ARQ uses both channel outputs.) For the remainder of this problem, assume the two a_i values are equally likely.

b. Explain why this is a diversity situation. What is the approximate cost in data rate for this retransmission in time if the same symbol constellation (same b) is used for each transmission? (1 pt)

c. Find a new SNR_{MFB} for this situation with a diversity receiver. (1 pt)

d. Find the new function $Q(D)$ for this diversity situation. (2 pts)

e. Determine the performance of the best DFE this time (SNR and P_e) and compare to the earlier single-instance receivers. (2 pts)

f. Compare the P_e of Part e with the product of the two P_e's found in Part a. Does this make sense? Comment. (2 pts)

g. Draw the receiver with RAKE illustrated as well as DFE, unbiasing, and decision device. (phase splitter can be ignored in diagram and all quantities can be assumed complex.) (2 pts).

3.46 *Precoder Diversity - 7 pts*

A system with 4 PAM transmits over two discrete-time channels shown with the two independent AWGN channels shown in Figure 3.99. ($\bar{\mathcal{E}}_x = 1$)

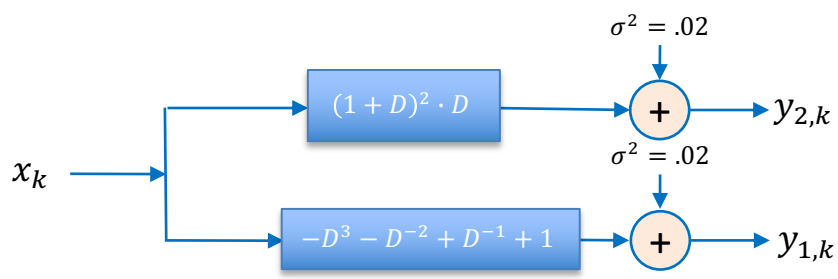

Figure 3.99: Transmission system for Problem 3.46.

a. Find the RAKE matched filter(s) for this system ? (1 pt)

b. Find the single feedforward filter for a ZF-DFE? (1 pt)

c. Show the best precoder for the system created in Part b. (1 pt)

d. Find the SNR at the detector for this precoded system? (1 pt)

e. Find the loss in SNR with respect to the of either single channel. (1 pt)

f. Find the P_e for this precoded diversity system. (1 pt)

g. Find the probability that a packet of 1540 bytes contains one or more errors. What might you do to improve? (1 pt)

3.47 *Equalizer Performance and Means - 10 pts*

Recall that arithmetic mean, geometric mean, and harmonic mean are of the form $\frac{1}{n}\sum_{i=1}^{n} x_i$, $(\prod_{i=1}^{n} x_i)^{\frac{1}{n}}$, $\left(\frac{1}{n}\sum_{i=1}^{n}\frac{1}{x_i}\right)^{-1}$, respectively. Furthermore, they satisfy the following inequalities:

$$\frac{1}{n}\sum_{i=1}^{n} x_i \quad \geq \quad \left(\prod_{i=1}^{n} x_i\right)^{\frac{1}{n}} \quad \geq \quad \left(\frac{1}{n}\sum_{i=1}^{n}\frac{1}{x_i}\right)^{-1},$$

with equality when $x_1 = x_2 = \cdots = x_n$

a. Express SNR_{ZFE}, SNR_{ZF-DFE}, SNR_{MFB} in terms of SNR_{MFB} and frequency response of the autocorrelation function q_k. Prove that $SNR_{ZFE} \leq SNR_{ZF-DFE} \leq SNR_{MFB}$ using above inequalities. When does equality hold? *hint*: use $\int_a^b x(t)dt = \lim_{n\to\infty}\sum_{k=1}^{n} x(\frac{b-a}{n}k + a)\cdot\frac{b-a}{n}$. (4 pts)

b. Similarly, prove that $SNR_{MMSE-LE,U} \leq \mathrm{SNR}_{MMSE-DFE,U} \leq SNR_{MFB}$ using above inequalities. When does equality hold? (4 pts)

c. Compare SNR_{ZFE} and $\mathrm{SNR}_{MMSE-LE}$. Which scheme has better performance? (2 pts)

3.48 *Unequal Channels and Basic Loading – Malkin- 26 pts*

Use the gap approximation for this problem. A sequence of 16-QAM symbols with in-phase component a_k and quadrature component b_k at time k is transmitted on a passband channel by the modulated signal

$$x(t) = \sqrt{2}\left\{\left[\sum_k a_k \cdot \varphi(t-kT)\right]\cdot cos(\omega_c t) - \left[\sum_k b_k \cdot \varphi(t-kT)\right]\cdot sin(\omega_c t)\right\}, \tag{3.835}$$

where $T = 40$ ns, $f_c = 2.4$ GHz, and the transmit power is 700 μW.

The transmit filter/basic function is $\varphi(t)$

$$\varphi(t) = \frac{1}{\sqrt{T}}\cdot sinc\left(\frac{t}{T}\right) \quad , \tag{3.836}$$

and the baseband channel response is a frequency translation given by $H(f) = e^{-j5\pi fT}$. The received signal is thus

$$y(t) = h(t) * x(t) + n(t) \tag{3.837}$$

where $n(t)$ is an additive white Gaussian noise random process with two-sided PSD of -100 dBm/Hz.

a. What is the data rate of this system? (1 pts)

b. What are $\mathcal{E}_x$, $\bar{\mathcal{E}}_x$ and d_{min} for this constellation? (2 pts)

c. What is $\tilde{x}_{bb}(t)$? (1.5 pts)

d. What is the ISI characterizing function $q(t)$? what is q_k? (1.5 pts)

e. What are P_e and $\bar{P}_e$ for an optimal ML detector? (2 pts)

For the remainder of this problem: The implementation of the baseband demodulator is faulty and the additive Gaussian noise power in the quadrature component is $\alpha = 4$ times what it should be. That is, the noise variance of the quadrature component is $\alpha\frac{N_0}{2} = 2N_0$ while the noise variance in the in-phase dimension is $\frac{N_0}{2}$. Answer the following questions for this situation.

f. What is the receiver SNR? Is this SNR meaningful any longer in terms of the gap formula? (2.5 pts)

g. What are P_e and $\bar{P}_e$? (3 pts)

h. Instead of using QAM modulation as above, two independent 4-PAM constellations (with half the total energy allocated for each constellation) are now transmitted on the in-phase and quadrature channels, respectively. What is P_e averaged over both of the PAM constellations? (1.5 pts)

i. The system design may allocate different energies for the in-phase and quadrature channels (**but this design still uses QAM modulation with the same number of bits on each of the in-phase and quadrature channels, and the transmit power remains at 700 μW). Use different inphase and quadrature energies to improve the $\bar{P}_e$ performance from Part (g).** What is the best energy allocation for the in-phase and quadrature channels? For the given $\bar{P}_e = 10^{-6}$, what is $\bar{b}$ and the achievable data rate? (3 pts)

j. Using the results from part (i) find the minimal increase in transmit power needed to guarantee $\bar{P}_e = 10^{-6}$ for 16-QAM transmission? (2.5 pts)

The design may now reduce losses. Given this increased noise in the quadrature dimension, tthe design may use only the in-phase dimension for transmission (but subject to the original transmit power constraint of 700 μW).

k. What data rate can be then supported that gives $\bar{P}_e = 10^{-6}$? (2.5 pts)

l. Using a fair comparison, compare the QAM transmission system from part (i) to the single-dimensional scheme ($N = 1$) from part (k). Which scheme is better? (3 pts)

m. Design a new transmission scheme that uses both the in-phase and quadrature channels to get a higher data rate than part (i), subject to the same $\bar{P}_e = 10^{-6}$, and original symbol rate and power constraint of 700 μW. (3 pts)

3.49 *A Specific One-Pole Channel (9 pts)*

A transmission system uses the basis function $\varphi(t) = sinc(t)$ with $\frac{1}{T} = 1$ Hz. The Fourier transform of the channel impulse response is:

$$H(f) = \begin{cases} \frac{1}{1-0.5j\cdot e^{-j2\pi f}}, & \text{for} |f| \leq \frac{1}{2} \\ 0, & \text{for} |f| > \frac{1}{2}\,. \end{cases} \tag{3.838}$$

and $SNR = \frac{\bar{\mathcal{E}}_x}{\sigma^2} = 10$ dB.

a. Find $||h||^2$ and Q(D). (1 pt)

b. Find $W_{ZFE}(D)$ and $W_{MMSE-LE}(D)$. (1 pt)

c. Find $W(D)$ and $B(D)$ for ZF-DFE. (1 pt)

d. Find $W(D)$ and $B(D)$ for MMSE-DFE. (2 pts)

e. What is SNR_{ZF-DFE}? (0.5 pt)

f. Design a Tomlinson precoder based on the ZF-DFE. Show both the precoder and the corresponding receiver (for any M). (1.5 pts)

g. Design a Laroia precoder based on the ZF-DFE. Assume the system uses 4-QAM modulation. Show both the precoder and the corresponding receiver. The kind of constellation used at each SBS detector should be shown. (2 pts)

3.50 *Infinite Diversity - Malkin (7 pts)*

A receiver has access to an infinite number of diversity channels where the output of channel i at time k is

$$y_{k,i} = x_k + 0.9 \cdot x_{k+1} + n_{k,i}, \qquad i = 0, 1, 2, \ldots$$

where $n_{k,i}$ is a Gaussian noise process independent across time and across all the channels, and with variance $\sigma_i^2 = 1.2^i \cdot 0.181$. Also, $\bar{\mathcal{E}}_x = 1$.

a. Find $SNR_{MFB,i}$, the SNR_{MFB} for channel i. (1 pt)

b. What is the matched filter for each diversity channel? (2 pts)

c. What is the resulting $Q(D)$ for this diversity system? (1.5 pts)

d. What is the detector SNR for this system for a MMSE-DFE receiver? (2.5 pts)

3.51 *Infinite Feedforward and Finite Feedback - Malkin (9 pts)*

A symbol-rate sampled MMSE-DFE structure, where the received signal is filtered by a continuous time matched filter, uses an *infinite-length feedforward filter*. However, the MMSE-DFE *feedback filter* has finite length N_b.

a. Formulate the optimization problem that solves to find the optimal feedforward and feedback coefficients to minimize the mean squared error (Hint: Don't approach this as a finite-length equalization problem as in Section 3.7).

   Assume that $\frac{N_0}{2} = .181$, $\mathcal{E}_x = 1$, and $H(D) = 1 + .9 \cdot D^{-1}$. (and $SNR_{MFB} = 10$ dB). (2 pts)

b. Using only 1 feedback tap ($N_b = 1$), determine the optimal feedforward and feedback filters (Hint: This is easy - you have already seen the solution before). (2 pts)

c. Now consider the ZF-DFE version of this problem. State the optimization problem for this situation (analogous to Part a). (2 pts)

   Now, change the channel to the infinite-impulse response of $H(D) = \frac{1}{1+0.9 \cdot D^{-1}}$ (and $\|h\|^2 = \frac{1}{1-0.9^2} = \frac{1}{0.19}$).

d. Determine the optimal feedforward and feedback filters for the ZF-DFE formulation using only 1 feedback tap ($N_b = 1$). (3 pts)

3.52 *Packet Processing - Malkin (10 pts)*

Suppose that in a packet-based transmission system, a receiver makes a decision from the set of transmit symbols x_1, x_2, x_3 based on the channel outputs y_1, y_2, y_3, where

$$\begin{bmatrix} y_3 \\ y_2 \\ y_1 \end{bmatrix} = \begin{bmatrix} p_{11} & p_{12} & p_{13} \\ 0 & p_{22} & p_{23} \\ 0 & 0 & p_{33} \end{bmatrix} \begin{bmatrix} x_3 \\ x_2 \\ x_1 \end{bmatrix} + \begin{bmatrix} n_3 \\ n_2 \\ n_1 \end{bmatrix} = \begin{bmatrix} 0.6 & 1.9 & -3.86 \\ 0 & 1.8 & 3.3 \\ 0 & 0 & 1.2 \end{bmatrix} \begin{bmatrix} x_3 \\ x_2 \\ x_1 \end{bmatrix} + \begin{bmatrix} n_3 \\ n_2 \\ n_1 \end{bmatrix} \tag{3.839}$$

and where the noise autocorrelation matrix is given by

$$R_n = E\left(\begin{bmatrix} n_3 \\ n_2 \\ n_1 \end{bmatrix} \begin{bmatrix} n_3^* & n_2^* & n_1^* \end{bmatrix} \right) = \begin{bmatrix} 0.3 & 0 & 0 \\ 0 & 0.5 & 0 \\ 0 & 0 & 0.1 \end{bmatrix}. \tag{3.840}$$

The inverse of the channel matrix is given by

$$\begin{bmatrix} 0.6 & 1.9 & -3.86 \\ 0 & 1.8 & 3.3 \\ 0 & 0 & 1.2 \end{bmatrix}^{-1} = \begin{bmatrix} 1.67 & -1.76 & 10.19 \\ 0 & 0.56 & -1.52 \\ 0 & 0 & 0.83 \end{bmatrix}. \tag{3.841}$$

The transmit symbols are i.i.d with $\mathcal{E}_{x_1} = \mathcal{E}_{x_2} = \mathcal{E}_{x_3} = 20$.

a. What is the 3-tap zero-forcing equalizer for x_1 based on the observation y_1, y_2, y_3? Repeat for x_2 and x_3.(1.5 pts)

b. What is the matrix ZFE for detecting x_1, x_2, and x_3? (Hint: This is easy - all the work occurred in the previous part) (1 pt)

c. What is the detection SNR for x_1 using a ZFE? Answer the same for x_2 and x_3. (1.5 pts)

d. An engineer now realizes that the performance could be improved through use previous decisions when detecting the current symbol. If the receiver starts by detecting x_1, then x_2, and finally x_3, describe how this modified ZF detector would work? (1 pt)

e. Assuming previous decisions are correct, what is now the detection SNR for each symbol? (1.5 pts)

f. The approach above does not necessarily minimize the MMSE. How would a packet MMSE-DFE work? How would you describe the feedback structure? (Don't solve for the optimal matrices - just describe the signal processing that would take place). (1 pt)

g. Can the THP also be implemented for this packet based system? Describe how this would be done (a description is sufficient response). (1 pt)

3.53 *DFEcolor Program with Nontrivial Complex Channel – 10 pts*

Use of the dfecolor.m program in Matlab produces:

```
>> h = [0 - 0.2500i   0.5000 + 0.5000i   1.0000 + 0.1250i   0.3000 - 0.2500i]
>> [snr,w]=dfecolor(1,h,7,3,6,1,.03*[1 zeros(1,6)])
snr = 15.2754
w = Columns 1 through 5
0.0006 + 0.0019i  -0.0064 + 0.0002i   0.0103 + 0.0198i   0.0249 + 0.0341i   0.2733 - 0.0231i
Columns 6 through 10
0.6038 - 0.6340i  -0.0000 + 0.2402i  -0.6392 + 0.5137i   0.0074 + 0.1009i  -0.0601 - 0.0721i
```

a. What is equalizer output (before bias removal), $E\left[z_k/x_{k-\Delta}\right]$, for the equalizer as output above? (1 pt)

b. If the noise vector in the matlab command above becomes .02*[1.5 -.5+.5*i], what will happen to DFE performance (improve/degrade)? Why? (1 pt)

c. Find $B_U(D)$ for the original (white) noise. (1 pt)

d. What is the maximum (uncoded QAM) data rate if the symbol rate is 100 MHz and $\bar{P}_e = 10^{-6}$? (Assume no error propagation and arbitrary constellations with SBS decisions in the MMSE-DFE.) (1 pt)

e. What is the maximum data rate that can be achieved if a Tomlinson precoder is used? (1 pt)

f. If the carrier frequency is 75 MHz, what are possible pulse-response samples for the actual channel, presuming the given h_k are baseband equivalents? (1 pt)

g. Assuming the channel has the minimum bandwidth for the pulse response given, what is the loss with respect to the matched filter bound? (1 pt)

h. When bias is absorbed into the feedforward equalizer, what is the magnitude of the "center" tap? Convolve this unbiased feedforward filter with the channel h and interpret in terms of the given command into dfecolor and its results. (2 pts)

i. For a flexible precoder in the transmitter and uncoded QAM transmission that will have $P_e < 10^{-6}$, what is the maximum number of points in the first corresponding two-dimensional decision device used in the receiver? (1 pt)

3.54 *Finite-Length Equalizer Design with Diversity – 17 pts*

A receiver designer has two options for the two-path channel described below. The designer may use only a single antenna (Parts a to c) that receives both paths' outputs added together with a single AWGN power spectral density of -110 dBm/Hz. Or as this problem progresses in Parts d and beyond, the designer may instead use two antennas that are directional with one receiver only on the first path with AWGN at -113 dBm/Hz and the second receiver only only the second path with AWGN also at -113 dBm/Hz (the noise that was present on the channel is presumably split evenly in this case). The transmit power is $P_x = \frac{\mathcal{E}_{\boldsymbol{x}}}{T} \leq 20$ dBm. The symbol rate is 1 MHz. The target probability of error is 10^{-6} and only integer number of bits/symbol are allowed. The system is sampled at instants $kT/2 = kT'$ for integer $k \geq 0$

The two paths' sampled (at pulse responses are:

$$\begin{aligned} h_1(t') &= e^{-10^6 t} \cdot u(t) \\ h_2(t) &= e^{-0.5 \cdot 10^6 \cdot (t - 0.5\mu\text{s})} \cdot u(t - 0.5\mu\text{s}) \ , \end{aligned}$$

where μs$= 10^{-6}$s.

a. Is there aliasing even with a sampling rate of $2/T$? Find by continuous integration $\|h_1\|^2$, $\|h_2\|^2$, and $\|h_1 + h_2\|^2$ and comment on the latter with respect to the sum of the former. Repeat this exercise for $\|p_1(kT')\|^2$, $\|\|h_2(kT')\|^2$ and $\|h\cdot(kT') + h_2(kT')\|^2$, and comment on their size relative to the true norms found by continuous integration relative to the choice of symbol rate (and thus also sampling rate). (4 pts)

b. Find ν and the FIR pulse response that approximates the actual response so that less than .25 dB error[62] in $\|h\|^2$ (that is, the norm square of the difference between the actual $\boldsymbol{h}$ and the truncated $\boldsymbol{h}$ is less than $(10^{.025} - 1) \cdot \|h\|^2$).

   Now find the Ex input for the dfecolor program, the vector $\boldsymbol{h}$ input that would be input to the DFECOLOR matlab program, and the CORRESPONDING noise vector that would be input. Please find these presuming that the anti-alias filter for $1/T'$ sampling is normalized. (3 pts)

c. Design an FIR DFE that achieves within .1 dB of the infinite-length performance for Part b's inputs. Record the smallest numbers of feedforward and feedback taps for which the equalizer can achieve this performance and the corresponding delay Δ. An acceptable response is the equalizer coefficient vector from Matlab decomposed separately into feedforward and feedback taps. Find the SNR and corresponding data rate for the design (3 pts).

d. Continue Part b except now find the two FIR pulse responses that approximates the pulse response so that less than .25 dB error in the overall $\|\boldsymbol{h}\|^2$ occurs, and provide the larger value of ν. (2 pts)

e. Now find the Ex input for the dfecolor program, the vector (rows) of p input that would be input to the DFERAKE matlab program, and the CORRESPONDING noise vector that would be input. Please find these presuming that the anti-alias filter for $1/T'$ sampling is normalized on both antennas. (2 pts)

[62] Readers should note that .25 dB accuracy is only about 6% of the energy; however, this is close enough to estimate equalizer behavior of the actual system. In practice, an adaptive implementation would tune the equalizer to get roughly the same performance as is derived here for the truncated approximation to the response $p(kT/2)$ over all time.

f. Design an FIR DFE that achieves within .1 dB of the infinite-length performance for Part d's pulse responses. Record the smallest numbers of feedforward and feedback taps that can achieve this performance and the corresponding delay Δ. An acceptable response is the equalizer coefficient vector from Matlab. Find the SNR and corresponding data rate for your design. (3 pts).

3.55 *Optimizing the DFE Transmit Filter – 3 pts*

A discrete-time channel is described by $y(D) = H(D) \cdot X(D) + N(D)$, where $X(D)$ is the transmit symbol sequence, $E(D)$ is the error sequence, and $N(D)$ is AWGN with variance $\frac{\mathcal{N}_0}{2}$. These notes so far have always assumed that the transmit sequence x_k is white (messages are independent). Suppose the transmitter could filter the symbol sequence before transmission, though the filtered symbol sequence must have the same power $\mathcal{E}_{\boldsymbol{x}}$. Call the magnitude squared of the transmit filter $\|H(e^{-\jmath\omega T})|^2$.

a. Given a MMSE-DFE receiver, find the transmit filter (squared magnitude) that maximizes the MMSE-DFE detection SNR. (2 pts)

b. Find the best transmit filter (squared magnitude) for the ZF-DFE (1 pt).

3.56 *Multi-User Scenario – 22 pts*

A single receiver receives transmissions from two independent users with symbol sequences $X_1(D)$ and $X_2(D)$, respectively. The two received signals are (with a and b real).

$$\begin{aligned} Y_1(D) &= (1 + a \cdot D)) \cdot X_1(D) - X_2(D) + N_1(D) \\ Y_2(D) &= X_1(D) + (1 - b \cdot D^2) \cdot X_2(D) + (1 - b \cdot D^2) \cdot N_2(D) + b \cdot D^2 \cdot Y_2(D) \quad , \end{aligned}$$

where $N_1(D)$ is AWGN with variance $\frac{\mathcal{N}_0}{2}$, and similarly $N_2(D)$ is AWGN with variance $\frac{\mathcal{N}_0}{2}$. The quantites a and b are real. The following are the energies

$$\begin{aligned} \mathbb{E}\left[X_1(D)X_1(D^{-*}\right] &= \mathcal{E}_1 \\ \mathbb{E}\left[X_2(D)X_2(D^{-*}\right] &= \mathcal{E}_2 \quad . \end{aligned}$$

The noises $N_1(D)$ and $N_2(D)$ are independent of one another and all mutually independent of the two transmitted data sequences $X_1(D)$ and $X_2(D)$. For this problem treat all ISI and "crosstalk" interference as if it came from a normal distribution, unless specifically treated otherwise as in Parts f and beyond. Matlab may be useful in this problem, particularly the routines "conv" "roots," and "integral."

The receiver will use both $Y_1(D)$ and $Y_2(D)$ for detection in all parts.

a. The receiver here will use both $Y_1(D)$ and $Y_2(D)$ for optimum detection of user 1 ($X_1(D)$), but treat $X_2(D)$ as noise. Find the noise-equivalent channel $\boldsymbol{H}(D)$ and the resulting $Q(D)$ for the case when $\mathcal{E}_2 = \frac{\mathcal{N}_0}{2}$. The Matlab Function "chol" may be useful in finding a noise-whitening filter. (3 pts)

b. For $\mathcal{E}_1 = 10$, $\mathcal{E}_2 = 1$, $\frac{\mathcal{N}_0}{2} = 1$, $a = 1$, and $b = 0.7$, find $Q(D)$, SNR_{MFB}, $\tilde{Q}(D)$, and the feed-forward and feedback filters for an infinite length MMSE-DFE for Part a's. The "integral function" may be convenient to compute the norm of channel elements. The "roots" and "conv" commands may also reduce labor to solve. (5 pts)

c. Show a Tomlinson precoder implementation of the structure in part b if M-PAM is transmitted. (1 pt)

d. Suppose, instead, the receiver instead first detects user 2's signal $X_2(D)$ based on both $Y_1(D)$ and $y_2(D)$ by using a ZF-DFE receiver. Please specify all the filters and the SNR_{ZF-DFE}, given that $\mathcal{E}_1 = 1$, $\mathcal{E}_2 = 30$, $\frac{\mathcal{N}_0}{2} = 1$, $a = 1$, and $b = 7$. Noise whitening may need to presume a triangular form as in Part a except that now the elements are functions of D - just solve it, 3 equations in 3 unknown functions of D - not that hard for first two elements, 3rd is ratio of 3rd order polynomials The integral and conv Matlab functions are again useful. (4 pts)

e. Show a Laroia implementation of the structure in Part d if M-PAM is transmitted. (2 pts)

f. This sub question investigates the system in Part b if $x_{2,k}$ is known and its effects removed at the receiver? Suppose a structure like that found in Parts b and c to detect $x_{2,k}$ reliably. (Since $\mathcal{E}_1 = 10$ is large, the data rate for the channel from $x_{2,k}$ to the receiver may be very low relative to the correct response for Part b.) Show a receiver for $x_{1,k}$ that makes use of a known $x_{2,k}$. Does this receiver look familiar in some way? What is roughly the new gap-based data rate achievable for x_1? (3 pts)

g. Repeat Part f for the numbers in Part d except that $x_{1,k}$ is detected and its affects removed. (2 pts)

h. Suppose time-sharing of the two systems ($\mathcal{E}_1 = 10$ or $\mathcal{E}_2 = 30$) is allowed (long blocks are assumed so any beginning or end effects are negligible). What data rate pairs for x_1 and x_2 might be possible (think of plot in two dimensions)? (2 pts)

3.57 Mutual Information and Parallel Independent AWGN Channels (3 pts)

This problem considers a set of parallel, independent, and one-real-dimensional AWGN channels of the form:

$$y_k = h_k \cdot x_k + n_k \quad ,$$

where the noises all have variance σ^2 with zero mean.

a. (1 pt) Use probability densities factoring to show that this channel set's mutual information is the sum of the set's individual mutual information quantities.

b. (1 pt) If the set of parallel channels has a total energy constraint that is equal to the sum of the energy constraints, what energy $\mathcal{E}_k$, $k = 1, ..., N$ should be allocated to each of the channels to maximize the mutual information? The answer may use the definition that the subchannel gains are given as $g_n = \frac{|h_k|^2}{\sigma^2}$ (so that the individual SNRs would then be $SNR_n = \mathcal{E}_k \cdot g_k$).

c. (1 pt) Find the overall $SNR_{overall}$ for a single AWGN that is equivalent to this problem's set of parallel channels in terms of mutual information.

3.58 Innovations (6 pts)

Find the innovations variance per real dimension, entropy per dimension, and linear prediction filter for the following Gaussian processes (let $T = 1$):

a. (2 pts) A real process with autocorrelation $R_{xx}(D) = .0619 \cdot D^{-2} + .4691 \cdot D^{-1} + 1 + .4691 \cdot D + .0619 \cdot D^2$.

b. (2 pts) A complex discrete-time process with power spectral density $10 \cdot [1.65 + 1.6 \cdot cos(\omega)]$.

c. (2 pts) A complex process that has a maximum of only 3 nonzero terms in its autocorrelation function and a notch exactly in the middle of its band (i.e., at normalized frequency 1/4) and total power 2.

3.59 Multibands (14 pts)

Three bands of transmission result from infinite-length water-filling as shown below with a gap of 5.8 dB at $P_e = 10^{-6}$. The lowest band uses baseband PAM transmission, and the other two bands use QAM transmission. Each band has an MMSE-DFE receiver with the SNR shown in Figure 3.100.

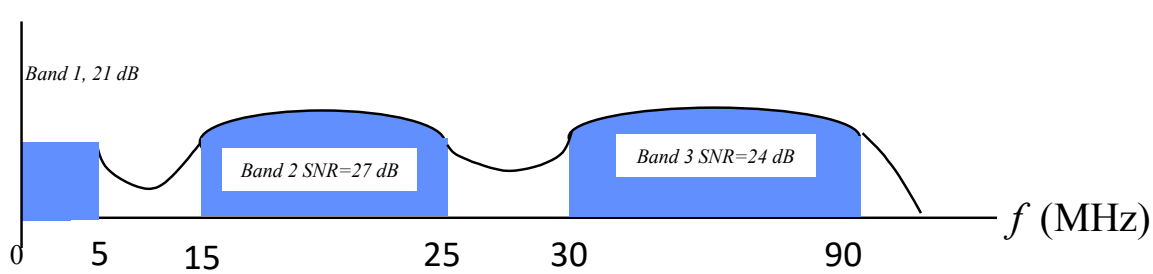

Figure 3.100: Multiband transmission for Problem 3.59

a. (3 pts) Find the optimum symbol rates $1/T_i^*$, $1/\bar{T}_i^*$, and the optimum carrier frequencies $f_{c,i}^*$ for each of the 3 bands shown in Figure 3.100.

b. (3 pts) Find $\bar{b}_1$, $\bar{b}_2$, and $\bar{b}_3$, as well as b_1, b_2, and b_3 for each of these 3 bands. Also find the data rate R for the entire 3-band system.

c. (1 pt) Find $1/T^*$.

d. (2 pts) Find the overall best SNR and $\bar{b}$ for a single AWGN that is equivalent to the set of channels in terms of mutual information.

e. (2 pts) The noise is such that (two-sided) $\bar{\mathcal{E}}_{\boldsymbol{x}} = -70$ dBm/Hz in all used bands. Find the total energy per symbol period T^* that is used and the power used.
The answers can be specified in terms of dBm/Hz and dBm.

Suppose baseband PAM with a symbol rate of $1/T$ =200 MHz is used instead with the same power, and energy equally divided on all dimensions (i.e., successive PAM symbols are independent).

f. (1 pts) What is $\bar{\mathcal{E}}_{x,PAM}$ =?

g. (2 pts) Find approximate $SNR_{mmse-dfe,PAM,u}$ and new data rate for this alternative single-band PAM design remembering that the non-zero gap increases the wasted-bandwidth loss. You may assume that the intervals between the transmit bands show carry very little (assume zero) data rate.

3.60 CDEF (10 pts)

An AWGN with intersymbol interference sustains successful transmission using a MMSE-DFE receiver with 256 QAM with Gap of $\Gamma = 8.8$ dB with a margin of 1.2 dB at $\bar{P}_e = 10^{-6}$.

a. (2 pts) What is the mutual information in bits per symbol for this channel? In bits per dimension?

b. (2 pts) Suppose optimization of the transmit filter increased the margin to 2.5 dB. What is the capacity (bits/dimension) of this new transmit-optimized channel at this symbol rate?

Returning (for the remainder of this problem) to the well-known $1 + .9 \cdot D^{-1}$ channel with $SNR_{MFB} = 10$ dB with $T = 1$ and PAM transmission:

c. (2 pts) What is the capacity of this system if energy increases such that $T^* = 1$ becomes the optimum symbol rate?

d. (3 pts) What would be the new (smallest) symbol energy per dimension for the situation in Part c?

e. (1 pt) Suppose this optimized system transmits with code with gap of 6 dB for probability of error 10^{-6} at $\bar{b} = 1$. What is margin at this data rate? (fractional bits per symbol are ok for inclusion in results and use of all formulas.)

Bibliography

[1] John G. Proakis and Mahsoud Salehi. *"Digital Communications - Fifth Edition"*. McGraw Hill, India, 2008.

[2] Thomas Kailath, Ali H. Sayed, and Babak Hassibi. *"Linear Estimation"*. Prentice Hall, USA, 2000.

[3] Lasha Ephremidze. *"An Elementary Proof of the Ploynomial Matrix Spectral Factorization Theorem"*. Proceedings of the Royal Society of Edinburgh Section A: Mathematics, DOI: https://doi.org/10.1017/S0308210512001552Published online by Cambridge University Press: 24 July 2014. AMS Subject Classification (2010): 47A68.

[4] Jack Salz. *"On Mean-Square Decision Feedback Equalization and Timing Phase"*. IEEE Transactions on Communications, Vol. 7, No. 5/6, March 1971, pp. 1138-139.

[5] M. Tomlinson. *"New Automatic Equaliser Employing Modulo Arithmetic"*. *Electronics Letters,* Vol. 25, No. 12, December 1977, pp. 1471-1476.

[6] Rajiv Laroia and Steven A. Tretter and Nariman Farvardin. *"A Simple and Effective Precoding Scheme for Noise Whitening on Intersymbol Interference Channels"*. *IEEE Transactions on Communications,* Vol. 41, No. 10, October 1993, pp. 1460-1463.

[7] Adam Lender. *"The Duobinary Technique for High-Speed Data Transmission"*. *IEEE Transactions on Magnetics,* Vol. 23, No. 5, September 1987, pp. 3666-3668.

[8] Hemant Thapar and Arvind Patel. *"A Class of Partial-Response Systems for Increasing Storage Density in Digital Magnetic Recording"*. *IEEE Transactions on Communication Electronics,* Vol. 82, No. 5, May 1963, pp. 214-218.

[9] Robert Price and Paul E. Green. *"A Communication Technique for Multipath Channels"*. *Proceedings of the IRE,* Vol. 46, No. 3, March 1958, pp. 555-570.

[10] Benard Widrow and M.E. Hoff Jr. *"Adaptive switching circuits"*. *1960 IRE WESCON Convention Record,* Part 4, New York: IRE, pp. 96-104.

[11] H. Robbins and S. Monro *"A Stochastic Approximation Method"*. *The Annals of Mathematical Statistics.,* Vol. 22, No. 3, pp.400-407.

Index